



National Library
of Canada

Acquisitions and
Bibliographic Services Branch

395 Wellington Street
Ottawa, Ontario
K1A 0N4

Bibliothèque nationale
du Canada

Direction des acquisitions et
des services bibliographiques

395, rue Wellington
Ottawa (Ontario)
K1A 0N4

Your file Votre référence

Our file Notre référence

NOTICE

The quality of this microform is heavily dependent upon the quality of the original thesis submitted for microfilming. Every effort has been made to ensure the highest quality of reproduction possible.

If pages are missing, contact the university which granted the degree.

Some pages may have indistinct print especially if the original pages were typed with a poor typewriter ribbon or if the university sent us an inferior photocopy.

Reproduction in full or in part of this microform is governed by the Canadian Copyright Act, R.S.C. 1970, c. C-30, and subsequent amendments.

AVIS

La qualité de cette microforme dépend grandement de la qualité de la thèse soumise au microfilmage. Nous avons tout fait pour assurer une qualité supérieure de reproduction.

S'il manque des pages, veuillez communiquer avec l'université qui a conféré le grade.

La qualité d'impression de certaines pages peut laisser à désirer, surtout si les pages originales ont été dactylographiées à l'aide d'un ruban usé ou si l'université nous a fait parvenir une photocopie de qualité inférieure.

La reproduction, même partielle, de cette microforme est soumise à la Loi canadienne sur le droit d'auteur, SRC 1970, c. C-30, et ses amendements subséquents.

The University of Alberta

Theory of Simple Conjugate Surfaces and its Application in Hypoid Gearing

By

Yuri Wang

A thesis submitted to the Faculty of Graduate Studies and Research in partial fulfillment of the requirements for the degree of **DOCTOR OF PHILOSOPHY**.

Department of Mechanical Engineering

Edmonton, Alberta

Fall, 1995



National Library
of Canada

Bibliothèque nationale
du Canada

Acquisitions and
Bibliographic Services Branch

Direction des acquisitions et
des services bibliographiques

395 Wellington Street
Ottawa, Ontario
K1A 0N4

395, rue Wellington
Ottawa (Ontario)
K1A 0N4

Your file Votre référence

Our file Notre référence

THE AUTHOR HAS GRANTED AN
IRREVOCABLE NON-EXCLUSIVE
LICENCE ALLOWING THE NATIONAL
LIBRARY OF CANADA TO
REPRODUCE, LOAN, DISTRIBUTE OR
SELL COPIES OF HIS/HER THESIS BY
ANY MEANS AND IN ANY FORM OR
FORMAT, MAKING THIS THESIS
AVAILABLE TO INTERESTED
PERSONS.

L'AUTEUR A ACCORDE UNE LICENCE
IRREVOCABLE ET NON EXCLUSIVE
PERMETTANT A LA BIBLIOTHEQUE
NATIONALE DU CANADA DE
REPRODUIRE, PRETER, DISTRIBUER
OU VENDRE DES COPIES DE SA
THESE DE QUELQUE MANIERE ET
SOUS QUELQUE FORME QUE CE SOIT
POUR METTRE DES EXEMPLAIRES DE
CETTE THESE A LA DISPOSITION DES
PERSONNE INTERESSEES.

THE AUTHOR RETAINS OWNERSHIP
OF THE COPYRIGHT IN HIS/HER
THESIS. NEITHER THE THESIS NOR
SUBSTANTIAL EXTRACTS FROM IT
MAY BE PRINTED OR OTHERWISE
REPRODUCED WITHOUT HIS/HER
PERMISSION.

L'AUTEUR CONSERVE LA PROPRIETE
DU DROIT D'AUTEUR QUI PROTEGE
SA THESE. NI LA THESE NI DES
EXTRAITS SUBSTANTIELS DE CELLE-
CI NE DOIVENT ETRE IMPRIMES OU
AUTREMENT REPRODUITS SANS SON
AUTORISATION.

ISBN 0-612-06307-0

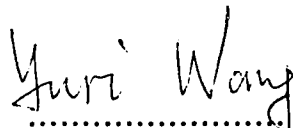
Canada

University of Alberta
Library Release Form

Name of Author : Yuri Wang
Title of Thesis : Theory of Simple Conjugate Surfaces and its Application
in Hypoid Gearing
Degree : Doctor of Philosophy
Year this Degree Granted: 1995

Permission is hereby granted to the University of Alberta Library to reproduce single copies of this thesis and to lend or sell such copies for private, scholarly or scientific research purpose only.

The author reserves all other publication and other rights in association with the copyright in the thesis, and except as hereinbefore provided neither the thesis nor any substantial portion thereof may be printed or otherwise reproduced in any material form whatever without the author prior written permission.

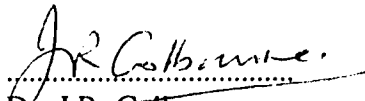

.....

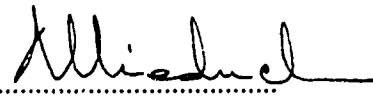
#2A,9101-112 Street
Edmonton, Alberta
T6C 5G2
CANADA

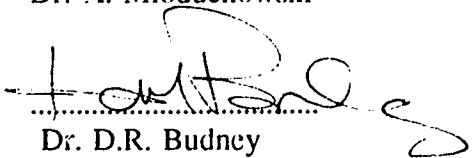
October 5th, 1995


UNIVERSITY OF ALBERTA
FACULTY OF GRADUATE STUDIES AND RESEARCH

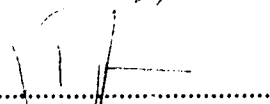
The undersigned certify that they have read, and recommended to the faculty of graduate studies and research for acceptance, a thesis entitled **Theory of Conjugate Surfaces and its Application in Hypoid Gearing** submitted by **Yu-Ri Wang** in partial fulfilment of the requirements for the degree of **Doctor of Philosophy**.

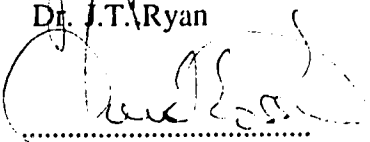

.....
Dr. J.R. Colbourne
(Supervisor)


.....
Dr. A. Mioduchowski


.....
Dr. D.R. Budney


.....
Dr. K.R. Fyfe


.....
Dr. J.T. Ryan


.....
Dr. C. Gosselin

Abstract

Conjugate surfaces with point contact have been widely used in the practice of gearing. The author of the present thesis has applied the theory of conjugate surfaces to develop the basic principles for designing and manufacturing a pair of point-contacting surfaces with controlled properties of transmission and contact at any position. An encompassing mathematical model was developed, based on Gleason No. 16 Bevel-Gear Generator, and a computer program for this mathematical model was written. Finally, the computer program was used to provide a numerical example.

Acknowledgements

In the entire course of completing this thesis, my supervisor, Dr. John R. Colbourne, has created all necessary conditions for me to accomplish this project and given me valuable suggestions and all other help. Here, I take this opportunity to express my sincere appreciation to him. Without him, it is quite questionable for me to finish this thesis.

I am also grateful to the other members of my supervisor group, Dr. David R. Budney and Dr. Andrew Mioduchowski, Dr. J.T. Ryan and Dr. K.R. Fyfe and the external examiner Dr. C Gosselin for their encouragement and valuable suggestions.

Gratitudes are also given to all the professors who ever give me lectures. Finally, I express my thanks to Mr. Allan M. Muir, Mr. Donald Fuhr and Mr. Max Schubert for their cooperations.

Contents

1	Introduction	1
2	Theory of Simple Conjugate Surfaces	4
2.1	Rotation of a Vector	4
2.1.1	The Expression for the Rotation of a Vector	4
2.1.2	Combination of Successive Rotations	5
2.1.3	Sequence-Reciprocation of Successive Rotations	6
2.1.4	Resolution of a Rotation	7
2.2	Introduction to Differential Geometry	8
2.2.1	The Expression for a Boundary Surface	8
2.2.2	The Unit Vector Normal to a Boundary Surface at an Arbitrary Point	8
2.2.3	Curvature of a Surface	9
2.2.4	Normal Curvature	9
2.2.5	Torsional Curvature	9
2.2.6	Geometric Angular Velocity of a Surface	10
2.2.7	Relation of Torsional Curvatures Between Two Mutually Perpendicular Directions	10
2.2.8	Relations of Normal and Torsional Curvatures Between Different Tangential Directions	12
2.2.9	Conjugate Normal and Torsional Curvatures	14
2.2.10	Relative Curvature, Relative Normal and Torsional Curvatures	14

2.2.11	Relations Between Relative Normal and Torsional Curvatures in Different Tangential Directions	16
2.2.12	Compatible Equation of Surface Curvatures	16
2.2.13	Curvature Difference	17
2.2.14	Intersecting Curve	18
2.2.15	The Unit Vector Tangent to the Intersecting Curve at Any Point	19
2.2.16	The Unit Normal to the Intersecting Curve at Any Point and the Effective Normal Zone	19
2.2.17	The Unit Principle Normal and Curvatures of the Intersecting Curve at Any Point	20
2.2.18	The Unit Binormal Vector to the Intersecting Curve at Any Point	23
2.2.19	The Torsional Curvature of the Intersecting Curve at Any Point	23
2.2.20	Geometric Angular Velocity of the Intersecting Curve	25
2.2.21	The Relative Geometric Angular Velocity of the Intersecting Curve with Respect to the Boundary Surface	26
2.2.22	The Relative Curvature and Relative Torsional Curvature of the Intersecting Curve with Respect to the Boundary Surface	27
2.2.23	Geodesic	28
2.3	Kinematics of Conjugacy	29
2.3.1	Motion of a Rigid Body and Conjugate Motion	29
2.3.2	The Simple Conjugate Motion with a Single Degree of Freedom	33
2.4	Geometry of Conjugate Configuration	44
2.4.1	Conjugate Configuration	44
2.4.2	Global Geometry of Line-Contacting Simple Conjugate Sur- faces with Single Degree of Freedom	47
2.4.3	Geometry in Infinitesimal Region of Line-Contacting Simple Conjugate Surface with Single Degree of Freedom	53

3	Basic Principle for the Design of Gear Blanks	77
3.1	The Kinematic Characteristics of Hypoid Gearing	77
3.2	Gear Blank Pitch Surface	80
3.3	The Conjugate Stagnant Curve, Conjugate Boundary Curve and Conjugate Varied Curve on Line – Contacting Conjugate Surfaces	83
3.4	The Analytical Expression for the Conjugate Boundary Curve under the Condition of Special Simple Conjugate Motion	87
3.5	The Boundary Curve of Curvature Interference on the Line-Contacting Conjugate Surface	88
3.6	Basic Geometry of the Gear Tooth under the Condition of Constant Transmission Ratio, Fixed Axes and No Axial Translation	88
4	Design of the Gear Blank	100
4.1	Calculation of the Basic Shape Parameters	100
4.2	Calculation of the Gear Blank Parameters for the Gear and the Pinion	104
5	Determination of Machine-Setting Parameters for the Generation of the Gear Tooth Surface	112
5.1	Expressions for the Cutter Surface	114
5.2	Cutting Position of the Reference Point P_b on the Workpiece	117
5.3	The Relationship between the Cutter Surface and the Gear Tooth Surface	118
5.4	Four Auxiliary Conditions	121
5.5	Simultaneous Equations for Determining the Machine-Setting Parameters and Discussion of the Degrees of Freedom for the Cutting Process	123
6	Calculation of Curvature for the Gear Tooth Surface	129
6.1	Calculation of Curvatures for Conical and Cylindrical Helicoids with Constant Rate of Lead and Rotating Surface	129
6.2	Selection of the Fundamental Contact point and Determination of the Cutting Position of the Fundamental Contact Point	135
6.3	Determination of the Curvature Properties of the Gear Tooth Surface	141

7	Calculation of Curvatures for the Pinion Tooth Surface with Line Contact	149
7.1	Determination of the Conjugate Contact Position at the Fundamental Contact Point P_f of the Gear Relative to the Pinion	149
7.2	Calculation of Curvatures	151
8	Calculation of the Quantity for the Curvature Modification to the Pinion Tooth Surface to Obtain Point Contact	158
8.1	Angle between the Virtual Instantaneous Line of Contact and the Contact Locus.	159
8.2	The Modification $\Delta K'_{2e}$ of the Conjugate Normal Curvature to the Pinion Tooth Surface in the Direction of the Instantaneous Line of Contact.	160
8.3	The Modification $\Delta G'_{2e}$ of the Conjugate Torsional Curvature in the Direction of the Instantaneous Line of Contact	164
8.4	The Modification $\Delta K'_{2g}$ of the Conjugate Normal Curvature in Direction \mathbf{g} Perpendicular to Direction \mathbf{e}	165
9	Determination of Machine-Setting Parameters for the Generation of the Pinion Tooth Surface	172
9.1	The Cutting Position Vector of the Point on the Cutter Corresponding to the Fundamental Contact Point	172
9.2	The Cutting Position Vector of the Fundamental Contact Point on the Pinion	175
9.3	Calculation of Curvatures for the Pinion Tooth Surface	177
9.4	Simultaneous Equations for Machine-Setting Parameters of the Pinion Tooth Surface	182
10	Summary of the Procedure for Design and Calculation	185
11	Immediate Future Challenge	188
A	Numerical Example	192
A.1	Design of Gear Blank	192

A.2	Machine-Setting Parameters for Gear	197
A.3	Calculation of Curvatures for the Gear Tooth Surface	200
A.4	Calculation of Curvatures for the Pinion Tooth Surface with Line Contact	203
A.5	Calculation of the Quantity for the Curvature Modification to the Pinion Tooth Surface	206
A.6	Determination of Machine-Setting Parameters for the Pinion Tooth Surface	208
A.7	Calculation of Curvatures for the Gear Tooth Surface	211
A.8	Calculation of Curvatures for the Pinion Tooth Surface with Line Contact	215
A.9	Calculation of the Quantity for the Curvature Modification to the Pinion Tooth Surface	218
A.10	Determination of Machine-Setting Parameters for the Pinion Tooth Surface	220

List of Figures

2.1	Rotation of a vector	5
2.2	Successive rotations about two axes	6
2.3	Two mutually perpendicular tangential directions	13
2.4	Fundamental surface and substituting surface	17
2.5	Unit normal and effective normal zone	19
2.6	Dual coordinate systems	35
2.7	Double branches of involute tooth surface	53
2.8	Relationships among three fundamental differential quantities	54
2.9	Several special tangential vectors	60
2.10	Reduced relative motion	63
3.1	Dual coordinate systems	78
3.2	Two types of common tangential cases	85
3.3	Two types of special tangential cases	86
3.4	The regions of conjugate solution and no conjugate solution	87
3.5	Conjugate valid and invalid zones	89
3.6	Relation among the unit normals	96
4.1	Approximate determination of the sum of the dedendum angles.	106
4.2	Blank parameters of gear	109
5.1	Dual coordinate systems for determination of the machine-setting	113

5.2	The initial position of cutting edge	114
5.3	Relationship among coordinate systems	116
5.4	Relationship among the coordinate systems	119
5.5	The phase angle for gear	122
5.6	The phase angle for cradle	123
5.7	Dimension of cutter	124
6.1	The position of the fundamental contact point	136
7.1	Several tangential vectors	155
8.1	Determination of $2F_{Ge}$	161
8.2	Curvature Modification	162
8.3	Normal intersection in direction e of instantaneous line of contact . .	163
8.4	Contact locus	166
8.5	Motion diagram	167
8.6	Motion diagram and contact locus	168
8.7	Diagrams for motion analyses	171
9.1	Relationship among coordinate systems	173

Nomenclature

\otimes	Operational Sign of Rotation
K_τ	The Normal Curvature of a Surface in Direction τ
G_τ	The Torsional Curvature of a Surface in Direction τ
K'_τ	The Conjugate Normal Curvature of a Surface in Direction τ
G'_τ	The Conjugate Torsional Curvature of the Surface in Direction τ
Ω_τ	The Geometric Angular Velocity
\overline{K}_τ	The Relative Normal Curvature in Direction τ
\overline{G}_τ	The Relative Torsional Curvature in Direction τ
$\overline{\Omega}_\tau$	The Geometric Angular Velocity
\mathbf{v}_p^{ij}	The Velocity of Body i with respect to j at Point P
η_p	The Equivalent Projection Component of the Relative Angular Velocity
\mathbf{J}_p	The Conjugate Relative Acceleration
N_g	The Number of Gear Teeth
N_p	The Number of Pinion Teeth
f_{gp}	The Hypoid Offset
ρ_b	The Radial Distance of the Reference Point on Gear
μ_b	The Phase Angle of the Reference Point on Gear
z_b	The Axial Distance of the Reference Point on Gear
F_G	The Face Width of the Gear
r_c	The Nominal Radius of Cutter
M_{gp}	Transmission Ratio of Hypoid Gearing
γ_g	Gear Pitch Angle
ρ'_b	The Radial Distance of Reference Point on Pinion
μ'_b	The Phase Angle of Reference Point on Pinion
z'_b	The Axial Distance of Reference Point on Pinion
γ_p	Pinion Pitch Angle
ψ_g	Gear Spiral Angle
ψ_p	Pinion Spiral Angle
\mathbf{N}_{1b}	Unit Normal to the Gear Blank Pitch Surface
A_b	The Component of \mathbf{N}_{1b} in the Coordinate Axis i
B_b	The Component of \mathbf{N}_{1b} in the Coordinate Axis j
C_b	The Component of \mathbf{N}_{1b} in the Coordinate Axis k

ϕ_o	Limit Pressure Angle
Φ_g	Average Pressure Angle of Gear
ϕ_{gi}	Gear Pressure Angle on Convex Side
ϕ_{go}	Gear Pressure Angle on Concave Side
k_1	Depth Factor
c_1	Mean Addendum Factor
k_2	Clearance Factor
h	Mean Working Depth
a_g	Mean Addendum for Gear
a_p	Mean Addendum for Pinion
b_g	Mean Dedendum for Gear
b_p	Mean Dedendum for Pinion
c	Clearance
A_{mG}	Mean Pitch Cone Distance
$\Sigma\delta_D$	Sum of Dedendum Angle
δ_g	Dedendum Angle of Gear
α_g	Addendum Angle of Gear
γ_{gf}	Face Angle of Gear
γ_{gr}	Root Angle of Gear
Z_{go}	Pitch Apex Beyond Crossing Point
Z_{gf}	Face Apex Beyond Crossing Point
Z_{gr}	Root Apex Beyond Crossing Point
γ_{pf}	Face Angle of Pinion
γ_{pr}	Root Angle of Pinion
Z_{pf}	Face Apex Beyond Crossing Point
Z_{pr}	Root Apex Beyond Crossing Point
f_{mg}	Vertical Position of Gear
L	Horizontal Position of Gear
W_p	The Point Width of Cutter
M_{mg}	The Ratio of Roll for Gear
ε_g^o	The Phase Angle Gear Cutting Position on Concave
ε_g^i	The Phase Angle Gear Cutting Position on Convex
σ^o	The Phase Angle for Cutting Edge of Outer Side
σ^i	The Phase Angle for Cutting Edge of Inner Side
x_c^o	The Coordinate of Cutter Center at the Cutting Position Corresponding to the Outer Side of Gear
y_c^o	The Coordinate of Cutter Center at the Cutting Position Corresponding to the Outer Side of Gear

z_c^o	The Coordinate of Cutter Center at the Cutting Position Corresponding to the Outter Side of Gear
x_c^i	The Coordinate of Cutter Center at the Cutting Position Corresponding to the Inner Side of Gear
y_c^i	The Coordinate of Cutter Center at the Cutting Position Corresponding to the Inner Side of Gear
z_c^i	The Coordinate of Cutter Center at the Cutting Position Corresponding to the Inner Side of Gear
N_c	Unit Normal to the Cutter Surface
N_g	Unit Normal to the Gear Tooth Surface
ρ_c^o	Cutter Radius on Outter Side
ρ_c^i	Cutter Radius on Inner Side
R_{mb}	The Cutting Position Vector of Reference Point on Cutter
R_{gb}	The Cutting Position Vector of Reference Point on Gear
ε_c^o	The Phase Angle of Cutter Center Corresponding to the Concave Side of Gear
ε_c^i	The Phase Angle of Cutter Center Corresponding to the Convex Side of Gear
ξ_f	The Local Coordinate of Fundamental Contact Point
a_f	The Local Coordinate of Fundamental Contact Point
f_{mp}	Vertical Position of Pinion
L_p	Horizontal Position of Pinion
M_{mp}	The Ratio of Roll for Pinion
$\delta\varepsilon_p^f$	The Increment of Phase Angle for Pinion Cutting
σ_p	The Phase Angle of Cutting Edge for Pinion
x_{cp}	The Coordinate of Cutter Center at the Cutting Position
y_{cp}	The Coordinate of Cutter Center at the Cutting Position
z_{cp}	The Coordinate of Cutter Center at the Cutting Position

Chapter 1

Introduction

Hypoid gearing is an important machine element widely employed in industry. In comparison with spiral bevel gearing, a pair of hypoid gearing can be used to provide an offset between the axes of pinion and gear, that is, it can transmit the motion and power between a pair of non-intersecting axes. Besides, under the condition of the same size of gear member and transmission ratio, the size of the pinion member in the case of hypoid gearing can be made bigger than that of the pinion member in the case of spiral bevel gearing and this property can increase the strength of the gearing. According to the differences of the tooth depth for hypoid gearing, there are two different types of tooth surfaces: one is the uniform depth tooth and the other is the tapered depth tooth. Gleason machine tools are used to make hypoid gearing with tapered depth teeth, while Oerlikon machine tools are used to make hypoid gearing with uniform depth teeth. The theoretical research and the practice of production have proved that hypoid gearing with tapered depth teeth has obvious advantages over that of uniform depth teeth. Especially in the toe end of hypoid gearing, the tapered depth teeth have higher tooth strength.

Many researchers and gear manufacturing companies have conducted research on hypoid gearing. For various reasons, there are gaps in the principles regarding the design and manufacture of hypoid gearing which handicap our understanding and inquiry into hypoid gearing. In order to ensure that we will be able to grasp, deeply and comprehensively, the principles regarding hypoid gearing, and to employ these principles to design and manufacture hypoid gearing, there is still a need to re-investigate these principles from the most fundamental level, and further, to make necessary improvements on some of the principles and conclusions.

E. Wildhaber[1-3] and B. Shtipelman[10] used method of projective geometry to research hypoid gearing and derive mathematical expressions and equations. F.

Litvin[16,17] used matrix to research hypoid gearing. As for general principles, the methods used by E. Wildhaber, B. Shtipelman and F. Litvin are quite similar. Since Shtipelman's book[10] gives very much detail of the whole process of derivation of all expressions and equations, we can use his book as an example to analyse their methods. First of all, Shtipelman explored features of hypoid gear engagement and obtained some expressions applicable to the case of a pair of hypoid gears. This work was also done by E. Wildhaber, M. Baxter[9] and F. Litvin. Then, with the aid of an imaginary crown gear, the mathematical expressions and equations obtained in hypoid gear engagement can be applied to determine the machine-setting parameters for gear and pinion and their curvature calculations. As an example, we consider their way to determine the ratio of roll and the vertical offset of the machine-setting parameters for a gear tooth surface. From the analysis of hypoid gear engagement, it is known that once the relative position of both axes, the tooth numbers of gear and pinion, and a calculating reference point are given, then the transmission ratio, the spiral angles and some other parameters are uniquely determined. For example, the transmission ratio of a pair of hypoid gears can be determined from expressions (1.75) and (1.41) in B. Shtipelman's book[10]. In order to determine the ratio of roll for cutting a tooth surface, an imaginary crown gear can be introduced, and then the imaginary crown gear and the workpiece together make a hypoid drive having an offset E_G and a shaft angle $(90^\circ + \Gamma_R)$, where, Γ_R is the root angle of the gear. Finally, the ratio of roll for the gear tooth surface can be determined by expression (3.6) which is a direct application of expression (1.75). The offset E_G can be determined by expression (3.1) with the aid of Fig. 3.1 in Shtipelman's book. In addition, the blade angles of the cutter must be equal to the pressure angles of the gear tooth surfaces which were determined in the section of gear blank design, or a tilt device must be used in their methods. Since such a method is based on the introduction of an imaginary crown gear, the parameters of the gear blanks with respect to the reference cones must be transferred to the parameters with respect to the root cones. Finally, the results of these calculation are not quite satisfactory. For example, the position of mean point can not be precisely controlled, although they intend the mean point to be a contact point. M. Baxter[9], F. Litvin[16,17], T. Krenzer[14], C. Gosselin[12,13,15,24], L. Cloutier[12,13,15,24], H.J. Stadtfeld[18] and J.R. Colbourne[23] have also suggested methods to improve the results of calculation. M. Baxter[9] developed the TCA (tooth contact analysis) program to improve the machine settings in order to improve the qualities of transmission and contact. The changes in machine settings required to produce a good bearing pattern are found by trial and error, and the choice of the final settings depends heavily on the individual's subjective judgement and experience. C. Gosselin and L. Cloutier[12,13,15,24] have investigated the effects of the machine settings on the kinematical motion error, and

provided some numerical methods to optimize the machine-setting parameters which can make the TCA method more efficient.

The present thesis derives mathematical expressions directly from the fundamental requirements of conjugate surfaces. The fundamental method is different from the methods mentioned above. Mathematical models in this thesis include functional relationships among all the parameters of adjustment provided by the Gleason No.16 Bevel-Gear Generator. This system of design and calculation can precisely control the position and curvature values of any specified contact point, and approximately control the contact pattern without using the TCA program. The whole procedure of design and manufacture of hypoid gearing in this system is as follows:

1. According to the requirements submitted by the users of hypoid gearing, design a pair of hypoid gear blanks;
2. According to the requirements for a gear tooth surface A_g obtained in the gear blank design, design a cutter surface A_{cg} and a pair of conjugate motions (ϕ_{cg}, ϕ_g) between cutter surface A_{cg} and workpiece of gear A_g , and then a gear tooth surface A_g is formed;
3. According to the conjugate requirements for a pair of line contact conjugate surfaces, define a pinion tooth surface A_p in terms of A_g and (ϕ_g, ϕ_p) ;
4. According to the requirements for transmission and contact, perform curvature modification to a pinion tooth surface A_p , and then obtain a new surface A_p^* which is used as the real pinion tooth surface;
5. According to the obtained tooth surface A_p^* , design a cutter surface A_{cp} and a pair of conjugate motions (ϕ_{cp}, ϕ_p) between the cutter and the pinion workpiece. Finally, the pinion tooth surface A_p^* is formed.

Chapter 2 of this thesis briefly introduces the contents of the theory of simple conjugate surfaces, which is one part of the theory of conjugate surfaces contributed by Chih-Hsin Chen[4,5]. Then, the author of this thesis uses this theory to describe the basic concepts in hypoid gearing, to research the basic principles for design and manufacture of hypoid gearing, and to establish mathematical models which enable the manufacturers of hypoid gearing to make good use of all the freedoms of adjustment provided by Gleason machine tools to produce hypoid gearing. This method of design and calculation can be suitable for both the Formate method and the generating method, with or without the tilt device, and is therefore very general. Furthermore, this method provides the firm foundation for the future development of research on hypoid gearing.

Chapter 2

Theory of Simple Conjugate Surfaces

2.1 Rotation of a Vector

2.1.1 The Expression for the Rotation of a Vector

Given an arbitrary point-vector \mathbf{A} and an arbitrary unit vector ω , let \mathbf{A} rotate an angle ε (by the right-hand rule) about ω as an axis, and then a new point-vector \mathbf{a} sharing the same origin with the vector \mathbf{A} as shown in fig.2.1 is obtained. Now introducing a new operational sign " \otimes ", the new point-vector \mathbf{a} can be expressed as

$$\mathbf{a} = (\varepsilon\omega) \otimes \mathbf{A} \quad (2.1)$$

The expression (2.1) is referred to as the expression for the rotation of a vector.

With the view of fig.2.1, we obtain

$$\begin{aligned} \mathbf{a} &= (\varepsilon\omega) \otimes \mathbf{A} \\ &= \vec{OB} \\ &= \vec{OE} + \vec{ED} + \vec{DB} \end{aligned}$$

Due to

$$\begin{aligned} \vec{OE} &= \frac{|\vec{OE}|}{|\vec{OA}|} \vec{OA} = \frac{|\vec{CD}|}{|\vec{CA}|} \mathbf{A} \\ &= \frac{|\vec{CD}|}{|\vec{CB}|} \mathbf{A} = \cos \varepsilon \mathbf{A} \end{aligned}$$

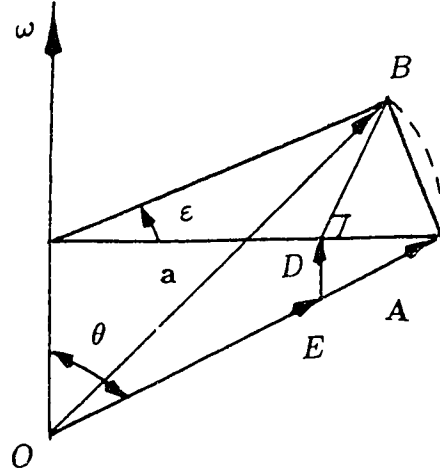


Figure 2.1: Rotation of a vector

$$\begin{aligned}
 \vec{ED} &= \frac{|\vec{ED}|}{|\vec{OC}|} |\vec{OC}| \omega = \frac{|\vec{DA}|}{|\vec{CA}|} (\omega \cdot \mathbf{A}) \omega \\
 &= \frac{|\vec{CA} - \vec{CD}|}{|\vec{CA}|} (\omega \cdot \mathbf{A}) \omega = (1 - \frac{|\vec{CD}|}{|\vec{CB}|}) (\omega \cdot \mathbf{A}) \omega \\
 &= (1 - \cos \varepsilon) (\omega \cdot \mathbf{A}) \omega
 \end{aligned}$$

$$\begin{aligned}
 \vec{DB} &= |\vec{DB}| \frac{\omega \times \mathbf{A}}{|\omega \times \mathbf{A}|} = |\vec{CB}| \sin \varepsilon \frac{\omega \times \mathbf{A}}{|\omega \times \mathbf{A}| \sin \theta} \\
 &= |\vec{CA}| \sin \varepsilon \frac{\omega \times \mathbf{A}}{|\omega \times \mathbf{A}|} = \sin \varepsilon (\omega \times \mathbf{A})
 \end{aligned}$$

Therefore, the expression for the rotation of a vector is of the form

$$\begin{aligned}
 \mathbf{a} &= (\varepsilon \omega) \otimes \mathbf{A} \\
 &= \cos \varepsilon \mathbf{A} + (1 - \cos \varepsilon) (\omega \cdot \mathbf{A}) \omega + \sin \varepsilon \omega \times \mathbf{A}
 \end{aligned} \tag{2.2}$$

2.1.2 Combination of Successive Rotations

Suppose that a rigid body rotates first about an axis ω_1 through an angle θ_1 and then about ω_2 through θ_2 , the origin being the same. It is possible to obtain the final orientation of the rigid body by a single rotation, i.e., by simply rotating the body about an axis ω through θ with the same origin. This fact means that two successive rotations with a common origin can be combined into a single rotation with the same origin, i.e.,

$$(\theta_2 \omega_2) \otimes [(\theta_1 \omega_1) \otimes \mathbf{R}] = (\theta \omega) \otimes \mathbf{R} \tag{2.3}$$

with \mathbf{R} being an arbitrary point-vector as shown in fig. 2.2.

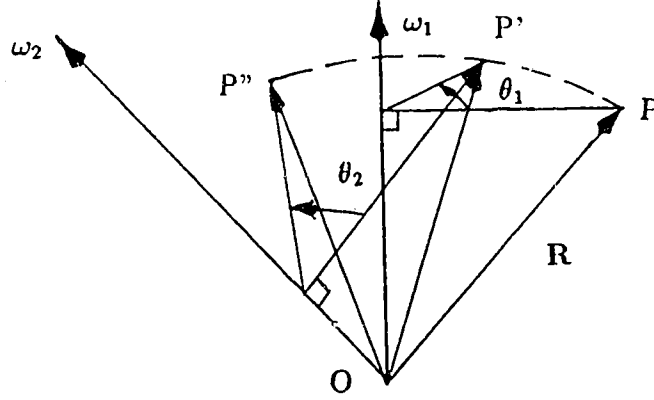


Figure 2.2: Successive rotations about two axes

Equation (2.3) will lead to the following two equations, expressing θ , ω in terms of θ_1 , ω_1 , θ_2 , ω_2 .

$$\tan \frac{\theta}{2} = \frac{\sqrt{1 - [\cos \frac{\theta_1}{2} \cos \frac{\theta_2}{2} - \sin \frac{\theta_1}{2} \sin \frac{\theta_2}{2} (\omega_1 \cdot \omega_2)]^2}}{[\cos \frac{\theta_1}{2} \cos \frac{\theta_2}{2} - \sin \frac{\theta_1}{2} \sin \frac{\theta_2}{2} (\omega_1 \cdot \omega_2)]} \quad (2.4)$$

$$\omega = \frac{\sin \frac{\theta_1}{2} \cos \frac{\theta_2}{2} \omega_1 + \cos \frac{\theta_1}{2} \sin \frac{\theta_2}{2} \omega_2 - \sin \frac{\theta_1}{2} \sin \frac{\theta_2}{2} (\omega_1 \times \omega_2)}{\sqrt{1 - [\cos \frac{\theta_1}{2} \cos \frac{\theta_2}{2} - \sin \frac{\theta_1}{2} \sin \frac{\theta_2}{2} (\omega_1 \cdot \omega_2)]^2}} \quad (2.5)$$

2.1.3 Sequence-Reciprocation of Successive Rotations

Suppose a rigid body rotates about ω_1 as an axis through an angle θ_1 first, and then rotates about an axis ω_2 through an angle θ_2 , both axes sharing the same origin O. The final point-vector, with respect to O, of any point \mathbf{R} on the rigid body after rotation will be $(\theta_2 \omega_2) \otimes [(\theta_1 \omega_1) \otimes \mathbf{R}]$. This point-vector can be alternatively obtained through an equivalent pair of rotations in the opposite order, that is, first, rotate about an axis ω_2 through an angle θ_2 , and secondly, rotate about an axis $(\theta_2 \omega_2) \otimes \omega_1$ through an angle θ_1 , i.e.,

$$(\theta_2 \omega_2) \otimes [(\theta_1 \omega_1) \otimes \mathbf{R}] = \{\theta_1 [(\theta_2 \omega_2) \otimes \omega_1]\} \otimes [(\theta_2 \omega_2) \otimes \mathbf{R}] \quad (2.6)$$

Alternatively, first, rotate about an axis $(-\theta_1 \omega_1) \otimes \omega_2$ through an angle θ_2 , and then, rotate about an axis ω_1 through an angle θ_1 , i.e.,

$$(\theta_2 \omega_2) \otimes [(\theta_1 \omega_1) \otimes \mathbf{R}] = (\theta_1 \omega_1) \otimes \{ \{ \theta_2 [(-\theta_1 \omega_1) \otimes \omega_2] \} \otimes \mathbf{R} \} \quad (2.7)$$

where \mathbf{R} is any point-vector.

2.1.4 Resolution of a Rotation

A rotation about ω through θ can be resolved into three successive rotations about two prescribed mutually perpendicular axes of rotation, ω_1 and ω_0 ($\omega_1 \cdot \omega_0 = 0$), with a common origin on the axis ω as follows:

$$(\theta \omega) \otimes \mathbf{R} = (\theta_1 \omega_1) \otimes \{ (\theta_0 \omega_0) \otimes [(\theta_2 \omega_1) \otimes \mathbf{R}] \} \quad (2.8)$$

with \mathbf{R} being any point-vector, and $\theta_0, \theta_1, \theta_2$ being determined by the following equations

$$\theta_0 = 2 \arcsin \{ \sqrt{[1 - (\omega \cdot \omega_1)^2]} \sin \frac{\theta}{2} \} \quad (2.9)$$

$$(0 \leq \theta_0 \leq \pi)$$

$$\left. \begin{array}{ll} (if & \omega \cdot \omega_0 \geq 0) \\ \theta_1 = \delta_1 + \delta_2 & or \\ \theta_2 = \delta_1 - \delta_2 & or \end{array} \right\} \begin{array}{ll} (if & \omega \cdot \omega_0 < 0) \\ \pi + \delta_1 - \delta_2 & \\ \delta_1 + \delta_2 - \pi & \end{array} \quad (2.10)$$

where

$$\left. \begin{array}{l} \delta_1 = \arctan[(\omega \cdot \omega_1) \tan \frac{\theta}{2}] \\ \quad (-\frac{\pi}{2} \leq \delta_1 \leq \frac{\pi}{2}) \\ \delta_2 = \arctan[\frac{\omega \cdot (\omega_1 \times \omega_0)}{(\omega \cdot \omega_0)}] \\ \quad (-\frac{\pi}{2} \leq \delta_2 \leq \frac{\pi}{2}) \end{array} \right\} \quad (2.11)$$

2.2 Introduction to Differential Geometry

2.2.1 The Expression for a Boundary Surface

Consider a coordinate system, say, $O-\mathbf{i}, \mathbf{j}, \mathbf{k}$. A boundary surface can be expressed in following two forms.

1. Functional Form.

Assume the coordinates of any point on the boundary surface are x, y, z . Then the boundary surface equation can be of the form

$$F(x, y, z) = 0 \quad (2.12)$$

2. Parametric Form.

Assume a point-vector, relative to the origin O , of any point on the boundary surface be \mathbf{R} , and let u, v be two parametric variables. Then the boundary surface can be expressed in the following parametric form

$$\mathbf{R}(u, v) = x(u, v)\mathbf{i} + y(u, v)\mathbf{j} + z(u, v)\mathbf{k} \quad (2.13)$$

2.2.2 The Unit Vector Normal to a Boundary Surface at an Arbitrary Point

The vector $\frac{\partial \mathbf{R}}{\partial u}$ is tangential to the curve $v = \text{const.}$ at the point \mathbf{R} ; for its direction is that of the displacement $d\mathbf{R}$ due to a variation du in the first parameter only. We take the positive direction along the parametric curve $v = \text{const.}$ as that for which u increases. This is the direction of the vector $\frac{\partial \mathbf{R}}{\partial u}$. Similarly $\frac{\partial \mathbf{R}}{\partial v}$ is tangential to the curve $u = \text{const.}$ in the positive sense, which corresponds to increase of v . The normal to the boundary surface at any point is perpendicular to every tangent line through that point, and is therefore perpendicular to each of the vectors $\frac{\partial \mathbf{R}}{\partial u}$ and $\frac{\partial \mathbf{R}}{\partial v}$. The unit normal to the boundary surface is therefore of the form

$$\begin{aligned} \mathbf{N}(u, v) &= \pm \frac{\frac{\partial \mathbf{R}}{\partial u} \times \frac{\partial \mathbf{R}}{\partial v}}{|\frac{\partial \mathbf{R}}{\partial u} \times \frac{\partial \mathbf{R}}{\partial v}|} \\ &= A\mathbf{i} + B\mathbf{j} + C\mathbf{k} \end{aligned} \quad (2.14)$$

where by substituting the expression (2.13) into the expression above, it follows that

$$\left. \begin{aligned} A &= \frac{1}{Q} \left(\frac{\partial y}{\partial u} \frac{\partial z}{\partial v} - \frac{\partial y}{\partial v} \frac{\partial z}{\partial u} \right) \\ B &= \frac{1}{Q} \left(\frac{\partial z}{\partial u} \frac{\partial x}{\partial v} - \frac{\partial z}{\partial v} \frac{\partial x}{\partial u} \right) \\ C &= \frac{1}{Q} \left(\frac{\partial x}{\partial u} \frac{\partial y}{\partial v} - \frac{\partial x}{\partial v} \frac{\partial y}{\partial u} \right) \end{aligned} \right\} \quad (2.15)$$

where

$$Q = \pm \sqrt{\left(\frac{\partial y}{\partial u} \frac{\partial z}{\partial v} - \frac{\partial y}{\partial v} \frac{\partial z}{\partial u}\right)^2 + \left(\frac{\partial z}{\partial u} \frac{\partial x}{\partial v} - \frac{\partial z}{\partial v} \frac{\partial x}{\partial u}\right)^2 + \left(\frac{\partial x}{\partial u} \frac{\partial y}{\partial v} - \frac{\partial x}{\partial v} \frac{\partial y}{\partial u}\right)^2}$$

The sign " \pm " can be chosen so that the positive direction of the unit normal points from the body to the space.

2.2.3 Curvature of a Surface

1. Definition.

Let \mathbf{R} be the position vector on a surface of any point P and \mathbf{N} the unit normal there. Let $\mathbf{R} + d\mathbf{R}$ be an adjacent point P' in any direction τ on the surface from the point P, and $\mathbf{N} + (d\mathbf{N})_\tau$ the unit normal at this point, and ds the length of the displacement $d\mathbf{R}$ from point P to P' along the direction τ . The limit vector $(\frac{d\mathbf{N}}{ds})_\tau$ when ds tends to zero is defined as the curvature of the surface along the direction τ at that point.

2. Expression.

Since \mathbf{N} is a vector of constant length, its first derivatives are perpendicular to \mathbf{N} and therefore tangential to the surface. $(\frac{d\mathbf{N}}{ds})_\tau$ may be expressed in the form

$$(\frac{d\mathbf{N}}{ds})_\tau = K_\tau \tau + G_\tau (\mathbf{N} \times \tau) \quad (2.16)$$

2.2.4 Normal Curvature

The component K_τ in the direction τ of curvature $(\frac{d\mathbf{N}}{ds})_\tau$ is defined as the normal curvature of the surface along the direction τ at the point P.

2.2.5 Torsional Curvature

The projection of the curvature $(\frac{d\mathbf{N}}{ds})_\tau$ in the direction $\mathbf{N} \times \tau$ is defined as the torsional curvature G_τ of the surface along the direction τ at the point P.

2.2.6 Geometric Angular Velocity of a Surface

Due to $(\frac{d\mathbf{N}}{ds})_\tau \cdot \mathbf{N} = 0$, $(\frac{d\mathbf{N}}{ds})_\tau$ can be considered as the virtual linear velocity formed by the end point of vector \mathbf{N} rotating with the geometric angular velocity Ω_τ (here, the geometric parameter s can be regarded as the time parameter); that is,

$$(\frac{d\mathbf{N}}{ds})_\tau = \Omega_\tau \times \mathbf{N} \quad (2.17)$$

Since any component of Ω in the direction \mathbf{N} does not have any effect on the value of the virtual linear velocity $\Omega_\tau \times \mathbf{N}$, Ω_τ could be assumed to lie on the tangent plane through the point P, that is,

$$\Omega_\tau \cdot \mathbf{N} = 0 \quad (2.18)$$

Forming the vector products of both sides of equation (2.17) with \mathbf{N} respectively and using equation (2.16), (2.18), it follows that

$$\Omega_\tau = K_\tau(\mathbf{N} \times \tau) - G_\tau \tau \quad (2.19)$$

2.2.7 Relation of Torsional Curvatures Between Two Mutually Perpendicular Directions

Select arbitrarily two mutually perpendicular unit vectors \mathbf{p} , \mathbf{q} on the tangent plane through any regular point of a surface, that is,

$$\mathbf{p} \cdot \mathbf{N} = 0, \mathbf{q} \cdot \mathbf{N} = 0, \mathbf{p} \cdot \mathbf{q} = 0$$

Without any loss of generality, let \mathbf{p} , after rotating about \mathbf{N} an angle $\frac{\pi}{2}$, reach \mathbf{q} , that is, $\mathbf{p} \times \mathbf{q} = \mathbf{N}$.

It can be verified that the torsional curvature G_p on the direction \mathbf{p} equals the negative value of the torsional curvature G_q on the direction \mathbf{q} , that is,

$$G_p = -G_q \quad (2.20)$$

Proof:

First of all, it is always possible to perform such a transformation of parametric variables of the parametric expression (2.13) for a boundary surface

$$\left. \begin{aligned} u &= u(p, q) \\ v &= v(p, q) \end{aligned} \right\} \quad (2.21)$$

such that the parametric expression $\mathbf{R} = \mathbf{R}(p, q)$ for the boundary surface after the transformation satisfies the following requirement at the corresponding point of the surface,

$$\left. \begin{aligned} \mathbf{p} &= \frac{\partial \mathbf{R}}{\partial p} \\ \mathbf{q} &= \frac{\partial \mathbf{R}}{\partial q} \end{aligned} \right\} \quad (2.22)$$

Where p and q are arc lengths of the surface in directions \mathbf{p} and \mathbf{q} respectively.

With the aid of expression (2.22), and taking into account $\mathbf{N} = \mathbf{p} \times \mathbf{q}$, we obtain

$$\mathbf{N} = \mathbf{p} \times \mathbf{q} = \frac{\partial \mathbf{R}}{\partial p} \times \frac{\partial \mathbf{R}}{\partial q} \quad (2.23)$$

Consequently,

$$\begin{aligned} \left(\frac{d\mathbf{N}}{ds}\right)_{\mathbf{p}} &= \frac{\partial \mathbf{N}}{\partial p} = \frac{\partial^2 \mathbf{R}}{\partial p^2} \times \frac{\partial \mathbf{R}}{\partial q} + \frac{\partial \mathbf{R}}{\partial p} \times \frac{\partial^2 \mathbf{R}}{\partial p \partial q} \\ &= \frac{\partial^2 \mathbf{R}}{\partial p^2} \times \mathbf{q} + \mathbf{p} \times \frac{\partial^2 \mathbf{R}}{\partial p \partial q} \end{aligned}$$

And

$$\begin{aligned} \left(\frac{d\mathbf{N}}{ds}\right)_{\mathbf{q}} &= \frac{\partial \mathbf{N}}{\partial q} = \frac{\partial^2 \mathbf{R}}{\partial q \partial p} \times \frac{\partial \mathbf{R}}{\partial q} + \frac{\partial \mathbf{R}}{\partial p} \times \frac{\partial^2 \mathbf{R}}{\partial q^2} \\ &= \frac{\partial^2 \mathbf{R}}{\partial q \partial p} \times \mathbf{q} + \mathbf{p} \times \frac{\partial^2 \mathbf{R}}{\partial q^2} \end{aligned}$$

With the aid of above two expressions and expression (2.16), consequently,

$$\begin{aligned} G_p &= \left(\frac{d\mathbf{N}}{ds}\right)_{\mathbf{p}} \cdot (\mathbf{N} \times \mathbf{p}) = \left(\mathbf{p} \times \frac{\partial^2 \mathbf{R}}{\partial p \partial q}\right) \cdot (\mathbf{N} \times \mathbf{p}) \\ &= -\frac{\partial^2 \mathbf{R}}{\partial p \partial q} \cdot \mathbf{N}, \end{aligned}$$

And

$$\begin{aligned}
G_q &= \left(\frac{d\mathbf{N}}{ds}\right)_q \cdot (\mathbf{N} \times \mathbf{q}) = \left(\frac{\partial^2 \mathbf{R}}{\partial q \partial p} \times \mathbf{q}\right) \cdot (\mathbf{N} \times \mathbf{q}) \\
&= \frac{\partial^2 \mathbf{R}}{\partial q \partial p} \cdot \mathbf{N}.
\end{aligned}$$

Since \mathbf{R} represents a regular point of the surface, $\frac{\partial^2 \mathbf{R}}{\partial p \partial q} = \frac{\partial^2 \mathbf{R}}{\partial q \partial p}$, we conclude from foregoing two expressions

$$G_p = -G_q$$

In agreement with the expression (2.20).

2.2.8 Relations of Normal and Torsional Curvatures Between Different Tangential Directions

Suppose that on the tangential plane through a point P there are two pairs of mutually perpendicular unit tangential vectors \mathbf{u} , $\mathbf{v} = \mathbf{N} \times \mathbf{u}$ and \mathbf{t} , $\mathbf{q} = \mathbf{N} \times \mathbf{t}$. If the angle through which \mathbf{u} rotates about \mathbf{N} as an axis to \mathbf{t} is θ_{ut} , then it follows that, as shown in Figure 2.3,

$$\begin{aligned}
\mathbf{u} &= [(-\theta_{ut})\mathbf{N}] \otimes \mathbf{t} = \cos \theta_{ut} \mathbf{t} - \sin \theta_{ut} \mathbf{q} \\
\mathbf{v} &= [(\frac{\pi}{2} - \theta_{ut})\mathbf{N}] \otimes \mathbf{t} = \sin \theta_{ut} \mathbf{t} + \cos \theta_{ut} \mathbf{q}
\end{aligned} \tag{2.24}$$

Let the normal curvatures along directions \mathbf{u} , \mathbf{v} , \mathbf{t} , be K_u , K_v , K_t and the torsional curvatures G_u , G_v , G_t . Since \mathbf{u} , \mathbf{v} are perpendicular to each other, from the equation (2.20), then $G_v = -G_u$.

Now suppose that after a small displacement ds of a point P in the direction \mathbf{t} to point P' shown in fig. 2.3, the increment of the unit normal of point P' with respect to point P is $(\Delta \mathbf{N})_{P-P'}$, in virtue of (2.16), approximating to the first order infinitesimal, $(\Delta \mathbf{N})_{P-P'}$ may be given by

$$(\Delta \mathbf{N})_{P-P'} = \left(\frac{d\mathbf{N}}{ds}\right)_t ds = (K_t \mathbf{t} + G_t \mathbf{q}) ds$$

On the other hand, $(\Delta \mathbf{N})_{P-P'}$ can be obtained by summing increment $(\Delta \mathbf{N})_{P-P_1}$ of small displacement $\cos \theta_{ut} ds$ of point P on direction \mathbf{u} to point P_1 and the increment

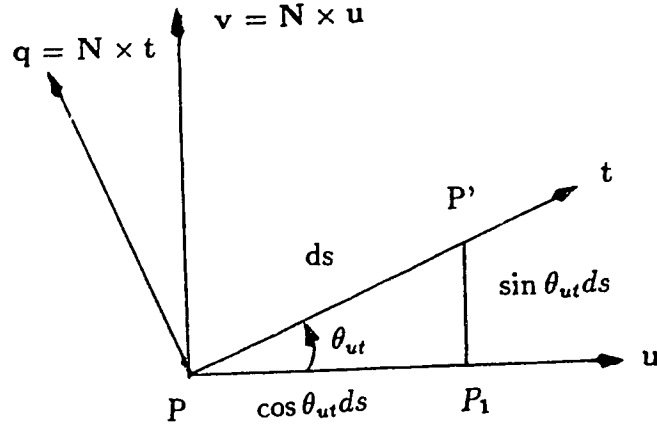


Figure 2.3: Two mutually perpendicular tangential directions

$(\Delta N)_{P_1-P'}$ of the small displacement $\sin \theta_{ut} ds$ of point P_1 on the direction \mathbf{v} to point P' , as shown in fig. 2.3, that is,

$$(\Delta N)_{P-P'} = (\Delta N)_{P-P_1} + (\Delta N)_{P_1-P'}$$

in virtue of expression (2.16)

$$(\Delta N)_{P-P_1} = \left(\frac{dN}{ds}\right)_u \cos \theta_{ut} ds = (K_u \mathbf{u} + G_u \mathbf{v}) \cos \theta_{ut} ds$$

and

$$(\Delta N)_{P_1-P'} = \left(\frac{dN}{ds}\right)_v \sin \theta_{ut} ds = (K_v \mathbf{v} + G_v \mathbf{u}) \sin \theta_{ut} ds$$

It follows that

$$(K_t \mathbf{t} + G_t \mathbf{q}) ds = [(K_u \mathbf{u} + G_u \mathbf{v}) \cos \theta_{ut} + (K_v \mathbf{v} + G_v \mathbf{u}) \sin \theta_{ut}] ds$$

Dividing each side of the expression above by ds and substituting from expression (2.24), the relations of the normal and torsional curvatures between different tangential directions therefore are expressed as

$$K_t = K_u \cos^2 \theta_{ut} + K_v \sin^2 \theta_{ut} + 2G_u \sin \theta_{ut} \cos \theta_{ut} \quad (2.25)$$

and

$$G_t = -(K_u - K_v) \sin \theta_{ut} \cos \theta_{ut} + G_u (\cos^2 \theta_{ut} - \sin^2 \theta_{ut}) \quad (2.26)$$

2.2.9 Conjugate Normal and Torsional Curvatures

In order to facilitate derivation of expressions and calculations in subsequent sections, we can express the curvature $(\frac{d\mathbf{N}}{ds})_\tau$ of a surface in the following form.

1. Definition.

If the curvature $(\frac{d\mathbf{N}}{ds})_\tau$ of a surface is resolved in the mutually perpendicular directions τ and $\tau \times \mathbf{N}$, the projection K'_τ of $(\frac{d\mathbf{N}}{ds})_\tau$ in the direction τ is defined as the conjugate normal curvature in the direction τ , and similarly the projection G'_τ of $(\frac{d\mathbf{N}}{ds})_\tau$ in the direction $\tau \times \mathbf{N}$ is defined as the conjugate torsional curvature in the direction τ , that is,

$$(\frac{d\mathbf{N}}{ds})_\tau = K'_\tau \tau + G'_\tau (\tau \times \mathbf{N}) \quad (2.27)$$

2. Relations of Conjugate Normal and Torsional Curvatures with Respect to Normal and Torsional Curvatures.

On comparing expressions (2.16) with (2.26), it follows that

$$\left. \begin{aligned} K'_\tau &= K_\tau \\ G'_\tau &= -G_\tau \end{aligned} \right\} \quad (2.28)$$

It follows from the above expression that under the same tangential direction, the conjugate normal curvature is identical to the normal curvature, and the conjugate torsional curvature is identical to the torsional curvature in magnitude and opposite in sign.

2.2.10 Relative Curvature, Relative Normal and Torsional Curvatures

If two surfaces, S_1 and S_2 , tangentially touch each other at a point P and let their outward pointing unit normals to surfaces S_1 and S_2 at the point P of common contact be \mathbf{N}_1 and \mathbf{N}_2 respectively, thus it follows that

$$\mathbf{N}_2 = -\mathbf{N}_1 \quad (2.29)$$

Next suppose that in any tangent direction τ , the curvature of surface S_1 is $(\frac{d\mathbf{N}_1}{ds})_\tau$ and the curvature of surface S_2 is $(\frac{d\mathbf{N}_2}{ds})_\tau$, the relative curvature of S_1 to S_2 at point P in direction τ is defined as

$$\left(\frac{d\bar{\mathbf{N}}}{ds}\right)_\tau = \left(\frac{d\mathbf{N}_1}{ds}\right)_\tau + \left(\frac{d\mathbf{N}_2}{ds}\right)_\tau \quad (2.30)$$

Using expression (2.16), we have

$$\left(\frac{d\mathbf{N}_1}{ds}\right)_\tau = K_{1\tau}\tau + G_{1\tau}(\mathbf{N}_1 \times \tau) \quad (2.31)$$

and with the aid of expressions (2.27), (2.29), it follows that

$$\begin{aligned} \left(\frac{d\mathbf{N}_2}{ds}\right)_\tau &= K'_{2\tau}\tau + G'_{2\tau}(\tau \times \mathbf{N}_2) \\ &= K'_{2\tau}\tau + G'_{2\tau}(\mathbf{N}_1 \times \tau) \end{aligned} \quad (2.32)$$

The substitution of above two expressions in expression (2.30) yields

$$\left(\frac{d\bar{\mathbf{N}}}{ds}\right)_\tau = (K_{1\tau} + K'_{2\tau})\tau + (G_{1\tau} + G'_{2\tau})(\mathbf{N}_1 \times \tau) \quad (2.33)$$

The relative normal curvature \bar{K}_τ and the relative torsional curvature \bar{G}_τ of surfaces S_1 and S_2 at point P of common contact in the direction τ are defined respectively as

$$\left. \begin{aligned} \bar{K}_\tau &= K_{1\tau} + K'_{2\tau} \\ \bar{G}_\tau &= G_{1\tau} + G'_{2\tau} \end{aligned} \right\} \quad (2.34)$$

Consequently, expression (2.33) may be expressed in the form.

$$\left(\frac{d\bar{\mathbf{N}}}{ds}\right)_\tau = \bar{K}_\tau\tau + \bar{G}_\tau(\mathbf{N} \times \tau) \quad (2.35)$$

The relative curvature $\left(\frac{d\bar{\mathbf{N}}}{ds}\right)_\tau$ can be represented as the virtual linear velocity formed by the end point of vector \mathbf{N}_1 rotating with the relative geometric angular velocity $\bar{\boldsymbol{\Omega}}_\tau$, that is,

$$\left(\frac{d\bar{\mathbf{N}}}{ds}\right)_\tau = \bar{\boldsymbol{\Omega}}_\tau \times \mathbf{N}_1 \quad (2.36)$$

in which

$$\begin{aligned} \bar{\boldsymbol{\Omega}}_\tau &= \bar{K}_\tau(\mathbf{N}_1 \times \tau) - \bar{G}_\tau\tau \\ &= \boldsymbol{\Omega}_{1\tau} - \boldsymbol{\Omega}_{2\tau} \end{aligned} \quad (2.37)$$

2.2.11 Relations Between Relative Normal and Torsional Curvatures in Different Tangential Directions

Let the relative normal curvature and the relative torsional curvature in any direction \mathbf{t} be \overline{K}_t and \overline{G}_t and \mathbf{u}, \mathbf{v} be two mutually perpendicular tangential directions in the common tangential plane of S_1, S_2 , and $\mathbf{v} = \mathbf{N}_1 \times \mathbf{u}$. Let the normal and torsional curvatures of S_1 in directions \mathbf{u}, \mathbf{v} be K_{1u}, K_{1v} and $G_{1u} = -G_{1v}$ and the conjugate normal and torsional curvatures of S_2 in directions \mathbf{u}, \mathbf{v} be K'_{2u}, K'_{2v} and $G'_{2u} = -G'_{2v}$. The relative normal and torsional curvatures in directions \mathbf{u}, \mathbf{v} are then in the form

$$\left. \begin{aligned} \overline{K}_u &= K_{1u} + K'_{2u} \\ \overline{K}_v &= K_{1v} + K'_{2v} \\ \overline{G}_u &= G_{1u} + G'_{2u} = -(G_{1v} + G'_{2v}) = -\overline{G}_v \end{aligned} \right\} \quad (2.38)$$

Next, suppose that the angle of \mathbf{u} rotating about \mathbf{N}_1 to \mathbf{t} is θ_{ut} , due to $\mathbf{N}_2 = -\mathbf{N}_1$, the angle of \mathbf{u} rotating about \mathbf{N}_2 to \mathbf{t} is $(-\theta_{ut})$. Consequently, by virtue of expressions (2.25), (2.26) and (2.27), we obtain

$$\left. \begin{aligned} K_{1t} &= K_{1u} \cos^2 \theta_{ut} + K_{1v} \sin^2 \theta_{ut} + 2G_{1u} \sin \theta_{ut} \cos \theta_{ut} \\ G_{1t} &= -(K_{1u} - K_{1v}) \sin \theta_{ut} \cos \theta_{ut} + G_{1u} (\cos^2 \theta_{ut} - \sin^2 \theta_{ut}) \\ K'_{2t} &= K'_{2u} \cos^2 (-\theta_{ut}) + K'_{2v} \sin^2 (-\theta_{ut}) + 2(-G'_{2v}) \sin(-\theta_{ut}) \cos(-\theta_{ut}) \\ &= K'_{2u} \cos^2 \theta_{ut} + K'_{2v} \sin^2 \theta_{ut} + 2G'_{2v} \sin \theta_{ut} \cos \theta_{ut} \\ G'_{2t} &= (K'_{2u} - K'_{2v}) \sin(-\theta_{ut}) \cos(-\theta_{ut}) \\ &\quad - (-G'_{2u}) [\cos^2(-\theta_{ut}) - \sin^2(-\theta_{ut})] \\ &= -(K'_{2u} - K'_{2v}) \sin \theta_{ut} \cos \theta_{ut} + G'_{2u} (\cos^2 \theta_{ut} - \sin^2 \theta_{ut}) \end{aligned} \right\} \quad (2.39)$$

With the aid of expressions (2.34) and (2.38), the relative normal curvature \overline{K}_t and the relative torsional curvature \overline{G}_t in direction \mathbf{t} are given by

$$\left. \begin{aligned} \overline{K}_t &= K_{1t} + K'_{2t} \\ &= \overline{K}_u \cos^2 \theta_{ut} + \overline{K}_v \sin^2 \theta_{ut} + 2\overline{G}_u \sin \theta_{ut} \cos \theta_{ut} \\ \overline{G}_t &= G_{1t} + G'_{2t} \\ &= -(\overline{K}_u - \overline{K}_v) \sin \theta_{ut} \cos \theta_{ut} + \overline{G}_u (\cos^2 \theta_{ut} - \sin^2 \theta_{ut}) \end{aligned} \right\} \quad (2.40)$$

2.2.12 Compatible Equation of Surface Curvatures

With the aid of expressions (2.25) and (2.26), it follows that

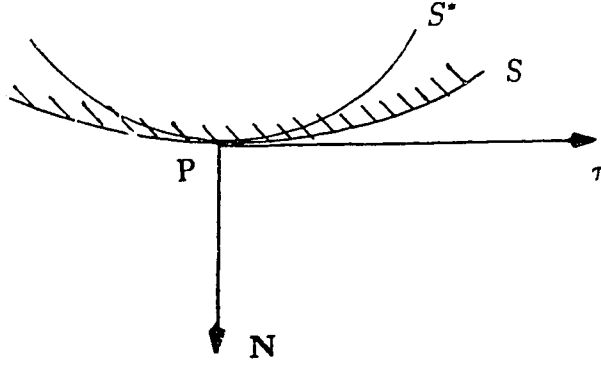


Figure 2.4: Fundamental surface and substituting surface

$$\left. \begin{aligned} (K_t - K_u) &= [-(K_u - K_v) \sin \theta_{ut} + 2G_u \cos \theta_{ut}] \sin \theta_{ut} \\ (G_u + G_t) &= [-(K_u - K_v) \sin \theta_{ut} + 2G_u \cos \theta_{ut}] \cos \theta_{ut} \end{aligned} \right\} \quad (2.41)$$

Provided that $\tan \theta_{ut} \neq \frac{2G_u}{(K_u - K_v)}$, i.e., $-(K_u - K_v) \sin \theta_{ut} + 2G_u \cos \theta_{ut} \neq 0$, expression (2.41) yields

$$\tan \theta_{ut} = \frac{K_t - K_u}{G_u + G_t} \quad (2.42)$$

Expression (2.42) is referred to as the harmonic equation of the surface curvature.

2.2.13 Curvature Difference

1. Fundamental Surface and Substituting Surface.

Given a boundary surface S , select any point P on S , and construct another boundary surface S^* tangent to S at point P , as shown in fig. 2.4. Then, S is called the fundamental boundary surface, P is the fundamental point for substitution, S^* is the substituting boundary surface. Here, S and S^* have the same unit normal at point P .

2. Definition.

At the fundamental point P for substitution, along an arbitrary tangential direction τ , the difference vector between the surface curvature $(\frac{dN}{ds})_\tau^*$ of the substituting boundary surface and the surface curvature $(\frac{dN}{ds})_\tau$ of the fundamental boundary surface is defined as curvature difference $\Delta(\frac{dN}{ds})_\tau$ at point P of S , S^* in direction τ , that is,

$$\Delta(\frac{dN}{ds})_\tau = (\frac{dN}{ds})_\tau^* - (\frac{dN}{ds})_\tau \quad (2.43)$$

3. Normal Curvature Difference and Torsional Curvature Difference .

Suppose normal curvatures at point P of S, S^* in direction τ are K_τ , K_τ^* , and torsional curvatures G_τ , G_τ^* , then,

$$\begin{aligned} \left(\frac{d\mathbf{N}}{ds}\right)_\tau &= K_\tau \tau + G_\tau (\mathbf{N} \times \tau) \\ \left(\frac{d\mathbf{N}}{ds}\right)_\tau^* &= K_\tau^* \tau + G_\tau^* (\mathbf{N} \times \tau) \end{aligned}$$

Substituting in the expression (2.43)

$$\begin{aligned} \Delta\left(\frac{d\mathbf{N}}{ds}\right)_\tau &= (K_\tau^* - K_\tau)\tau + (G_\tau^* - G_\tau)(\mathbf{N} \times \tau) \\ &= \Delta K_\tau \tau + \Delta G_\tau (\mathbf{N} \times \tau) \end{aligned} \quad (2.44)$$

where ΔK_τ is defined as the normal curvature difference of S, S^* in the direction τ ; ΔG_τ as the torsional curvature difference of S, S^* in the direction τ ; and with the aid of expression (2.44), we obtain

$$\left. \begin{aligned} \Delta K_\tau &= K_\tau^* - K_\tau \\ \Delta G_\tau &= G_\tau^* - G_\tau \end{aligned} \right\} \quad (2.45)$$

2.2.14 Intersecting Curve

1. Definition.

The intersection of two boundary surfaces is called the intersecting curve.

2. Expressions for the Intersecting Curve.

(1) The functional expression:

The combination of the functional expressions for two surfaces, that is,

$$\left. \begin{aligned} \text{The first surface: } & F_I(x, y, z) = 0 \\ \text{The second surface: } & F_{II}(x, y, z) = 0 \end{aligned} \right\} \quad (2.46)$$

(2) Parametric expression:

$$\left. \begin{aligned} \text{The first surface: } & \mathbf{R} = \mathbf{R}_I(u, v) \\ \text{The second surface: } & \mathbf{R} = \mathbf{R}_{II}(q, t) \end{aligned} \right\} \quad (2.47)$$

Where u,v,q and t are parametric variables. Due to expressions (2.47), only one of the variables u,v,q and t is independent.

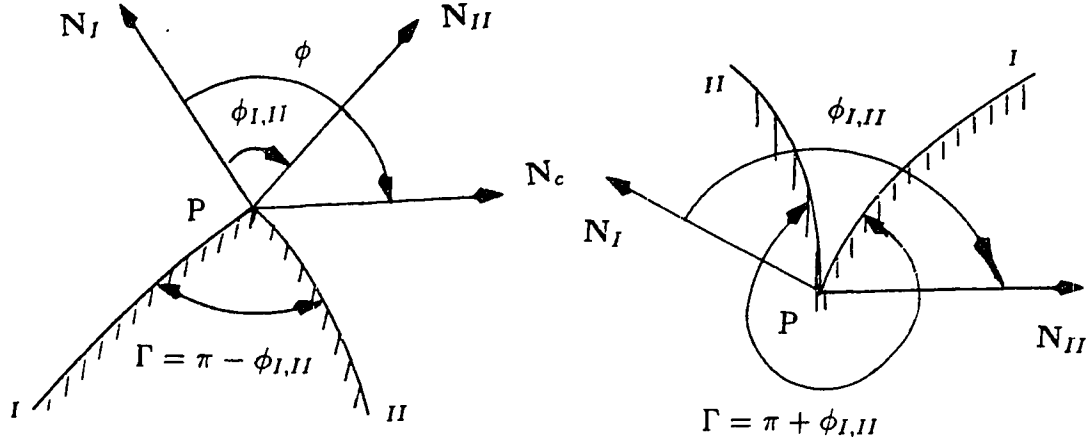


Figure 2.5: Unit normal and effective normal zone

2.2.15 The Unit Vector Tangent to the Intersecting Curve at Any Point

Suppose the unit normals to the first and second surfaces at any point P of the intersecting curve are, respectively, N_I and N_{II} , and if the first surface is chosen as the basic standard surface, the unit vector tangential to the intersecting curve at point P is perpendicular to both normals, and is therefore given by

$$\mathbf{w} = \frac{\mathbf{N}_I \times \mathbf{N}_{II}}{|\mathbf{N}_I \times \mathbf{N}_{II}|} \quad (2.48)$$

2.2.16 The Unit Normal to the Intersecting Curve at Any Point and the Effective Normal Zone

1. Definition.

Any unit vector at point P perpendicular to \mathbf{w} is defined as a unit normal N_c to the intersecting curve. If N_I is chosen as the initial unit normal vector, then any other unit normal vector N_c can be regarded as formed by rotation of N_I about \mathbf{w} an angle ϕ as shown in fig.2.5

$$\mathbf{N}_c = (\phi \mathbf{w}) \otimes \mathbf{N}_I \quad (2.49)$$

2. The Angle $\phi_{I,II}$.

The angle $\phi_{I,II}$ of rotation of \mathbf{N}_I about \mathbf{w} to \mathbf{N}_{II} can be found from expression (2.48),

$$0 < \phi_{I,II} < \pi \quad (2.50)$$

3. The Effective Normal Zone.

If the value of ϕ satisfies the condition

$$0 \leq \phi \leq \phi_{I,II} \quad (2.51)$$

then, the unit normal vector which is determined by expression (2.49) is referred to as the effective unit normal vector. The zone defined by $\phi_{I,II}$ is called the effective normal zone.

2.2.17 The Unit Principle Normal and Curvatures of the Intersecting Curve at Any Point

1. Definition.

Suppose the rate of change of the unit tangential vector to the intersecting curve at any point P with respect to the arc length s of this intersecting curve is $\frac{d\mathbf{w}}{ds}$, and the unit vector in the direction $\frac{d\mathbf{w}}{ds}$ is defined as the unit principle normal vector ξ at the point P of the intersecting curve, i.e.,

$$\xi = \frac{\frac{d\mathbf{w}}{ds}}{\left| \frac{d\mathbf{w}}{ds} \right|} \quad (2.52)$$

The magnitude of $\frac{d\mathbf{w}}{ds}$ is defined as the curvature k_c of the intersecting curve at the point P, i.e.,

$$k_c = \sqrt{\left(\frac{d\mathbf{w}}{ds} \right) \cdot \left(\frac{d\mathbf{w}}{ds} \right)} = \left| \frac{d\mathbf{w}}{ds} \right| \quad (2.53)$$

2. Derivation of an Expression for $\left(\frac{d\mathbf{w}}{ds} \right)$.

Use of the expression (2.48) gives

$$\begin{aligned} \frac{d\mathbf{w}}{ds} &= \frac{d}{ds} \left(\frac{\mathbf{N}_I \times \mathbf{N}_{II}}{|\mathbf{N}_I \times \mathbf{N}_{II}|} \right) \\ &= \frac{\left(\frac{d\mathbf{N}_I}{ds} \right) \times \mathbf{N}_{II}}{|\mathbf{N}_I \times \mathbf{N}_{II}|} + \frac{\mathbf{N}_I \times \left(\frac{d\mathbf{N}_{II}}{ds} \right)}{|\mathbf{N}_I \times \mathbf{N}_{II}|} \\ &\quad - \frac{\mathbf{w}}{|\mathbf{N}_I \times \mathbf{N}_{II}|} \frac{d}{ds} (|\mathbf{N}_I \times \mathbf{N}_{II}|) \end{aligned} \quad (2.54)$$

With the aid of the expression (2.16)

$$\left(\frac{d\mathbf{N}_I}{ds}\right)_{\mathbf{w}} = K_{Iw}\mathbf{w} + G_{Iw}(\mathbf{N}_I \times \mathbf{w}) \quad (2.55)$$

$$\left(\frac{d\mathbf{N}_{II}}{ds}\right)_{\mathbf{w}} = K_{IIw}\mathbf{w} + G_{IIw}(\mathbf{N}_{II} \times \mathbf{w}) \quad (2.56)$$

With the aid of expressions (2.16), (2.55) and (2.56)

$$\begin{aligned} \frac{d}{ds}(|\mathbf{N}_I \times \mathbf{N}_{II}|) &= \frac{d}{ds}[\sqrt{(\mathbf{N}_I \times \mathbf{N}_{II}) \cdot (\mathbf{N}_I \times \mathbf{N}_{II})}] \\ &= \frac{1}{2\sqrt{(\mathbf{N}_I \times \mathbf{N}_{II}) \cdot (\mathbf{N}_I \times \mathbf{N}_{II})}} \frac{d}{ds}[(\mathbf{N}_I \times \mathbf{N}_{II}) \cdot (\mathbf{N}_I \times \mathbf{N}_{II})] \\ &= \frac{\left\{ \left[\left(\frac{d\mathbf{N}_I}{ds}\right)_{\mathbf{w}} \times \mathbf{N}_{II} \right] + \left[\mathbf{N}_I \times \left(\frac{d\mathbf{N}_{II}}{ds}\right)_{\mathbf{w}} \right] \right\} \cdot (\mathbf{N}_I \times \mathbf{N}_{II})}{|\mathbf{N}_I \times \mathbf{N}_{II}|} \\ &= [\mathbf{w} \times \left(\frac{d\mathbf{N}_I}{ds}\right)_{\mathbf{w}}] \cdot \mathbf{N}_{II} + \mathbf{N}_I \cdot \left[\left(\frac{d\mathbf{N}_{II}}{ds}\right)_{\mathbf{w}} \times \mathbf{w}\right] \\ &= (G_{Iw} - G_{IIw})(\mathbf{N}_I \cdot \mathbf{N}_{II}) \end{aligned} \quad (2.57)$$

Substitution of expressions (2.55), (2.56) and (2.57) into (2.54) yields

$$\frac{d\mathbf{w}}{ds} = \frac{-K_{Iw}(\mathbf{N}_{II} \times \mathbf{w}) + K_{IIw}(\mathbf{N}_I \times \mathbf{w})}{|\mathbf{N}_I \times \mathbf{N}_{II}|} \quad (2.58)$$

Due to $|\mathbf{N}_I \times \mathbf{N}_{II}| = \sin \phi_{I,II}$, Then

$$\frac{d\mathbf{w}}{ds} = \frac{K_{IIw}(\mathbf{N}_I \times \mathbf{w}) - K_{Iw}(\mathbf{N}_{II} \times \mathbf{w})}{\sin \phi_{I,II}} \quad (2.59)$$

3. The Value of k_c .

Substitution of expression (2.59) into (2.53) leads to the curvature k_c of the intersecting curve

$$k_c = \sqrt{\frac{K_{Iw}^2 - 2K_{Iw}K_{IIw} \cos \phi_{I,II} + K_{IIw}^2}{\sin \phi_{I,II}}} \quad (2.60)$$

4. The Angle of Rotation of \mathbf{N}_I about \mathbf{w} as an Axis to ξ .

Substitution of expressions (2.53), (2.59) and (2.60) into (2.51) yields

$$\xi = \frac{K_{IIw}(\mathbf{N}_I \times \mathbf{w}) - K_{Iw}(\mathbf{N}_{II} \times \mathbf{w})}{\sqrt{K_{Iw}^2 - 2K_{Iw}K_{IIw} \cos \phi_{I,II} + K_{IIw}^2}} \quad (2.61)$$

With the aid of expression (2.61), we find angle $\phi_{I\xi}$

$$\left. \begin{aligned} \sin \phi_{I\xi} &= (\mathbf{N}_I \times \xi) \cdot \mathbf{w} \\ &= \frac{K_{Iw} \cos \phi_{I,II} - K_{IIw}}{\sqrt{K_{Iw}^2 - 2K_{Iw}K_{IIw} \cos \phi_{I,II} + K_{IIw}^2}} \\ \cos \phi_{I\xi} &= \mathbf{N}_I \cdot \xi \\ &= \frac{-K_{Iw} \sin \phi_{I,II}}{\sqrt{K_{Iw}^2 - 2K_{Iw}K_{IIw} \cos \phi_{I,II} + K_{IIw}^2}} \\ &= -\frac{K_{Iw}}{k_c} \end{aligned} \right\} \quad (2.62)$$

5. The Angle $\phi_{II\xi}$ of Rotation of \mathbf{N}_{II} about \mathbf{w} as an Axis to ξ .

Again, using expression (2.61), we find the angle $\phi_{II\xi}$

$$\left. \begin{aligned} \sin \phi_{II\xi} &= (\mathbf{N}_{II} \times \xi) \cdot \mathbf{w} \\ &= \frac{K_{Iw} - K_{IIw} \cos \phi_{I,II}}{\sqrt{K_{Iw}^2 - 2K_{Iw}K_{IIw} \cos \phi_{I,II} + K_{IIw}^2}} \\ \cos \phi_{II\xi} &= \mathbf{N}_{II} \cdot \xi \\ &= \frac{-K_{IIw} \sin \phi_{I,II}}{\sqrt{K_{Iw}^2 - 2K_{Iw}K_{IIw} \cos \phi_{I,II} + K_{IIw}^2}} \\ &= -\frac{K_{IIw}}{k_c} \end{aligned} \right\} \quad (2.63)$$

6. The Curvature Condition for a Curve Lying on the Surface.

Expressions (2.62) and (2.63) lead to

$$k_c = -\frac{K_{Iw}}{\cos \phi_{I\xi}} = -\frac{K_{IIw}}{\cos \phi_{II\xi}} = -\frac{K_{IIw}}{\cos(\phi_{I\xi} - \phi_{I,II})} \quad (2.64)$$

It can be concluded from expression (2.64) that the normal curvature K_w of a surface in the direction tangential to the intersecting curve is equal to the negative value of the product of the curvature of this curve and the cosine of angle $\phi_{N\xi}$ between the normal vector to the surface and the principle normal vector to the curve

$$K_w = -k_c \cos \phi_{N\xi} \quad (2.65)$$

Expression (2.65) is referred to as the curvature condition for a curve lying on the surface.

2.2.18 The Unit Binormal Vector to the Intersecting Curve at Any Point

The unit normal vector formed by the rotation of the unit principle normal about the unit tangential vector \mathbf{w} a right angle $\frac{\pi}{2}$ is defined as the unit binormal vector β to the intersecting curve at point P, that is,

$$\beta = \left(\frac{\pi}{2}\mathbf{w}\right) \otimes \xi = \mathbf{w} \times \xi \quad (2.66)$$

Substitution of expressions (2.61) into (2.66) yields

$$\beta = \frac{K_{IIw}\mathbf{N}_I - K_{Iw}\mathbf{N}_{II}}{\sqrt{K_{Iw}^2 - 2K_{Iw}K_{IIw}\cos\phi_{I,II} + K_{IIw}^2}} \quad (2.67)$$

2.2.19 The Torsional Curvature of the Intersecting Curve at Any Point

1. Definition.

Since the unit principle normal vector ξ is a unit vector, and then $\frac{d\xi}{ds} \cdot \xi = 0$, it follows that the derivative of ξ can have components in only the \mathbf{w} and β directions.

$$\frac{d\xi}{ds} = \left(\frac{d\xi}{ds} \cdot \mathbf{w}\right)\mathbf{w} + \left(\frac{d\xi}{ds} \cdot \beta\right)\beta$$

Since $\xi \cdot \mathbf{w} = 0$, we use expressions (2.52) and (2.53) to obtain

$$\frac{d\xi}{ds} \cdot \mathbf{w} = -\xi \cdot \frac{d\mathbf{w}}{ds} = -k_c$$

Combination of the two expressions above yields

$$\frac{d\xi}{ds} = -k_c\mathbf{w} + \left(\frac{d\xi}{ds} \cdot \beta\right)\beta \quad (2.68)$$

The projection of $\frac{d\xi}{ds}$ in direction β is defined as the torsional curvature κ_c of the intersecting curve, that is,

$$\kappa_c = \frac{d\xi}{ds} \cdot \beta \quad (2.69)$$

2. The Expression for the Calculation of κ_c .

Due to

$$\begin{aligned}\xi &= (\phi_{I\xi} \mathbf{w}) \otimes \mathbf{N}_I \\ &= \cos \phi_{I\xi} \mathbf{N}_I + \sin \phi_{I\xi} \mathbf{w} \times \mathbf{N}_I\end{aligned}\quad (2.70)$$

Consequently

$$\begin{aligned}\frac{d\xi}{ds} &= -(\sin \phi_{I\xi} \mathbf{N}_I + \cos \phi_{I\xi} \mathbf{N}_I \times \mathbf{w}) \frac{d\phi_{I\xi}}{ds} \\ &\quad + \cos \phi_{I\xi} \left(\frac{d\mathbf{N}_I}{ds} \right)_{\mathbf{w}} - \sin \phi_{I\xi} \left[\frac{d}{ds} (\mathbf{N}_I \times \mathbf{w}) \right]_{\mathbf{w}}\end{aligned}\quad (2.71)$$

Substitution of expression (2.70) into (2.66) yields

$$\beta = -(\sin \phi_{I\xi} \mathbf{N}_I + \cos \phi_{I\xi} \mathbf{N}_I \times \mathbf{w}) \quad (2.72)$$

Substitution of expressions (2.71) and (2.72) into (2.69), with the aid of expression (2.55), gives the required expression for κ_c .

$$\begin{aligned}\kappa_c &= \frac{d\phi_{I\xi}}{ds} - (\mathbf{N}_I \times \mathbf{w}) \cdot \left(\frac{d\mathbf{N}_I}{ds} \right)_{\mathbf{w}} \\ &= \frac{d\phi_{I\xi}}{ds} - G_{Iw}\end{aligned}\quad (2.73)$$

3. Rate of Change of Angle $\phi_{I\xi}$ along the Intersection Curve.

Due to $|\mathbf{N}_I \times \mathbf{N}_{II}| = \sin \phi_{I,II}$, $\mathbf{N}_I \cdot \mathbf{N}_{II} = \cos \phi_{I,II}$, we can find from expression (2.57)

$$\frac{d}{ds} (\sin \phi_{I,II}) = \cos \phi_{I,II} \frac{d\phi_{I,II}}{ds} = (G_{Iw} - G_{IIw}) \cos \phi_{I,II}$$

That is

$$\frac{d\phi_{I,II}}{ds} = G_{Iw} - G_{IIw} \quad (2.74)$$

From expression (2.65)

$$K_{Iw} \cos(\phi_{I\xi} - \phi_{I,II}) = K_{IIw} \cos \phi_{I\xi} \quad (2.75)$$

The value of $\frac{d\phi_{I\xi}}{ds}$ can be obtained by taking the derivative of the above expression with respect to the arc lengths of the intersecting curve, and using expression (2.74)

$$\frac{d\phi_{I\xi}}{ds} = \frac{\left\{ K_{Iw} (G_{Iw} - G_{IIw}) \sin(\phi_{I\xi} - \phi_{I,II}) + \cos(\phi_{I\xi} - \phi_{I,II}) \left(\frac{dK_{Iw}}{ds} \right)_{\mathbf{w}} - \cos \phi_{I\xi} \left(\frac{dK_{IIw}}{ds} \right)_{\mathbf{w}} \right\}}{K_{Iw} \sin(\phi_{I\xi} - \phi_{I,II}) - K_{IIw} \sin \phi_{I\xi}} \quad (2.76)$$

Then with the aid of expressions (2.66), (2.68), and (2.69), we obtain

$$\begin{aligned}
\frac{d\beta}{ds} &= \frac{d}{ds}(\mathbf{w} \times \xi) \\
&= \frac{d\mathbf{w}}{ds} \times \xi + \mathbf{w} \times \frac{d\xi}{ds} \\
&= \mathbf{w} \times (-k_c \mathbf{w} + \kappa_c \beta) \\
&= -\kappa_c \xi
\end{aligned} \tag{2.77}$$

Finally, expressions (2.52), (2.68), (2.69) and (2.77) lead to the following three relations,

$$\left. \begin{aligned}
\frac{d\mathbf{w}}{ds} &= k_c \xi \\
\frac{d\xi}{ds} &= -k_c \mathbf{w} + \kappa_c \beta \\
\frac{d\beta}{ds} &= -\kappa_c \xi
\end{aligned} \right\} \tag{2.78}$$

Expressions (2.78) are called the Serret-Frenet Formulas.

2.2.20 Geometric Angular Velocity of the Intersecting Curve

By regarding the arc length as a time parameter, the rate of change $\frac{d\mathbf{w}}{ds}$, $\frac{d\xi}{ds}$, $\frac{d\beta}{ds}$ of the three coordinate directions \mathbf{w} , ξ , β can be considered as the velocities of their end points if the vectors were to rotate with an imaginary angular velocity ω_c , that is

$$\left. \begin{aligned}
\frac{d\mathbf{w}}{ds} &= \omega_c \times \mathbf{w} \\
\frac{d\xi}{ds} &= \omega_c \times \xi \\
\frac{d\beta}{ds} &= \omega_c \times \beta
\end{aligned} \right\} \tag{2.79}$$

Substitution of expression (2.78) into (2.79) yields

$$\omega_c = \kappa_c \mathbf{w} + k_c \beta \tag{2.80}$$

ω_c defined by expression (2.80) is called the geometric angular velocity of the intersecting curve.

2.2.21 The Relative Geometric Angular Velocity of the Intersecting Curve with Respect to the Boundary Surface

1. Definition.

The subtraction of the geometric angular velocity Ω_w of either of the boundary surfaces in the direction tangential to the intersecting curve, from the geometric angular velocity ω_c of the intersecting curve, is defined as the relative geometric angular velocity $\Delta\omega_c$ of the intersecting curve with respect to the boundary surface, that is,

$$\Delta\omega_c = \omega_c - \Omega_w \quad (2.81)$$

2. Formula for Calculation.

Substituting expression (2.72) into (2.80), thus

$$\omega_c = \kappa_c \mathbf{w} - k_c \cos \phi_{I\xi} \mathbf{N}_I \times \mathbf{w} - k_c \sin \phi_{I\xi} \mathbf{N}_I \quad (2.82)$$

In a similar way

$$\omega_c = \kappa_c \mathbf{w} - k_c \cos \phi_{II\xi} \mathbf{N}_{II} \times \mathbf{w} - k_c \sin \phi_{II\xi} \mathbf{N}_{II} \quad (2.83)$$

With the aid of expressions (2.19), (2.55) and (2.56), it follows

$$\Omega_{Iw} = K_{Iw}(\mathbf{N}_I \times \mathbf{w}) - G_{Iw} \mathbf{w} \quad (2.84)$$

and

$$\Omega_{IIw} = K_{IIw}(\mathbf{N}_{II} \times \mathbf{w}) - G_{IIw} \mathbf{w} \quad (2.85)$$

The relative geometric angular velocity $\Delta_I \omega_c$ of the intersecting curve with respect to the first boundary surface can be found by substituting expressions (2.82), (2.84) into (2.81) as

$$\begin{aligned} \Delta_I \omega_c = & (\kappa_c + G_{Iw}) \mathbf{w} - (k_c \cos \phi_{I\xi} + K_{Iw})(\mathbf{N}_I \times \mathbf{w}) \\ & - k_c \sin \phi_{I\xi} \mathbf{N}_I \end{aligned} \quad (2.86)$$

Due to expression (2.64), i.e., $k_c \cos \phi_{I\xi} + K_{Iw} = 0$, then

$$\Delta_I \omega_c = (\kappa_c + G_{Iw}) \mathbf{w} - k_c \sin \phi_{I\xi} \mathbf{N}_I \quad (2.87)$$

Similarly, the relative geometric angular velocity $\Delta_{II} \omega_c$ of the intersecting curve with respect to the second boundary surface is found as

$$\Delta_{II} \omega_c = (\kappa_c + G_{IIw}) \mathbf{w} - k_c \sin \phi_{II\xi} \mathbf{N}_{II} \quad (2.88)$$

2.2.22 The Relative Curvature and Relative Torsional Curvature of the Intersecting Curve with Respect to the Boundary Surface

1. Definition.

It can be found from expressions (2.87) and (2.88) that the relative geometric angular velocity $\Delta\omega_c$ of the intersecting curve with respect to the boundary surface has components only in directions \mathbf{w} and \mathbf{N} . This is because expression (2.64) has to be satisfied, thus, $\Delta\omega_c$ has no component in direction $\mathbf{N} \times \mathbf{w}$, otherwise, the intersecting curve would deviate from the boundary surface. The projection component of $\Delta\omega_c$ in the direction \mathbf{N} normal to the boundary surface is defined as the relative curvature Δk_c of the intersecting curve with respect to the boundary surface, i.e.,

$$\Delta k_c = \Delta\omega_c \cdot \mathbf{N} \quad (2.89)$$

The projection component of $\Delta\omega_c$ in the direction \mathbf{w} tangential to the intersecting curve is defined as the relative torsional curvature $\Delta\kappa_c$ of the intersecting curve with respect to the boundary surface, i.e.,

$$\Delta\kappa_c = \Delta\omega_c \cdot \mathbf{w} \quad (2.90)$$

2. Formula for Calculation.

In accordance with expression (2.73), it can be found

$$\begin{aligned} \kappa_c + G_{Iw} &= \frac{d\phi_{I\xi}}{ds} \\ \kappa_c + G_{IIw} &= \frac{d\phi_{II\xi}}{ds} \end{aligned}$$

By designating the angle of rotation of \mathbf{N} (\mathbf{N}_I or \mathbf{N}_{II}) about \mathbf{w} to ξ as $\phi_{N\xi}$, the above two expressions can be combined as

$$\kappa_c + G_w = \frac{d\phi_{N\xi}}{ds} \quad (2.91)$$

Substitution of expressions (2.87), (2.88), and (2.91) into (2.89) and (2.90) yields

$$\Delta k_c = -k_c \sin \phi_{N\xi} \quad (2.92)$$

$$\Delta\kappa_c = \frac{d\phi_{N\xi}}{ds} \quad (2.93)$$

2.2.23 Geodesic

If the relative geometric angular velocity of the curve relative to the surface at any point is identical to zero, i.e.,

$$\Delta k_c = -k_c \sin \phi_{N\xi} = 0 \quad (2.94)$$

$$\Delta \kappa_c = \frac{d\phi_{N\xi}}{ds} = \kappa_c + G_w = 0 \quad (2.95)$$

then this curve is said to be a geodesic of this surface.

2.3 Kinematics of Conjugacy

2.3.1 Motion of a Rigid Body and Conjugate Motion

Degrees of Freedom for Motion of a Rigid Body

Motion of a rigid body, strictly speaking, refers to the motion, measured in a specific time parameter, of a rigid body relative to a specific reference frame. Displacement in a reference frame of any rigid body can be resolved into two parts, i.e., translation and rotation. Let \mathbf{R}_0 be a point-vector, relative to the origin of a reference frame, of any point of a rigid body at the initial instant, and after an elapse of time t , due to displacements, \mathbf{R}_0 becomes \mathbf{R}_p

$$\mathbf{R}_p = (\theta\omega) \otimes \mathbf{R}_0 + \mathbf{s} \quad (2.96)$$

where $(\theta\omega) \otimes \mathbf{R}_0$ represents the part of rotation, ω being an axis of rotation and θ an angle of rotation; \mathbf{s} represents the part of translation. Expression (2.96) represents rotation first and then translation. If a rigid body takes translation first and then rotation, it comes

$$\mathbf{R}_p = (\theta\omega) \otimes (\mathbf{R}_0 + \mathbf{s}_t) \quad (2.97)$$

From expressions (2.96) and (2.97), it follows that if

$$\mathbf{s} = (\theta\omega) \otimes \mathbf{s}_t \quad (2.98)$$

then, expressions (2.96) and (2.97) are equivalent to each other.

Since ω is a unit vector and \mathbf{s} , \mathbf{s}_t are vectors, therefore, six parametric variables, i.e., θ , ω , \mathbf{s} or \mathbf{s}_t , are required to determine the displacement of a rigid body, although they are all functions of the time parameter, that is,

$$\left. \begin{aligned} \theta &= \theta(t), & \omega &= \omega(t), \\ \mathbf{s} &= \mathbf{s}(t), & \mathbf{s}_t &= \mathbf{s}_t(t) \end{aligned} \right\} \quad (2.99)$$

Expression (2.99) represents nine equations which must satisfy three conditions represented by (2.98); that is, only six functional expressions can be arbitrarily prescribed, therefore, the number of degrees of freedom for a rigid body, without any constraint in a reference frame, is six. The above six functional expressions are not independent of each other whenever the motion of a rigid body is subjected to constraints. Let C_r be the number of independent relations to be satisfied among θ , ω , \mathbf{s} , or \mathbf{s}_t , i.e., the number of degree of constraint for the motion of a rigid body be C_r , and thus the number of degree of freedom for the motion of a rigid body are

$$D_r = 6 - C_r \quad (2.100)$$

where $0 \leq C_r \leq 5$, then $1 \leq D_r \leq 6$.

Motion of Rigid Bodies Subject to a Constraint of Boundary Geometric Configuration — Conjugate Motions

Suppose that rigid body I is fixed to the reference frame which measures the motion of rigid body II, and thus, the motion of rigid body II is exactly the relative motion of rigid body II to body I. Next suppose the boundary geometric configurations of rigid bodies I and II are A and \bar{A} (including surface, curve and point) respectively. It is now assumed that a constraint in the relative motion between I and II is such that A, \bar{A} always keep contact with each other during the whole process of motion. Such relative motion is called the motion of rigid bodies subject to a constraint of boundary geometric configuration. Obviously, an arbitrary alternative of choice of a reference frame does not affect the relative motion itself except for the form of expression for the relative motion. Now select arbitrarily a reference frame O to measure motions of rigid bodies I, II, and let motions of I, II relative to O be ϕ_1, ϕ_2 respectively, and thus a pair of motions (ϕ_1, ϕ_2) represents the relative motion between rigid body I and body II under the constraint (A, \bar{A}) , and consequently, (ϕ_1, ϕ_2) is called conjugate motion and correspondingly, we will refer to this constraint (A, \bar{A}) as the conjugate configuration. Conjugate motion has three characteristics:

1. Coexistence.

Any conjugate motion is composed of a pair of motions (ϕ_1, ϕ_2) . In the general case, ϕ_1, ϕ_2 are of the form similar to expression (2.96) or (2.97).

2. Interdependency with Conjugate Configuration.

Conjugate motion represents the relative motion of both rigid bodies subject to constraints, and therefore, the conjugate motion and the conjugate configuration are interdependent. Conjugate motion is the kinematic (time) manifestation of the conjugate configuration, and the conjugate configuration is the geometric manifestation of conjugate motion.

3. Versatility of Form.

Under the same constraint, i.e., (A, \bar{A}) , the conjugate motions (ϕ_1, ϕ_2) , because of the different reference frames selected, are of different forms but they represent the identical relative motion. The interchange among varieties of form (ϕ_1, ϕ_2) corresponding to the identical conjugate configurations (A, \bar{A}) is called interchangeability of conjugate motions.

The Canonical Form of Conjugate Motion.

First let the reference frame O_I be fixed with one of the rigid bodies, say, rigid body I, and consequently, ϕ_1 of the conjugate motion (ϕ_1, ϕ_2) becomes static; that is, if a point-vector of any point on the rigid body I at the initial instant is \mathbf{R}_1 , after an elapse of time t , the point-vector of this point is \mathbf{r}_{1t} , and then $\mathbf{r}_{1t} = \mathbf{R}_1$. Meanwhile, ϕ_2 of the conjugate motion (ϕ_1, ϕ_2) will be simply the relative motion ϕ_{21} of rigid body II to body I. The most general form ϕ_{21} is a combination of rotation and translation. If the point-vector of any point on the rigid body II, at the initial instant, is \mathbf{R}_2 , and at the time t , \mathbf{r}_{2t} , from the expression (2.96), we obtain

$$\mathbf{r}_{2t} = (\theta\omega) \otimes \mathbf{R}_2 + \mathbf{s} \quad (2.101)$$

Now select arbitrarily two mutually perpendicular fixed unit vectors ω_1, ω_0 ($\omega_1 \cdot \omega_0 = 0$) which do not vary with time, in virtue of expression (2.8), expression (2.101) becomes

$$\mathbf{r}_{2t} = (-\varepsilon_1\omega_1) \otimes \{(-\alpha\omega_0) \otimes [(-\varepsilon_2\omega_1) \otimes \mathbf{R}_2]\} + \mathbf{s} \quad (2.102)$$

Next select a reference frame O and suppose that O_I , with respect to O , takes a screw displacement consisting of first a rotation about an axis ω_1 and then a translation parallel to ω_1 , that is, at the instant t , the point-vector \mathbf{r}_t fixed with O_I will correspond to the point-vector \mathbf{R}_t in a reference frame O

$$\mathbf{R}_t = (\varepsilon_1\omega_1) \otimes \mathbf{r}_t + \sigma_1\omega_1 \quad (2.103)$$

ε_1 being an angle of rotation, and σ_1 being a translation along the axis ω_1 . By making use of $\mathbf{r}_{1t} = \mathbf{R}_1$, and expressions (2.102), (2.103), conjugate motion (ϕ_1, ϕ_2) with respect to the reference frame O can be found as follows;

$$\left. \begin{array}{l} \phi_1 : \quad \mathbf{R}_{1t} = (\varepsilon_1\omega_1) \otimes \mathbf{R}_1 + \sigma_1\omega_1 \\ \phi_2 : \quad \mathbf{R}_{2t} = (-\alpha\omega_0) \otimes [(-\varepsilon_2\omega_1) \otimes \mathbf{R}_2] + \rho\mathbf{q} \end{array} \right\} \quad (2.104)$$

where $\rho\mathbf{q} = (\varepsilon_1\omega_1) \otimes \mathbf{s} + \sigma_1\omega_1$.

Expression (2.104) is regarded as the canonical form of conjugate motion. The characteristic feature of the canonical form of conjugate motion is that among the rotation parts of two motions ϕ_1, ϕ_2 comprising conjugate motion, the more complicated one, i.e., ϕ_2 in expression (2.104), is a composition of just two successive rotations about the two fixed axes. Comparing to expression (2.102) which contains three successive rotations, this one is much simpler and therefore much more convenient for carrying out analyses.

The Classification of Conjugate Motions

In the canonical form of conjugate motions, i.e., expression (2.104), $\alpha, \varepsilon_1, \varepsilon_2$ vary generally with time, and the corresponding conjugate motions (ϕ_1, ϕ_2) are called the general conjugate motion. If among three parameters $\alpha, \varepsilon_1, \varepsilon_2$, at least one parameter is constant, then, the corresponding conjugate motions (ϕ_1, ϕ_2) are regarded as simple conjugate motions.

The Equivalent Conjugate Motions and Their Degrees of Freedom

Suppose that a rigid body I is connected with a rigid body II through a conjugate pair 1 and the rigid body II is connected with a rigid body III through a conjugate pair 2, and thus, the motion of rigid body I relative to rigid body III is subjected to constraints of conjugate pairs 1, 2, and this motion is the sum of both the conjugate motion between rigid bodies I and II and the conjugate motion between rigid bodies II and III. Such relative motion between two rigid bodies subject to constraints of two or more conjugate pairs is also a conjugate motion and therefore referred to as the equivalent conjugate motion.

The number of degrees of freedom D_e for the equivalent conjugate motion is the sum of the number of degrees of freedom for all individual conjugate pairs D_{ci} ($i = 1, 2, \dots, n$), that is,

$$D_e = \sum_{i=1}^n D_{ci} = D_{ci} \quad (2.105)$$

Due to $n \geq 2$, $D_{ci} \geq 1$. from expression (2.105), it follows $D_e \geq 2$, i.e., there is a minimum value of 2 for the number of degrees of freedom of equivalent conjugate motion but no maximum limitation.

The canonical form for the equivalent conjugate motion is still expression (2.104), but six parametric variables $\alpha, \varepsilon_1, \varepsilon_2, \rho\mathbf{q}$ in expression (2.104) are functions of D_e independent parametric variables (assuming $\theta_1, \theta_2, \dots, \theta_{D_e}$), that is,

$$\left. \begin{aligned} \alpha &= \alpha(\theta_1, \theta_2, \dots, \theta_{D_e}) \\ \varepsilon_1 &= \varepsilon_1(\theta_1, \theta_2, \dots, \theta_{D_e}) \\ \varepsilon_2 &= \varepsilon_2(\theta_1, \theta_2, \dots, \theta_{D_e}) \\ \rho\mathbf{q} &= \rho\mathbf{q}(\theta_1, \theta_2, \dots, \theta_{D_e}) \end{aligned} \right\} \quad (2.106)$$

Where $\theta_1, \theta_2, \dots, \theta_{D_e}$ are independent of each other and functions of time t as a parameter, i.e.,

$$\theta_j = \theta_j(t), \quad j = 1, 2, \dots, D_e \quad (2.107)$$

Therefore, the condition $D_e > 6$ does not change the number of parametric variables which describe the relative motion of both rigid bodies, i.e., six parametric variables, $\alpha, \varepsilon_1, \varepsilon_2, \rho\mathbf{q}$, but the condition $D_e > 6$ enlarges the active scope of the relative displacement of both rigid bodies.

2.3.2 The Simple Conjugate Motion with a Single Degree of Freedom

The Canonical Form of the Simple Conjugate Motion

We call the motion simple conjugate motion, when among the three parametric variables $\alpha, \varepsilon_1, \varepsilon_2$ of the canonical form of conjugate motion (2.104), at least one is constant. First consider the case that α is constant. In virtue of expression (2.6), ϕ_2 in expression (2.104) becomes

$$\mathbf{R}_{2t} = \{-\varepsilon_2[(-\alpha\omega_0) \otimes \omega_1]\} \otimes [(-\alpha\omega_0) \otimes \mathbf{R}_2] + \rho\mathbf{q} \quad (2.108)$$

Due to ω_1, ω_0 being constant unit vectors, α being a constant, $(-\alpha\omega_0) \otimes \omega_1$ must be a constant unit vector and assumed as

$$\omega_2 = -(-\alpha\omega_0) \otimes \omega_1 \quad (2.109)$$

In the case $\cos \alpha \neq 0$, $\omega_2, \omega_0, \omega_1 \times \omega_0$ are non-coplanar, therefore, $\rho\mathbf{q}$ can be resolved along the directions of these three unit vectors.

$$\rho\mathbf{q} = \sigma_2\omega_2 + f\omega_0 + h\omega_1 \times \omega_0 \quad (2.110)$$

In the case $\cos \alpha = 0$, $\omega_2, \omega_0, \omega_1$ are non-coplanar, $\rho\mathbf{q}$ can be resolved as

$$\rho\mathbf{q} = \sigma_2\omega_2 + f\omega_0 + \sigma'_1\omega_1 \quad (2.111)$$

Let

$$\left. \begin{aligned} l\mathbf{p} &= f\omega_0 + h\omega_1 \times \omega_0, & (\cos \alpha \neq 0) \\ l\mathbf{p} &= f\omega_0 + \sigma'_1\omega_1, & (\cos \alpha = 0) \end{aligned} \right\} \quad (2.112)$$

Combine expressions (2.110) and (2.111) into

$$\rho \mathbf{q} = \sigma_2 \omega_2 + l \mathbf{p} \quad (2.113)$$

Suppose

$$\mathbf{R}' = (-\alpha \omega_2) \otimes \mathbf{R}_2 \quad (2.114)$$

With substitution into expression (2.108) from expressions (2.109), (2.113) and (2.114), ϕ_2 may be expressed as

$$\mathbf{R}_{2t} = (\varepsilon_2 \omega_2) \otimes \mathbf{R}'_2 + \sigma_2 \omega_2 + l \mathbf{p} \quad (2.115)$$

\mathbf{R}_{1t} and \mathbf{R}_{2t} in expression (2.104) share the same origin. In order to suit such a special case as simple conjugate motion, the origin of a point-vector of a point on rigid body I remains the initial origin and the origin of a point-vector of a point on rigid body II is adjusted to the end-point of the vector $l \mathbf{p}$. The point-vectors of points on rigid bodies I, II with double origins are represented by $\mathbf{R}_{1p}, \mathbf{R}_{2p}$ respectively for discrimination. That is

$$\left. \begin{aligned} \mathbf{R}_{1p} &= \mathbf{R}_{1t} \\ \mathbf{R}_{2p} &= \mathbf{R}_{2t} - l \mathbf{p} \end{aligned} \right\} \quad (2.116)$$

Since α is a constant, and ω_0 is a constant unit vector, the expression (2.114) represents the fact that the rigid body II rotates about ω_0 through a fixed angle α and this indicates a change of the initial orientation of rigid body II. If the orientation after changing is assumed as the original orientation, then \mathbf{R}'_2 may be rewritten as \mathbf{R}_2 , consequently, in virtue of expressions (2.115), (2.116), together with the expression (2.104), the canonical form of simple conjugate motion is found as

$$\left. \begin{aligned} \phi_1 : \quad \mathbf{R}_{1p} &= \mathbf{R}_{1t} = (\varepsilon_1 \omega_1) \otimes \mathbf{R}_1 + \sigma_1 \omega_1 \\ \phi_2 : \quad \mathbf{R}_{2p} &= \mathbf{R}_{2t} - l \mathbf{p} = (\varepsilon_2 \omega_2) \otimes \mathbf{R}_2 + \sigma_2 \omega_2 \end{aligned} \right\} \quad (2.117)$$

Where $l \mathbf{p}$ can be found from the expression (2.112).

When among the three parametric variables, ε_2 is constant and α, ε_1 are variables, replacing $(-\varepsilon_2 \omega_1) \otimes \mathbf{R}_2$ by \mathbf{R}'_2 and α by ε_2 will transform the canonical form from expression (2.104) to expression (2.117), where $\omega_2 = \omega_0$.

When among the three parametric variables, ε_1 is constant and α, ε_2 are variables, obviously, just exchanging the indices of the rigid bodies I, II will reduce this case to the same case as that of ε_2 being constant, and therefore the motion can also be represented by the canonical form (2.117).

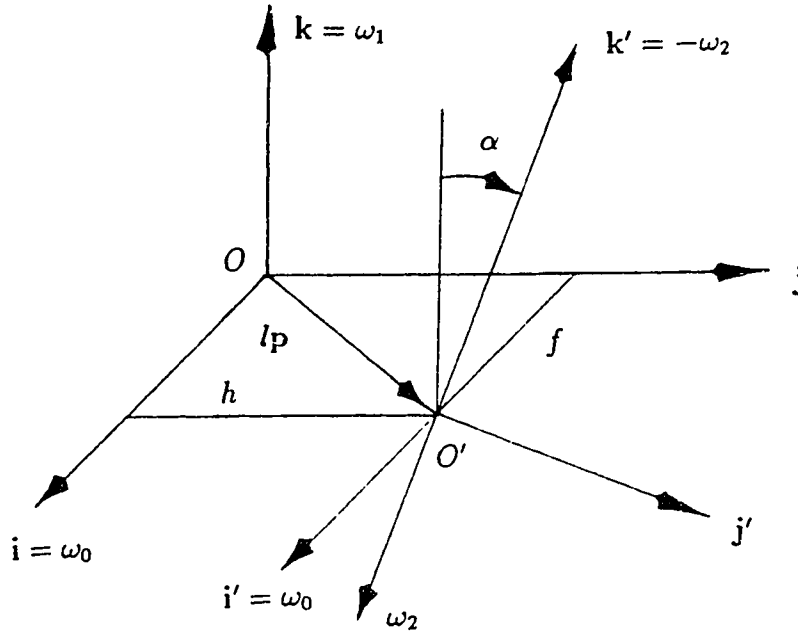


Figure 2.6: Dual coordinate systems

Dual Coordinate Systems for a Simple Conjugate Motion

With angle α being constant, we can adopt the dual coordinate systems, i.e., $O - i, j, k$ for body I and $O' - i', j', k'$ for body II. The relationships between the dual coordinates shown in fig. 2.6. are as follows.

$$\left. \begin{aligned} i &= \omega_0, & j &= \omega_1 \times \omega_0, & k &= \omega_1 \\ i' &= \omega_0, & j' &= \omega_0 \times \omega_2, & k' &= -\omega_2 \end{aligned} \right\} \quad (2.118)$$

With the aid of expressions (2.109) and (2.118), we obtain

$$\left. \begin{aligned} i' &= i, & j' &= \cos \alpha j - \sin \alpha k, & k' &= \sin \alpha j + \cos \alpha k \\ i &= i', & j &= \cos \alpha j' + \sin \alpha k', & k &= -\sin \alpha j' + \cos \alpha k' \end{aligned} \right\} \quad (2.119)$$

and making use of expressions (2.112) and (2.118)

$$\left. \begin{aligned} l_p &= \overline{OO'} = f i + h j & (\cos \alpha \neq 0) \\ l_p &= \overline{OO'} = f i + \sigma'_1 k & (\cos \alpha = 0) \end{aligned} \right\} \quad (2.120)$$

Displacement of a Point of a Rigid Body in a Simple Conjugate Motion with a Single Degree of Freedom

1. Independent Parametric Variable.

Due to the single degree of freedom, there exists only one independent variable among $\varepsilon_1, \varepsilon_2, \sigma_1, \sigma_2, f, h$ (or σ'_1). In principle, any one among these six parametric variables can be selected as an independent parametric variable, and usually, ε_1 is selected as the independent parametric variable, that is,

$$\left. \begin{aligned} \varepsilon_2 &= \varepsilon_2(\varepsilon_1), & \sigma_1 &= \sigma_1(\varepsilon_1), & \sigma_2 &= \sigma_2(\varepsilon_1) \\ f &= f(\varepsilon_1), & h &= h(\varepsilon_1) & \text{or } \sigma'_1 &= \sigma'_1(\varepsilon_1) \end{aligned} \right\} \quad (2.121)$$

2. Displacement of a Point P on Rigid Body I.

Let the initial ($\varepsilon_1 = 0$) point-vector of a point P in body I with respect to $O - \mathbf{i}, \mathbf{j}, \mathbf{k}$ be $\mathbf{R}_1 = x\mathbf{i} + y\mathbf{j} + z\mathbf{k}$. After an elapse of time ε_1 (here the angle ε_1 can also be regarded as a time parameter), the corresponding point-vector $\mathbf{R}_{1p} = x_p\mathbf{i} + y_p\mathbf{j} + z_p\mathbf{k}$ of the point (P_d) will be

$$\left. \begin{aligned} \mathbf{R}_{1p} &= (\varepsilon_1\omega_1) \otimes \mathbf{R}_1 + \sigma_1\omega_1 = (\varepsilon_1\mathbf{k}) \otimes \mathbf{R}_1 + \sigma_1\mathbf{k} \\ x_p &= x \cos \varepsilon_1 - y \sin \varepsilon_1 \\ y_p &= x \sin \varepsilon_1 + y \cos \varepsilon_1 \\ z_p &= z + \sigma_1 \end{aligned} \right\} \quad (2.122)$$

3. The Common Point of Rigid Body II.

Suppose that point P_d is the common point[†] of body I and body II at the instant ε_1 , and thus, its point-vector \mathbf{R}_{2p} , as a point in body II, with the origin O' is in the form

$$\left. \begin{aligned} \mathbf{R}_{2p} &= \mathbf{R}_{1p} - l\mathbf{p} = x'_p\mathbf{i}' + y'_p\mathbf{j}' + z'_p\mathbf{k}' \\ x'_p &= x_p - f \\ y'_p &= (y_p - h) \cos \alpha - z_p \sin \alpha \\ z'_p &= (y_p - h) \sin \alpha + z_p \cos \alpha \end{aligned} \right\} \quad (2.123)$$

4. The Initial Corresponding Point \bar{P} in Rigid Body II.

A point \bar{P} in rigid body II at the initial instant, corresponding to the common point P_d at the instant ε_1 , i.e., corresponding to the initial point P in rigid body I, is called the initial corresponding point in rigid body II, and its point-vector $\mathbf{R}_2 = x'\mathbf{i}' + y'\mathbf{j}' + z'\mathbf{k}'$ with respect to the origin O' is given by

$$\mathbf{R}_2 = (-\varepsilon_2\omega_2) \otimes \mathbf{R}_{2p} - \sigma_2\omega_2 \quad (2.124)$$

With the aid of expressions (2.122) and (2.123), the foregoing expression may be expanded as

$$\left. \begin{aligned} \mathbf{R}_2 &= (-\varepsilon_2 \omega_2) \otimes [(\varepsilon_1 \omega_1) \otimes \mathbf{R}_1 + \sigma_1 \omega_1 - l\mathbf{p}] - \sigma_2 \omega_2 \\ x' &= x(\cos \varepsilon_1 \cos \varepsilon_2 - \cos \alpha \sin \varepsilon_1 \sin \varepsilon_2) \\ &\quad - y(\sin \varepsilon_1 \cos \varepsilon_2 + \cos \alpha \cos \varepsilon_1 \sin \varepsilon_2) \\ &\quad + (z + \sigma_1) \sin \alpha \sin \varepsilon_2 - f \cos \varepsilon_2 + h \cos \alpha \sin \varepsilon_2 \\ y' &= x(\cos \varepsilon_1 \sin \varepsilon_2 + \cos \alpha \sin \varepsilon_1 \cos \varepsilon_2) \\ &\quad + y(\cos \alpha \cos \varepsilon_1 \cos \varepsilon_2 - \sin \varepsilon_1 \sin \varepsilon_2) \\ &\quad - (z + \sigma_1) \sin \alpha \cos \varepsilon_2 - f \sin \varepsilon_2 - h \cos \alpha \cos \varepsilon_2 \\ z' &= x \sin \alpha \sin \varepsilon_1 + y \sin \alpha \cos \varepsilon_1 + (z + \sigma_1) \cos \alpha \\ &\quad - h \sin \alpha + \sigma_2 \end{aligned} \right\} \quad (2.125)$$

Where $\varepsilon_2, \sigma_1, \sigma_2, f, h$ are all functions of ε_1 .

Velocity of a Point in Simple Conjugate Motion with a Single Degree of Freedom

1. The velocity \mathbf{v}_p , with respect to coordinate system $O - \mathbf{i}, \mathbf{j}, \mathbf{k}$, of the point P_d (\mathbf{R}_{1p}) in rigid body I at instant ε_1 is

$$\begin{aligned} \mathbf{v}_p &= \frac{d\mathbf{R}_{1p}}{d\varepsilon_1} = \omega_1 \times \mathbf{R}_{1p} + \frac{d\sigma_1}{d\varepsilon_1} \omega_1 \\ &= -y_p \mathbf{i} + x_p \mathbf{j} + \frac{d\sigma_1}{d\varepsilon_1} \mathbf{k} \end{aligned} \quad (2.126)$$

2. The velocity \mathbf{v}'_p , with respect to coordinate system $O - \mathbf{i}, \mathbf{j}, \mathbf{k}$, of the common point $P_d(\mathbf{R}_{2p})$ in the rigid body II at instant ε_1 is

$$\mathbf{v}'_p = M \omega_2 \times \mathbf{R}_{2p} + \frac{d\sigma_2}{d\varepsilon_1} \omega_2 + \frac{d(l\mathbf{p})}{d\varepsilon_1} \quad (2.127)$$

Where

$$M = \frac{d\varepsilon_2}{d\varepsilon_1} \quad (2.128)$$

3. The relative velocity $\mathbf{v}_p^{12} = v_{p1}^{12} \mathbf{i} + v_{p2}^{12} \mathbf{j} + v_{p3}^{12} \mathbf{k}$ at the point $P_d(\mathbf{R}_{1p})$ of body I to body II at instant ε_1 is

$$\left. \begin{aligned} \mathbf{v}_p^{12} &= \mathbf{v}_p - \mathbf{v}'_p \\ &= \omega_1 \times \mathbf{R}_{1p} + \frac{d\sigma_1}{d\varepsilon_1} \omega_1 - [M \omega_2 \times \mathbf{R}_{2p} + \frac{d\sigma_2}{d\varepsilon_1} \omega_2 + \frac{d(l\mathbf{p})}{d\varepsilon_1}] \\ v_{p1}^{12} &= -(1 + M \cos \alpha) y_p + M z_p \sin \alpha + M h \cos \alpha - \frac{df}{d\varepsilon_1} \\ v_{p2}^{12} &= (1 + M \cos \alpha) x_p - M f \cos \alpha + \frac{d\sigma_2}{d\varepsilon_1} \sin \alpha - \frac{dh}{d\varepsilon_1} \\ v_{p3}^{12} &= -M x_p \sin \alpha + M f \sin \alpha + \frac{d\sigma_1}{d\varepsilon_1} + \frac{d\sigma_2}{d\varepsilon_1} \cos \alpha \end{aligned} \right\} \quad (2.129)$$

4. The velocity \mathbf{v}_p^{21} at point P_d of body II relative to body I at instant ε_1 is

$$\begin{aligned}\mathbf{v}_p^{21} &= \mathbf{v}'_p - \mathbf{v}_p = -\mathbf{v}_p^{12} \\ &= M\omega_2 \times \mathbf{R}_{2p} + \frac{d\sigma_2}{d\varepsilon_1}\omega_2 + \frac{d(l\mathbf{p})}{d\varepsilon_1} - \omega_1 \times (\mathbf{R}_{2p} + l\mathbf{p}) - \frac{d\sigma_1}{d\varepsilon_1}\omega_1\end{aligned}\quad (2.130)$$

Relative Angular Velocity of Simple Conjugate Motion with Single Degree of Freedom

1. The angular velocity Ω_{12} of rigid body I relative to rigid body II at instant ε_1 is

$$\begin{aligned}\Omega_{12} &= \omega_1 - M\omega_2 \\ &= M \sin \alpha \mathbf{j} + (1 + M \cos \alpha) \mathbf{k}\end{aligned}\quad (2.131)$$

2. The projection component $\Omega_{sp}\mathbf{N}_{1p}$ of the relative angular velocity of rigid body I relative to rigid body II at instant ε_1 on the unit vector $\mathbf{N}_{1p} = A_p\mathbf{i} + B_p\mathbf{j} + C_p\mathbf{k}$ normal to the boundary surface of rigid body I at point P is

$$\begin{aligned}\Omega_{sp} &= \Omega_{12} \cdot \mathbf{N}_{1p} \\ &= B_p M \sin \alpha + C_p(1 + M \cos \alpha)\end{aligned}\quad (2.132)$$

3. The equivalent projection component η_p of the relative angular velocity of body I relative to body II at the instant ε_1 on the common tangent plane at P is

$$\left. \begin{aligned}\eta_p &= (\omega_1 - M\omega_2) \times \mathbf{N}_{1p} \\ &= \eta_{p1}\mathbf{i} + \eta_{p2}\mathbf{j} + \eta_{p3}\mathbf{k} \\ \eta_{p1} &= -B_p(1 + M \cos \alpha) + C_p M \sin \alpha \\ \eta_{p2} &= A_p(1 + M \cos \alpha) \\ \eta_{p3} &= -A_p M \sin \alpha \\ |\eta_p| &= \sqrt{\eta_{p1}^2 + \eta_{p2}^2 + \eta_{p3}^2}\end{aligned}\right\} \quad (2.133)$$

4. The projection component η_p^* of Ω_{12} on the plane with the normal \mathbf{N}_{1p} .

$$\eta_p^* = \Omega_{12} - \Omega_{sp}\mathbf{N}_{1p} = \mathbf{N}_{1p} \times (\Omega_{12} \times \mathbf{N}_{1p}) \quad (2.134)$$

5. The angle of rotation $\theta_{v\eta}$ about \mathbf{N}_{1p} axis from \mathbf{v}_p^{12} to η_p is found as follows

$$\left. \begin{aligned}\sin \theta_{v\eta} &= \frac{\mathbf{N}_{1p} \cdot (\mathbf{v}_p^{12} \times \eta_p)}{|\mathbf{v}_p^{12}| |\eta_p|} \\ \cos \theta_{v\eta} &= \frac{\mathbf{v}_p^{12} \cdot \eta_p}{|\mathbf{v}_p^{12}| |\eta_p|}\end{aligned}\right\} \quad (2.135)$$

Pitch Surfaces and Condition of Their Existence in Simple Conjugate Motion with a Single Degree of Freedom

1. Definition.

A surface, between body I and body II, composed of points with $\mathbf{v}_p^{12} = 0$ is defined as the pitch surface.

2. The Condition of the Existence of a Pitch Surface.

Since any point on the pitch surface must satisfy requirements $v_{p1}^{12} = v_{p2}^{12} = v_{p3}^{12} = 0$, thus, when ε_1 is regarded as the time parameter, the elimination of x_p from the last two equations of (2.129) will yield the condition of the existence of a pitch surface which must be satisfied by the simple conjugate motion with a single degree of freedom as follows

$$M(f - \frac{dh}{d\varepsilon_1}) \sin \alpha + (1 + M \cos \alpha) \frac{d\sigma_1}{d\varepsilon_1} + (M + \cos \alpha) \frac{d\sigma_2}{d\varepsilon_1} = 0 \quad (2.136)$$

3. The Equation of the Pitch Surface.

If the condition of the existence of a pitch surface in the case of simple conjugate motion with a single degree of freedom, i.e., (2.136), is satisfied, with the use of ε_1 as a time parameter, the application of the first two equations in (2.129) and expression (2.122) will provide the equation of the pitch surface on body I with the origin O at the initial position, i.e., $\varepsilon_1 = 0$, in the following form

$$\left. \begin{aligned} \mathbf{R}_0 &= x_0 \mathbf{i} + y_0 \mathbf{j} + z_0 \mathbf{k} \\ x_0 &= \frac{1}{(1+M \cos \alpha)} \left\{ [Mh \cos \alpha + M(z_0 + \sigma_1) \sin \alpha - \frac{df}{d\varepsilon_1}] \sin \varepsilon_1 \right. \\ &\quad \left. + (Mf \cos \alpha + \frac{dh}{d\varepsilon_1} - \sin \alpha \frac{d\sigma_2}{d\varepsilon_1}) \cos \varepsilon_1 \right\} \\ y_0 &= \frac{1}{(1+M \cos \alpha)} \left\{ [Mh \cos \alpha + M(z_0 + \sigma_1) \sin \alpha - \frac{df}{d\varepsilon_1}] \cos \varepsilon_1 \right. \\ &\quad \left. - (Mf \cos \alpha + \frac{dh}{d\varepsilon_1} - \sin \alpha \frac{d\sigma_2}{d\varepsilon_1}) \sin \varepsilon_1 \right\} \end{aligned} \right\} \quad (2.137)$$

where z_0, ε_1 are the two independent parametric variables, and $M, f, h, \sigma_1, \sigma_2$ are functions of ε_1 , as in expression (2.121).

Application of expressions (2.125) and (2.137) yields the equation of the pitch

surface on body II with the origin O' at the initial position as follows

$$\left. \begin{aligned} \mathbf{R}'_0 &= x'_0 \mathbf{i}' + y'_0 \mathbf{j}' + z'_0 \mathbf{k}' \\ x'_0 &= \frac{1}{(1+M \cos \alpha)} \left\{ \left(-f + \frac{dh}{d\varepsilon_1} - \sin \alpha \frac{d\sigma_2}{d\varepsilon_1} \right) \cos \varepsilon_2 - [-h \right. \\ &\quad \left. + M(z_0 + \sigma_1) \sin \alpha - \frac{df}{d\varepsilon_1} \right] \cos \alpha \sin \varepsilon_2 \} + (z_0 + \sigma_1) \sin \alpha \sin \varepsilon_2 \\ y'_0 &= \frac{1}{(1+M \cos \alpha)} \left\{ \left(-f + \frac{dh}{d\varepsilon_1} - \sin \alpha \frac{d\sigma_2}{d\varepsilon_1} \right) \sin \varepsilon_2 + [-h \right. \\ &\quad \left. + M(z_0 + \sigma_1) \sin \alpha - \frac{df}{d\varepsilon_1} \right] \cos \alpha \cos \varepsilon_2 \} - (z_0 + \sigma_1) \sin \alpha \cos \varepsilon_2 \\ z'_0 &= \frac{1}{(1+M \cos \alpha)} [-h + M(z_0 + \sigma_1) \sin \alpha - \frac{df}{d\varepsilon_1}] \sin \alpha + (z_0 + \sigma_1) \cos \alpha \\ &\quad + \sigma_2 \end{aligned} \right\} \quad (2.138)$$

where again z_0, ε_1 are the two independent parametric variables, and ε_2 is a function of ε_1 .

4. Equation for The Set of Pitch Points with Respect to the Fixed Coordinate Frame.

It follows from substitution of expressions (2.137) into (2.122) that the equation for the engagement of pitch surfaces is found in the form as follows

$$\left. \begin{aligned} \mathbf{r}_0 &= X_0 \mathbf{i} + Y_0 \mathbf{j} + Z_0 \mathbf{k} \\ X_0 &= \frac{1}{1+M \cos \alpha} \left(Mf \cos \alpha + \frac{dh}{d\varepsilon_1} - \sin \alpha \frac{d\sigma_2}{d\varepsilon_1} \right) \\ Y_0 &= \frac{1}{1+M \cos \alpha} \left[Mh \cos \alpha + M(z_0 + \sigma_1) \sin \alpha - \frac{df}{d\varepsilon_1} \right] \\ Z_0 &= z_0 + \sigma_1 \end{aligned} \right\} \quad (2.139)$$

Surfaces of Screw Axes Under Simple Conjugate Motion with Single Degree of Freedom

1. Surfaces of Screw Axes.

We will assume the angular velocity Ω_{12} of body I relative to body II is different from zero, i.e., $\Omega_{12} \neq 0$, and we consider points satisfying the requirement:

$$\Omega_{12} \times \mathbf{v}_p^{12} = 0 \quad (2.140)$$

In other words, the relative velocity of the points is parallel with the relative angular velocity of the bodies. Then a surface formed by any such points is called a surface of screw axes.

2. Equations for the Surfaces of Screw Axes.

With ε_1 being the time parameter, substitution of expression (2.121) into (2.139) together with the consideration $\Omega_{12} \neq 0$ yields

$$\left. \begin{aligned} v_{p1}^{12} &= 0 \\ v_{p2}^{12}(1 + M \cos \alpha) &= v_{p3}^{12} M \sin \alpha \end{aligned} \right\} \quad (2.141)$$

In virtue of expressions (2.122), (2.129), it follows from expression (2.140) that the equation for the surface of screw axes in body I at the initial position with the origin O is in the form

$$\left. \begin{aligned} \mathbf{R}_a &= x_a \mathbf{i} + y_a \mathbf{j} + z_a \mathbf{k} \\ x_a &= E \cos \varepsilon_1 + F \sin \varepsilon_1 \\ y_a &= -E \sin \varepsilon_1 + F \cos \varepsilon_1 \end{aligned} \right\} \quad (2.142)$$

where

$$\left. \begin{aligned} E &= \frac{Mf(M + \cos \alpha) + (1 + M \cos \alpha) \frac{dh}{d\varepsilon_1} + M \sin \alpha \frac{d\sigma_1}{d\varepsilon_1} - \sin \alpha \frac{d\sigma_2}{d\varepsilon_1}}{(1 + M \cos \alpha)^2 + M^2 \sin^2 \alpha} \\ F &= \frac{M(z_a + \sigma_1) \sin \alpha + Mh \cos \alpha - \frac{df}{d\varepsilon_1}}{(1 + M \cos \alpha)} \end{aligned} \right\} \quad (2.143)$$

As before z_a, ε_1 are the two independent parametric variables, and $M, f, h, \sigma_1, \sigma_2$ are functions of ε_1 .

With the aid of expressions (2.125) and (2.141), the equation for the surface of screw axes in body II with the origin O' at the initial position may be found as

$$\left. \begin{aligned} \mathbf{R}'_a &= x'_a \mathbf{i}' + y'_a \mathbf{j}' + z'_a \mathbf{k}' \\ x'_a &= E \cos \varepsilon_2 - F \cos \alpha \sin \varepsilon_2 + (z_a + \sigma_1) \sin \alpha \sin \varepsilon_2 - f \cos \varepsilon_2 \\ &\quad + h \cos \alpha \sin \varepsilon_2 \\ y'_a &= E \sin \varepsilon_2 + F \cos \alpha \cos \varepsilon_2 - (z_a + \sigma_1) \sin \alpha \cos \varepsilon_2 - f \sin \varepsilon_2 \\ &\quad - h \cos \alpha \cos \varepsilon_2 \\ z'_a &= F \sin \alpha + (z_a + \sigma_1) \cos \alpha - h \sin \alpha + \sigma_2 \end{aligned} \right\} \quad (2.144)$$

where, E, F are defined in expression (2.142).

3. Screw Axes.

It may be seen from expressions (2.141) to (2.143) that $x_a, y_a, x'_a, y'_a, z'_a$ are all linear functions of z_a at any given instant ε_1 , and there are thus two straight lines in bodies I and II respectively which are called the screw axes corresponding to the given time ε_1 . Surfaces of screw axes are just composed of screw axes corresponding to all different times, and they must therefore be ruled surfaces.

4. Equation for the Set of Screw Axes with Respect to the Fixed Reference Frame.

Expression (2.141) can be substituted into (2.122) to obtain the equation for the Set of screw axes as follows

$$\left. \begin{aligned} \mathbf{r}_a &= X_a \mathbf{i} + Y_a \mathbf{j} + Z_a \mathbf{k} \\ X_a &= \frac{Mf(M+\cos\alpha) + (1+M\cos\alpha)\frac{dh}{d\varepsilon_1} + M\sin\alpha\frac{d\sigma_1}{d\varepsilon_1} - \sin\alpha\frac{d\sigma_2}{d\varepsilon_1}}{(1+M\cos\alpha)^2 + M^2\sin^2\alpha} \\ Y_a &= \frac{M(z_a + \sigma_1)\sin\alpha + Mh\cos\alpha - \frac{df}{d\varepsilon_1}}{1+M\cos\alpha} \\ Z_a &= z_a + \sigma_1 \end{aligned} \right\} \quad (2.145)$$

Conjugate Relative Acceleration

At instant ε_1 , the velocity \mathbf{v}_p^{12} of body I relative to II at the common point P_d can be determined by the expression (2.129). Likewise, the velocity \mathbf{v}_p^{21} of body II relative to I at the common point P_d is $\mathbf{v}_p^{21} = -\mathbf{v}_p^{12}$. At instant $(\varepsilon_1 + \Delta\varepsilon_1)$, the point P_d on body I will move to the position $P'_d(\mathbf{R}_{1p'})$ which may be given by the first expression of (2.117).

$$\mathbf{R}_{1p'} = \mathbf{R}_{1p} + (\omega_1 \times \mathbf{R}_{1p} + \frac{d\sigma_1}{d\varepsilon_1}\omega_1)\Delta\varepsilon_1 \quad (2.146)$$

With the aid of expressions (2.129) and (2.143), omitting all the infinitesimals higher than the second order, the velocity of body I relative to II at point $P'_d(\mathbf{R}_{1p'})$ at instant $(\varepsilon_1 + \Delta\varepsilon_1)$ may be put in the form

$$\begin{aligned} \mathbf{v}_{p'}^{12} &= \mathbf{v}_p^{12} + \left\{ \omega_1 \times (\omega_1 \times \mathbf{R}_{1p} + \frac{d\sigma_1}{d\varepsilon_1}\omega_1) + \frac{d^2\sigma_1}{d\varepsilon_1^2}\omega_1 \right. \\ &\quad \left. - \frac{dM}{d\varepsilon_1}\omega_2 \times (\mathbf{R}_{1p} - l\mathbf{p}) - \frac{d^2\sigma_1}{d\varepsilon_1^2}\omega_2 - \frac{d^2(l\mathbf{p})}{d\varepsilon_1^2} \right. \\ &\quad \left. - M\omega_2 \times [\omega_1 \times \mathbf{R}_{1p} + \frac{d\sigma_1}{d\varepsilon_1}\omega_1 - \frac{d(l\mathbf{p})}{d\varepsilon_1}] \right\} \Delta\varepsilon_1 \end{aligned} \quad (2.147)$$

Likewise, at instant $(\varepsilon_1 + \Delta\varepsilon_1)$, the velocity of body II relative to I at the point $P'_d(\mathbf{R}_{1p'})$ of the body I is found as

$$\mathbf{v}_{p'}^{21} = -\mathbf{v}_{p'}^{12} \quad (2.148)$$

Since at instant $(\varepsilon_1 + \Delta\varepsilon_1)$, body I has already rotated about ω_1 as an axis through an angle $\Delta\varepsilon_1$, with respect to the body I at the instant ε_1 , the velocity of body II relative to I at the point P'_d becomes $(-\Delta\varepsilon_1\omega_1) \otimes \mathbf{v}_{p'}^{21}$. Consequently, the conjugate acceleration of body II relative to I is in the form

$$\mathbf{J}_p = \lim_{\Delta\varepsilon_1 \rightarrow 0} \frac{(-\Delta\varepsilon_1\omega_1) \otimes \mathbf{v}_{p'}^{21} - \mathbf{v}_p^{21}}{\Delta\varepsilon_1} \quad (2.149)$$

Substitution of expressions (2.148) into (2.149), together with the use of (2.123) (2.130) and (2.147), yields

$$\begin{aligned} \mathbf{J}_p &= \left. \begin{aligned} &\frac{dM}{d\varepsilon_1} \omega_2 \times (\mathbf{R}_{1p} - l\mathbf{p}) + \frac{d^2\sigma_2}{d\varepsilon_1^2} \omega_2 + \frac{d^2(l\mathbf{p})}{d\varepsilon_1^2} - \frac{d^2\sigma_1}{d\varepsilon_1^2} \omega_1 \\ &+ M\omega_2 \times \left[\omega_1 \times \mathbf{R}_{1p} + \frac{d\sigma_1}{d\varepsilon_1} \omega_1 - \frac{d(l\mathbf{p})}{d\varepsilon_1} \right] \\ &- \omega_1 \times \left[M\omega_2 \times (\mathbf{R}_{1p} - l\mathbf{p}) + \frac{d\sigma_2}{d\varepsilon_1} \omega_2 + \frac{d(l\mathbf{p})}{d\varepsilon_1} \right] \end{aligned} \right\} \quad (2.150) \\ &= J_{p1}\mathbf{i} + J_{p2}\mathbf{j} + J_{p3}\mathbf{k} \end{aligned}$$

where

$$\begin{aligned} J_{p1} &= \left. \begin{aligned} &M \left[\left(f - \frac{dh}{d\varepsilon_1} \right) \cos \alpha - \frac{d\sigma_1}{d\varepsilon_1} \sin \alpha \right] + \frac{dh}{d\varepsilon_1} - \frac{d\sigma_2}{d\varepsilon_1} \sin \alpha \\ &+ \frac{d^2f}{d\varepsilon_1^2} + \frac{dM}{d\varepsilon_1} \left[(y_p - h) \cos \alpha - z_p \sin \alpha \right] \end{aligned} \right\} \\ J_{p2} &= \left. \begin{aligned} &M \left[\left(h + \frac{df}{d\varepsilon_1} \right) \cos \alpha + z_p \sin \alpha \right] - \frac{dM}{d\varepsilon_1} (x_p - f) \cos \alpha \\ &- \frac{df}{d\varepsilon_1} - \frac{d^2\sigma_2}{d\varepsilon_1^2} \sin \alpha + \frac{d^2h}{d\varepsilon_1^2} \end{aligned} \right\} \quad (2.151) \\ J_{p3} &= \left. \begin{aligned} &-M \left(y_p + \frac{df}{d\varepsilon_1} \right) \sin \alpha + \frac{dM}{d\varepsilon_1} (x_p - f) \sin \alpha \\ &- \frac{d^2\sigma_1}{d\varepsilon_1^2} - \frac{d^2\sigma_2}{d\varepsilon_1^2} \cos \alpha \end{aligned} \right\} \end{aligned}$$

The parameter \mathbf{J}_p is a very important one which will be used in calculation of curvature values and other second order differential parameters.

2.4 Geometry of Conjugate Configuration

2.4.1 Conjugate Configuration

Conjugate Configurations, Quasi-Conjugate Configurations and Conjugate Surfaces

Suppose that motions of bodies I, II with respect to reference frame O are ϕ_1 and ϕ_2 respectively, if in the whole course of motion, the boundary configurations A, \bar{A} of bodies I, II can remain in continuous contact with each other without any interference, (A, \bar{A}) may then be recognized as a pair of conjugate configurations under the conjugate motion (ϕ_1, ϕ_2) . Conjugate configuration and conjugate motion are interdependent on each other, and their composition is called the conjugate pair. The geometric foundation of a conjugate pair is a pair of conjugate configurations (A, \bar{A}) , and the behaviour with respect to time (or with respect to a kinematic variable) of a conjugate pair is a pair of conjugate motions.

If the boundary configurations A, \bar{A} of rigid bodies I, II can keep continuous contact with each other without any interference during only part of the motion, while in the remaining part of the motion A and \bar{A} do not directly come into contact with each other, that is, there exists neither contact nor interference between bodies I and II, (A, \bar{A}) are then said to be quasi-conjugate configurations under the conjugate motion (ϕ_1, ϕ_2) . Either one of a pair of quasi-conjugate configurations is referred to as the fundamental conjugate configuration, while the other one is called the limit conjugate configuration. The composition of the quasi-conjugate configuration and conjugate motion is regarded as the quasi-conjugate pair.

Although the boundary configurations A and \bar{A} of rigid bodies I, II can contain curves and points, surfaces are required for conjugation. In order to highlight this fact, conjugate configurations (A, \bar{A}) are also usually referred to as the conjugate surfaces (A, \bar{A}) .

Conjugate Contact Point and Conjugate Point

1. Definition.

At any instant, points in contact between a pair of conjugate configurations are defined as a pair of conjugate contact points at the given instant. At any other instant, due to the conjugate motion of bodies I, II, the original pair of conjugate contact points will be separated from each other and consequently become a pair of

corresponding points respectively on the individual conjugate surface. Such a pair of points are defined as a pair of conjugate points.

2. Conditions to be Satisfied by Conjugate Contact Points.

(1). The conjugate contact point $\mathbf{R}_{1t}(\mathbf{R}_{1p})$ of body I must coincide with the conjugate contact point $\mathbf{R}_{2t}(\mathbf{R}_{2p})$ of body II, that is,

In the general conjugate motion,

$$\mathbf{R}_{1t} = \mathbf{R}_{2t} \quad (2.152)$$

In the simple conjugate motion,

$$\mathbf{R}_{1p} - \mathbf{R}_{2p} = l\mathbf{p} \quad (2.153)$$

(2). Coincidence of the unit normal, i.e.,

In the general conjugate motion,

$$\mathbf{N}_{1t} = -\mathbf{N}_{2t} \quad (2.154)$$

In the simple conjugate motion,

$$\mathbf{N}_{1p} = -\mathbf{N}_{2p} \quad (2.155)$$

(3). Relative velocity having no component along the common normal. i.e.,

In the general conjugate motion,

$$\mathbf{N}_{1t} \cdot \mathbf{v}_t^{12} = 0 \quad (2.156)$$

In the simple conjugate motion,

$$\mathbf{N}_{1p} \cdot \mathbf{v}_p^{12} = 0 \quad (2.157)$$

(4). No interference in the neighborhood of the contact point, i.e., the relative normal curvature \overline{K}_τ at that point along any tangential direction τ must satisfy

$$\overline{K}_\tau = K_{1\tau} + K_{2\tau} \geq 0 \quad (2.158)$$

Instantaneous Line of Contact and Line of Contact

In the case of line contact between a pair of conjugate surfaces, at any instant, a pair of conjugate surfaces come into contact with each other along one curve, and this curve is defined as the instantaneous line of contact at the given instant. At any other time, due to the conjugate motions of bodies I, and II, the initial instantaneous lines of contact will move apart from each other and become a pair of corresponding curves lying on the individual conjugate surfaces respectively, and such a pair of curves are defined as a pair of lines of contact. In certain special cases, there may be simultaneous contact along several lines of contact.

Surface of Engagement

A virtual geometrical surface, in the fixed reference space, composed of the totality of points of contact at different instants, is defined as the surface of engagement B.

The Five Types of Problems of Conjugate Surfaces or Curvatures

There are five types of problem which are frequently met in the geometry of conjugate surfaces and curvatures.

1. Problem Type 1.

Given a conjugate surface A and a pair of conjugate motions ϕ_1, ϕ_2 ; determine the conjugate surface \bar{A} and the surface of engagement B. This kind of problem is often encountered in the mechanical cutting process.

2. Problem Type 2.

Given a surface of engagement B and a pair of conjugate motions ϕ_1, ϕ_2 ; determine a pair of conjugate surfaces A and \bar{A} . This kind of problem arises in the design of tooth profiles for a gear pump.

3. Problem Type 3.

Given a pair of conjugate surfaces A, \bar{A} and a conjugate motion ϕ_1 or ϕ_2 ; determine the surface of engagement B and the conjugate motion ϕ_2 or ϕ_1 . This kind of problem occurs when tooth contact analysis is carried out.

4. Problem Type 4.

Given a conjugate surface A, a surface of engagement B and a conjugate motion ϕ_1 ; determine the conjugate surface \bar{A} and the conjugate motion ϕ_2 . The solution to this kind of problem is often required in measuring the accuracy of profiles formed by a cutting process.

5. Problem Type 5.

Given a pair of conjugate surfaces A, \bar{A} and a surface of engagement B; determine the pair of conjugate motions ϕ_1 and ϕ_2 . This type of problem is often encountered in the development of programs for a C.N.C. (computer-numerically-controlled) machine.

2.4.2 Global Geometry of Line-Contacting Simple Conjugate Surfaces with Single Degree of Freedom

Computation Procedure for the Solution to the First Kind of Problem of Conjugate Surfaces

1. Given Terms.

(1) The first conjugate surface A.

The parametric equation of A which is usually a surface.

$$\mathbf{R}_1 = x(u, v)\mathbf{i} + y(u, v)\mathbf{j} + z(u, v)\mathbf{k} \quad (2.159)$$

The unit normal \mathbf{N}_1 of A at the point \mathbf{R}_1 given by expressions (2.14) and (2.15)

$$\left. \begin{aligned} \mathbf{N}_1 &= A\mathbf{i} + B\mathbf{j} + C\mathbf{k} \\ A &= \frac{1}{Q} \left(\frac{\partial y}{\partial u} \frac{\partial z}{\partial v} - \frac{\partial y}{\partial v} \frac{\partial z}{\partial u} \right) \\ B &= \frac{1}{Q} \left(\frac{\partial z}{\partial u} \frac{\partial x}{\partial v} - \frac{\partial z}{\partial v} \frac{\partial x}{\partial u} \right) \\ C &= \frac{1}{Q} \left(\frac{\partial x}{\partial u} \frac{\partial y}{\partial v} - \frac{\partial x}{\partial v} \frac{\partial y}{\partial u} \right) \\ Q &= \pm \sqrt{\left(\frac{\partial y}{\partial u} \frac{\partial z}{\partial v} - \frac{\partial y}{\partial v} \frac{\partial z}{\partial u} \right)^2 + \left(\frac{\partial z}{\partial u} \frac{\partial x}{\partial v} - \frac{\partial z}{\partial v} \frac{\partial x}{\partial u} \right)^2 + \left(\frac{\partial x}{\partial u} \frac{\partial y}{\partial v} - \frac{\partial x}{\partial v} \frac{\partial y}{\partial u} \right)^2} \end{aligned} \right\} \quad (2.160)$$

Where, the sign " \pm " is so defined that the positive direction of \mathbf{N}_1 points from the body to the space.

(2) Conjugate motions ϕ_1 and ϕ_2 .

Due to the single degree of freedom, there exists only one independent parametric variable. Usually, the conjugate motion ϕ_1 of body I contains rotation, therefore ε_1

can be taken as the independent parametric variable, and all the other parametric variables of conjugate motions are functions of ε_1 . Given conjugate motions ϕ_1 and ϕ_2 implies that the following expressions are known,

$$\left. \begin{aligned} \varepsilon_2 &= \varepsilon_2(\varepsilon_1), \quad \sigma_1 = \sigma_1(\varepsilon_1), \quad \sigma_2 = \sigma_2(\varepsilon_1). \\ f &= f(\varepsilon_1), \quad h = h(\varepsilon_1) \end{aligned} \right\} \quad (2.161)$$

2. Terms to be Solved.

The surface of engagement B and the second conjugate surface \bar{A} .

The surface of engagement B can be given in the coordinate system $O - i, j, k$

$$\mathbf{r}_1 = x_1 \mathbf{i} + y_1 \mathbf{j} + z_1 \mathbf{k} \quad (2.162)$$

The second conjugate surface \bar{A} can be expressed in the coordinate system $O' - i', j', k'$

$$\mathbf{R}_2 = x' \mathbf{i}' + y' \mathbf{j}' + z' \mathbf{k}' \quad (2.163)$$

3. Steps of The Computation Procedure.

(1) Determine the values of the coordinates and the unit normal on a point of the surface A. Choosing a pair of values (u,v), use expressions (2.159) and (2.160) to obtain \mathbf{R}_1 and \mathbf{N}_1 .

(2) Find the corresponding value of ε_1 . After the elapse of time ε_1 , \mathbf{R}_1 and \mathbf{N}_1 will reach the position of conjugate contact, i.e., becoming a conjugate contact point. At that time, \mathbf{R}_1 will become \mathbf{R}_{1p} and \mathbf{N}_1 will become \mathbf{N}_{1p} . The use of expression (2.122) gives

$$\left. \begin{aligned} \mathbf{R}_{1p} &= (\varepsilon_1 \mathbf{k}) \otimes \mathbf{R}_1 + \sigma_1 \mathbf{k} \\ \mathbf{N}_{1p} &= (\varepsilon_1 \mathbf{k}) \otimes \mathbf{N}_1 \end{aligned} \right\} \quad (2.164)$$

Being conjugate contact points, requirement (2.157) must be satisfied, i.e., $\mathbf{N}_{1p} \cdot \mathbf{v}_p^{12} = 0$. Substitution of expressions (2.129) and (2.164) into (2.157) will yield

$$U \cos \varepsilon_1 - V \sin \varepsilon_1 = W \quad (2.165)$$

Where, U, V, W are determined by the followings

$$\left. \begin{aligned} U &= A[Mh \cos \alpha + M(z + \sigma_1) \sin \alpha - \frac{df}{d\varepsilon_1}] \\ &\quad - B(Mf \cos \alpha + \frac{dh}{d\varepsilon_1} - \sin \alpha \frac{d\sigma_2}{d\varepsilon_1}) - CMx \sin \alpha \\ V &= A(Mf \cos \alpha + \frac{dh}{d\varepsilon_1} - \sin \alpha \frac{d\sigma_2}{d\varepsilon_1}) \\ &\quad + B[Mh \cos \alpha + M(z + \sigma_1) \sin \alpha - \frac{df}{d\varepsilon_1}] - CM y \sin \alpha \\ W &= (1 + M \cos \alpha)(Ay - Bx) \\ &\quad - C(Mf \sin \alpha + \frac{d\sigma_1}{d\varepsilon_1} + \cos \alpha \frac{d\sigma_2}{d\varepsilon_1}) \end{aligned} \right\} \quad (2.166)$$

Here, $M = \frac{d\varepsilon_2}{d\varepsilon_1}$.

Expression (2.165) can be rewritten in the form,

$$\varepsilon_1 = \arccos\left(\frac{W}{\sqrt{U^2 + V^2}}\right) - \arctan\left(\frac{V}{U}\right) \quad (2.167)$$

In the general case, U , V and W are functions of ε_1 , so the solution to ε_1 can not be calculated directly from expression (2.167) and must be found numerically. In engineering practice, the case being often faced is that M , f , h , σ_1 , $\frac{d\sigma_2}{d\varepsilon_1}$ are constants. In this case, it is known from expression (2.166) that U , V and W are not functions of ε_1 , expression (2.167) will directly provide the value of ε_1 .

(3). Determine the corresponding values of ε_2 , σ_1 , σ_2 , f , h . The substitution of the value of ε_1 obtained in (2) into expression (2.161) yields the corresponding values.

(4). Determine the corresponding point \mathbf{r}_1 of the surface of engagement B. \mathbf{r}_1 in the coordinate system $O - \mathbf{i}, \mathbf{j}, \mathbf{k}$ can be found by substituting the values of ε_1 and σ_1 obtained in steps (2), (3) into expression (2.122)

$$\left. \begin{aligned} x_1 &= x \cos \varepsilon_1 - y \sin \varepsilon_1 \\ y_1 &= x \sin \varepsilon_1 + y \cos \varepsilon_1 \\ z_1 &= z + \sigma_1 \end{aligned} \right\} \quad (2.168)$$

(5). Determine the unit normal \mathbf{N}_{1p} to the first conjugate surface A at point \mathbf{r}_1 . The expansion of the second formula in expression (2.164) will give

$$\left. \begin{aligned} \mathbf{N}_{1p} &= A_p \mathbf{i} + B_p \mathbf{j} + C_p \mathbf{k} \\ A_p &= A \cos \varepsilon_1 - B \sin \varepsilon_1 \\ B_p &= A \sin \varepsilon_1 + B \cos \varepsilon_1 \\ C_p &= C \end{aligned} \right\} \quad (2.169)$$

(6). Determine the point-vector \mathbf{r}'_1 , with respect to coordinate system $O' - \mathbf{i}', \mathbf{j}', \mathbf{k}'$, corresponding to point \mathbf{r}_1 . Application of expressions (2.119), (2.120) and (2.153) will express the point-vector \mathbf{r}'_1 as

$$\left. \begin{aligned} \mathbf{r}'_1 &= \mathbf{R}_{2p} = x'_1 \mathbf{i}' + y'_1 \mathbf{j}' + z'_1 \mathbf{k}' \\ x'_1 &= x_1 - f \\ y'_1 &= (y_1 - h) \cos \alpha - z_1 \sin \alpha \\ z'_1 &= (y_1 - h) \sin \alpha + z_1 \cos \alpha \end{aligned} \right\} \quad (2.170)$$

(7) Determine the unit normal \mathbf{N}_{2p} to the second conjugate surface at the point \mathbf{r}_1 (i.e., \mathbf{r}'_1). The employment of expressions (2.119) and (2.155) will give

$$\left. \begin{aligned} \mathbf{N}_{2p} &= -\mathbf{N}_{1p} = A'_p \mathbf{i}' + B'_p \mathbf{j}' + C'_p \mathbf{k}' \\ A'_p &= -A_p \\ B'_p &= -B_p \cos \alpha + C_p \sin \alpha \\ C'_p &= -B_p \sin \alpha - C_p \cos \alpha \end{aligned} \right\} \quad (2.171)$$

(8). Determine the corresponding conjugate point \mathbf{R}_2 on the second conjugate surface \bar{A} . The use of expressions (2.118) and (2.125) yields

$$\left. \begin{aligned} \mathbf{R}_2 &= (\varepsilon_2 \mathbf{k}') \otimes \mathbf{r}'_1 + \sigma_2 \mathbf{k}' = x' \mathbf{i}' + y' \mathbf{j}' + z' \mathbf{k}' \\ x' &= x'_1 \cos \varepsilon_2 - y'_1 \sin \varepsilon_2 \\ y' &= x'_1 \sin \varepsilon_2 + y'_1 \cos \varepsilon_2 \\ z' &= z'_1 + \sigma_2 \end{aligned} \right\} \quad (2.172)$$

(9). Determine the unit normal \mathbf{N}_2 to the second conjugate surface \bar{A} at the point \mathbf{R}_2 . With the aid of expression (2.118), \mathbf{N}_2 can be found as

$$\left. \begin{aligned} \mathbf{N}_2 &= A' \mathbf{i}' + B' \mathbf{j}' + C' \mathbf{k}' \\ A' &= A'_p \cos \varepsilon_2 - B'_p \sin \varepsilon_2 \\ B' &= A'_p \sin \varepsilon_2 + B'_p \cos \varepsilon_2 \\ C' &= C'_p \end{aligned} \right\} \quad (2.173)$$

(10). Choose another value of a pair of parameters (u, v), and repeat the steps from (1) to (10), until the entire surfaces B and \bar{A} are obtained.

Line-Contacting Simple Conjugate Surfaces of Single Degree of Freedom with Double Branches

In the general case of simple conjugate motion with a single degree of freedom, points on a pair of line-contacting conjugate surfaces A and \bar{A} are one to one correspondent. When simple conjugate motion with a single degree of freedom meets some specific constraint conditions, one point on surface A might have two different corresponding conjugate points and one point on surface \bar{A} might also have two different corresponding conjugate points, and sometimes, on surface A or \bar{A} there may exist points that have no corresponding conjugate points.

1. Constraints to Conjugate Motion.

No variations in positions of axes of rotation; constant transmission ratio; no axial translation of the body I; constant velocity of axial translation of the body II, namely,

$$\left. \begin{aligned} f &= \text{constant} & h &= \text{constant} \\ M = \frac{d\varepsilon_2}{d\varepsilon_1} &= \text{constant} & \sigma_1 = \frac{d\sigma_1}{d\varepsilon_1} &= 0 & \frac{d\sigma_2}{d\varepsilon_1} &= \text{constant} \end{aligned} \right\} \quad (2.174)$$

2. Double Solutions.

The corresponding values of U , V , W can be found by substituting expression (2.174) into expression (2.166), that is,

$$\left. \begin{aligned} U &= AM(h \cos \alpha + z \sin \alpha) - B(Mf \cos \alpha - \sin \alpha \frac{d\sigma_2}{d\varepsilon_1}) - CMx \sin \alpha \\ V &= A(Mf \cos \alpha - \sin \alpha \frac{d\sigma_2}{d\varepsilon_1}) + BM(h \cos \alpha + z \sin \alpha) - CM y \sin \alpha \\ W &= (1 + M \cos \alpha)(Ay - Bx) - C(Mf \sin \alpha + \cos \alpha \frac{d\sigma_2}{d\varepsilon_1}) \end{aligned} \right\} \quad (2.175)$$

Since the unit normal vector $(Ai + Bj + Ck)$ to the surface A at a point is the function of the position $(xi + yj + zk)$ of the point, in view of expression (D.24), it is found that U , V , W are functions only of the position of the point, instead of functions of ε_1 , i.e.,

$$\left. \begin{aligned} U &= U(x, y, z) \\ V &= V(x, y, z) \\ W &= W(x, y, z) \end{aligned} \right\} \quad (2.176)$$

Once a point on surface A is specified, U , V , W are accordingly determined, and the corresponding value of ε_1 can be found directly from expression (2.167).

If U , V , W satisfy the following condition

$$U^2 + V^2 > W^2 \quad (2.177)$$

then, the term $\arccos(\frac{W}{\sqrt{U^2 + V^2}})$ in expression (2.167) will yield two solutions within the range of from $-\pi$ to π , i.e., the whole cycle (2π); that is, $\pm\theta$. The value of θ can be given as

$$\cos \theta = \frac{W}{\sqrt{U^2 + V^2}} \quad (2.178)$$

Where $\pi > \theta > 0$.

Therefore, double solutions corresponding to the value of ε_1 at the point on the surface arise; that is,

$$\varepsilon_1 = \theta - \delta \quad (2.179)$$

and

$$\varepsilon_1 = -\theta - \delta \quad (2.180)$$

where, the value of δ within the range of from 0 to 2π is calculated from equation (2.167) as

$$\left. \begin{aligned} \sin \delta &= \frac{V}{\sqrt{U^2+V^2}} \\ \cos \delta &= \frac{U}{\sqrt{U^2+V^2}} \end{aligned} \right\} \quad (2.181)$$

3. Double Branches of a Conjugate Surface.

Due to double solutions of the values of ε_1 , there are two conjugate points, instead of one, corresponding to one point of the surface A, thus, constituting two pieces of a surface, regarded as the first and second branch of the conjugate surface \bar{A} . Figure 2.7 shows double branches of the involute tooth surface. AB and A'B' in fig.2.7 are the same involute tooth surface in different positions, CD is accordingly the first branch of the conjugate surface and EF the second branch of the conjugate surface. Generally, the first and second branches of the conjugate surface intersect each other, and the line of intersection between the first and second branches corresponds to two different curves of the first conjugate surface A.

4. Condition for Tangency of Two Branches.

If on surface A there is a curve on which all points satisfy the condition

$$U^2 + V^2 = W^2 \quad (2.182)$$

then, $\theta = 0$ when $W > 0$, or $\theta = \pi$ when $W < 0$. $+\theta$ and $-\theta$ have no material difference. ε_1 no longer has double solutions but has a unique solution, that is, there is only one, rather than two, conjugate curve which corresponds to the curve on surface A. The two branches of the conjugate surface do not intersect each other any more but touch each other along a line.

5. Region of No Conjugate Solution.

If points within the area of surface A satisfy the following condition

$$U^2 + V^2 < W^2 \quad (2.183)$$

then, θ has no real solution, and consequently, ε_1 has no real solution. This implies that the points within this area will never reach the state of conjugate contact, and this area is called region of no conjugate solution.

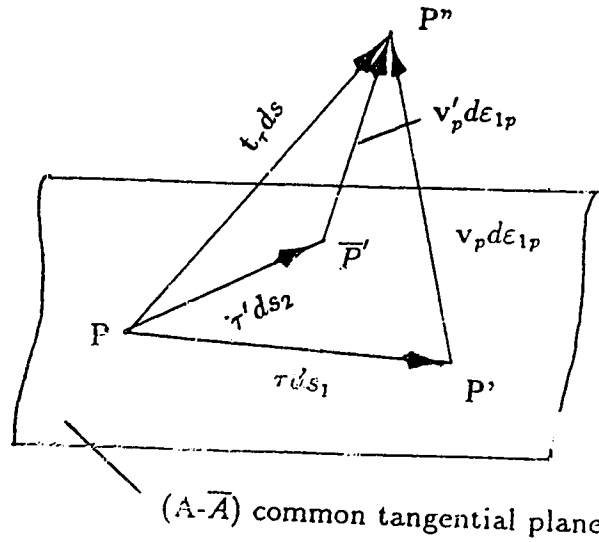


Figure 2.8: Relationships among three fundamental differential quantities

ds_2 and ds are called three fundamental differential quantities. They are related to each other. When $ds_1 \rightarrow 0$, ds_2 , ds will also tend to zero, i.e., $ds_2 \rightarrow 0$, $ds \rightarrow 0$, and therefore, when $ds_1 \rightarrow 0$, \bar{P}' will lie on the common tangential plane to the point P of surfaces $(A-\bar{A})$ as well.

2. Angular (i.e., Time) Increment.

At instant ε_{1p} , P' and \bar{P}' are, in general, two separated points, but a pair of conjugate points, and therefore, eventually in some instant, say, $(\varepsilon_{1p} + d\varepsilon_{1p})$, both points P' and \bar{P}' will move to the common conjugate contact point P'' . The corresponding time increment $d\varepsilon_{1p}$ is also called the angular increment, which stands for the increment, calculated from ε_{1p} , of the rotating angle ε_1 of body I as the independent parametric variable of simple conjugate motion with a single degree of freedom.

3. The First Conjugate Relation.

Since $ds_1, d\varepsilon_{1p}$ are infinitesimal, the vector from point P' to P'' with precision of the first order infinitesimal may be thought of as the product of the velocity \mathbf{v}_p of point P on body I determined by expression (2.126) and the time (angular) increment $d\varepsilon_{1p}$. Then, the first conjugate relation is expressed as

$$\mathbf{t}_\tau ds = \vec{P\bar{P}''} = \vec{P\bar{P}'} + \vec{P'\bar{P}''} = \tau ds_1 + \mathbf{v}_p d\varepsilon_{1p} \quad (2.184)$$

4. The Second Conjugate Relation.

Similarly, the vector from point \bar{P}' to P'' can be seen to be equal to the product of \mathbf{v}'_p determined by expression (2.127) by the time (angular) increment $d\varepsilon_{1p}$,

$$\mathbf{t}_\tau ds = P\bar{P}'' = P\bar{P}' + \bar{P}'P'' = \tau' ds_2 + \mathbf{v}'_p d\varepsilon_{1p} \quad (2.185)$$

With the aid of expressions (2.184) and (2.185) and taking into account $\mathbf{v}_p - \mathbf{v}'_p = \mathbf{v}_p^{12}$, the second conjugate relation may be established as

$$\tau' ds_2 = \tau ds_1 + \mathbf{v}_p^{12} d\varepsilon_{1p} \quad (2.186)$$

Where, \mathbf{v}_p^{12} is given by expression (2.129).

5. The Third Conjugate Relation.

Suppose that at instant ε_{1p} , the unit normals at point P of surfaces A and \bar{A} are \mathbf{N}_{1p} , \mathbf{N}_{2p} respectively. Then due to point P being the conjugate contact point at instant ε_{1p} , expression (2.155), i.e., $\mathbf{N}_{1p} = -\mathbf{N}_{2p}$, must be satisfied. Use of expression (2.17) provides the unit normal \mathbf{N}'_{1p} at point P' of surface A at instant ε_{1p}

$$\mathbf{N}_{1p'} = \mathbf{N}_{1p} + (d\mathbf{N}_{1p})_\tau = \mathbf{N}_{1p} + \boldsymbol{\Omega}_{1\tau} \times \mathbf{N}_{1p} ds_1 \quad (2.187)$$

where, $\boldsymbol{\Omega}_{1\tau}$ is the geometric angular velocity at point P of surface A in direction τ , as defined in equation (2.19).

Analogously, unit normal $\mathbf{N}_{2p'}$ to point \bar{P}' of surface \bar{A} is given by

$$\mathbf{N}_{2p'} = \mathbf{N}_{2p} + (d\mathbf{N}_{2p})_{\tau'} = \mathbf{N}_{2p} + \boldsymbol{\Omega}_{2\tau'} \times \mathbf{N}_{2p} ds_2 \quad (2.188)$$

where, $\boldsymbol{\Omega}_{2\tau'}$ is the geometric angular velocity at point P of surface \bar{A} in direction τ' .

At instant $(\varepsilon_{1p} + d\varepsilon_{1p})$, points P' and \bar{P}' will move to the common point P'', and the corresponding unit normal vectors $\mathbf{N}_{1p''}$ and $\mathbf{N}_{2p''}$ retaining only the first order infinitesimals are

$$\mathbf{N}_{1p''} = (d\varepsilon_{1p}\omega_1) \otimes \mathbf{N}_{1p'} = \mathbf{N}_{1p} + \boldsymbol{\Omega}_{1\tau} \times \mathbf{N}_{1p} ds_1 + \omega_1 \times \mathbf{N}_{1p} d\varepsilon_{1p} \quad (2.189)$$

$$\mathbf{N}_{2p''} = (d\varepsilon_{2p}\omega_2) \otimes \mathbf{N}_{2p'} = \mathbf{N}_{2p} + \boldsymbol{\Omega}_{2\tau'} \times \mathbf{N}_{2p} ds_2 + \omega_2 \times \mathbf{N}_{2p} d\varepsilon_{2p} \quad (2.190)$$

Since point P'' is the conjugate contact point at the instant $(\varepsilon_{1p} + d\varepsilon_{1p})$, we know $\mathbf{N}_{1p''} = -\mathbf{N}_{2p''}$. Then, using expressions (2.189) and (2.190), and taking into account $\mathbf{N}_{1p} = -\mathbf{N}_{2p}$, $d\varepsilon_{2p} = M d\varepsilon_{1p}$, we obtain

$$\Omega_{2\tau'} \times N_{1p} ds_2 = \Omega_{1\tau} \times N_{1p} ds_1 + (\omega_1 - M\omega_2) \times N_{1p} d\varepsilon_{1p} \quad (2.191)$$

Substitution from expressions (2.133) to (2.191) produces the third conjugate relation

$$\Omega_{2\tau'} \times N_{1p} ds_2 = \Omega_{1\tau} \times N_{1p} ds_1 + \eta_p d\varepsilon_{1p} \quad (2.192)$$

where, η_p , defined in equation (2.133), is the equivalent projection component of the angular velocity of body I relative to body II. By using expression (2.19) to expand $\Omega_{1\tau}$ and $\Omega_{2\tau'}$ in terms of the conjugate normal curvature $K'_{2\tau'}$ and the conjugate torsional curvature $G'_{2\tau'}$, and taking into consideration $N_{2p} = -N_{1p}$, the third conjugate relation (2.192) can be rewritten as

$$[K'_{2\tau'}\tau' + G'_{2\tau'}(N_{1p} \times \tau')]ds_2 = -[K_{1\tau}\tau + G_{1\tau}(N_{1p} \times \tau)]ds_1 - \eta_p d\varepsilon_{1p} \quad (2.193)$$

Rate of Angular Increment

1. Definition.

The rate of change $(\frac{d\varepsilon_{1p}}{ds_1})_\tau$ of the rotational angle ε_{1p} with respect to the arc length ds_1 of the first conjugate surface A along the tangential direction τ is defined as the rate of angular increment at point P of surface A in direction τ . Since there is line contact, direction τ can be chosen arbitrarily in the tangent plane.

2. The Other Form of Harmonic Equation of Surface Curvatures.

Expression (2.42) gave a relation between the normal and torsional curvatures in directions \mathbf{t} and \mathbf{u} .

$$\frac{K_t - K_u}{G_u + G_t} = \tan \theta_{ut} = \frac{\sin \theta_{ut}}{\cos \theta_{ut}} = \frac{\mathbf{N} \cdot (\mathbf{u} \times \mathbf{t})}{\mathbf{u} \cdot \mathbf{t}} \quad (2.194)$$

then

$$[K_t \mathbf{t} + G_t(\mathbf{N} \times \mathbf{t})] \cdot \mathbf{u} = [K_u \mathbf{u} + G_u(\mathbf{N} \times \mathbf{u})] \cdot \mathbf{t}$$

With the aid of expression (2.16), the above expression can be rewritten as

$$(\frac{d\mathbf{N}}{ds})_u \cdot \mathbf{t} = (\frac{d\mathbf{N}}{ds})_t \cdot \mathbf{u} \quad (2.195)$$

In virtue of expression (2.17), expression (2.195) can be transformed into the other form of harmonic equation of surface curvatures

$$(\Omega_u \times \mathbf{N}) \cdot \mathbf{t} = (\Omega_t \times \mathbf{N}) \cdot \mathbf{u} \quad (2.196)$$

3. Calculating Formula.

From the definition of the conjugate relative acceleration, i.e., expression (2.149), and relation (2.130), that is, $\mathbf{v}_p^{21} = -\mathbf{v}_p^{12}$, the velocity \mathbf{v}_{dp}^{12} at point P of body I relative to body II at instant $(\varepsilon_{1p} + d\varepsilon_{1p})$, under the condition of body I returning to the position of the original instant ε_{1p} , may be found as

$$\mathbf{v}_{dp}^{12} = \mathbf{v}_p^{12} - \mathbf{J}_p d\varepsilon_{1p} \quad (2.197)$$

At instant $(\varepsilon_{1p} + d\varepsilon_{1p})$, the angular velocity of body I relative to body II is $[(\omega_1 - M\omega_2) + \frac{d(\omega_1 - M\omega_2)}{d\varepsilon_{1p}} d\varepsilon_{1p}]$, and then, at instant $(\varepsilon_{1p} + d\varepsilon_{1p})$, under the condition of body I returning to the position of initial instant ε_{1p} , the velocity at point P' as shown in fig. 2.8 of body I relative to body II, precise to the first order infinitesimal, is found as

$$\mathbf{v}_{dp'}^{12} = \mathbf{v}_{dp}^{12} + (\omega_1 - M\omega_2) \times \tau ds_1$$

Substitution of expression (2.197) into the foregoing expression may yield

$$\mathbf{v}_{dp'}^{12} = \mathbf{v}_{dp}^{12} - \mathbf{J}_p d\varepsilon_{1p} + (\omega_1 - M\omega_2) \times \tau ds_1 \quad (2.198)$$

Still remaining at instant $(\varepsilon_{1p} + d\varepsilon_{1p})$, and returning body I to the position of instant $(\varepsilon_{1p} + d\varepsilon_{1p})$, point P' will reach point P'' as shown in fig. 2.8, and then, the relative linear velocity $\mathbf{v}_{p''}^{12}$ at point P'' is in the form

$$\mathbf{v}_{p''}^{12} = (d\varepsilon_{1p}\omega_1) \otimes \mathbf{v}_{dp'}^{12} \quad (2.199)$$

Due to point P'' being the conjugate contact point at instant $(\varepsilon_{1p} + d\varepsilon_{1p})$, expression (2.157) must be satisfied, that is,

$$\mathbf{N}_{1p''} \cdot \mathbf{v}_{p''}^{12} = 0 \quad (2.200)$$

Substitution of expressions (2.189), (2.199) into (2.200) yields

$$\mathbf{N}_{1p'} \cdot \mathbf{v}_{dp'}^{12} = 0 \quad (2.201)$$

Substitution from expressions (2.187), (2.198) into (2.201), with the aid of $\mathbf{v}_p^{12} \cdot \mathbf{N}_{1p} = 0$ and neglecting any value higher than the first order infinitesimal, yields

$$(\boldsymbol{\omega}_1 \times \mathbf{N}_{1p}) \cdot \mathbf{v}_p^{12} ds_1 - \mathbf{N}_{1p} \cdot \mathbf{J}_p d\varepsilon_{1p} + \mathbf{N}_{1p} \cdot [(\omega_1 - M\omega_2) \times \tau] ds_1 = 0 \quad (2.202)$$

With the aid of expressions (2.133) and (2.196), expression (2.202) may be rewritten as

$$|\mathbf{v}_p^{12}|(\boldsymbol{\Omega}_{1v} \times \mathbf{N}_{1p}) \cdot \tau d\mathbf{s}_1 - \mathbf{N}_{1p} \cdot \mathbf{J}_p d\boldsymbol{\varepsilon}_{1p} - \eta_p \cdot \tau d\mathbf{s}_1 = 0 \quad (2.203)$$

Consequently, the expression for calculating the rate of angular increment may be found

$$\left(\frac{d\boldsymbol{\varepsilon}_{1p}}{ds_1}\right)_\tau = \frac{[|\mathbf{v}_p^{12}|(\boldsymbol{\Omega}_{1v} \times \mathbf{N}_{1p}) - \eta_p]}{\mathbf{N}_{1p} \cdot \mathbf{J}_p} \cdot \tau \quad (2.204)$$

where, $\boldsymbol{\Omega}_{1v}$ is the geometric angular velocity at point P of surface A in direction $\frac{\mathbf{v}_p^{12}}{|\mathbf{v}_p^{12}|}$.

Conjugate Angular Velocity and Its Equivalent Projection Component.

1. Conjugate Angular Velocity.

The angular velocity of body II relative to body I at instant $\boldsymbol{\varepsilon}_{1p}$ is $\boldsymbol{\Omega}_{21} = M\omega_2 - \omega_1$. The sliding velocity at the conjugate contact point P of body II relative to body I at instant $\boldsymbol{\varepsilon}_{1p}$ is $\mathbf{v}_p^{21} = -\mathbf{v}_p^{12}$, that is, body II slides a distance $-|\mathbf{v}_p^{12}|$ in the tangential direction $\frac{\mathbf{v}_p^{12}}{|\mathbf{v}_p^{12}|}$ with respect to body I within the unit time (angle). Since the first conjugate surface A at point P is curved and its geometric angular velocity in the tangential direction $\frac{\mathbf{v}_p^{12}}{|\mathbf{v}_p^{12}|}$ is $\boldsymbol{\Omega}_{1v}$, if surface A at point P is reduced to a plane, the equivalent angular velocity \mathbf{W}_p of body II relative to body I should include the angular velocity $[-(-|\mathbf{v}_p^{12}|)\boldsymbol{\Omega}_{1v}]$ in addition to the physical relative angular velocity $\boldsymbol{\Omega}_{21}$. This equivalent relative angular velocity is referred to as the conjugate angular velocity at point P, that is,

$$\mathbf{W}_p = [-(-|\mathbf{v}_p^{12}|)\boldsymbol{\Omega}_{1v}] + \boldsymbol{\Omega}'_p = |\mathbf{v}_p^{12}|\boldsymbol{\Omega}_{1v} - (\omega_1 - M\omega_2) \quad (2.205)$$

2. Equivalent Projection Component.

The equivalent projection component of the conjugate angular velocity is defined as

$$\mathbf{U}_p = \mathbf{W}_p \times \mathbf{N}_{1p} \quad (2.206)$$

Substitution of expressions (2.205) into (2.206) together with the aid of expression (2.133) may produce

$$\mathbf{U}_p = |\mathbf{v}_p^{12}|\boldsymbol{\Omega}_{1v} \times \mathbf{N}_{1p} - \eta_p = |\mathbf{v}_p^{12}|\left(\frac{d\mathbf{N}_{1p}}{ds_1}\right)_v - \eta_p \quad (2.207)$$

In view of expression (2.206), \mathbf{U}_p is perpendicular to \mathbf{N}_{1p} , and \mathbf{U}_p is therefore a vector on the common tangential plane at point P, and can be resolved along two mutually perpendicular directions $\frac{\mathbf{v}_p^{12}}{|\mathbf{v}_p^{12}|}$ and $\Delta_p = \mathbf{N}_{1p} \times \frac{\mathbf{v}_p^{12}}{|\mathbf{v}_p^{12}|}$

$$\mathbf{U}_p = D_p \frac{\mathbf{v}_p^{12}}{|\mathbf{v}_p^{12}|} + E_p \Delta_p \quad (2.208)$$

Where

$$\left. \begin{aligned} D_p &= K_{1v} |\mathbf{v}_p^{12}| - |\eta_p| \cos \theta_{v\eta} \\ E_p &= G_{1v} |\mathbf{v}_p^{12}| - |\eta_p| \sin \theta_{v\eta} \end{aligned} \right\} \quad (2.209)$$

3. The Three Components of the Conjugate Angular Velocity.

\mathbf{W}_p can be resolved along three mutually perpendicular directions, that is,

$$\mathbf{W}_p = (\mathbf{W}_p \cdot \frac{\mathbf{v}_p^{12}}{|\mathbf{v}_p^{12}|}) \frac{\mathbf{v}_p^{12}}{|\mathbf{v}_p^{12}|} + (\mathbf{W}_p \cdot \Delta_p) \Delta_p + (\mathbf{W}_p \cdot \mathbf{N}_{1p}) \mathbf{N}_{1p} \quad (2.210)$$

Substituting expressions (2.205) into (2.210), with the aid of expressions (2.17), (2.132), (2.133) and (2.209), gives

$$\mathbf{W}_p = -E_p \frac{\mathbf{v}_p^{12}}{|\mathbf{v}_p^{12}|} + D_p \Delta_p - \Omega_{sp} \mathbf{N}_{1p} \quad (2.211)$$

Expression (2.211) reveals that after reducing surface A at the point P into a plane, the angular velocity of body II relative to body I is the sum of three components of angular velocity, namely, angular velocity $-E_p$ in direction $\frac{\mathbf{v}_p^{12}}{|\mathbf{v}_p^{12}|}$; angular velocity D_p in direction Δ_p and angular velocity $-\Omega_{sp}$ in direction \mathbf{N}_{1p} .

Several Special Tangential Directions

There are seven special tangential directions in the common tangential plane at the conjugate contact point P of surfaces A, \bar{A} at instant ε_{1p} , namely, $\frac{\mathbf{v}_p^{12}}{|\mathbf{v}_p^{12}|}$, Δ_p , $\frac{\eta_p}{|\eta_p|}$, $\frac{\dot{\eta}_p}{|\dot{\eta}_p|}$, $\mathbf{g} = \frac{\mathbf{U}_p}{|\mathbf{U}_p|}$, \mathbf{e} , $\frac{\mathbf{W}_p}{|\mathbf{W}_p|}$, etc., as shown in fig.2.9.

1. The Direction of Relative Velocity $\frac{\mathbf{v}_p^{12}}{|\mathbf{v}_p^{12}|}$.

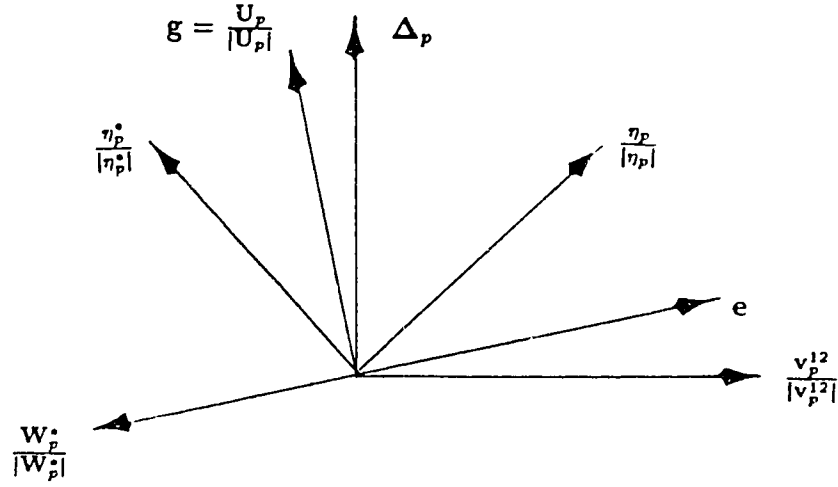


Figure 2.9: Several special tangential vectors

Since point P is a conjugate contact point, $\mathbf{N}_{1p} \cdot \mathbf{v}_p^{12} = 0$, that is, \mathbf{v}_p^{12} lies in the tangential plane, and thus, $\frac{\mathbf{v}_p^{12}}{|\mathbf{v}_p^{12}|}$ is a tangential direction at the point P.

2. The Tangential Direction Δ_p Perpendicular to \mathbf{v}_p^{12} .

Δ_p is defined as

$$\Delta_p = \mathbf{N}_{1p} \times \frac{\mathbf{v}_p^{12}}{|\mathbf{v}_p^{12}|} \quad (2.212)$$

Then, Δ_p lies in the common tangential plane, and is a unit tangential direction at point P.

3. The Direction of the Projection Component of the Relative Angular Velocity $\frac{\eta_p^*}{|\eta_p^*|}$.

It is known from definition (2.134) that η_p^* is perpendicular to \mathbf{N}_{1p} and lies in the common tangential plane, and $\frac{\eta_p^*}{|\eta_p^*|}$ is therefore a tangential direction at point P.

4. The Direction of the Equivalent Projection Component of the Relative Angular Velocity $\frac{\eta_p}{|\eta_p|}$.

It is known from expression (2.133) that η_p is perpendicular to \mathbf{N}_{1p} , and lies in the common tangential plane, and $\frac{\eta_p}{|\eta_p|}$ is therefore a tangential direction at point P.

5. The Direction of Maximum Rate of Angular Increment \mathbf{g} .

Substituting expressions (2.207) into (2.204), then

$$\left(\frac{d\varepsilon_{1p}}{ds_1}\right)_\tau = \frac{\mathbf{U}_p}{\mathbf{N}_{1p} \cdot \mathbf{J}_p} \cdot \boldsymbol{\tau} \quad (2.213)$$

In view of expression (2.213), when $\tau = \frac{\mathbf{U}_p}{|\mathbf{U}_p|}$, the corresponding value of $(\frac{d\varepsilon_{1p}}{ds_1})_\tau$ has its maximum value. Meanwhile, from the definition of \mathbf{U}_p , i.e., expression (2.206), \mathbf{U}_p is perpendicular to \mathbf{N}_{1p} and lies in the common tangential plane, and $\frac{\mathbf{U}_p}{|\mathbf{U}_p|}$ is therefore in the tangential direction at point P and is called the direction of the maximum rate of angular increment \mathbf{g} , that is,

$$\mathbf{g} = \frac{\mathbf{U}_p}{|\mathbf{U}_p|} = \frac{D_p}{\sqrt{D_p^2 + E_p^2}} \frac{\mathbf{v}_p^{12}}{|\mathbf{v}_p^{12}|} + \frac{E_p}{\sqrt{D_p^2 + E_p^2}} \Delta_p \quad (2.214)$$

By using expression (2.214), angle θ_{vg} of $\frac{\mathbf{v}_p^{12}}{|\mathbf{v}_p^{12}|}$ rotating about \mathbf{N}_{1p} to \mathbf{g} may be found

$$\left. \begin{aligned} \sin \theta_{vg} &= \frac{E_p}{\sqrt{D_p^2 + E_p^2}} \\ \cos \theta_{vg} &= \frac{D_p}{\sqrt{D_p^2 + E_p^2}} \end{aligned} \right\} \quad (2.215)$$

where, D_p , E_p are given by expressions (2.209).

The value g of the maximum rate of angular increment may be found

$$g = \left(\frac{d\varepsilon_{1p}}{ds_1} \right)_g = \frac{\sqrt{D_p^2 + E_p^2}}{\mathbf{N}_{1p} \cdot \mathbf{J}_p} \quad (2.216)$$

6. The Direction of the Instantaneous Line of Contact.

While $\tau = \mathbf{g} \times \mathbf{N}_{1p} = \frac{\mathbf{U}_p}{|\mathbf{U}_p|} \times \mathbf{N}_{1p}$, with the aid of expression (2.213), the corresponding value of $(\frac{d\varepsilon_{1p}}{ds_1})_\tau$ is equal to zero; that is, all the points on this tangential direction are conjugate contact points at the instant ε_{1p} , and hence, this direction is the direction of instantaneous line of contact \mathbf{e} . The use of expression (2.214) yields

$$\mathbf{e} = \mathbf{g} \times \mathbf{N}_{1p} = \frac{\mathbf{U}_p \times \mathbf{N}_{1p}}{|\mathbf{U}_p|} = \frac{E_p}{\sqrt{D_p^2 + E_p^2}} \frac{\mathbf{v}_p^{12}}{|\mathbf{v}_p^{12}|} - \frac{D_p}{\sqrt{D_p^2 + E_p^2}} \Delta_p \quad (2.217)$$

Angle θ_{ve} of $\frac{\mathbf{v}_p^{12}}{|\mathbf{v}_p^{12}|}$ rotating about \mathbf{N}_{1p} to \mathbf{e} can be found from the expression (2.217)

$$\left. \begin{aligned} \sin \theta_{ve} &= \frac{-D_p}{\sqrt{D_p^2 + E_p^2}} \\ \cos \theta_{ve} &= \frac{E_p}{\sqrt{D_p^2 + E_p^2}} \end{aligned} \right\} \quad (2.218)$$

7. The Direction of the Projection Component of the Conjugate Angular Velocity $\frac{\mathbf{W}_p^*}{|\mathbf{W}_p^*|}$

The projection component \mathbf{W}_p^* of the conjugate angular velocity \mathbf{W}_p on the common tangential plane is

$$\mathbf{W}_p^* = \mathbf{W}_p - (\mathbf{N}_{1p} \cdot \mathbf{W}_p) \mathbf{N}_{1p} = \mathbf{N}_{1p} \times (\mathbf{W}_p \times \mathbf{N}_{1p}) = \mathbf{N}_{1p} \times \mathbf{U}_p \quad (2.219)$$

Hence, unit vector $\frac{\mathbf{W}_p^*}{|\mathbf{W}_p^*|}$ is in a tangential direction at point P and use of expressions (2.214) and (2.217) yields

$$\frac{\mathbf{W}_p^*}{|\mathbf{W}_p^*|} = \mathbf{N}_{1p} \times \frac{\mathbf{U}_p}{|\mathbf{U}_p|} = \mathbf{N}_{1p} \times \mathbf{g} = -\mathbf{e} \quad (2.220)$$

Expression (2.220) shows that the direction of the projection component of the conjugate angular velocity is perpendicular to the direction of the maximum rate of angular increment and coincides with the direction of the instantaneous line of contact but in the opposite direction. After surface A at the conjugate contact point P is reduced to plane A^* , the motion of body II relative to body I can be represented by the reduced cylindric surface \bar{A}^* , i.e., the reduced surface corresponding to surface \bar{A} at the point P, rolling, sliding and twisting on plane A^* , i.e., the common tangential plane P of surfaces A and \bar{A} as shown in fig.2.12. After such a reduction, the kinematic meaning of expression (2.220) becomes very clear, that is, the straight line of contact \mathbf{e} between cylindric surface \bar{A}^* and plane A^* is just the rolling axis $\frac{\mathbf{W}_p^*}{|\mathbf{W}_p^*|}$ of the surface \bar{A}^* with respect to plane A^* except for the opposite direction. The rolling angular velocity of cylindric surface \bar{A}^* relative to plane A^* about $\frac{\mathbf{W}_p^*}{|\mathbf{W}_p^*|}$ as an axis is $|\mathbf{W}_p^*|$; the twisting angular velocity about \mathbf{N}_{1p} as an axis is $-\Omega_{sp}$, and furthermore, the relative sliding velocity is $-\mathbf{v}_p^{12}$.

Substitution of expressions (2.208) into (2.219) and using expression (2.212) may give rise to

$$\mathbf{W}_p^* = -\tilde{\mathbf{E}}_p \frac{\mathbf{v}_p^{12}}{|\mathbf{v}_p^{12}|} + D_p \Delta_p \quad (2.221)$$

Then

$$|\mathbf{W}_p^*| = |\mathbf{U}_p| = \sqrt{D_p^2 + E_p^2} \quad (2.222)$$

Formulas of Calculation for the Values of Line-Contacting Relative Curvatures

1. In Direction \mathbf{e} .

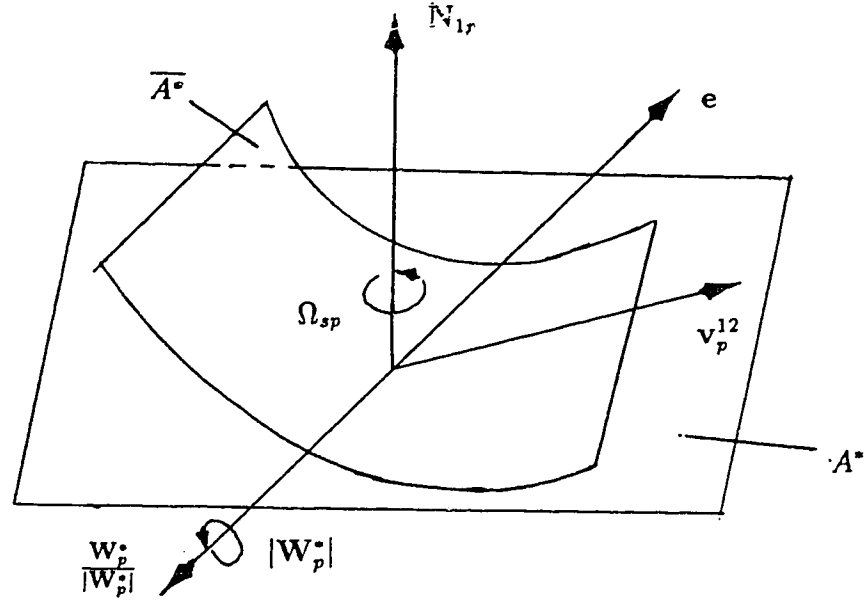


Figure 2.10: Reduced relative motion

Since we are considering line-contacting simple conjugate surfaces with a single degree of freedom, surfaces A and \bar{A} are completely coincident with each other in direction e ; that is, the relative geometric angular velocity $\bar{\Omega}_e$ in direction e is

$$\bar{\Omega}_e = 0 \quad (2.223)$$

With the aid of expression (2.37), expression (2.223) leads to the relative normal curvature \bar{K}_e and relative torsional curvature \bar{G}_e in direction e as follows

$$\left. \begin{aligned} \bar{K}_e &= 0 \\ \bar{G}_e &= 0 \end{aligned} \right\} \quad (2.224)$$

2. In Direction $\frac{v_p^{12}}{|v_p^{12}|}$.

When we consider direction $\tau = \frac{v_p^{12}}{|v_p^{12}|}$ in the surface tangent plane, expression (2.186) gives rise to

$$\left. \begin{aligned} \tau' &= \frac{v_p^{12}}{|v_p^{12}|} \\ \left(\frac{ds_2}{ds_1} \right)_\tau &= 1 + |v_p^{12}| \left(\frac{d\epsilon_{1p}}{ds_1} \right)_\tau \end{aligned} \right\} \quad (2.225)$$

Meanwhile, with the aid of expression (2.208), expression (2.213) gives

$$\left(\frac{d\varepsilon_{1p}}{ds_1}\right)_v = \frac{\mathbf{U}_p}{\mathbf{N}_{1p} \cdot \mathbf{J}_p} \cdot \frac{\mathbf{v}_p^{12}}{|\mathbf{v}_p^{12}|} = \frac{D_p}{\mathbf{N}_{1p} \cdot \mathbf{J}_p} \quad (2.226)$$

Furthermore, using expression (2.192),

$$\Omega_{2v} \times \mathbf{N}_{1p} ds_2 = \Omega_{1v} \times \mathbf{N}_{1p} ds_1 + \eta_p d\varepsilon_{1p}$$

With the aid of the definition in (2.37), i.e., $\bar{\Omega}_v = \Omega_{1v} - \Omega_{2v}$, expressions (2.225) and (2.226) are substituted into the above expression, to give relative geometric angular velocity $\bar{\Omega}_v$ in direction $\frac{\mathbf{v}_p^{12}}{|\mathbf{v}_p^{12}|}$

$$\bar{\Omega}_v \times \mathbf{N}_{1p} \left(\frac{ds_2}{ds_1}\right)_v = \Omega_{1v} \times \mathbf{N}_{1p} \left[\left(\frac{ds_2}{ds_1}\right)_v - 1\right] - \eta_p \left(\frac{d\varepsilon_{1p}}{ds_1}\right)_v$$

that is,

$$\bar{\Omega}_v \times \mathbf{N}_{1p} = \frac{(|\mathbf{v}_p^{12}| \Omega_{1v} \times \mathbf{N}_{1p} - \eta_p) D_p}{D_p |\mathbf{v}_p^{12}| + \mathbf{N}_{1p} \cdot \mathbf{J}_p} \quad (2.227)$$

or

$$\bar{\Omega}_v = \mathbf{N}_{1p} \times (\bar{\Omega}_v \times \mathbf{N}_{1p}) = \frac{D_p}{(D_p |\mathbf{v}_p^{12}| + \mathbf{N}_{1p} \cdot \mathbf{J}_p)} \mathbf{W}_p^* \quad (2.228)$$

With the aid of equations (2.37) and (2.221), expression (2.228) leads to the relative normal curvature \bar{K}_v and relative torsional curvature \bar{G}_v in the direction $\frac{\mathbf{v}_p^{12}}{|\mathbf{v}_p^{12}|}$ as follows

$$\left. \begin{aligned} \bar{K}_v &= \bar{\Omega}_v \cdot (\mathbf{N}_{1p} \times \frac{\mathbf{v}_p^{12}}{|\mathbf{v}_p^{12}|}) = \bar{\Omega}_v \cdot \Delta_p = \frac{D_p^2}{(D_p |\mathbf{v}_p^{12}| + \mathbf{N}_{1p} \cdot \mathbf{J}_p)} \\ \bar{G}_v &= \bar{\Omega}_v \cdot \left(-\frac{\mathbf{v}_p^{12}}{|\mathbf{v}_p^{12}|}\right) = \frac{D_p E_p}{(D_p |\mathbf{v}_p^{12}| + \mathbf{N}_{1p} \cdot \mathbf{J}_p)} \end{aligned} \right\} \quad (2.229)$$

3. Other Forms of Relations of Relative Curvatures between Different Tangential Directions.

By using expression (2.35) and

$$\begin{aligned} \sin \theta_{ut} &= \mathbf{N}_1 \cdot (\mathbf{u} \times \mathbf{t}) = (\mathbf{N}_1 \times \mathbf{u}) \cdot \mathbf{t} = \mathbf{v} \cdot \mathbf{t} \\ \cos \theta_{ut} &= \mathbf{u} \cdot \mathbf{t} \end{aligned}$$

where, $\mathbf{v} = \mathbf{N}_1 \times \mathbf{u}$.

Relation (2.40) of relative curvatures between different tangential directions can be rewritten in the form

$$\left(\frac{d\bar{N}}{ds}\right)_t = \left(\frac{d\bar{N}}{ds}\right)_u(\mathbf{u} \cdot \mathbf{t}) + \left(\frac{d\bar{N}}{ds}\right)_v(\mathbf{v} \cdot \mathbf{t}) \quad (2.230)$$

With the aid of expression (2.36), expression (2.230) gives rise to another form of relationship of relative curvatures between different tangential directions as follows,

$$\bar{\Omega}_t = \bar{\Omega}_u(\mathbf{u} \cdot \mathbf{t}) + \bar{\Omega}_v(\mathbf{v} \cdot \mathbf{t}) \quad (2.231)$$

4. In Direction \mathbf{g} —Perpendicular to the Instantaneous line of Contact.

Since $\mathbf{g} = \mathbf{N}_{1p} \times \mathbf{e}$, \mathbf{e} and \mathbf{g} can replace \mathbf{u} and \mathbf{v} in expression (2.231), and with $\mathbf{t} = \frac{\mathbf{v}_p^{12}}{|\mathbf{v}_p^{12}|}$, then,

$$\bar{\Omega}_v = \bar{\Omega}_e\left(\mathbf{e} \cdot \frac{\mathbf{v}_p^{12}}{|\mathbf{v}_p^{12}|}\right) + \bar{\Omega}_g\left(\mathbf{g} \cdot \frac{\mathbf{v}_p^{12}}{|\mathbf{v}_p^{12}|}\right)$$

Substitution of expressions (2.214), (2.223) and (2.228) into the above expression yields the relative geometric angular velocity $\bar{\Omega}_g$ in direction \mathbf{g}

$$\bar{\Omega}_g = \frac{\sqrt{D_p^2 + E_p^2}}{(D_p|\mathbf{v}_p^{12}| + \mathbf{N}_{1p} \cdot \mathbf{J}_p)} \mathbf{W}_p^* \quad (2.232)$$

With the aid of expressions (2.37), (2.214), (2.217) and (2.221), the relative normal curvature (the maximum absolute value of relative normal curvature) \bar{K}_g and the relative torsional curvature \bar{G}_g in direction \mathbf{g} can be found from the expression (2.232)

$$\left. \begin{aligned} \bar{K}_g &= \bar{\Omega}_g \cdot (\mathbf{N}_{1p} \times \mathbf{g}) = -\bar{\Omega}_g \cdot \mathbf{e} = \frac{(D_p^2 + E_p^2)}{(D_p|\mathbf{v}_p^{12}| + \mathbf{N}_{1p} \cdot \mathbf{J}_p)} \\ \bar{G}_g &= \bar{\Omega}_g \cdot (-\mathbf{g}) = 0 \end{aligned} \right\} \quad (2.233)$$

As a matter of interest, the radius of curvature of the reduced cylindric surface \bar{A}^* of the surface \bar{A} at the point P is equal to $\frac{1}{\bar{K}_g}$.

5. In an Arbitrary Tangential Direction.

Replacing \mathbf{t} , \mathbf{u} and \mathbf{v} in expression (2.231) with τ , \mathbf{e} and \mathbf{g} respectively and taking into account $\bar{\Omega}_e = 0$, then

$$\bar{\Omega}_\tau = \bar{\Omega}_g(\mathbf{g} \cdot \tau)$$

By substituting expression (2.232) into the above expression and using expressions (2.214) and (2.222), the relative geometric angular velocity $\bar{\Omega}_\tau$ in direction τ is given by

$$\bar{\Omega}_\tau = \frac{(\mathbf{U}_p \cdot \tau)}{(D_p |\mathbf{v}_p^{12}| + \mathbf{N}_{1p} \cdot \mathbf{J}_p)} \mathbf{W}_p^* \quad (2.234)$$

By using expressions (2.37), (2.214), (2.217), (2.219) and (2.222), expression (2.234) leads to the relative normal curvature \bar{K}_τ and relative torsional curvature \bar{G}_τ in the direction τ

$$\left. \begin{aligned} \bar{K}_\tau &= \bar{\Omega}_\tau \cdot (\mathbf{N}_{1p} \times \tau) = \frac{(\mathbf{U}_p \cdot \tau)^2}{(D_p |\mathbf{v}_p^{12}| + \mathbf{N}_{1p} \cdot \mathbf{J}_p)} = \frac{(D_p^2 + E_p^2) \sin^2 \theta_{e\tau}}{(D_p |\mathbf{v}_p^{12}| + \mathbf{N}_{1p} \cdot \mathbf{J}_p)} \\ \bar{G}_\tau &= \bar{\Omega}_\tau \cdot (-\tau) = \frac{(\mathbf{U}_p \cdot \tau)(\mathbf{U}_p \cdot (\mathbf{N}_{1p} \times \tau))}{(D_p |\mathbf{v}_p^{12}| + \mathbf{N}_{1p} \cdot \mathbf{J}_p)} = \frac{(D_p^2 + E_p^2) \sin \theta_{e\tau} \cos \theta_{e\tau}}{(D_p |\mathbf{v}_p^{12}| + \mathbf{N}_{1p} \cdot \mathbf{J}_p)} \end{aligned} \right\} \quad (2.235)$$

Formulas of Calculation for Values of Several Conjugate Parameters

1. Curvatures of the Second Conjugate Surface.

With the aid of expressions (2.37) and (2.234), the geometric angular velocity $\Omega_{2\tau}$ at the conjugate contact point P of the second conjugate surface \bar{A} in any tangential direction τ is found,

$$\Omega_{2\tau} = \Omega_{1\tau} - \bar{\Omega}_\tau = \Omega_{1\tau} - \frac{(\mathbf{U}_p \cdot \tau)}{(D_p |\mathbf{v}_p^{12}| + \mathbf{N}_{1p} \cdot \mathbf{J}_p)} \mathbf{W}_p^* \quad (2.236)$$

With the aid of expressions (2.37) and (2.235), conjugate normal curvature $K'_{2\tau}$ and conjugate torsional curvature $G'_{2\tau}$ of surface \bar{A} in direction τ are given by

$$\left. \begin{aligned} K'_{2\tau} &= \bar{K}_\tau - K_{1\tau} = \frac{(D_p^2 + E_p^2) \sin^2 \theta_{e\tau}}{(D_p |\mathbf{v}_p^{12}| + \mathbf{N}_{1p} \cdot \mathbf{J}_p)} - K_{1\tau} \\ G'_{2\tau} &= \bar{G}_\tau - G_{1\tau} = \frac{(D_p^2 + E_p^2) \sin \theta_{e\tau} \cos \theta_{e\tau}}{(D_p |\mathbf{v}_p^{12}| + \mathbf{N}_{1p} \cdot \mathbf{J}_p)} - G_{1\tau} \end{aligned} \right\} \quad (2.237)$$

When $\tau = \mathbf{e}$, i.e., in the direction of the instantaneous line of contact, expression (2.237) gives

$$\left. \begin{aligned} K'_{2e} &= -K_{1e} \\ G'_{2e} &= -G_{1e} \end{aligned} \right\} \quad (2.238)$$

When $\tau = \frac{\mathbf{v}_p^{12}}{|\mathbf{v}_p^{12}|}$, i.e., in the direction of the relative velocity, the application of expressions (2.218) and (2.237) yields

$$\left. \begin{aligned} K'_{2v} &= \frac{D_p^2}{(D_p|\mathbf{v}_p^{12}| + \mathbf{N}_{1p} \cdot \mathbf{J}_p)} - K_{1v} \\ G'_{2v} &= \frac{D_p E_p}{(D_p|\mathbf{v}_p^{12}| + \mathbf{N}_{1p} \cdot \mathbf{J}_p)} - G_{1v} \end{aligned} \right\} \quad (2.239)$$

When $\tau = \Delta_p$, i.e., in the direction perpendicular to the relative velocity, the application of expressions (2.212), (2.218) and (2.237) produces

$$\left. \begin{aligned} K'_{2\Delta} &= \frac{E_p^2}{(D_p|\mathbf{v}_p^{12}| + \mathbf{N}_{1p} \cdot \mathbf{J}_p)} - K_{1\Delta} \\ G'_{2\Delta} &= \frac{-D_p E_p}{(D_p|\mathbf{v}_p^{12}| + \mathbf{N}_{1p} \cdot \mathbf{J}_p)} - G_{1\Delta} = -G'_{2v} \end{aligned} \right\} \quad (2.240)$$

When $\tau = \mathbf{g}$, i.e., in the direction perpendicular to the instantaneous line of contact, expression (2.237) gives

$$\left. \begin{aligned} K'_{2g} &= \frac{(D_p^2 + E_p^2)}{(D_p|\mathbf{v}_p^{12}| + \mathbf{N}_{1p} \cdot \mathbf{J}_p)} - K_{1g} \\ G'_{2g} &= -G_{1g} \end{aligned} \right\} \quad (2.241)$$

2. Angle between Conjugate Tangential Directions.

The tangential directions τ and τ' in fig.2.8 are called mutually conjugate tangential directions at the conjugate contact point P. Assume the angle of rotation of τ about \mathbf{N}_{1p} to τ' be $\theta_{\tau\tau'}$ within the range of $-\pi \leq \theta_{\tau\tau'} \leq \pi$. Dot-multiplication of both sides of expression (2.186), i.e., the second conjugate relationship, by τ yields

$$\cos \theta_{\tau\tau'} ds_2 = \tau \cdot \tau' ds_2 = ds_1 + \mathbf{v}_p^{12} \cdot \tau d\varepsilon_{1p}$$

That is,

$$\cos \theta_{\tau\tau'} \left(\frac{ds_2}{ds_1} \right)_\tau = 1 + |\mathbf{v}_p^{12}| \cos \theta_{v\tau} \left(\frac{d\varepsilon_{1p}}{ds_1} \right)_\tau \quad (2.242)$$

Dot-multiplying both sides of expression (2.186) by $(\mathbf{N}_{1p} \times \tau)$ gives

$$\sin \theta_{\tau\tau'} \left(\frac{ds_2}{ds_1} \right)_\tau = (\mathbf{N}_{1p} \times \tau) \cdot \mathbf{v}_p^{12} \left(\frac{d\varepsilon_{1p}}{ds_1} \right)_\tau = -|\mathbf{v}_p^{12}| \sin \theta_{v\tau} \left(\frac{d\varepsilon_{1p}}{ds_1} \right)_\tau \quad (2.243)$$

Substitution of expressions (2.213) into (2.242) and (2.243) and use of expressions (2.214), (2.216) and (2.217) produces

$$\tan \theta_{\tau\tau'} = \frac{\sin \theta_{\tau\tau'}}{\cos \theta_{\tau\tau'}} = \frac{-g|\mathbf{v}_p^{12}| \sin \theta_{v\tau} \sin \theta_{e\tau}}{1 + g|\mathbf{v}_p^{12}| \cos \theta_{v\tau} \sin \theta_{e\tau}} \quad (2.244)$$

When $-g|\mathbf{v}_p^{12}|\sin\theta_{v\tau}\sin\theta_{e\tau} > 0$, $\theta_{\tau\tau'}$ lies in the interval $0 < \theta_{\tau\tau'} < \pi$; when $-g|\mathbf{v}_p^{12}|\sin\theta_{v\tau}\sin\theta_{e\tau} < 0$, $0 > \theta_{\tau\tau'} > -\pi$.

Since $\theta_{v\tau} = \theta_{ve} + \theta_{e\tau}$, expression (2.244) may be rewritten as follows

$$\tan\theta_{\tau\tau'} = \frac{-g|\mathbf{v}_p^{12}||\cos\theta_{ve} - \cos(2\theta_{e\tau} + \theta_{ve})|}{2 + g|\mathbf{v}_p^{12}|[-\sin\theta_{ve} + \sin(2\theta_{e\tau} + \theta_{ve})]} \quad (2.245)$$

Where, $|\mathbf{v}_p^{12}|$ is determined by expression (2.129); g is determined by expression (2.215) and θ_{ve} is determined by expression (2.218).

When $\tau = \pm\mathbf{e}$, $\theta_{e\tau} = 0$ or π , and then $\theta_{\tau\tau'} = 0$ will correspondingly result from expression (2.245), that is, τ and τ' are coincident with each other in \mathbf{e} or $-\mathbf{e}$.

When $\tau = \pm \frac{\mathbf{v}_p^{12}}{|\mathbf{v}_p^{12}|}$, $\theta_{e\tau} = \theta_{ev}$ or $(\pi + \theta_{ev})$, and then $\theta_{\tau\tau'} = 0$ may also be obtained from expression (2.245), that is, τ and τ' are coincident with each other in $\frac{\mathbf{v}_p^{12}}{|\mathbf{v}_p^{12}|}$ or $-\frac{\mathbf{v}_p^{12}}{|\mathbf{v}_p^{12}|}$.

An examination of expression (2.245) shows the following: when $g = 0$, which is equivalent to $D_p = 0$, and $E_p = 0$ with the aid of expression (2.216), or $|\mathbf{v}_p^{12}| = 0$, then $\theta_{\tau\tau'}$ is always equal to zero for any tangential direction τ , that is, τ coincides with τ' . In the general case when $g \neq 0$, $|\mathbf{v}_p^{12}| \neq 0$, then only when $\tau = \pm\mathbf{e}$ or $\tau = \pm \frac{\mathbf{v}_p^{12}}{|\mathbf{v}_p^{12}|}$ is the corresponding $\theta_{\tau\tau'}$ equal to zero. The value of $\theta_{\tau\tau'}$ corresponding to any other tangential direction τ is different from zero. If the following condition is satisfied,

$$(\sin\theta_{ve} - \frac{2}{g|\mathbf{v}_p^{12}|})^2 \leq 1 \quad (2.246)$$

and when $\theta_{e\tau}$ is given by

$$\theta_{e\tau} = \frac{1}{2}[-\theta_{ve} + \arcsin(\sin\theta_{ve} - \frac{2}{g|\mathbf{v}_p^{12}|})] \quad (2.247)$$

then the corresponding value of $\theta_{\tau\tau'}$ will be $|\theta_{\tau\tau'}| = \frac{\pi}{2}$, since the denominator term of expression (2.245) becomes zero. In other words, whenever inequality (2.246) is satisfied, there exists a tangential direction such that $|\theta_{\tau\tau'}| > \frac{\pi}{2}$. On the contrary, if expression (2.246) is not satisfied, i.e., when

$$(\sin\theta_{ve} - \frac{2}{g|\mathbf{v}_p^{12}|})^2 > 1 \quad (2.248)$$

then since the denominator term of expression (2.245) is different from zero, it is always true that $|\theta_{\tau\tau'}| < \frac{\pi}{2}$. In the general case of worm-gear drives, because values

of g and $|\mathbf{v}_p^{12}|$ are all very large, it is necessary to make the value of θ_{ve} as close as possible to $|\theta_{ve}| = \frac{\pi}{2}$ in order to satisfy the requirement of expression (2.248), and this is just the case in Niemann-worm drives (i.e., the Flender worm, now generally known as the Cavex worm).

By substituting expressions (2.216) and (2.218) into (2.248), expression (2.248) may be rewritten in another form as follows

$$(D_p |\mathbf{v}_p^{12}| + 2\mathbf{N}_{1p} \cdot \mathbf{J}_p)^2 > |\mathbf{v}_p^{12}|^2 (D_p^2 + E_p^2) \quad (2.249)$$

3. The Ratio of Conjugate Arc Lengths.

The ratio between the arc length ds_2 in the tangential direction τ' of body II and the arc length ds_1 in the tangential direction τ of body I, as shown in fig.2.8, is called the ratio of conjugate arc lengths at the conjugate contact point P in the direction τ (ds_1, ds_2 are specified as positive values). Application of expressions (2.242) and (2.243) gives

$$\left(\frac{ds_2}{ds_1}\right)_\tau^2 = 1 + 2|\mathbf{v}_p^{12}| \cos \theta_{v\tau} \left(\frac{d\varepsilon_{1p}}{ds_1}\right)_\tau + |\mathbf{v}_p^{12}|^2 \left(\frac{d\varepsilon_{1p}}{ds_1}\right)_\tau^2 \quad (2.250)$$

Substitution of expressions (2.213) into (2.250) together with use of expressions (2.214), (2.216) and (2.217) and $\theta_{v\tau} = \theta_{ve} + \theta_{e\tau}$ produces

$$\left(\frac{ds_2}{ds_1}\right)_\tau = \sqrt{\begin{aligned} & (1 - g|\mathbf{v}_p^{12}| \sin \theta_{vg} + \frac{g^2 |\mathbf{v}_p^{12}|^2}{2}) \\ & + g|\mathbf{v}_p^{12}| [\cos \theta_{ve} \sin 2\theta_{e\tau} + (\sin \theta_{ve} - \frac{g|\mathbf{v}_p^{12}|}{2}) \cos 2\theta_{e\tau}] \end{aligned}} \quad (2.251)$$

Formulas of Calculation for Values of Several Parameters on the Surface of Engagement

1. Unit Vector Normal to the Surface of Engagement.

When $\tau = \mathbf{e}$, expression (2.213) leads to $(\frac{d\varepsilon_{1p}}{ds_1})_e = 0$, and then, application of expression (2.184), i.e., the first conjugate relation, gives

$$\left. \begin{aligned} \mathbf{t}_e &= \mathbf{e} \\ \left(\frac{ds}{ds_1}\right)_e &= 1 \end{aligned} \right\} \quad (2.252)$$

When $\tau = \mathbf{g}$, substitution of expressions (2.216) into (2.184) yields

$$\mathbf{t}_g \left(\frac{ds}{ds_1}\right)_g = \mathbf{g} + g\mathbf{v}_p \quad (2.253)$$

In the general case, $(\mathbf{g} + g\mathbf{v}_p) \neq 0$, then, the unit vector Π_p normal to the conjugate contact point P of the surface of engagement is found from expressions (2.252) and (2.253)

$$\begin{aligned}\Pi_p &= \frac{\mathbf{t}_e \times \mathbf{t}_g}{|(\mathbf{t}_e \times \mathbf{t}_g)|} = \frac{\mathbf{e} \times (\mathbf{g} + g\mathbf{v}_p)}{|[\mathbf{e} \times (\mathbf{g} + g\mathbf{v}_p)]|} \\ &= \frac{\mathbf{N}_{1p} + g\mathbf{e} \times \mathbf{v}_p}{|(\mathbf{N}_{1p} + g\mathbf{e} \times \mathbf{v}_p)|}\end{aligned}\quad (2.254)$$

Since Π_p and \mathbf{N}_{1p} are both unit vectors perpendicular to \mathbf{e} , \mathbf{N}_{1p} can be rotated about \mathbf{e} to Π_p

$$\Pi_p = (\phi_{N\Pi}\mathbf{e}) \otimes \mathbf{N}_{1p} = \cos \phi_{N\Pi} \mathbf{N}_{1p} - \sin \phi_{N\Pi} \mathbf{g} \quad (2.255)$$

Expressions (2.254) and (2.255) directly lead to

$$\left. \begin{aligned}\sin \phi_{N\Pi} &= \Pi_p \cdot (-\mathbf{g}) = \frac{g(\mathbf{N}_{1p} \cdot \mathbf{v}_p)}{|(\mathbf{N}_{1p} + g\mathbf{e} \times \mathbf{v}_p)|} \\ \cos \phi_{N\Pi} &= \Pi_p \cdot \mathbf{N}_{1p} = \frac{1 + g(\mathbf{g} \cdot \mathbf{v}_p)}{|(\mathbf{N}_{1p} + g\mathbf{e} \times \mathbf{v}_p)|}\end{aligned}\right\} \quad (2.256)$$

Examination of expression (2.256) indicates that when $\mathbf{N}_{1p} \cdot \mathbf{v}_p = 0$; that is, when \mathbf{v}_p lies on the common tangential plane at conjugate contact point P, then, $\phi_{N\Pi} = 0$. In other words, Π_p and \mathbf{N}_{1p} are colinear, and the surface of engagement comes into tangent contact with the common tangential plane at the point P. If at any instant and at any conjugate contact point the requirement is satisfied for the surface of engagement and the common tangential plane to be in tangential contact with each other, then, the corresponding conjugate surface is called the gear blank pitch surface (assuming $\mathbf{v}_p \neq 0$).

2.The Relation between the Direction of the Contact Path and the Direction of the Common Tangent at the Contact point.

Since $\mathbf{t}_e = \mathbf{e}$ and \mathbf{t}_τ are all tangential directions to the surface of engagement and perpendicular to Π_p , \mathbf{t}_τ can be expressed by rotation of \mathbf{e} about Π_p ; that is,

$$\mathbf{t}_\tau = (\varphi_{et}\Pi_p) \otimes \mathbf{e} \quad (2.257)$$

Substituting expressions (2.255) into (2.257), then,

$$\mathbf{t}_\tau = \cos \varphi_{et} \mathbf{e} + \sin \varphi_{et} (\cos \phi_{N\Pi} \mathbf{g} + \sin \phi_{N\Pi} \mathbf{N}_{1p}) \quad (2.258)$$

Substituting expressions (2.258) into the first conjugate relation, i.e, expression (2.184), and making use of expressions (2.213), (2.214), (2.216) and (2.217), then,

$$(\cos \varphi_{et} \mathbf{e} + \sin \varphi_{et} \cos \phi_{N\Pi} \mathbf{g} + \sin \varphi_{et} \sin \phi_{N\Pi} \mathbf{N}_{1p}) \left(\frac{ds}{ds_1} \right)_\tau = \tau + g \sin \theta_{e\tau} \mathbf{v}_p \quad (2.259)$$

Dot-multiplying both sides of expression (2.259) by \mathbf{e} , \mathbf{g} and \mathbf{N}_{1p} respectively, then

$$\left. \begin{aligned} \cos \varphi_{et} \left(\frac{ds}{ds_1} \right)_\tau &= \cos \theta_{e\tau} + g \sin \theta_{e\tau} (\mathbf{e} \cdot \mathbf{v}_p) \\ \sin \varphi_{et} \cos \phi_{N\Pi} \left(\frac{ds}{ds_1} \right)_\tau &= \sin \theta_{e\tau} + g \sin \theta_{e\tau} (\mathbf{g} \cdot \mathbf{v}_p) \\ \sin \varphi_{et} \sin \phi_{N\Pi} \left(\frac{ds}{ds_1} \right)_\tau &= g \sin \theta_{e\tau} (\mathbf{N}_{1p} \cdot \mathbf{v}_p) \end{aligned} \right\} \quad (2.260)$$

With the aid of expression (2.256), expression (2.260) leads to the relationship between the tangential direction to the surface of engagement and the corresponding tangential direction to the first conjugate surface

$$\tan \varphi_{et} = \frac{|(\mathbf{N}_{1p} + g\mathbf{e} \times \mathbf{v}_p)| \sin \theta_{e\tau}}{\cos \theta_{e\tau} + g \sin \theta_{e\tau} (\mathbf{e} \cdot \mathbf{v}_p)} \quad (2.261)$$

When $\sin \theta_{e\tau} > 0$, $0 < \varphi_{et} < \pi$; and when $\sin \theta_{e\tau} < 0$, $0 > \varphi_{et} > -\pi$.

3. The Relation between the Arc Lengths of the Contact Path and Contacting Profiles

Assuming $ds_1 > 0$, $ds > 0$, the ratio between the arc length ds along \mathbf{t} of the surface of engagement and the corresponding arc length ds_1 in direction τ on rigid body I is found from expression (2.259) as follows

$$\begin{aligned} \left(\frac{ds}{ds_1} \right)_\tau &= \sqrt{(\tau + g \sin \theta_{e\tau} \mathbf{v}_p) \cdot (\tau + g \sin \theta_{e\tau} \mathbf{v}_p)} \\ &= \sqrt{1 + 2g \sin \theta_{e\tau} (\tau \cdot \mathbf{v}_p) + g^2 \sin^2 \theta_{e\tau} |\mathbf{v}_p|^2} \end{aligned} \quad (2.262)$$

Substituting $\tau = \cos \theta_{e\tau} \mathbf{e} + \sin \theta_{e\tau} \mathbf{g}$ into expression (2.262), then

$$\left(\frac{ds}{ds_1} \right)_\tau = \sqrt{1 + g(\mathbf{g} \cdot \mathbf{v}_p) + \frac{g^2 |\mathbf{v}_p|^2}{2} + g\{\sin 2\theta_{e\tau} (\mathbf{e} \cdot \mathbf{v}_p) - \cos 2\theta_{e\tau} [(\mathbf{g} \cdot \mathbf{v}_p) + \frac{g|\mathbf{v}_p|^2}{2}]\}} \quad (2.263)$$

The Procedure for the Calculation of Curvatures of the Second Conjugate Surface (The First Type of Problem of Conjugate Curvatures)

1. Given Quantities.

(1). The coordinate position of a specified point P on the first conjugate surface $\mathbf{R}_1 = x\mathbf{i} + y\mathbf{j} + z\mathbf{k}$,

- (2). The unit vector normal to this point of the first conjugate surface $\mathbf{N}_1 = A\mathbf{i} + B\mathbf{j} + C\mathbf{k}$,
- (3). A unit vector tangential to this point of the first conjugate surface $\mathbf{q} = q_1\mathbf{i} + q_2\mathbf{j} + q_3\mathbf{k}$,
- (4). Normal and torsional curvatures $K_{1q}, K_{1w}, G_{1q} = -G_{1w}$ at this point of the first conjugate surface in directions $\mathbf{q}, \mathbf{w} = \mathbf{N}_1 \times \mathbf{q}$.
- (5). The direction \mathbf{u} in the tangential plane in which the curvature of the second surface is to be formed. To define \mathbf{u} , we can use the angle θ_{qu} of rotation from \mathbf{q} to \mathbf{u} about the unit normal \mathbf{N}_{1p} .
- (6). Functional relations of conjugate motion: $\varepsilon_2 = \varepsilon_2(\varepsilon_1), \sigma_1 = \sigma_1(\varepsilon_1), \sigma_2 = \sigma_2(\varepsilon_1), f = f(\varepsilon_1), h = h(\varepsilon_1)$ and the value α .

2. Quantities to be Found.

- (1). The coordinate position of the corresponding conjugate point \bar{P} of the second conjugate surface $\mathbf{R}_2 = x'\mathbf{i}' + y'\mathbf{j}' + z'\mathbf{k}'$,
- (2). The unit vector normal to point \bar{P} of the second conjugate surface $\mathbf{N}_2 = A'\mathbf{i}' + B'\mathbf{j}' + C'\mathbf{k}'$,
- (3). The conjugate normal and torsional curvatures $K'_{2u}, K'_{2v}, G'_{2u} = -G'_{2v}$ of the second conjugate surface at point \bar{P} in the specified tangential directions $\mathbf{u}, \mathbf{v} = \mathbf{N}_2 \times \mathbf{u}$,

3. Steps of the Computation Procedure.

- (1). Using expressions (2.166) and (2.167), we obtain the corresponding value ε_{1p} .
- (2). Using the given functional relations of the conjugate motion, we obtain the corresponding values at the instant ε_{1p} : $\varepsilon_2, \sigma_1, \sigma_2, f, h, M = \frac{d\varepsilon_2}{d\varepsilon_1}, \frac{d\sigma_1}{d\varepsilon_1}, \frac{d\sigma_2}{d\varepsilon_1}, \frac{df}{d\varepsilon_1}, \frac{dh}{d\varepsilon_1}, \frac{dM}{d\varepsilon_1}, \frac{d^2\sigma_1}{d\varepsilon_1^2}, \frac{d^2\sigma_2}{d\varepsilon_1^2}, \frac{d^2f}{d\varepsilon_1^2}, \frac{d^2h}{d\varepsilon_1^2}$.
- (3). Using expression (2.168), we obtain the coordinate values of the corresponding conjugate contact point $\mathbf{R}_{1p} = x_p\mathbf{i} + y_p\mathbf{j} + z_p\mathbf{k}$.
- (4). Using expression (2.169), we obtain the unit vector normal to the first conjugate surface at the corresponding conjugate contact point $\mathbf{N}_{1p} = A_p\mathbf{i} + B_p\mathbf{j} + C_p\mathbf{k}$.
- (5). Using expressions (2.170) and (2.172), we obtain the coordinate position of the corresponding conjugate point \bar{P} of the second conjugate surface $\mathbf{R}_2 = x'\mathbf{i}' + y'\mathbf{j}' + z'\mathbf{k}'$.
- (6). Using expressions (2.171) and (2.173), we obtain the unit vector normal to point \bar{P} of the second conjugate surface $\mathbf{N}_2 = A'\mathbf{i}' + B'\mathbf{j}' + C'\mathbf{k}'$.
- (7). Using $\mathbf{q}_p = (\varepsilon_{1p}\mathbf{k}) \otimes \mathbf{q}$, we obtain \mathbf{q}_q .

(8). Using expression (2.129), we obtain \mathbf{v}_p^{12} , $|\mathbf{v}_p^{12}|$.

(9). Using expression (2.133), we obtain η_p , $|\eta_p|$.

(10). Using $\sin \theta_{qv} = \mathbf{N}_{1p} \cdot (\mathbf{q}_p \times \frac{\mathbf{v}_p^{12}}{|\mathbf{v}_p^{12}|})$, $\cos \theta_{qv} = \mathbf{q}_p \cdot \frac{\mathbf{v}_p^{12}}{|\mathbf{v}_p^{12}|}$, we obtain $\sin \theta_{qv}$, $\cos \theta_{qv}$ and θ_{qv} .

(11). Using

$$\begin{aligned} K_{1v} &= K_{1q} \cos^2 \theta_{qv} + K_{1w} \sin^2 \theta_{qv} + 2G_{1q} \sin \theta_{qv} \cos \theta_{qv}, \\ K_{1\Delta} &= K_{1q} \sin^2 \theta_{qv} + K_{1w} \cos^2 \theta_{qv} - 2G_{1q} \sin \theta_{qv} \cos \theta_{qv}, \\ G_{1v} &= -G_{1\Delta} = -(K_{1q} - K_{1w}) \sin \theta_{qv} \cos \theta_{qv} + G_{1q} (\cos^2 \theta_{qv} - \sin^2 \theta_{qv}) \end{aligned}$$

we obtain K_{1v} , $K_{1\Delta}$, $G_{1v} = -G_{1\Delta}$.

(12). Using (2.135), we obtain $\sin \theta_{v\eta}$, $\cos \theta_{v\eta}$.

(13). Using (2.209), we obtain D_p , E_p .

(14). Using (2.218), we obtain $\sin \theta_{ve}$, $\cos \theta_{ve}$, θ_{ve} .

(15). Using

$$\begin{aligned} K_{1e} &= K_{1v} \cos^2 \theta_{ve} + K_{1\Delta} \sin^2 \theta_{ve} + 2G_{1v} \sin \theta_{ve} \cos \theta_{ve}, \\ K_{1g} &= K_{1v} \sin^2 \theta_{ve} + K_{1\Delta} \cos^2 \theta_{ve} - 2G_{1v} \sin \theta_{ve} \cos \theta_{ve}, \\ G_{1e} &= -G_{1g} = -(K_{1v} - K_{1\Delta}) \sin \theta_{ve} \cos \theta_{ve} + G_{1v} (\cos^2 \theta_{ve} - \sin^2 \theta_{ve}). \end{aligned}$$

we obtain K_{1e} , K_{1g} , $G_{1e} = -G_{1g}$.

(16). Using (2.148), we obtain $\bar{\mathbf{J}}_p$ and $\mathbf{N}_{1p} \cdot \mathbf{J}_p = A_p J_{p1} + B_p J_{p2} + C_p J_{p3}$.

(17). Using (2.233), we obtain \bar{K}_p .

(18). Using (2.238), (2.241), we obtain K'_{2e} , K'_{2g} , $G'_{2e} = -G'_{2g}$.

(19). Using $\theta_{eu} = \theta_{ev} + \theta_{vq} + \theta_{qu} = -\theta_{ve} - \theta_{qv} + \theta_{qu}$, we obtain θ_{eu} , $\sin \theta_{eu}$, $\cos \theta_{eu}$.

(20). Using

$$\begin{aligned} K'_{2u} &= K'_{2e} \cos^2 \theta_{eu} + K'_{2g} \sin^2 \theta_{eu} + 2G'_{2e} \sin \theta_{eu} \cos \theta_{eu}, \\ K'_{2e} &= K'_{2e} \sin^2 \theta_{eu} + K'_{2g} \cos^2 \theta_{eu} - 2G'_{2e} \sin \theta_{eu} \cos \theta_{eu}, \\ G'_{2u} &= -G'_{2v} = -(K'_{2e} - K'_{2g}) \sin \theta_{eu} \cos \theta_{eu} + G'_{2e} (\cos^2 \theta_{eu} - \sin^2 \theta_{eu}). \end{aligned}$$

we obtain K'_{2u} , K'_{2v} , $G'_{2u} = -G'_{2v}$.

Calculation Formulas for the Unit Normal and the Curvatures of the First Conjugate Surface When the Second Conjugate Surface is an Intersecting Curve.

1. Given Quantities.

(1). Values of the following parameters corresponding to the instant ε_1 , i.e., $\varepsilon_2, \sigma_1, \sigma_2, f, h, M = \frac{d\varepsilon_2}{d\varepsilon_1}, \frac{d\sigma_1}{d\varepsilon_1}, \frac{d\sigma_2}{d\varepsilon_1}, \frac{df}{d\varepsilon_1}, \frac{dh}{d\varepsilon_1}, \frac{dM}{d\varepsilon_1}, \frac{d^2\sigma_1}{d\varepsilon_1^2}, \frac{d^2\sigma_2}{d\varepsilon_1^2}, \frac{d^2f}{d\varepsilon_1^2}, \frac{d^2h}{d\varepsilon_1^2}$, and the constant value α .

(2). The coordinate position of any point of the intersecting curve (the second conjugate surface) at instant ε_1 , i.e., $\mathbf{R}_{2p} = x'\mathbf{i}' + y'\mathbf{j}' + z'\mathbf{k}'$.

(3). The unit tangential direction of the intersecting curve at the point P, $\mathbf{w} = w'_1\mathbf{i}' + w'_2\mathbf{j}' + w'_3\mathbf{k}' = w_1\mathbf{i} + w_2\mathbf{j} + w_3\mathbf{k}$.

(4). The unit principal normal of the intersecting curve at point P $\xi = \xi'_1\mathbf{i}' + \xi'_2\mathbf{j}' + \xi'_3\mathbf{k}' = \xi_1\mathbf{i} + \xi_2\mathbf{j} + \xi_3\mathbf{k}$, and unit normal vectors $\mathbf{N}_I, \mathbf{N}_{II}$ of surfaces I, II comprising this intersecting curve.

(5). The curvature k_c of the intersecting curve at point P.

2. Computation Procedure.

(1). First, we find the coordinate position of the corresponding conjugate contact point P of the first conjugate surface $\mathbf{R}_{1p} = x_p\mathbf{i} + y_p\mathbf{j} + z_p\mathbf{k}$. Since point P is conjugate contact point P, $\mathbf{R}_{1p} = \mathbf{R}_{2p} + l\mathbf{p}$, then

$$\left. \begin{aligned} x_p &= x'_p + f \\ y_p &= y'_p \cos \alpha + z'_p \sin \alpha + h \\ z_p &= -y'_p \sin \alpha + z'_p \cos \alpha \end{aligned} \right\} \quad (2.264)$$

With the aid of expressions (2.129), (2.133), (2.148) and (2.264), and the given values of the conjugate motion parameters, $\mathbf{v}_p^{12}, \eta_p, \mathbf{J}_p$ can be correspondingly found.

(2). Next, the unit vector normal to the first conjugate surface at point \mathbf{R}_{1p} is $\mathbf{N}_{1p} = A_p\mathbf{i} + B_p\mathbf{j} + C_p\mathbf{k}$. Since the intersecting curve itself is an instantaneous line of contact whenever it comes into contact with the first conjugate surface, i.e., $\mathbf{w} = \pm\mathbf{e}$, \mathbf{w} is perpendicular to \mathbf{N}_{1p} and lies in the common tangential plane. Meanwhile, since \mathbf{R}_{1p} is the conjugate contact point, \mathbf{v}_p^{12} and \mathbf{N}_{1p} are perpendicular, therefore,

$$\mathbf{N}_{1p} = \pm \frac{\mathbf{w} \times \mathbf{v}_p^{12}}{|\mathbf{w} \times \mathbf{v}_p^{12}|} \quad (2.265)$$

Where, the sign " \pm " can be determined in the following way

$$\mathbf{w} \cdot (\mathbf{N}_I \times \mathbf{N}_{1p}) \leq 0 \quad (2.266)$$

The positive direction of \mathbf{w} can be determined by expression (B.37), so that the angle ϕ_{III} of \mathbf{N}_I rotating about \mathbf{w} to \mathbf{N}_{II} satisfies the requirement $0 < \phi_{III} < \pi$, i.e., the expression (2.50).

(3). The normal curvature K_{1w} at point \mathbf{R}_{1p} of the first conjugate surface in direction \mathbf{w} is found as follows. If the intersecting curve comes into contact with the first conjugate surface, this intersecting curve is a curve lying on the first conjugate surface. Use of the Meusnier theorem, i.e., expression (2.65), yields the normal curvature as

$$K_{1w} = -k_c(\mathbf{N}_{1p} \cdot \xi) \quad (2.267)$$

(4). Next, we find the torsional curvature G_{1w} at point \mathbf{R}_{1p} of the first conjugate surface in direction \mathbf{w} . Use of expressions (2.42), (2.209) and (2.218), taking into account $\mathbf{w} = \pm \mathbf{e}$, yields

$$\frac{K_{1w} - K_{1v}}{G_{1w} + G_{1v}} = \tan \theta_{vw} = \tan \theta_v = \frac{-D_p}{E_p} = \frac{-(K_{1v}|\mathbf{v}_p^{12}| - |\eta_p| \cos \theta_{v\eta})}{(G_{1v}|\mathbf{v}_p^{12}| - |\eta_p| \sin \theta_{v\eta})}$$

Then

$$\frac{K_{1w}|\mathbf{v}_p^{12}| - |\eta_p| \cos \theta_{v\eta}}{G_{1w}|\mathbf{v}_p^{12}| + |\eta_p| \sin \theta_{v\eta}} = \tan \theta_{vw} = \frac{\mathbf{N}_{1p}(\mathbf{v}_p^{12} \times \mathbf{w})}{\mathbf{v}_p^{12} \cdot \mathbf{w}} \quad (2.268)$$

Expression (2.268) gives the torsional curvature G_{1w} ,

$$G_{1w} = \frac{(\mathbf{v}_p^{12} \cdot \mathbf{w})}{\mathbf{N}_{1p} \cdot (\mathbf{v}_p^{12} \times \mathbf{w})} (K_{1w} - \frac{|\eta_p|}{|\mathbf{v}_p^{12}|} \cos \theta_{v\eta}) - \frac{|\eta_p|}{|\mathbf{v}_p^{12}|} \sin \theta_{v\eta} \quad (2.269)$$

(5). The normal curvature K_{1q} at point \mathbf{R}_{1p} of the first conjugate surface in direction $\mathbf{q} = \mathbf{N}_{1p} \times \mathbf{w}$ is the next quantity to be calculated. Since conjugate normal curvature K'_{2q} of the intersecting curve in direction \mathbf{q} is $K'_{2q} \rightarrow \infty$, then $\bar{K}'_q = \bar{K}_g = K_{1q} + K_{2q} \rightarrow \infty$, and application of expressions (2.209) and (2.233) yields

$$D_p|\mathbf{v}_p^{12}| + \mathbf{N}_{1p} \cdot \mathbf{J}_p = |\mathbf{v}_p^{12}|(K_{1v}|\mathbf{v}_p^{12}| - |\eta_p| \cos \theta_{v\eta}) + \mathbf{N}_{1p} \cdot \mathbf{J}_p = 0 \quad (2.270)$$

Expression (2.270) leads immediately to

$$K_{1v} = \frac{|\eta_p|}{|\mathbf{v}_p^{12}|} \cos \theta_{v\eta} - \frac{\mathbf{N}_{1p} \cdot \mathbf{J}_p}{|\mathbf{v}_p^{12}|^2} \quad (2.271)$$

Using expression (2.25), then

$$K_{1v} = K_{1w} \cos^2 \theta_{wv} + K_{1q} \sin^2 \theta_{wv} + 2G_{1w} \sin \theta_{wv} \cos \theta_{wv} \quad (2.272)$$

With the aid of expressions (2.271) and (2.272), the normal curvature K_{1q} can then be found

$$\begin{aligned} K_{1q} = & -\frac{(\mathbf{w} \cdot \mathbf{v}_p^{12})^2}{[\mathbf{N}_{1p} \cdot (\mathbf{w} \times \mathbf{v}_p^{12})]^2} K_{1w} - \frac{2(\mathbf{w} \cdot \mathbf{v}_p^{12})}{[\mathbf{N}_{1p} \cdot (\mathbf{w} \times \mathbf{v}_p^{12})]} G_{1w} \\ & + \frac{(|\mathbf{v}_p^{12}| |\eta_p| \cos \theta_{v\eta} - \mathbf{N}_{1p} \cdot \mathbf{J}_p)}{[\mathbf{N}_{1p} \cdot (\mathbf{w} \times \mathbf{v}_p^{12})]^2} \end{aligned} \quad (2.273)$$

(v). The torsional curvature G_{1q} at point \mathbf{R}_{1p} of the first conjugate surface in the direction \mathbf{q} is $G_{1q} = -G_{1w}$.

Chapter 3

Basic Principle for the Design of Gear Blanks

The basic principles for the gear blank design have been given by B. Shtipleman [10], M. Baxter [9], F. Litvin [15] and the Gleason Works [30]. Since some concepts such as the gear blank pitch surfaces are very important in the author's opinion, it is worthwhile to especially emphasize and explain them further. In order to ensure that we can use formulas of the AGMA 2005 standard[10] correctly to calculate the parameters of the gear blanks which will be used in the following sections, it is necessary to rederive the formulas. Some of these are different from those of the AGMA 2005 standard in appearance, but their calculating results are the same.

3.1 The Kinematic Characteristics of Hypoid Gearing

Referring to the dual coordinate system shown in Fig.3.1, assume the coordinate system $O-i, j, k$ corresponds to hypoid gear with $k = \omega_1$ being its axis of rotation and $O' - i', j', k'$ corresponds to hypoid pinion with $k' = -\omega_2$ being its axis of rotation. Such a choice of the coordinate systems will be used throughout this thesis. Conjugate motion of hypoid gearing is the motion of constant transmission ratio with fixed axes and no axial translation; this is,

$$\left. \begin{array}{l} \alpha = \text{constant}, \quad f = \text{constant}, \quad M = \frac{d\epsilon_2}{d\epsilon_1} = \text{constant}, \\ \sigma_1 = \sigma_2 = 0, \quad h = 0 \end{array} \right\} \quad (3.1)$$

where, α is the shaft angle; f is the offset of hypoid gearing; M is the transmission ratio; f and h together form the offset, but the axes can be chosen as that $h = 0$ as shown in fig.3.1.

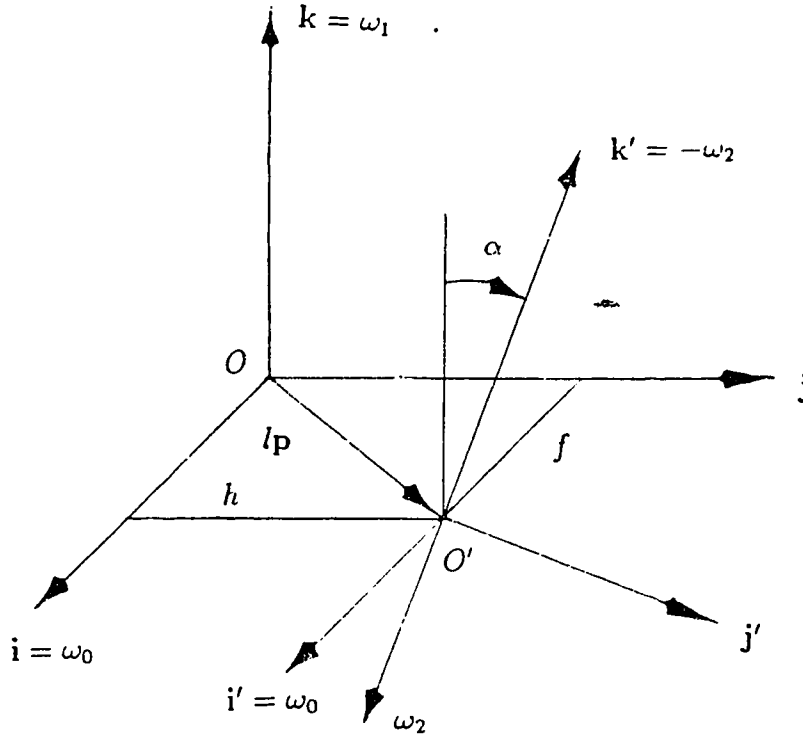


Figure 3.1: Dual coordinate systems

From the condition of conjugate motion of hypoid gearing, i.e., expression (3.1), the kinematic characteristics of hypoid gearing can be achieved as follows:

1. No Pitch Surface.

By substituting expression (3.1) into requirement (2.136) for the existence of a pitch surface, it can be seen that due to

$$M(f - \frac{dh}{d\varepsilon_1}) \sin \alpha + (1 + M \cos \alpha) \frac{d\sigma_1}{d\varepsilon_1} + (M + \cos \alpha) \frac{d\sigma_2}{d\varepsilon_1} = Mf \sin \alpha \neq 0 \quad (3.2)$$

thus there exists no pitch surface in hypoid gearing.

2. Surfaces of Screw Axes with Hyperboloid.

Substitution of condition (3.1) into expression (2.142) leads to the equation for the surface of the screw axes in the hypoid gear with reference to the coordinate system O-i,j,k as follows.

$$\left. \begin{aligned} \mathbf{R}_a &= x_a \mathbf{i} + y_a \mathbf{j} + z_a \mathbf{k} \\ x_a &= E \cos \varepsilon_1 + F \sin \varepsilon_1 \\ y_a &= -E \sin \varepsilon_1 + F \cos \varepsilon_1 \end{aligned} \right\} \quad (3.3)$$

where

$$\left. \begin{aligned} E &= \frac{Mf(M+\cos \alpha)}{(1+M \cos \alpha)^2 + M^2 \sin^2 \alpha} \\ F &= \frac{Mz_a \sin \alpha}{1+M \cos \alpha} \end{aligned} \right\} \quad (3.4)$$

Since the following requirement is fulfilled

$$\frac{x_a^2}{a^2} + \frac{y_a^2}{b^2} - \frac{z_a^2}{c^2} = 1 \quad (3.5)$$

where,

$$\left. \begin{aligned} a &= b = \frac{Mf(M+\cos \alpha)}{(1+M \cos \alpha)^2 + M^2 \sin^2 \alpha} \\ c &= \frac{f(1+M \cos \alpha)(M+\cos \alpha)}{[(1+M \cos \alpha)^2 + M^2 \sin^2 \alpha] \sin \alpha} \end{aligned} \right\} \quad (3.6)$$

thus, the surface of screw axes of the hypoid gear is a hyperboloid.

Likewise, substitution of condition (3.1) into expression (2.144) yields the equation for the surface of screw axes in the hypoid pinion with respect to coordinate system $\mathbf{O}' - \mathbf{i}', \mathbf{j}', \mathbf{k}'$ as follows

$$\left. \begin{aligned} \mathbf{R}'_a &= x'_a \mathbf{i}' + y'_a \mathbf{j}' + z'_a \mathbf{k}' \\ x'_a &= E \cos \varepsilon_2 - F \cos \alpha \sin \varepsilon_2 + z_a \sin \alpha \sin \varepsilon_2 - f \cos \varepsilon_2 \\ y'_a &= E \sin \varepsilon_2 + F \cos \alpha \cos \varepsilon_2 - z_a \sin \alpha \cos \varepsilon_2 - f \sin \varepsilon_2 \\ z'_a &= F \sin \alpha + z_a \cos \alpha \end{aligned} \right\} \quad (3.7)$$

Since the following requirement is fulfilled

$$\frac{x'^2_a}{a'^2} + \frac{y'^2_a}{b'^2} - \frac{z'^2_a}{c'^2} = 1 \quad (3.8)$$

where

$$\left. \begin{aligned} a' &= b' = E - f \\ c' &= \frac{(E-f)(M+\cos \alpha)}{\sin \alpha} \end{aligned} \right\} \quad (3.9)$$

Then, the surface of screw axes of the hypoid pinion is also a hyperboloid.

The spatial position of the screw axis of hypoid gearing may be found from expression (2.145) as following

$$\left. \begin{aligned} \mathbf{r}_a &= (\varepsilon_1 \omega_1) \otimes \mathbf{R}_a = X_a \mathbf{i} + Y_a \mathbf{j} + Z_a \mathbf{k} \\ X_a &= E = \frac{M f (M + \cos \alpha)}{(1 + M \cos \alpha)^2 + M^2 \sin^2 \alpha} \\ Y_a &= F = \frac{M z_a \sin \alpha}{1 + M \cos \alpha} \\ Z_a &= z_a \end{aligned} \right\} \quad (3.10)$$

That is, the screw axis intersects the coordinate axis \mathbf{i} between points O and O' and is perpendicular to the coordinate axis \mathbf{i} .

3.2 Gear Blank Pitch Surface

The definition of the gear blank pitch surface has been given in section 2.4.3. We use the requirement that the surface of engagement and the common tangential plane of both conjugate surfaces should be in contact with each other in any instant, i.e., $\phi_{N\Pi} = 0$, and the common tangential plane is defined as the gear blank pitch plane. An implication of this definition is that the conjugate surface is always on one side of the surface of engagement. Therefore, such surfaces will not cause any interference with each other, when they are used as boundary surfaces of both members of gearing. On the other hand, an examination of expression (2.256) shows that $\phi_{N\Pi}$ is equal to zero whenever $\mathbf{N}_{1p} \cdot \mathbf{v}_p = 0$ is fulfilled with the exception of $g = \infty$, i.e., $\mathbf{N}_{1p} \cdot \mathbf{J}_p = 0$, which is the singular case and will be discussed in the following section. The fact $\mathbf{N}_{1p} \cdot \mathbf{v}_p = 0$ implies that the contact transmission will be realized only by friction, instead of by an active force. From the point of view of energy transmission, conjugate surfaces of this type are unacceptable. However, use of such surfaces as the boundary surfaces of the corresponding conjugate surfaces is most ideal, since this is very similar to the case of transmission between two friction wheels and thus no interference will occur.

With the aid of $\mathbf{N}_{1p} \cdot \mathbf{v}_p^{12} = 0$, the requirement of $\mathbf{N}_{1p} \cdot \mathbf{v}_p = 0$ yields the unit normal \mathbf{N}_b to the gear blank pitch surface in the following form

$$\mathbf{N}_{1p} = \pm \frac{\mathbf{v}_p \times \mathbf{v}_p^{12}}{|\mathbf{v}_p \times \mathbf{v}_p^{12}|} \quad (3.11)$$

where, \mathbf{v}_p^{12} is found from expression (2.129) and sign " \pm " is so defined that the positive direction of \mathbf{N}_{1p} points away from the axis $\omega_1 = \mathbf{k}$.

In the special case of conjugate motion for constant transmission ratio, fixed axes and no axial translation, i.e., expression (2.1), the velocity \mathbf{v}_p , with respect to coordinate system $\mathbf{O-i,j,k}$, of point $P_d(\mathbf{R}_{1p})$ in rigid body I at instant ε_1 is found from expression (2.129) as follows

$$\mathbf{v}_p = \omega_1 \times \mathbf{R}_{1p} \quad (3.12)$$

and the velocity \mathbf{v}_p^{12} at point $P_d(\mathbf{R}_{1p})$ of body I relative to body II at the instant ε_1 is found from expression (2.129)

$$\mathbf{v}_p^{12} = \omega_1 \times \mathbf{R}_{1p} - M\omega_2 \times \mathbf{R}_{2p} \quad (3.13)$$

Then the unit normal \mathbf{N}_b to the gear blank pitch surface can be calculated from expression (2.11), that is,

$$\begin{aligned} \mathbf{N}_b &= \pm \frac{\mathbf{v}_p \times \mathbf{v}_p^{12}}{|\mathbf{v}_p \times \mathbf{v}_p^{12}|} \\ &= \pm \frac{(\omega_1 \times \mathbf{R}_{1p}) \times (M\omega_2 \times \mathbf{R}_{2p})}{|(\omega_1 \times \mathbf{R}_{1p}) \times (M\omega_2 \times \mathbf{R}_{2p})|} \end{aligned} \quad (3.14)$$

Since \mathbf{N}_b is perpendicular to \mathbf{v}_p and \mathbf{v}_p^{12} , we have the following relations,

$$\left. \begin{aligned} \mathbf{N}_b \cdot (\omega_1 \times \mathbf{R}_{1p}) &= 0 \\ \mathbf{N}_b \cdot (\omega_2 \times \mathbf{R}_{2p}) &= 0 \end{aligned} \right\} \quad (3.15)$$

As a consequence, \mathbf{N}_b intersects simultaneously with ω_1 and ω_2 , i.e., the axes of rotation of gear and pinion, respectively.

It is worth notice that a gear blank pitch surface is neither a pitch surface nor a surface of screw axes. The three types of surface are defined quite differently. There exist the following three major differences in the geometric properties:

1. The pitch surface does not exist in any condition of conjugate motion and at any conjugate contact point. Only when the condition of the existence of a pitch surface is fulfilled, and the conjugate contact point is in the position determined by expression (2.139) does a pitch surface exist. Surfaces of screw axes are available in any condition of conjugate motion but only in the spatial position of the conjugate contact point found from expression (2.145).

On the contrary, a gear blank pitch surface exists in any condition of conjugate motion and any spatial position of the conjugate contact point.

2. Once the conjugate motion is given, the corresponding pitch surfaces (if existing) and surfaces of screw axes are uniquely determined; that is, there exist only one pair of pitch surfaces and one pair of surfaces of screw axes. The pitch surface

is just the special case of the surface of screw axes in the condition of $\mathbf{v}_p^{12} = \mathbf{0}$. In other words, the pitch surface and the surface of screw axes are simply the geometric representation of conjugate motion.

On the contrary, the unit normal \mathbf{N}_b to a gear blank pitch surface is determined by expression (3.11), and curvature properties of the first gear blank pitch surface can be arbitrarily prescribed, as for the curvature properties of the second gear blank pitch surface, this can be given from the solution to the first type of problem of conjugate curvatures, referring to section 2.4.3. This implies that there exist a series of pairs of gear blank pitch surfaces, due to sharing the same unit normal \mathbf{N}_b , being tangent of each other under any condition of conjugate motion and any position of the conjugate contact point.

3. At the position of the pitch point, i.e., $\mathbf{v}_p^{12} = \mathbf{0}$, it is seen from expression (3.11) that the direction of \mathbf{N}_b is indefinite. In other words, any pair of conjugate surfaces through the pitch point can be used as a pair of gear blank pitch surfaces. But in the current practice of gear design for non-hypoid gears, a pair of corresponding pitch surfaces through the pitch point is widely used as a pair of gear blank pitch surfaces. This might be the reason for the confusion between the concepts of pitch surface, surface of screw axes and gear blank pitch surface. It should be remembered that the use of the pitch surface as the gear blank pitch surface is just a special case but is not a necessary requirement. Here, strictly distinguishing the gear blank pitch surface from the pitch surface and the surface of screw axes has a decisive effect on the gear blank design, and will open the train of thought in the practice of gear design.

If we look to the practical function, it is also worthwhile to distinguish the following five different surfaces. The functions of pitch surface and surface of screw axes are the geometric representations of the conjugate motion. The requirement of the pitch surface is $\mathbf{v}_p^{12} = \mathbf{0}$, i.e., expression (2.136) and the requirement of the surface of screw axes is $\boldsymbol{\Omega}_{12} \times \mathbf{v}_p^{12} = \mathbf{0}$, i.e., expression (2.140). The function of the gear blank pitch surface is mainly its use as the boundary surface of the corresponding conjugate surface, instead of as a surface which accomplishes the task of transmission. The requirement of the gear blank pitch surface is $\mathbf{N}_b \cdot \mathbf{v}_p = 0$ or $\mathbf{N}_b = \frac{\mathbf{v}_p \times \mathbf{v}_p^{12}}{|\mathbf{v}_p \times \mathbf{v}_p^{12}|}$, i.e., expression (3.11). The transmission of motion and power are completed through a pair of gear tooth surfaces. Whether a pair of gear tooth surfaces is designed better or worse directly affects transmission properties of motion and power, strength of contact and bending, life expectancy, vibration, noise, lubrication and so on. Therefore, the gear tooth surfaces are the major object of gear research. In the course of gear design, in order to define some parameters, it is necessary to introduce a reference surface. There are no specific requirements for the reference surface other than convenience. In the current practice of gear design, pitch surfaces (if existing) are usually used

as a pair of reference surfaces for gear and pinion respectively, or a pair of gear blank pitch surfaces, as in the case of hypoid gearing, is used as a pair of reference surfaces.

3.3 The Conjugate Stagnant Curve, Conjugate Boundary Curve and Conjugate Varied Curve on Line – Contacting Conjugate Surfaces

1. Conjugate Stagnant Curve.

We consider the case when a point on a conjugate surface reaches the position of conjugate contact, and the following condition is satisfied simultaneously in addition to the fulfillment of the condition $\mathbf{N}_{1p} \cdot \mathbf{v}_p^{12} = 0$,

$$\mathbf{N}_{1p} \cdot \mathbf{J}_p = 0 \quad (3.16)$$

where, \mathbf{J}_p is defined in expression (2.149).

Then, the curve composed of points satisfying these conditions is called the conjugate stagnant curve on a conjugate surface. It can be deduced from the definition of \mathbf{J}_p , i.e., expression (2.149), that if a point P on the conjugate stagnant curve reaches the position of conjugate contact at the instant ε_1 , i.e., $\mathbf{N}_{1p} \cdot \mathbf{v}_p^{12} = 0$, then, the relative velocity $\mathbf{v}_{p'}^{12}$ at the same point P on the conjugate surface but at the instant $(\varepsilon_{1p} + \Delta\varepsilon_{1p})$ is expressed in the form

$$\begin{aligned} \mathbf{v}_{p'}^{12} &= (\Delta\varepsilon_{1p}\omega_1) \otimes (\mathbf{v}_p^{12} - \mathbf{J}_p\Delta\varepsilon_{1p}) \\ &= \mathbf{v}_p^{12} + (\omega_1 \times \mathbf{v}_p^{12} - \mathbf{J}_p)\Delta\varepsilon_{1p} \end{aligned} \quad (3.17)$$

Meanwhile, the unit normal $\mathbf{N}_{1p'}$ at this point and this instant, i.e., $(\varepsilon_{1p} + \Delta\varepsilon_{1p})$ is found in the form

$$\begin{aligned} \mathbf{N}_{1p'} &= (\Delta\varepsilon_{1p}\omega_1) \otimes \mathbf{N}_{1p} \\ &= \mathbf{N}_{1p} + \omega_1 \times \mathbf{N}_{1p}\Delta\varepsilon_{1p} \end{aligned} \quad (3.18)$$

Since the point on the conjugate stagnant curve satisfies expression (3.16), the combination of expressions (3.17) and (3.18) leads to

$$\mathbf{N}_{1p'} \cdot \mathbf{v}_{p'}^{12} = \mathbf{N}_{1p} \cdot \mathbf{v}_p^{12} - \mathbf{N}_{1p} \cdot \mathbf{J}_p\Delta\varepsilon_{1p} = 0 \quad (3.19)$$

The implication of the above expression is that at instant $(\varepsilon_{1p} + \Delta\varepsilon_{1p})$, this point will still be a conjugate contact point and, therefore, is called the stagnant point of

conjugate contact. Consequently, the curve composed of such kinds of points is called the conjugate stagnant curve.

2. The Tangential Direction to a Conjugate Stagnant Curve.

Assume that P and P' are two adjacent points on the conjugate stagnant curve, and the vector from P to P' is $P\vec{P}' = \mathbf{e}_s ds_1$, thus, when $ds_1 \rightarrow 0$, \mathbf{e}_s becomes the unit vector at point P tangential to the conjugate stagnant curve. If at instant ε_{1p} , point P reaches the position of conjugate contact, then, requirement (2.203) will be satisfied. When $\tau = \mathbf{e}_s$, it follows from expression (2.203) that

$$|\mathbf{v}_p^{12}|[(\boldsymbol{\Omega}_{1v} \times \mathbf{N}_{1p}) \cdot \mathbf{e}_s ds_1 - \mathbf{N}_{1p} \cdot \mathbf{J}_p d\varepsilon_{1p} - \eta_p \cdot \mathbf{e}_s ds_1] = 0 \quad (3.20)$$

Since point P is the point on the conjugate stagnant curve, condition (3.16) is fulfilled, and thus, with the aid of expression (2.207), expression (3.20) becomes

$$\mathbf{U}_p \cdot \mathbf{e}_s ds_1 = 0 \quad (3.21)$$

Expression (3.21) indicates that the tangential direction to the conjugate stagnant curve coincides with the tangential direction to the instantaneous line of contact; that is, at every point of the conjugate stagnant curve, the conjugate stagnant curve is tangential to the instantaneous line of contact which passes through that point as shown in fig. 3.2

3. Two Kinds of Common Tangential States.

The common tangential state of the conjugate stagnant curve with the lines of contact can be classified into two types. One type is when all the lines of contact stay on one side of the conjugate stagnant curve as shown in fig.3.2 (a). The conjugate stagnant curve in this case is referred to as the conjugate boundary curve. The other type is when every line of contact crosses over the conjugate stagnant curve and is tangent to the conjugate stagnant curve as shown in fig.3.2 (b). The conjugate stagnant curve in this case is called the conjugate varied curve.

4. Two Special Tangential Cases.

When the conjugate stagnant curve coincides with one of the lines of contact, the conjugate stagnant curve will no longer meet and be tangent to the other lines of contact. This is a special case which can also be classified into two types. One type is when all the lines of contact stay on one side of the conjugate stagnant curve except for the one coinciding with the conjugate stagnant curve as shown fig.3.3 (a). At this time, the conjugate stagnant curve becomes the conjugate boundary curve. The other type is when lines of contact can be found on both sides of the conjugate

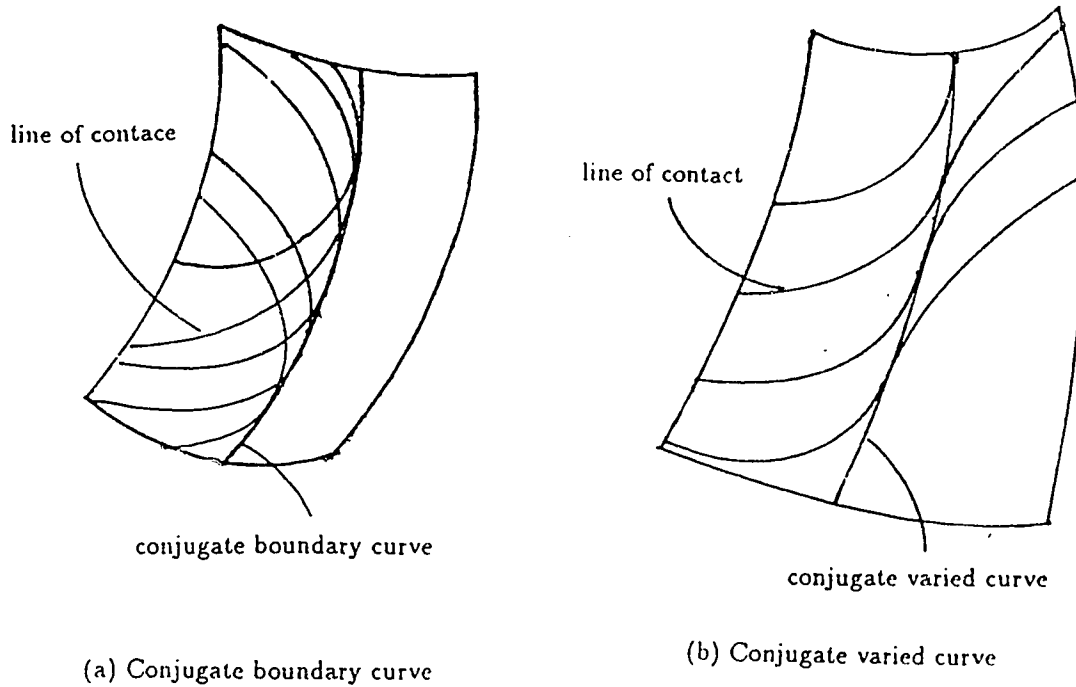


Figure 3.2: Two types of common tangential cases

stagnant curve and the conjugate stagnant curve coincides with one of the lines of contact as shown fig.3.3 (b). The conjugate stagnant curve at this time is called the conjugate varied curve.

5. Conjugate Boundary Curve.

If the values D_p and E_p , determined by expression (2.209), at every point on the conjugate stagnant curve satisfy the following condition; i.e.,

$$D_p^2 + E_p^2 > 0 \quad (3.22)$$

then it follows from expressions (2.216) and (3.16) that the corresponding value $g = (\frac{d\varepsilon_{1p}}{ds_1})_g$ becomes $g \rightarrow \pm\infty$. The implication is that after being in tangent contact with the conjugate stagnant curve, lines of contact will be back toward the original side of the conjugate stagnant curve as shown in fig.3.4. Then, the conjugate stagnant curve when condition (3.22) is satisfied must be the conjugate boundary curve as shown in fig.3.2 (a) and fig. 3.3 (a). The conjugate boundary curve divides a conjugate surface into two regions: one region accommodates all the lines of contact and is therefore called the region of conjugate solution; and the other region has no lines of contact, and is therefore called the region of no conjugate solution.

6. Conjugate Varied Curve.

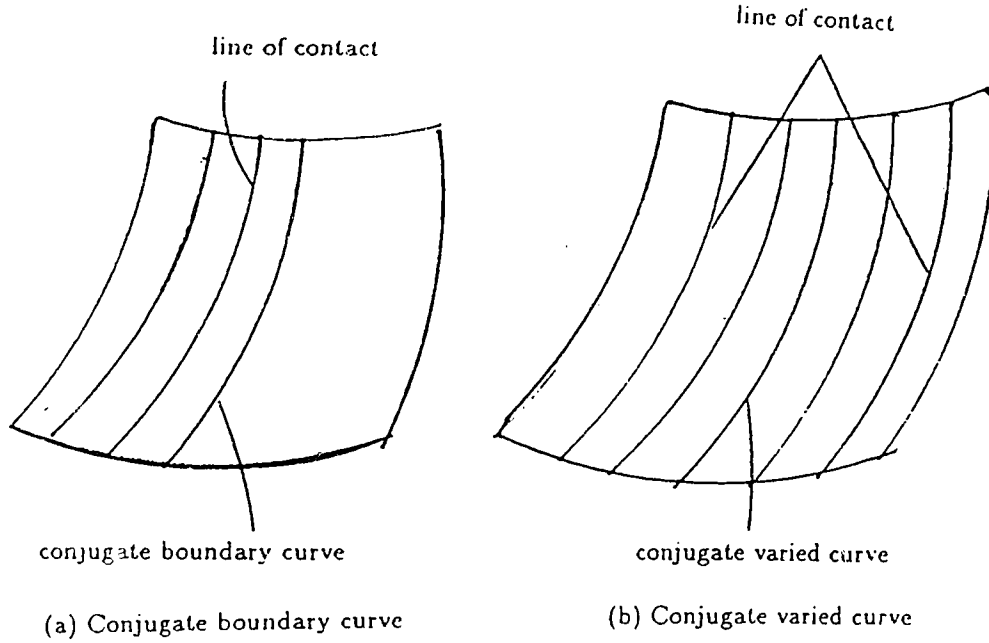


Figure 3.3: Two types of special tangential cases

If the values D_p and E_p and g satisfy the following condition, i.e.,

$$\left. \begin{aligned} D_p^2 + E_p^2 &= 0 \\ g &= \frac{\sqrt{D_p^2 + E_p^2}}{N_{1p} \cdot J_p} = \frac{0}{0} = \text{definite limiting value} \neq \pm\infty \end{aligned} \right\} \quad (3.23)$$

then, after being in tangent contact with the conjugate stagnant curve, lines of contact will cross over the conjugate stagnant curve. Therefore, the conjugate stagnant curve when condition (3.23) is satisfied must be the conjugate varied curve. Since condition (3.23) is much more stringent than condition (3.22), in most cases, the conjugate stagnant curve on an arbitrarily prescribed conjugate surface, i.e., satisfying condition (3.16), is generally a conjugate boundary curve.

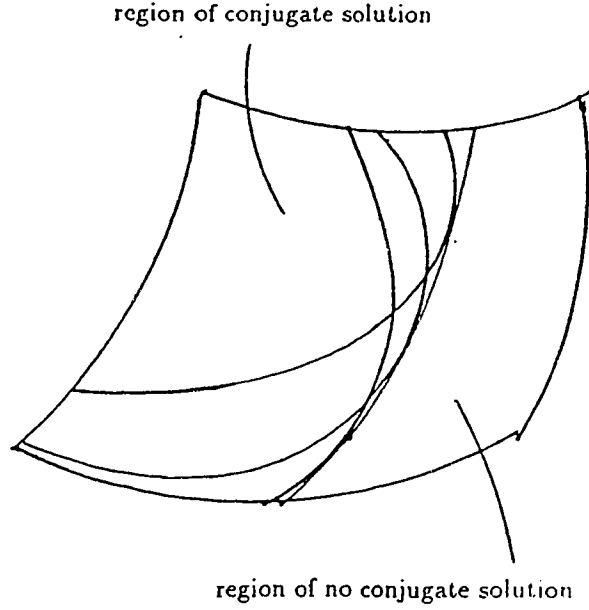


Figure 3.4: The regions of conjugate solution and no conjugate solution

3.4 The Analytical Expression for the Conjugate Boundary Curve under the Condition of Special Simple Conjugate Motion

As has been analysed in section 2.4.2, when the condition of conjugate motion satisfies expression (2.174), the requirement $\mathbf{N}_{1p} \cdot \mathbf{v}_p^{12} = 0$ yields

$$U \cos \varepsilon_1 - V \sin \varepsilon_1 = W \quad (3.24)$$

where, U , V and W are functions only of the position of the point and can be determined by expression (2.175).

With the aid of expression (2.118) and (2.122), the expression of \mathbf{J}_p can be written as

$$\left. \begin{aligned} \mathbf{J}_p &= J_{p1}\mathbf{i} + J_{p2}\mathbf{j} + J_{p3}\mathbf{k} \\ J_{p1} &= Mf \cos \alpha - \frac{d\sigma_2}{d\varepsilon_1} \sin \alpha \\ J_{p2} &= Mz \sin \alpha + Mh \cos \alpha \\ J_{p3} &= -M(x \sin \varepsilon_1 + y \cos \varepsilon_1) \sin \alpha \end{aligned} \right\} \quad (3.25)$$

Substitution of expression (3.25) and (2.169) into expression $\mathbf{N}_{1p} \cdot \mathbf{J}_p = 0$ produces

$$U \sin \varepsilon_1 + V \cos \varepsilon_1 = 0 \quad (3.26)$$

Combination of expression (3.24) and (3.26) leads to

$$U^2 + V^2 = W^2 \quad (3.27)$$

This is the analytical expression for the conjugate boundary curve in the condition of conjugate motion represented by expression (2.174).

3.5 The Boundary Curve of Curvature Interference on the Line-Contacting Conjugate Surface

If the point within the region of conjugate solution on the conjugate surface, when it reaches the position of conjugate contact, i.e., fulfillment of the requirement $\mathbf{N}_{1p} \cdot \mathbf{v}_p^{12} = 0$, satisfies the following requirement

$$D_p |\mathbf{v}_p^{12}| + \mathbf{N}_{1p} \cdot \mathbf{J}_p = 0 \quad (3.28)$$

then the curve composed of such points divides the region of conjugate solution into two sub-regions, in one sub-region, $(D_p |\mathbf{v}_p^{12}| + \mathbf{N}_{1p} \cdot \mathbf{J}_p) > 0$; and in the other sub-region, $(D_p |\mathbf{v}_p^{12}| + \mathbf{N}_{1p} \cdot \mathbf{J}_p) < 0$, and thus, the curve composed of points satisfying condition (3.28) is called the boundary curve of curvature interference on the conjugate surface. The boundary curve of curvature interference divides the region of conjugate solution into two sub-regions. Within one sub-region, where $(D_p |\mathbf{v}_p^{12}| + \mathbf{N}_{1p} \cdot \mathbf{J}_p) > 0$, the value of the corresponding relative normal curvature determined by expression (2.233) becomes $\overline{K_g} > 0$; that is, there is no curvature interference between rigid bodies I and II, and therefore, this sub-region is called the conjugate valid zone as shown in fig. 3.5. Within the other sub-region, where $(D_p |\mathbf{v}_p^{12}| + \mathbf{N}_{1p} \cdot \mathbf{J}_p) < 0$, the value of the corresponding relative normal curvature becomes $\overline{K_g} < 0$; that is, there is curvature interference between rigid bodies I and II at contact points within this sub-region. Therefore, this sub-region is regarded as the conjugate invalid zone as shown in fig.3.5.

3.6 Basic Geometry of the Gear Tooth under the Condition of Constant Transmission Ratio, Fixed Axes and No Axial Translation

1. Gear Blank Pitch Surface of Rotation.

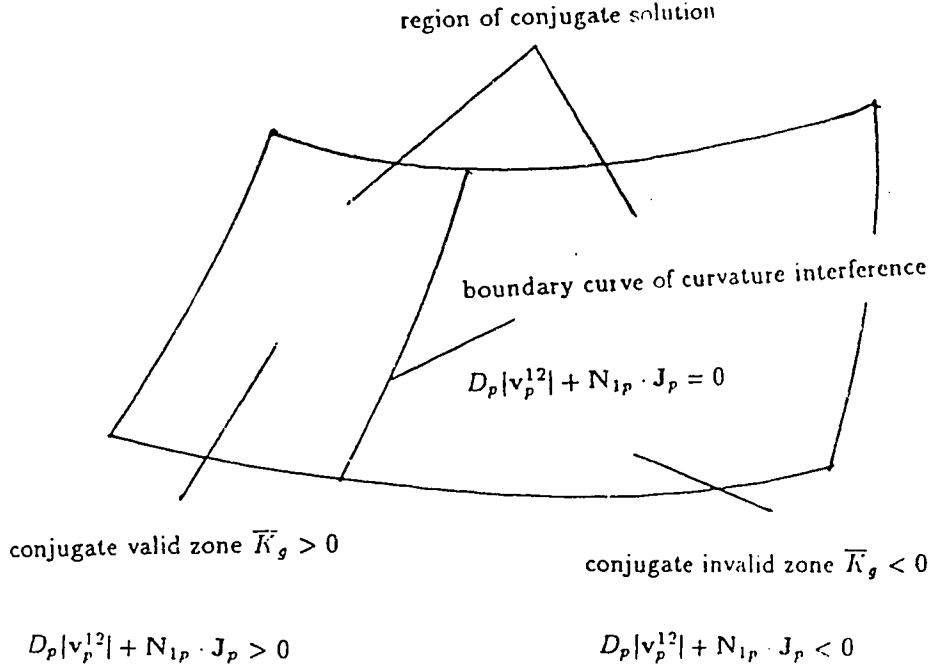


Figure 3.5: Conjugate valid and invalid zones

The conjugate motion for constant transmission ratio, fixed axes and no axial translation is given by expression (3.1). Assume that the positions of the conjugate contact point in coordinate systems $O - \mathbf{i}, \mathbf{j}, \mathbf{k}$ and $O' - \mathbf{i}', \mathbf{j}', \mathbf{k}'$ are respectively represented in the forms

$$\begin{aligned} \mathbf{R}_{1p} &= x_p \mathbf{i} + y_p \mathbf{j} + z_p \mathbf{k} \\ &= \rho \cos \mu \mathbf{i} + \rho \sin \mu \mathbf{j} + z_p \mathbf{k} \end{aligned} \quad (3.29)$$

where, ρ is the radial distance of the conjugate contact point P from the axis $\omega_1 = \mathbf{k}$; μ is the phase angle made by rotating axis \mathbf{i} about axis $\mathbf{k} = \omega_1$ to the radial vector of point P; and z_p is the axial distance from point P to origin O along the direction $\mathbf{k} = \omega_1$. Similarly, in the second coordinate system

$$\begin{aligned} \mathbf{R}_{2p} &= x'_p \mathbf{i}' + y'_p \mathbf{j}' + z'_p \mathbf{k}' \\ &= \rho' \cos \mu' \mathbf{i}' + \rho' \sin \mu' \mathbf{j}' + z'_p \mathbf{k}' \end{aligned} \quad (3.30)$$

where, ρ' is the radial distance of conjugate contact point P from the axis $\omega_2 = -\mathbf{k}'$; μ' is the phase angle made by rotating axis \mathbf{i}' about axis $\mathbf{k}' = -\omega_2$ to the radial vector of conjugate contact point P; and z'_p is the axial distance from point P to origin O' along axis $\mathbf{k}' = -\omega_2$.

Employing expressions (2.153) and (2.120) and using expression (C.23) leads to

$$\begin{aligned}\mathbf{R}_{2p} &= \mathbf{R}_{1p} - l\mathbf{p} \\ &= (\rho \cos \mu - f)\mathbf{i}' + (\rho \sin \mu \cos \alpha - z_p \sin \alpha)\mathbf{j}' \\ &\quad + (\rho \sin \mu \sin \alpha + z_p \cos \alpha)\mathbf{k}'\end{aligned}\quad (3.31)$$

Comparison of expressions (3.30) with (3.31) gives

$$\left. \begin{aligned}\rho' \cos \mu' &= \rho \cos \mu - f \\ \rho' \sin \mu' &= \rho \sin \mu \cos \alpha - z_p \sin \alpha \\ z_p' &= \rho \sin \mu \sin \alpha + z_p \cos \alpha\end{aligned}\right\} \quad (3.32)$$

and consequently,

$$\rho' = \sqrt{(\rho \cos \mu - f)^2 + (\rho \sin \mu \cos \alpha - z_p \sin \alpha)^2} \quad (3.33)$$

Substitution of expression (3.29) and the condition of conjugate motion, i.e., expression (3.1) into (2.129) gives the relative velocity at the conjugate contact point P as follows

$$\left. \begin{aligned}\mathbf{v}_p^{12} &= v_{p1}^{12}\mathbf{i} + v_{p2}^{12}\mathbf{j} + v_{p3}^{12}\mathbf{k} \\ v_{p1}^{12} &= -\rho(1 + M \cos \alpha) \sin \mu + M z_p \sin \alpha \\ v_{p2}^{12} &= \rho(1 + M \cos \alpha) \cos \mu - M f \cos \alpha \\ v_{p3}^{12} &= -M(\rho \cos \mu - f) \sin \alpha \\ |\mathbf{v}_p^{12}| &= \sqrt{(v_{p1}^{12})^2 + (v_{p2}^{12})^2 + (v_{p3}^{12})^2}\end{aligned}\right\} \quad (3.34)$$

Also, \mathbf{v}_p^{12} can be rewritten in the coordinate system $\mathbf{O}' - \mathbf{i}', \mathbf{j}', \mathbf{k}'$ with the aid of expression (2.119)

$$\left. \begin{aligned}\mathbf{v}_p^{12} &= v_{p1}^{12'}\mathbf{i}' + v_{p2}^{12'}\mathbf{j}' + v_{p3}^{12'}\mathbf{k}' \\ v_{p1}^{12'} &= v_{p1}^{12} = -\rho(1 + M \cos \alpha) \sin \mu + M z_p \sin \alpha \\ v_{p2}^{12'} &= v_{p2}^{12} \cos \alpha - v_{p3}^{12} \sin \alpha \\ &= \rho(\cos \alpha + M) \cos \mu - M f \\ v_{p3}^{12'} &= v_{p2}^{12} \sin \alpha + v_{p3}^{12} \cos \alpha = \rho \cos \mu \sin \alpha\end{aligned}\right\} \quad (3.35)$$

Further, substitution of expressions (3.29) and (3.1) into (2.126) yields the velocity as follows

$$\mathbf{v}_p = -\rho \sin \mu \mathbf{i} + \rho \cos \mu \mathbf{j} \quad (3.36)$$

Substitution of expressions (3.1) and (3.29) into (2.150) yields

$$\left. \begin{aligned} \mathbf{J}_p &= J_{p1}\mathbf{i} + J_{p2}\mathbf{j} + J_{p3}\mathbf{k} \\ J_{p1} &= Mf \cos \alpha \\ J_{p2} &= Mz_p \sin \alpha \\ J_{p3} &= -My_p \sin \alpha = -M\rho \sin \mu \sin \alpha \end{aligned} \right\} \quad (3.37)$$

Consequently, the unit normal to the first gear blank pitch surface can be found from the definition, i.e., expression (3.11), and by using expression (3.34) and (3.36). The unit normal then takes the form

$$\left. \begin{aligned} \mathbf{N}_{1b} &= \pm \frac{\mathbf{v}_p \times \mathbf{v}_p^{12}}{|\mathbf{v}_p \times \mathbf{v}_p^{12}|} = A_b\mathbf{i} + B_b\mathbf{j} + C_b\mathbf{k} \\ A_b &= \frac{(\rho \cos \mu - f) \sin \alpha \cos \mu}{Q_b} \\ B_b &= \frac{(\rho \cos \mu - f) \sin \alpha \sin \mu}{Q_b} \\ C_b &= \frac{(z_p \cos \mu \sin \alpha - f \sin \mu \cos \alpha)}{Q_b} \end{aligned} \right\} \quad (3.38)$$

where, $Q_b = \pm \sqrt{(\rho \cos \mu - f)^2 \sin^2 \alpha + (z_p \cos \mu \sin \alpha - f \sin \mu \cos \alpha)^2}$, and sign " \pm " is so defined that the positive direction of \mathbf{N}_{1b} points from the body to the space.

With the aid of expressions (2.119), (3.32) and (3.38), the unit normal to the second gear blank pitch surface is given from the requirement (2.155) as following

$$\left. \begin{aligned} \mathbf{N}_{2b} &= -\mathbf{N}_{1b} = A'_b\mathbf{i}' + B'_b\mathbf{j}' + C'_b\mathbf{k}' \\ A'_b &= -A_b = \frac{-\rho' \cos \mu \sin \alpha \cos \mu'}{Q_b} \\ B'_b &= -B_b \cos \alpha + C_b \sin \alpha \\ &= \frac{-\rho' \cos \mu \sin \alpha \sin \mu'}{Q_b} \\ C'_b &= -B_b \sin \alpha - C_b \cos \alpha \\ &= \frac{-(\rho \sin \mu \sin \alpha + z_p \cos \alpha) \cos \mu \sin \alpha + f \sin \mu}{Q_b} \end{aligned} \right\} \quad (3.39)$$

It can be seen from the above analyses that once the position of the conjugate contact point is found, i.e., the parameters ρ, μ and z_p and the conditions of conjugate motion in expression (3.1) are given, then the unit normals to the gear blank pitch surfaces are accordingly determined. Then, the shape of the first gear blank pitch surface can be, in effect, arbitrarily prescribed under the fulfillment of the requirement for the unit normal. It is just for convenience that the surface of revolution through the conjugate contact point with the axis $\omega_1 = \mathbf{k}$ is used as the first gear blank pitch surface. The second gear blank pitch surface should be, strictly speaking, the conjugate surface corresponding to the first gear blank pitch surface of revolution. Thus, the second gear blank pitch surface may not certainly be a surface of revolution

with the axis $\omega_2 = -\mathbf{k}'$. But as noted before, the function of the gear blank pitch surface is just to secure no interference between the conjugate surfaces rather than to accomplish the task of transmission. Therefore, to facilitate manufacturing, the practice of using the surface of revolution as the second gear blank pitch surface is, of course, completely permitted, although somewhat differences of curvature arise. This is just the situation in the current practice of gearing. However, such difference of curvature must make conjugate surfaces separate.

2. Pitch Angle of the Gear Blank.

In the formation of the surface of revolution, the curve in the axial intersection with the surface of revolution is usually used as generatrix. Let the unit vector tangent to the generatrix of the first gear blank pitch surface be \mathbf{S} , then,

$$\mathbf{S} = \frac{\mathbf{N}_{1b} \times (\mathbf{k} \times \mathbf{R}_{1p})}{|\mathbf{N}_{1b} \times (\mathbf{k} \times \mathbf{R}_{1p})|} \quad (3.40)$$

Substitution of expressions (3.29) and (3.38) into (3.40) yields

$$\left. \begin{aligned} \mathbf{S} &= S_1 \mathbf{i} + S_2 \mathbf{j} + S_3 \mathbf{k} \\ S_1 &= \frac{-(z_p \cos \mu \sin \alpha - f \sin \mu \cos \alpha) \cos \mu}{Q_b} \\ S_2 &= \frac{-(z_p \cos \mu \sin \alpha - f \sin \mu \cos \alpha) \sin \mu}{Q_b} \\ S_3 &= \frac{(\rho \cos \mu - f) \sin \alpha}{Q_b} \end{aligned} \right\} \quad (3.41)$$

Analogously, let the unit vector tangent to the generatrix of the second gear blank pitch surface be \mathbf{S}' , then,

$$\mathbf{S}' = \frac{\mathbf{N}_{2b} \times (\mathbf{k}' \times \mathbf{R}_{2p})}{|\mathbf{N}_{2b} \times (\mathbf{k}' \times \mathbf{R}_{2p})|} \quad (3.42)$$

Substitution of expressions (3.31) and (3.39) into (3.42) yields

$$\left. \begin{aligned} \mathbf{S}' &= S'_1 \mathbf{i}' + S'_2 \mathbf{j}' + S'_3 \mathbf{k}' \\ S'_1 &= \frac{(\rho \cos \mu - f)[(\rho \sin \mu \sin \alpha + z_p \cos \alpha) \cos \mu \sin \alpha - f \sin \mu]}{Q_b \sqrt{(\rho \cos \mu - f)^2 + (\rho \sin \mu \cos \alpha - z_p \sin \alpha)^2}} \\ S'_2 &= \frac{(\rho \sin \mu \cos \alpha - z_p \sin \alpha)[(\rho \sin \mu \sin \alpha + z_p \cos \alpha) \cos \mu \sin \alpha - f \sin \mu]}{Q_b \sqrt{(\rho \cos \mu - f)^2 + (\rho \sin \mu \cos \alpha - z_p \sin \alpha)^2}} \\ S'_3 &= \frac{-\cos \mu \sin \alpha \sqrt{(\rho \cos \mu - f)^2 + (\rho \sin \mu \cos \alpha - z_p \sin \alpha)^2}}{Q_b} \end{aligned} \right\} \quad (3.43)$$

The pitch angle γ_g of the first gear blank pitch surface can be found from the dot-product of \mathbf{S} with the axis $\omega_1 = \mathbf{k}$ as follows

$$\cos \gamma_g = |\mathbf{S} \cdot \mathbf{k}| = \left| \frac{(\rho \cos \mu - f) \sin \alpha}{Q_b} \right| \quad (3.44)$$

where, $0 \leq \gamma_g \leq \frac{\pi}{2}$

Likewise, the pitch angle γ_p of the second gear blank pitch surface can be found as follows

$$\begin{aligned} \cos \gamma_p &= |\mathbf{S}' \cdot \mathbf{k}'| \\ &= \left| \frac{-\cos \mu \sin \alpha \sqrt{(\rho \cos \mu - f)^2 + (\rho \sin \mu \cos \alpha - z_p \sin \alpha)^2}}{Q_b} \right| \end{aligned} \quad (3.45)$$

where, $0 \leq \gamma_p \leq \frac{\pi}{2}$.

3. Spiral Angle.

Since the common normal to any pair of conjugate surfaces must be perpendicular to the relative velocity \mathbf{v}_p^{12} at the conjugate contact point P, then, \mathbf{v}_p^{12} must be perpendicular both to the common normal $\mathbf{N}_{1b} = -\mathbf{N}_{2b}$ to the pair of gear blank pitch surfaces, and to the common normal to the pair of conjugate surfaces which, in effect, undertake the task of transmission. In other words, the tangential direction of the intersection between the gear blank pitch surface and the conjugate surface really undertaking the task of transmission is colinear with \mathbf{v}_p^{12} at the conjugate contact point P. Consequently, the spiral angle of the first conjugate surface, i.e., the tooth surface of the gear, can be defined to be the angle made by the tangential direction to the intersection between the tooth surface of the gear and the first gear blank pitch surface with the direction \mathbf{S} of the generatrix of the first gear blank pitch surface, that is,

$$\begin{aligned} \cos \psi_g &= \frac{|\mathbf{S} \cdot \mathbf{v}_p^{12}|}{|\mathbf{v}_p^{12}|} \\ &= \frac{|S_1 v_{p1}^{12} + S_2 v_{p2}^{12} + S_3 v_{p3}^{12}|}{|\mathbf{v}_p^{12}|} \end{aligned} \quad (3.46)$$

where, $|\mathbf{v}_p^{12}|$, v_p^{12} , v_p^{12} , and v_p^{12} can be found in expression (3.34), and S_1 , S_2 and S_3 can be determined from expression (3.41), for a right-hand gear $0^\circ < \psi_g < 90^\circ$; for a left-hand gear $90^\circ < \psi_g < 180^\circ$.

Analogously, the spiral angle of the second conjugate surface, i.e., the tooth surface of the pinion, can be defined to be the angle made by the tangential direction to the intersection between the tooth surface of the pinion and the second gear blank pitch surface with direction \mathbf{S}' of the generatrix of the second gear blank pitch surface; that is,

$$\begin{aligned} \cos \psi_p &= \frac{|\mathbf{S}' \cdot \mathbf{v}_p^{12}|}{|\mathbf{v}_p^{12}|} \\ &= \frac{|S'_1 v_{p1}^{12'} + S'_2 v_{p2}^{12'} + S'_3 v_{p3}^{12'}|}{|\mathbf{v}_p^{12}|} \end{aligned} \quad (3.47)$$

where, S'_1 , S'_2 and S'_3 can be found in expression (3.43), and $v_{p1}^{12'}$, $v_{p2}^{12'}$ and $v_{p3}^{12'}$ can be found by expression (2.35), for a right-hand pinion $0^\circ < \psi_p < 90^\circ$; for a left-hand pinion $90^\circ < \psi_p < 180^\circ$.

4. The Pressure Angle of the Gear Tooth Surface and the Tooth Curvature.

Since the unit common normal $\mathbf{N}_{1b} = -\mathbf{N}_{2b}$ to the gear blank pitch surfaces and the unit common normal $\mathbf{N}_{1p} = -\mathbf{N}_{2p}$ to the conjugate tooth surfaces are simultaneously perpendicular to the relative velocity $\frac{\mathbf{v}_p^{12}}{|\mathbf{v}_p^{12}|}$, and $\frac{\mathbf{v}_p^{12}}{|\mathbf{v}_p^{12}|}$ coincides with the tangential direction \mathbf{t} to the intersection between the conjugate tooth surface and the gear blank pitch surface, thus, the unit normal \mathbf{N}_{1p} to the tooth surface of the gear can be obtained by a rotation of \mathbf{N}_{1b} about \mathbf{t} through an angle $(\phi_g - 90^\circ)$ and ϕ_g is called the pressure angle of the gear.

The tangential direction \mathbf{t} to the intersection between the conjugate tooth surface and the gear blank pitch surface can be found in the form

$$\left. \begin{aligned} \mathbf{t} &= (-\psi_g \mathbf{N}_{1b}) \otimes \mathbf{S} = t_1 \mathbf{i} + t_2 \mathbf{j} + t_3 \mathbf{k} \\ t_1 &= S_1 \cos \psi_g - (B_b S_3 - C_b S_2) \sin \psi_g \\ t_2 &= S_2 \cos \psi_g - (C_b S_1 - A_b S_3) \sin \psi_g \\ t_3 &= S_3 \cos \psi_g - (A_b S_2 - B_b S_1) \sin \psi_g \end{aligned} \right\} \quad (3.48)$$

where, \mathbf{N}_{1b} is determined by expression (3.38), \mathbf{S} is calculated from expression (3.41) and ψ_g is the spiral angle of the gear determined by expression (3.46).

Then, the unit normal \mathbf{N}_{1p} to the tooth surface of the gear is given as follows

$$\mathbf{N}_{1p} = [(\phi_g - 90^\circ) \mathbf{t}] \otimes \mathbf{N}_{1b} = \sin \phi_g \mathbf{N}_{1b} - \cos \phi_g \mathbf{t} \times \mathbf{N}_{1b} \quad (3.49)$$

As discussed previously, the point at which the conditions $\mathbf{N}_{1p} \cdot \mathbf{v}_p^{12} = 0$ and $\mathbf{N}_{1p} \cdot \mathbf{J}_p = 0$ are fulfilled is called the conjugate stagnant point. In other words, the unit normal at the conjugate stagnant point of the tooth surface of the gear is equal to

$$\mathbf{N}_{op} = \frac{\mathbf{v}_p^{12} \times \mathbf{J}_p}{|\mathbf{v}_p^{12} \times \mathbf{J}_p|} \quad (3.50)$$

which is regarded as the unit limit normal. The pressure angle corresponding to the unit limit normal is defined as the limit pressure angle ϕ_0 .

To derive an expression for the limit pressure angle, we set equation (3.49) equal to expression (3.50), i.e.,

$$\frac{\mathbf{v}_p^{12} \times \mathbf{J}_p}{|\mathbf{v}_p^{12} \times \mathbf{J}_p|} = \sin \phi_0 \mathbf{N}_{1b} - \cos \phi_0 \mathbf{t} \times \mathbf{N}_{1b} \quad (3.51)$$

Dot-multiplication of both sides in the above expression with \mathbf{J}_p yields the limit pressure angle as follows

$$\tan \phi_o = \frac{\mathbf{J}_p \cdot (\mathbf{t} \times \mathbf{N}_{1b})}{\mathbf{J}_p \cdot \mathbf{N}_{1b}} \quad (3.52)$$

where, \mathbf{J}_p , \mathbf{N}_{1b} and \mathbf{t} can be determined by expressions (3.37), (3.38) and (3.48) respectively.

Since only the section on one side of the conjugate stagnant curve can enter the position of conjugate contact, this situation is, of course, undesirable. In order to exclude the conjugate stagnant curve from the active section of the tooth surface, the actual pressure angle of the gear should be different from the limit pressure angle.

From the analyses in section (3.5), it can be seen that when $D_p |\mathbf{v}_p^{12}| + \mathbf{N}_{1p} \cdot \mathbf{J}_p = 0$, curvature interference would occur. Since in hypoid gearing, the relative velocity $|\mathbf{v}_p^{12}|$ is always different from zero, curvature interference would arise whenever $\mathbf{N}_{1p} \cdot \mathbf{J}_p = 0$ and $D_p = 0$ simultaneously. The curvature corresponding to $D_p = 0$ with the limit normal is called the limit normal curvature K_o and it can be found from definition (2.209) as follows

$$K_o = \frac{|\eta_p| \cos \theta_{v\eta}}{|\mathbf{v}_p^{12}|} = \frac{\mathbf{v}_p^{12} \cdot (\boldsymbol{\Omega}_{12} \times \mathbf{N}_{op})}{|\mathbf{v}_p^{12}|^2} \quad (3.53)$$

where, $|\mathbf{v}_p^{12}|$, $|\eta_p|$ and $\cos \theta_{v\eta}$ can be determined from expressions (3.34), (2.133) and (2.135) respectively.

The limit curvature k_c^o of the intersection between the gear tooth surface and the gear blank pitch plane, i.e., the reference plane, is found by using the Meusnier theorem, i.e., expression (2.65)

$$K_o = k_c^o \cos \phi_o \quad (3.54)$$

Correspondingly, the limit curvature radius r_{no} of the intersection of the gear tooth surface with the gear blank pitch plane can be defined to be

$$r_{no} = \frac{|\mathbf{v}_p^{12}| \cos \phi_o}{|\eta_p| \cos \theta_{v\eta}} \quad (3.55)$$

5. Relation of the Surface of Engagement with the Gear Blank Pitch Plane.

Application of expression (2.184) yields a unit vector tangential to the surface of engagement as follows

$$\mathbf{t}_\tau = \frac{[\boldsymbol{\tau} + \mathbf{v}_p \left(\frac{d\epsilon_{1p}}{ds_1} \right)_\tau]}{\left(\frac{ds}{ds_1} \right)_\tau} \quad (3.56)$$

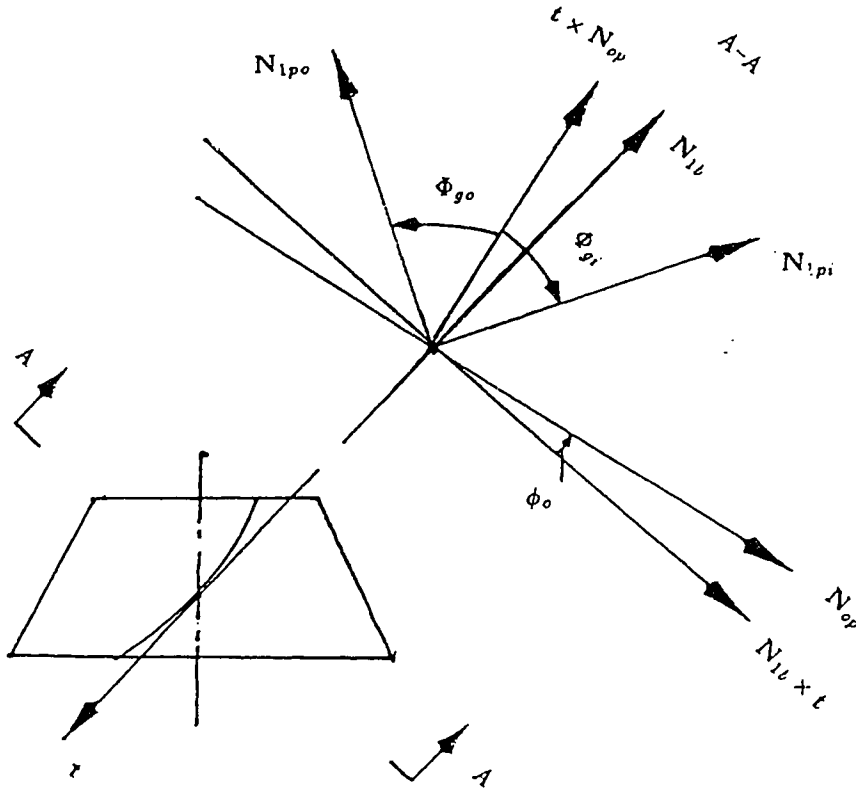


Figure 3.6: Relation among the unit normals

Writing $\tau = \frac{\mathbf{v}_p^{12}}{|\mathbf{v}_p^{12}|}$, expression (2.56) becomes

$$\mathbf{t}_v = \frac{\left[\frac{\mathbf{v}_p^{12}}{|\mathbf{v}_p^{12}|} + \mathbf{v}_p \left(\frac{d\varepsilon_{1p}}{ds_1} \right)_v \right]}{\left(\frac{ds}{ds_1} \right)_v} \quad (3.57)$$

With the aid of expression (3.38), i.e., $\mathbf{N}_{1b} = \frac{\mathbf{v}_p \times \mathbf{v}_p^{12}}{|\mathbf{v}_p \times \mathbf{v}_p^{12}|}$, then, $\mathbf{t}_v \cdot \mathbf{N}_{1b} = 0$, that is, \mathbf{t}_v is the unit vector tangent to the intersection of the surface of engagement with the gear blank pitch plane.

In virtue of fig.3.6, the actual unit normal to the gear tooth surface on the convex side is found

$$\mathbf{N}_{1pi} = \sin \Phi_{gi} \mathbf{N}_{op} + \cos \Phi_{gi} \mathbf{t} \times \mathbf{N}_{op} \quad (3.58)$$

where, Φ_g is the angle between \mathbf{N}_{1p} and $\mathbf{t} \times \mathbf{N}_{op}$.

With the aid of expression (3.50), we obtain

$$\mathbf{N}_{1pi} \cdot \mathbf{J}_p = \cos \Phi_{gi} (\mathbf{t} \times \mathbf{N}_{op}) \cdot \mathbf{J}_p \quad (3.59)$$

where, \mathbf{J}_p , \mathbf{t} and \mathbf{N}_{op} can be determined by expressions (3.37), (3.48) and (3.50).

Let the actual curvature of the intersection between the gear tooth surface on the convex side and the gear blank pitch plane be the sum of the limit curvature k_c^o and the incremental value Δk_{ci} , i.e., $k_c^o + \Delta k_{ci}$. In this case, the actual normal curvature K_{gvi} of the gear tooth surface on the convex side in the direction of the relative velocity $\frac{\mathbf{v}_p^{12}}{|\mathbf{v}_p^{12}|}$ is found by using expression (2.65)

$$K_{gvi} = (k_c^o + \Delta k_{ci}) \sin(\Phi_{gi} - \phi_o) \quad (3.60)$$

Substitution of expressions (3.34), (2.133), (2.135) and (3.60) into (2.209) and using (3.53), (3.54) yields the quantity D_{gpi}

$$\begin{aligned} D_{gpi} &= K_{gvi} |\mathbf{v}_p^{12}| - |\eta_p| \cos \theta_{v\eta} \\ &= -k_c^o |\mathbf{v}_p^{12}| \cos \Phi_{gi} \sin \phi_o + \Delta k_{ci} |\mathbf{v}_p^{12}| \sin(\Phi_{gi} - \phi_o) \\ &\quad - \frac{\mathbf{v}_p^{12} \cdot [\boldsymbol{\Omega}_{12} \times (\mathbf{t} \times \mathbf{N}_{op})]}{|\mathbf{v}_p^{12}|} \cos \Phi_{gi} \end{aligned} \quad (3.61)$$

where, $\boldsymbol{\Omega}_{12}$ is calculated in expression (2.131).

Consequently, with the aid of expressions (3.59) and (3.61), application of expression (2.226) yields the rate of angular increment along the direction of the relative velocity on the convex side in the following form

$$\begin{aligned} \left(\frac{d\varepsilon_{1p}}{ds_1} \right)_{gvi} &= \frac{D_{gpi}}{\mathbf{N}_{1pi} \cdot \mathbf{J}_p} \\ &= -\frac{k_c^o |\mathbf{v}_p^{12}|^2 \sin \phi_o + \mathbf{v}_p^{12} \cdot [\boldsymbol{\Omega}_{12} \times (\mathbf{t} \times \mathbf{N}_{op})]}{|\mathbf{v}_p^{12}| (\mathbf{t} \times \mathbf{N}_{op}) \cdot \mathbf{J}_p} + \frac{\Delta k_{ci} |\mathbf{v}_p^{12}| \sin(\Phi_{gi} - \phi_o)}{(\mathbf{t} \times \mathbf{N}_{op}) \cdot \mathbf{J}_p \cos \Phi_{gi}} \end{aligned} \quad (3.62)$$

Finally, expression (3.57) gives the unit vector tangential to the intersection of the surface of engagement corresponding to the convex side with the gear blank pitch plane as follows

$$\mathbf{t}_{gvi} = \frac{\frac{\mathbf{v}_p^{12}}{|\mathbf{v}_p^{12}|} + \mathbf{v}_p \left(\frac{d\varepsilon_{1p}}{ds_1} \right)_{gvi}}{\left(\frac{ds}{ds_1} \right)_{gvi}} \quad (3.63)$$

Likewise, the actual unit normal to the gear tooth surface on the concave side is given, as shown in fig.3.6

$$\mathbf{N}_{1po} = -\sin \Phi_{go} \mathbf{N}_{op} + \cos \Phi_{go} (\mathbf{t} \times \mathbf{N}_{op}) \quad (3.64)$$

then

$$\mathbf{N}_{1po} \cdot \mathbf{J}_p = \cos \Phi_{go} (\mathbf{t} \times \mathbf{N}_{op}) \cdot \mathbf{J}_p \quad (3.65)$$

where, \mathbf{J}_p , \mathbf{t} and \mathbf{N}_{op} can be determined by expressions (3.37), (3.48) and (3.50).

As we did with the convex side, we let the actual curvature of the intersection of the gear tooth surface on the concave side with the gear blank pitch plane be the sum of the limit curvature k_{co}^o and the modification value Δk_c . Again, the actual normal curvature K_{gvo} of the gear tooth surface on the concave side along the direction of relative velocity $\frac{\mathbf{v}_p^{12}}{|\mathbf{v}_p^{12}|}$ is found in the following form

$$K_{gvo} = -(k_c^o + \Delta k_{co}) \sin(\Phi_{go} + \phi_o) \quad (3.66)$$

Substitution of expressions (3.34), (2.133), (2.135) and (3.66) into (2.209) and using expressions (3.53) and (3.54) yields

$$\begin{aligned} D_{gpo} &= K_{gvo} |\mathbf{v}_p^{12}| - |\eta_p| \cos \theta_{v\eta} \\ &= -k_c^o |\mathbf{v}_p^{12}| \cos \Phi_{go} \sin \phi_o - \Delta k_{co} |\mathbf{v}_p^{12}| \sin(\Phi_{go} + \phi_o) \\ &\quad - \frac{\mathbf{v}_p^{12} \cdot [\boldsymbol{\Omega}_{12} \times (\mathbf{t} \times \mathbf{N}_{op})]}{|\mathbf{v}_p^{12}|} \cos \Phi_{go} \end{aligned} \quad (3.67)$$

Consequently, the rate of angular increment in the direction of the relative velocity on the concave side is found

$$\begin{aligned} \left(\frac{d\epsilon_{1p}}{ds_1} \right)_{gvo} &= \frac{D_{gpo}}{\mathbf{N}_{1po} \cdot \mathbf{J}_p} \\ &= - \frac{k_c^o |\mathbf{v}_p^{12}|^2 \sin \phi_o + \mathbf{v}_p^{12} \cdot [\boldsymbol{\Omega}_{12} \times (\mathbf{t} \times \mathbf{N}_{op})]}{|\mathbf{v}_p^{12}| (\mathbf{t} \times \mathbf{N}_{op}) \cdot \mathbf{J}_p} - \frac{\Delta k_{co} |\mathbf{v}_p^{12}| \sin(\Phi_{go} + \phi_o)}{(\mathbf{t} \times \mathbf{N}_{op}) \cdot \mathbf{J}_p \cos \Phi_{go}} \end{aligned} \quad (3.68)$$

Finally, the unit vector tangent to the intersection of the surface of engagement corresponding to the concave side with the gear blank pitch plane is given

$$\mathbf{t}_{vo} = \frac{\frac{\mathbf{v}_p^{12}}{|\mathbf{v}_p^{12}|} + \mathbf{v}_p \left(\frac{d\epsilon_{1p}}{ds_1} \right)_{gvo}}{\left(\frac{ds}{ds_1} \right)_{gvo}} \quad (3.69)$$

It can be seen from the examination of expressions (3.63) and (3.69) that once the following requirement is satisfied, i.e.,

$$\frac{\Delta k_{ci} \sin(\Phi_{gi} - \phi_o)}{\cos \Phi_{gi}} = - \frac{\Delta k_{co} \sin(\Phi_{go} + \phi_o)}{\cos \Phi_{go}} \quad (3.70)$$

then, $t_{vo} = t_{vi}$; that is, both surfaces of engagement corresponding to the convex and the concave sides intersect in a line which is in tangential contact with the gear blank pitch plane.

It can also be seen that if using the limit normal and limit normal curvature of the gear tooth surface as the actual unit normal and the curvature of the gear tooth surface, then, due to $\mathbf{N}_{1p} \cdot \mathbf{J}_p = \mathbf{N}_{op} \cdot \mathbf{J}_p = 0$ and $D_p = 0$, the corresponding rate of angular increment would become indefinite, i.e., $(\frac{d\varepsilon_{1p}}{ds_1})_v = \frac{0}{0}$. This implies from expression (3.57) that the tangential direction of the intersection between the gear blank pitch plane and the surface of engagement is indefinite, in other words, the gear blank pitch surface is in tangential contact but not intersection with the surface of engagement.

It should be mentioned here that in order to eliminate the possibilities of both the conjugate boundary curve and of curvature interference, the current practice of gear design is to prescribe the pressure angle of the gear different from the limit pressure angle, i.e., $\mathbf{N}_{1p} \cdot \mathbf{J}_p \neq 0$, and use the limit curvature radius as the practical curvature radius of the gear, i.e., $D_p \neq 0$, finally, $D_p|\mathbf{v}_p^{12}| + \mathbf{N}_{1p} \cdot \mathbf{J}_p \neq 0$. But, on the other hand, due to $D_p \neq 0$, it can be seen from expression (2.218) that $\theta_{ve} \neq 0$, that is, there exist bias contacts. In the author's opinion, there is no need to consider the factor of the limit curvature, and just the limit pressure angle is taken into consideration for designing the tooth surface with point contact.

Chapter 4

Design of the Gear Blank

Some expressions in this section are cited directly from AGMA 2005 standard, and some other expressions are different from the AGMA 2005 standard in appearance but the same in principle.

4.1 Calculation of the Basic Shape Parameters

Let the number of teeth for the gear and the pinion be N_g and N_p respectively, and the theoretical transmission ratio between gear and pinion is in the form

$$M_{gp} = \frac{N_g}{N_p} \quad (4.1)$$

The face width F_G of the gear and the hypoid offset f_{gp} are specified by the users of hypoid gearing.

Although the shaft angle between the gear and the pinion in hypoid gearing can be any value, the right angle is most widely used in the industry practice. In order to simplify the calculation, this thesis is confined to discuss only the case of a right angle between the gear and the pinion shafts, i.e., $\alpha = -90^\circ$ in condition (3.1), but the principle used here can be applied in the case of a shaft angle with any value.

We select the tooth surface of the gear as the fundamental surface and then, the tooth surface of the pinion is the mating surface. Further, we prescribe a point P_b on the fundamental surface as the reference point, and the gear blank pitch surfaces through the reference point P_b are used as reference surfaces (reference cones) to define nominal parameters such as pressure angles, spiral angles and so on. The position of

the reference point is not strictly prescribed but is usually at the mean point of the tooth width and the center of a tooth space on the reference cones. Its position can be defined by the following three parameters,

Parameter 1: The radial distance of the reference point P_b to axis $\omega_1 = k$ — ρ_b ;

Parameter 2: The phase angle made by rotating axis i about axis k to the radial vector of the reference point P_b — μ_b ;

Parameter 3: The axial distance of reference point P_b from origin point O along axis k — z_b .

Once these three position parameters for reference point P_b are prescribed, the basic shape parameters, i.e., pitch angles, spiral angles and pressure angles, can be accordingly determined as following

1. Pitch Angles.

(1). Gear pitch angle γ_g .

Replacing ρ , μ , z_p and f in expression (3.44) by ρ_b , μ_b , z_b and f_{gp} respectively and considering $\alpha = -90^\circ$ yields the gear pitch angle as follows

$$\cos \gamma_g = \frac{|(\rho_b \cos \mu_b - f_{gp})|}{Q_b} \quad (4.2)$$

$$0 < \gamma_g \leq 90^\circ$$

where, f_{gp} is the offset between the gear and the pinion, and Q_b is found in the form

$$Q_b = \sqrt{(\rho_b \cos \mu_b - f_{gp})^2 + z_b^2 \cos^2 \mu_b} \quad (4.3)$$

(2). Pinion pitch angle γ_p .

The position parameters for point P'_b on the pinion corresponding to the reference point P_b on gear can be found by using expression (3.32) as follows

$$\left. \begin{aligned} \rho'_b &= \sqrt{(\rho_b \cos \mu_b - f_{gp})^2 + z_b^2} \\ \tan \mu'_b &= \frac{z_b}{\rho_b \cos \mu_b - f_{gp}} \\ z'_b &= -\rho_b \sin \mu_b \end{aligned} \right\} \quad (4.4)$$

where, ρ'_b is the radial distance of point P'_b from axis $k' = -\omega_2$; μ'_b is the phase angle made by rotating axis i' to the radial vector of point P'_b , and z'_b is the axial distance from point P'_b to origin point O' along axis $k' = -\omega_2$.

Then, application of expression (3.45) leads to the pinion pitch angle as follows

$$\cos \gamma_p = \frac{|\cos \mu_b \sqrt{(\rho_b \cos \mu_b - f_{gp})^2 + z_b^2}|}{Q_b} \quad (4.5)$$

$$0 < \gamma_p \leq 90^\circ$$

2. Spiral Angles.

(1). Gear spiral angle ψ_g .

Application of expression (3.34) and setting $\alpha = -90^\circ$ yields the velocity at the reference point P_b of the gear relative to point P_b on the pinion as follows

$$\left. \begin{aligned} \mathbf{v}_b^{12} &= v_{b1}^{12}\mathbf{i} + v_{b2}^{12}\mathbf{j} + v_{b3}^{12}\mathbf{k} \\ v_{b1}^{12} &= -\rho_b \sin \mu_b - M_{gp} z_b \\ v_{b2}^{12} &= \rho_b \cos \mu_b \\ v_{b3}^{12} &= M_{gp}(\rho_b \cos \mu_b - f_{gp}) \\ |\mathbf{v}_b^{12}| &= \sqrt{(v_{b1}^{12})^2 + (v_{b2}^{12})^2 + (v_{b3}^{12})^2} \end{aligned} \right\} \quad (4.6)$$

and expression (3.41) gives the generatrix of the gear reference cone in the form

$$\left. \begin{aligned} \mathbf{S}_b &= S_{b1}\mathbf{i} + S_{b2}\mathbf{j} + S_{b3}\mathbf{k} \\ S_{b1} &= \frac{z_b \cos^2 \mu_b}{Q_b} \\ S_{b2} &= \frac{z_b \cos \mu_b \sin \mu_b}{Q_b} \\ S_{b3} &= \frac{-(\rho_b \cos \mu_b - f_{gp})}{Q_b} \end{aligned} \right\} \quad (4.7)$$

Then, substitution of expressions (4.6) and (4.7) into (3.46) yields the gear spiral angle ψ_g as follows

$$\cos \psi_g = \frac{|v_{b1}^{12}S_{b1} + v_{b2}^{12}S_{b2} + v_{b3}^{12}S_{b3}|}{|\mathbf{v}_b^{12}|} \quad (4.8)$$

where, if $f_{gp} > 0$, then $0^\circ < \psi_g < 90^\circ$; if $f_{gp} < 0$, then $90^\circ < \psi_g < 180^\circ$.

(2). Pinion spiral angle ψ_p .

Expression (3.43) gives the generatrix of the pinion reference cone in the form

$$\left. \begin{aligned} \mathbf{S}'_b &= S'_{b1}\mathbf{i}' + S'_{b2}\mathbf{j}' + S'_{b3}\mathbf{k}' \\ S'_{b1} &= \frac{(\rho_b \cos \mu_b - f_{gp})^2 \sin \mu_b}{Q_b \sqrt{(\rho_b \cos \mu_b - f_{gp})^2 + z_b^2}} \\ S'_{b2} &= \frac{z_b(\rho_b \cos \mu_b - f_{gp}) \sin \mu_b}{Q_b \sqrt{(\rho_b \cos \mu_b - f_{gp})^2 + z_b^2}} \\ S'_{b3} &= \frac{\cos \mu_b \sqrt{(\rho_b \cos \mu_b - f_{gp})^2 + z_b^2}}{Q_b} \end{aligned} \right\} \quad (4.9)$$

and expression (3.35) gives

$$\left. \begin{aligned} \mathbf{v}_b^{12} &= v_{b1'}^{12}\mathbf{i}' + v_{b2'}^{12}\mathbf{j}' + v_{b3'}^{12}\mathbf{k}' \\ v_{b1'}^{12} &= v_{b1}^{12} \\ v_{b2'}^{12} &= v_{b3}^{12} \\ v_{b3'}^{12} &= -v_{b2}^{12} \end{aligned} \right\} \quad (4.10)$$

Then, substitution of expressions (4.9) and (4.10) into (3.47) yields the pinion spiral angle as follows

$$\cos \psi_p = \frac{|S'_{b1}v_{b1'}^{12} + S'_{b2}v_{b2'}^{12} + S'_{b3}v_{b3'}^{12}|}{|v_b^{12}|} \quad (4.11)$$

where, if $f_{gp} > 0$, then $90^\circ < \psi_p < 180^\circ$; if $f_{gp} < 0$, then $0^\circ < \psi_p < 90^\circ$.

3. Pressure Angles.

The gear pressure angle ϕ_g can be prescribed as long as its value is different from the limit pressure angle ϕ_o . Replacing M , f , ρ , μ and z_p in expression (3.37) by M_{gp} , f_{gp} , ρ_b , μ_b and z_b and setting $\alpha = -90^\circ$ yields

$$\left. \begin{aligned} J_b &= J_{b1}\mathbf{i} + J_{b2}\mathbf{j} + J_{b3}\mathbf{k} \\ J_{b1} &= 0 \\ J_{b2} &= -M_{gp}z_b \\ J_{b3} &= M_{gp}\rho_b \sin \mu_b \end{aligned} \right\} \quad (4.12)$$

Expression (3.38) can be further simplified in the form

$$\left. \begin{aligned} N_{1b} &= A_b\mathbf{i} + B_b\mathbf{j} + C_b\mathbf{k} \\ A_b &= -\frac{(\rho_b \cos \mu_b - f_{gp}) \cos \mu_b}{Q_b} \\ B_b &= -\frac{(\rho_b \cos \mu_b - f_{gp}) \sin \mu_b}{Q_b} \\ C_b &= -\frac{z_b \cos \mu_b}{Q_b} \end{aligned} \right\} \quad (4.13)$$

where, Q_b is given by expression (4.3).

Substitution of expressions (3.48), (4.12) and (4.13) into (3.52) yields the limit pressure angle

$$\tan \phi_o = \frac{\rho_b(t_1B_b - t_2A_b) \sin \mu_b - z_b(t_3A_b - t_1C_b)}{\rho_bC_b \sin \mu_b - z_bB_b} \quad (4.14)$$

Then, the gear pressure angles are in the following forms

(1). Pressure angle on the convex face, ϕ_{gi} .

$$\phi_{gi} = \phi_{gm} + \phi_o \quad (4.15)$$

where, $0^\circ < \phi_{gm} < 90^\circ$ and $0 < \phi_{gi} < 90^\circ$.

(2). Pressure angle on the concave face, ϕ_{go} .

$$\phi_{go} = 180 - \phi_{gm} + \phi_o \quad (4.16)$$

where, $90^\circ < \phi_{go} < 180^\circ$.

(3). Average pressure angle of gear, Φ_g .

$$\Phi_g = \frac{180^\circ - \phi_{go} + \phi_{gi}}{2} \quad (4.17)$$

The pressure angle of the pinion depends on the condition of conjugate motion and the requirement of the curvature modification and is directly influenced by the pressure angle of the gear.

4.2 Calculation of the Gear Blank Parameters for the Gear and the Pinion

1. Select Depth Factor k_1 , Mean Addendum Factor c_1 and Clearance Factor k_2 .

The depth factor k_1 can be found from table 6—1 in the AGMA standard [8].

The mean addendum factor c_1 can be found from table 6—2 in the AGMA standard.

The clearance factor k_2 can be found from chapter 6.5 in the AGMA standard.

2. Depth Parameters at the Reference point on the Gear.

(1). Mean working depth h .

The mean working depth h can be calculated from table 6—7 in the AGMA standard in the following form

$$h = \frac{2k_1\rho_b \cos \psi_g}{N_g} \quad (4.18)$$

(2). Mean addendum.

With the aid of table 6—7 in the AGMA standard, the mean addendum values can be determined in the following form.

Mean addendum for the gear a_g .

$$a_g = c_1 h \quad (4.19)$$

Mean addendum for the pinion a_p .

$$a_p = h - a_g \quad (4.20)$$

(3). Mean dedendum.

With the aid of table 6—7 in the AGMA standard, the mean dedendum values can be found as follows:

Mean dedendum for the gear b_g .

$$b_g = h(1 + k_2 - c_1) \quad (4.21)$$

Mean dedendum for the pinion b_p .

$$b_p = b_g + a_g - a_p \quad (4.22)$$

(4). Clearance c .

With the aid of table 6—7 in the AGMA standard, the clearance c is found in the form

$$c = k_2 h \quad (4.23)$$

3. Depthwise taper parameters of the gear.

(1). Sum of the dedendum angles, $\Sigma\delta_D$

Figure 4.1 (a) exhibits the shape of the tooth slot on the gear pitch cone. It can be seen from fig. 4.1 (a) that

$$\beta_1 = \frac{MN}{Ob} \quad (4.24)$$

due to

$$MN = \frac{\pi \rho_b}{N_g} \quad (4.25)$$

and with the aid of fig.4.1 (b), we obtain

$$\overline{ob} = \frac{\rho_b}{\sin \gamma_g} \quad (4.26)$$

where, γ_g is found in expression (4.2).

Thus, substitution of expressions (4.25), (4.26) into (4.24) leads to

$$\beta_1 = \frac{\pi \sin \gamma_g}{N_g} \quad (4.27)$$

Examination of fig.4.1 (a) gives

$$\beta_2 = \frac{mn}{\overline{O_c b}} \quad (4.28)$$

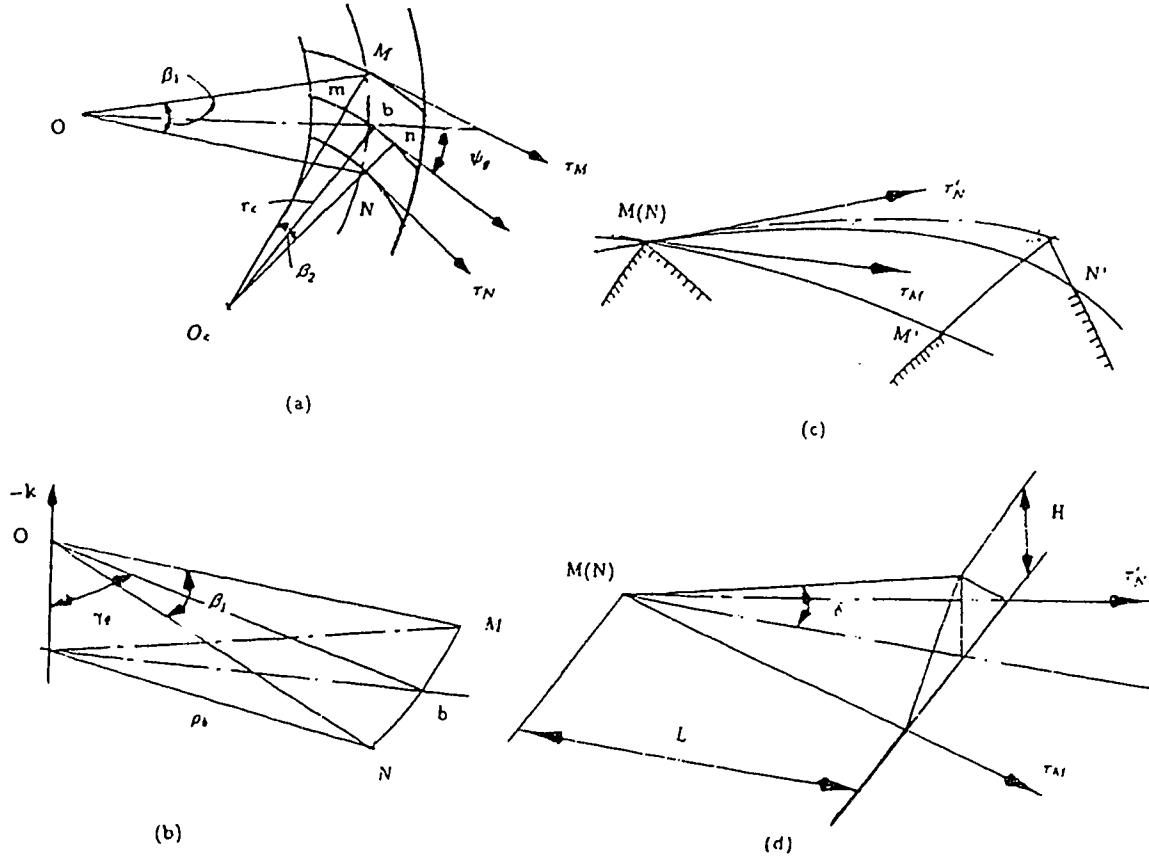


Figure 4.1: Approximate determination of the sum of the dedendum angles.

due to

$$\left. \begin{aligned} mn &\approx MN \sin \psi_g \\ \overline{O_c b} &= r_c \end{aligned} \right\} \quad (4.29)$$

where, r_c is the nominal radius of the cutter.

With the aid of expression (4.25), substitution of expressions (4.29) into (4.28) yields

$$\beta_2 = \frac{\pi \rho_b \sin \psi_g}{r_c N_g} \quad (4.30)$$

After rotating the convex flank about the axis $-k$ until point N coincides with point M on the concave flank, as shown in fig.4.1 (c), the unit vector τ_N becomes τ'_N given by the following expression

$$\begin{aligned}
\tau'_N &= (-\beta_1 \mathbf{k}) \otimes \tau_N \\
&= (-\beta_1 \mathbf{k}) \otimes [(\beta_2 \mathbf{k}) \otimes \tau_M] \\
&= [(\beta_2 - \beta_1) \mathbf{k}] \otimes \tau_M
\end{aligned} \tag{4.31}$$

On the other hand, τ'_N can be expressed in the form

$$\tau'_N = (-\lambda \mathbf{k}) \otimes \tau_M \tag{4.32}$$

in which λ is the angle made by rotating τ_M about the axis $-\mathbf{k}$ to τ'_N .

A Comparison of expressions (4.31) and (4.32) yields

$$\lambda = \beta_1 - \beta_2 \tag{4.33}$$

By replacing the actual tooth surfaces on both sides with the tangential planes at points M and N, as shown in fig.4.1 (d), we obtain

$$H \tan \Phi_g \approx L \frac{\lambda}{2} \tag{4.34}$$

where, Φ_g is found in expression (4.17).

On the other hand, H can be found as following

$$H \approx L\delta \tag{4.35}$$

Therefore, the combination of expressions (4.34) and (4.35) leads to

$$\begin{aligned}
\delta &= \frac{\lambda}{2 \tan \Phi_g} = \frac{\beta_1 - \beta_2}{2 \tan \Phi_g} \\
&= \frac{1}{2 \tan \Phi_g} \left(\frac{\pi \sin \gamma_g}{N_g} - \frac{\pi \rho_b \sin \psi_g}{r_c N_g} \right)
\end{aligned} \tag{4.36}$$

Finally, the sum of the dedendum angles in the case of duplex depth taper can be found in the form

$$\begin{aligned}
\Sigma \delta_D &= \frac{2\delta}{|\cos \psi_g|} \\
&= \frac{\pi}{N_g \tan \Phi_g |\cos \psi_g|} \left(\sin \gamma_g - \frac{\rho_b \sin \psi_g}{r_c} \right)
\end{aligned} \tag{4.37}$$

By defining the mean pitch cone distance of the gear as

$$A_{mG} = \frac{\rho_b}{\sin \gamma_g} \tag{4.38}$$

expression (4.37) can be rewritten in the form

$$\Sigma\delta_D = \frac{\pi \sin \gamma_g}{N_g \tan \Phi_g |\cos \psi_g|} \left(1 - \frac{A_{mG} \sin \psi_g}{r_c}\right) \quad (4.39)$$

Since the diametral pitch of gear is defined as

$$P_d = \frac{N_g}{D} \quad (4.40)$$

and the outer cone distance is found in the form

$$A_{oG} = \frac{D}{2 \sin \gamma_g} \quad (4.41)$$

in which D is the pitch diameter, then $\Sigma\delta_D$ can be expressed in the form

$$\Sigma\delta_D = \frac{90^\circ}{P_d A_{oG} \tan \Phi_g |\cos \psi_g|} \left(1 - \frac{A_{mG} \sin \psi_g}{r_c}\right) \quad (4.42)$$

(2). Dedendum angle of the gear, δ_g .

Table 6—4 in the AGMA standard yields

$$\delta_g = \Sigma\delta_D - \Sigma\delta_D \left(\frac{a_g}{h}\right) \quad (4.43)$$

(3). Addendum angle of the gear, α_g .

Table 6—7 in the AGMA standard gives

$$\alpha_g = \Sigma\delta_D - \delta_g \quad (4.44)$$

4. Blank parameters of the gear.

With the aid of fig.4.2, the blank parameters of the gear can be found as follows:

(1). Face angle of gear, γ_{gf} .

Table 6—7 in the AGMA standard gives the relation

$$\gamma_{gf} = \gamma_g + \alpha_g \quad (4.45)$$

(2). Root angle of the gear, γ_{gr} .

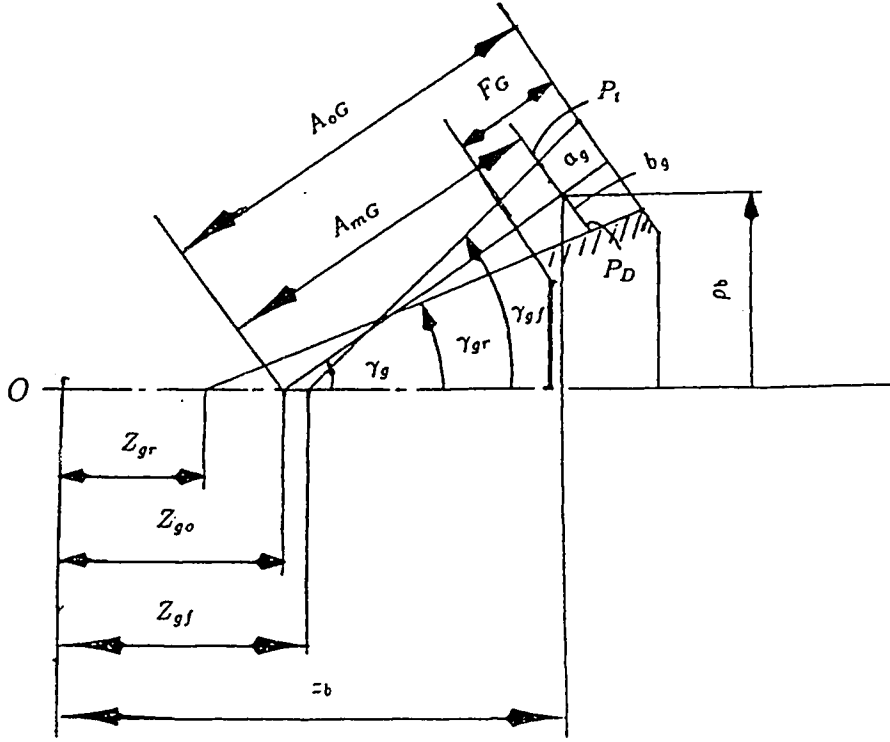


Figure 4.2:Blank parameters of gear

Table 6—7 in the AGMA standard gives

$$\gamma_{gr} = \gamma_g - \delta_g \quad (4.46)$$

(3). Pitch apex beyond the crossing point (including sign), Z_{go} .

Examination of fig. 4.2 yields

$$Z_{go} = z_b - \frac{\rho_b}{\tan \gamma_g} \quad (4.47)$$

(4). Face apex beyond the crossing point (including sign), Z_{gf} .

With the aid of fig.4.2, we can see that

$$Z_{gf} = z_b - \left(\frac{\rho_b + a_g \cos \gamma_g}{\tan \gamma_{gf}} + a_g \sin \gamma_g \right) \quad (4.48)$$

(5). Root apex beyond the crossing point (including sign), Z_{gr} .

The coordinate Z_{gr} is found in the same way

$$Z_{gr} = z_b - \left(\frac{\rho_b - b_g \cos \gamma_g}{\tan \gamma_{gr}} - b_g \sin \gamma_g \right) \quad (4.49)$$

5. Blank parameters of the pinion.

(1). Face angle of the pinion, γ_{pf} .

The parameters of point P_D shown in fig.4.2 are found in the form

$$\left. \begin{aligned} \rho_D &= \rho_b - (b_g - c) \cos \gamma_g \\ z_D &= z_b + (b_g - c) \sin \gamma_g \end{aligned} \right\} \quad (4.50)$$

We construct a cone through point P_D with cone angle equal to root angle γ_{gr} of the gear. Then application of expression (3.44), setting $\alpha = -90^\circ$, yields the phase angle μ_D of point P_D as follows

$$\cos \mu_D = \frac{f_{gp} \tan \gamma_{gr}}{z_D + \rho_D \tan \gamma_{gr}} \quad (4.51)$$

Employment of expression (3.45) gives the angle γ_{pf} of the pinion as follows

$$\cos \gamma_{pf} = \left| \frac{\cos \mu_D \sqrt{(\rho_D \cos \mu_D - f_{gp})^2 + z_D^2}}{Q_D} \right| \quad (4.52)$$

where

$$Q_D = \sqrt{(\rho_D \cos \mu_D - f_{gp})^2 + z_D^2 \cos^2 \mu_D} \quad (4.53)$$

(2). Root angle of the pinion, γ_{pr} .

Likewise, parameters of point P_t shown in fig.4.2 are found in the form

$$\left. \begin{aligned} \rho_t &= \rho_b + (a_g + c) \cos \gamma_g \\ z_t &= z_b - (a_g + c) \sin \gamma_g \end{aligned} \right\} \quad (4.54)$$

Again, we construct a cone through point P_t with cone angle equal to the face angle γ_{gf} of the gear. Then application of expression (3.44), setting $\alpha = -90^\circ$, yields the phase angle μ_t of point P_t as follows

$$\cos \mu_t = \frac{f_{gp} \tan \gamma_{gf}}{z_t + \rho_t \tan \gamma_{gf}} \quad (4.55)$$

Employment of expression (3.45) leads to the root angle γ_{pr} of the pinion as follows

$$\cos \gamma_{pr} = \left| \frac{\cos \mu_t \sqrt{(\rho_t \cos \mu_t - f_{gp})^2 + z_t^2}}{Q_t} \right| \quad (4.56)$$

where

$$Q_t = \sqrt{(\rho_t \cos \mu_t - f_{gp})^2 + z_t^2 \cos^2 \mu_t} \quad (4.57)$$

(3). Face apex beyond the crossing point (including sign), Z_{pf} .

$$Z_{pf} = -\rho_D \sin \mu_D - \frac{\rho'_D}{\tan \gamma_{pf}} \quad (4.58)$$

where, with the aid of expression (3.33), ρ'_D can be determined in the form

$$\rho'_D = \sqrt{(\rho_D \cos \mu_D - f_{gp})^2 + z_D^2} \quad (4.59)$$

(4). Root apex beyond the crossing point (including sign), Z_{pr} .

$$Z_{pr} = -\rho_t \sin \mu_t - \frac{\rho'_t}{\tan \gamma_{pr}} \quad (4.60)$$

where, with the aid of expression (3.33), ρ'_t can be determined in the form

$$\rho'_t = \sqrt{(\rho_t \cos \mu_t - f_{gp})^2 + z_t^2} \quad (4.61)$$

Chapter 5

Determination of Machine-Setting Parameters for the Generation of the Gear Tooth Surface

In processing a pair of hypoid gears, the fundamental surface, i.e., the tooth surface of the gear, is usually cut first, and then, according to the fundamental surface obtained, the adaptability of a pair of tooth surfaces to errors and the requirement for transmission precision, the tooth surface of the mating gear, i.e., the tooth surface of the pinion, is finally produced through proper curvature modifications. Therefore, there is no unique specification for the shape of the fundamental surface, and this facilitates the design and manufacture of the gear tooth surface.

The current method for determining the machine-setting parameters is to introduce an imaginary crown gear and then to try to find a relationship between the imaginary crown gear and the workpiece. This method lacks a theoretical basis. Since the essence of the problem for calculating the machine-setting parameters is to determine the relationship between a pair of motions, i.e., the motions of cutter ϕ_1 and workpiece ϕ_2 , and a pair of surfaces, i.e., the cutter surface A and the tooth surface \bar{A} , it is necessary to satisfy the requirements of conjugation, i.e., expressions (2.153), (2.155), (2.157) and (2.158). Furthermore, the tooth surface \bar{A} is formed by the cutter surface A under the motions of cutter ϕ_1 and workpiece ϕ_2 , and therefore, the machine-setting parameters can be calculated with the aid of the solution to the first kind of problem of conjugate surfaces given in section 2.4.2.

The Gleason No. 16 Bevel-Gear Generator enables us to produce a tooth surface of hypoid gearing by the Formate method or by generation with or without the tilt device. In the case of Formate, a cutter surface, i.e., a cone formed by rotation of

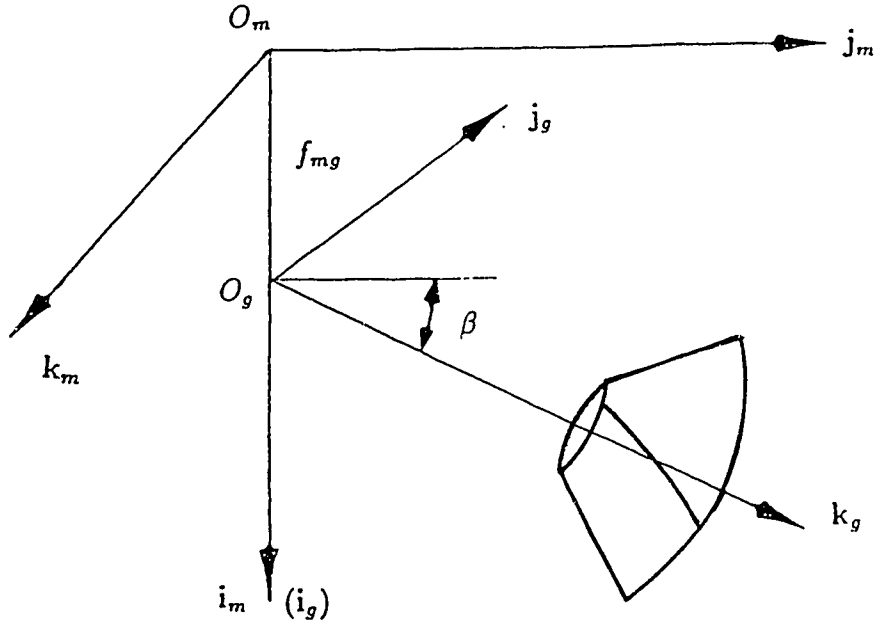


Figure 5.1: Dual coordinate systems for determination of the machine-setting

cutting edge, takes no motion with respect to the workpiece and the tooth surface obtained is the complement of the cutter surface. In the case of the generating method, the cutter surface rotates about the cradle axis, and the workpiece rotates about its own axis. Hence, the tooth surface of the workpiece is the envelope surface of the cutter surface under the motion of the cutter relative to the workpiece. In the case of the generating method without a tilt device, the axis of the cutter is parallel to that of the cradle; while in the case of the generating method with a tilt device, the axis of the cutter is not parallel to that of the cradle.

The orientation of the cutter axis relative to the cradle axis is defined by the tilt angle and the swivel angle. The angle between the cradle axis and the cutter axis is called the tilt angle which is used to compensate the difference of the pressure angle of the workpiece and to obtain the required root angle. The swivel angle is used to adjust the orientation of the inclined angle of the cutter axis with respect to the cradle.

Similarly to section 2.3.2, we use dual coordinate systems $O_m - i_m, j_m, k_m$ and

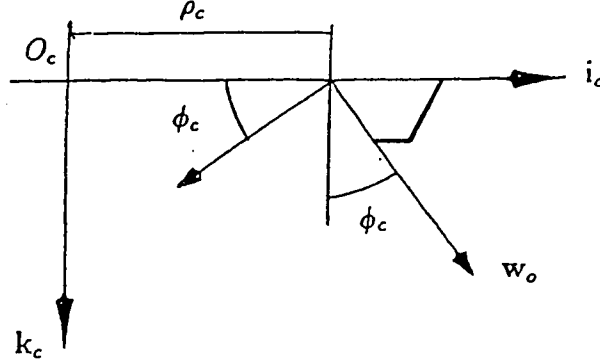


Figure 5.2: The initial position of cutting edge

$O_g - i_g, j_g, k_g$ as shown in fig.5.1, and we choose coordinate system $O_m - i_m, j_m, k_m$ corresponding to the machine frame, k_m being coincident with the axis of the cradle, and i_m being vertically down. The coordinate system $O_g - i_g, j_g, k_g$ corresponds to the workpiece, k_g being coincident with the rotating axis of the workpiece. The relationship between $O_m - i_m, j_m, k_m$ and $O_g - i_g, j_g, k_g$ is found as follows,

$$\left. \begin{aligned} \vec{O_m O_g} &= f_{mg} i_m \\ i_g &= i_m \\ j_g &= (\beta i_m) \otimes (-k_m) = -\cos \beta k_m + \sin \beta j_m \\ k_g &= (\beta i_m) \otimes j_m = \sin \beta k_m + \cos \beta j_m \end{aligned} \right\} \quad (5.1)$$

5.1 Expressions for the Cutter Surface

Cutter surface A_c can be expressed in coordinate system $O_c - i_c, j_c, k_c$ as shown in fig.5.2. k_c coincides with the axis of the cutter.

Let w_o be the tangential direction of the cutting edge in the coordinate plane $i_c - O_c - j_c$ as follows

$$w_o = \sin \phi_c i_c + \cos \phi_c k_c \quad (5.2)$$

where, $0^\circ < \phi_c < 180^\circ$.

Then, the expression for the cutter surface can be obtained by rotating the cutting

edge about axis \mathbf{k}_c as follows

$$\begin{aligned}\mathbf{R}_c &= (\sigma \mathbf{k}_c) \otimes (\rho_c \mathbf{i}_c + s \mathbf{w}_o) \\ &= (\rho_c + s \sin \phi_c) \cos \sigma \mathbf{i}_c + (\rho_c + s \sin \phi_c) \sin \sigma \mathbf{j}_c + s \cos \phi_c \mathbf{k}_c\end{aligned}\quad (5.3)$$

where, in the case of the concave side, $\sigma = \sigma^o$, $s = s^o$, $\phi_c = \phi_c^o$, $\rho_c = \rho_c^o$, and in the case of the convex side, $\sigma = \sigma^i$, $s = s^i$, $\phi_c = \phi_c^i$, $\rho_c = \rho_c^i$.

Correspondingly, the unit normal \mathbf{N}_c to the cutter surface may be expressed in the form

$$\begin{aligned}\mathbf{N}_c &= (\sigma \mathbf{k}_c) \otimes (-\cos \phi_c \mathbf{i}_c + \sin \phi_c \mathbf{k}_c) \\ &= -\cos \phi_c \cos \sigma \mathbf{i}_c - \cos \phi_c \sin \sigma \mathbf{j}_c + \sin \phi_c \mathbf{k}_c\end{aligned}\quad (5.4)$$

Now, we embed coordinate system $O_c - \mathbf{i}_c, \mathbf{j}_c, \mathbf{k}_c$ into $O_m - \mathbf{i}_m, \mathbf{j}_m, \mathbf{k}_m$, as shown in fig.5.3 and the coordinate systems $O_c - \mathbf{i}_c, \mathbf{j}_c, \mathbf{k}_c$ and $O_m - \mathbf{i}_m, \mathbf{j}_m, \mathbf{k}_m$ are related as follows

$$\left. \begin{aligned}\mathbf{i}_c &= (\Theta \mathbf{k}_m) \otimes \mathbf{i}_m = \cos \Theta \mathbf{i}_m + \sin \Theta \mathbf{j}_m \\ \mathbf{k}_c &= (\zeta \mathbf{i}_c) \otimes \mathbf{k}_m = \sin \zeta \sin \Theta \mathbf{i}_m - \sin \zeta \cos \Theta \mathbf{j}_m + \cos \zeta \mathbf{k}_m \\ \mathbf{j}_c &= \mathbf{k}_c \times \mathbf{i}_c = -\cos \zeta \sin \Theta \mathbf{i}_m + \cos \zeta \cos \Theta \mathbf{j}_m + \sin \zeta \mathbf{k}_m\end{aligned}\right\} \quad (5.5)$$

where, Θ is the swivel angle, and ζ is the tilt angle. For the concave side: $\Theta = \Theta^o$; for the convex side: $\Theta = \Theta^i$.

Without the tilt device, i.e., $\Theta = \zeta = 0$, the relationship above will be simplified as follows

$$\left. \begin{aligned}\mathbf{i}_c &= \mathbf{i}_m \\ \mathbf{j}_c &= \mathbf{j}_m \\ \mathbf{k}_c &= \mathbf{k}_m\end{aligned}\right\} \quad (5.6)$$

and

$$\vec{O_m O_c} = x_c \mathbf{i}_m + y_c \mathbf{j}_m + z_c \mathbf{k}_m \quad (5.7)$$

where, for the concave flank: $x_c = x_c^o$, $y_c = y_c^o$, $z_c = z_c^o$; for the convex flank: $x_c = x_c^i$, $y_c = y_c^i$, $z_c = z_c^i$.

Then, with the aid of expression (5.5), the cutter surface A_c can be expressed in coordinate system $O_m - \mathbf{j}_m, \mathbf{j}_m, \mathbf{k}_m$ as follows

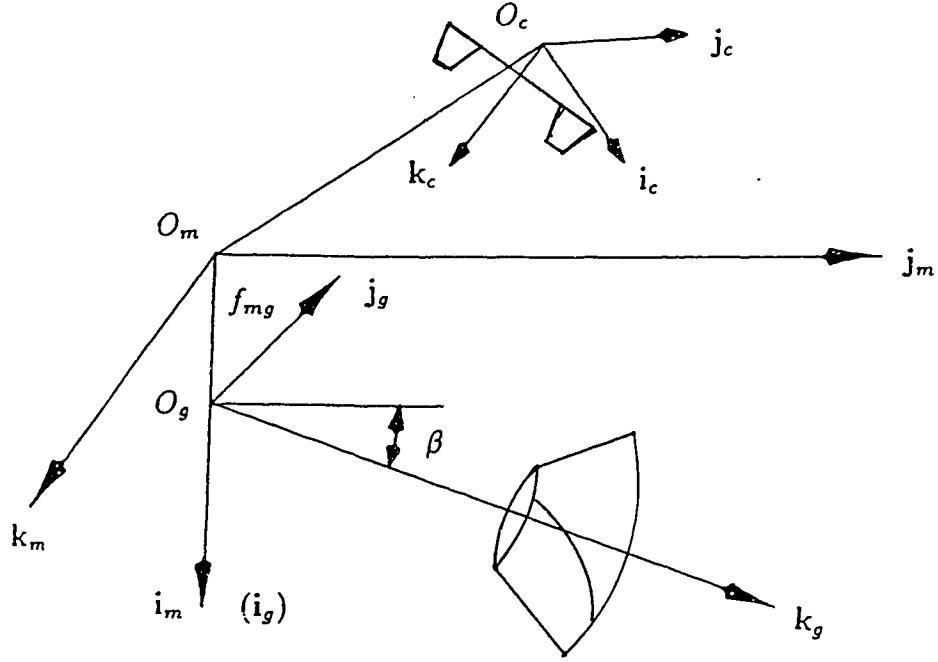


Figure 5.3: Relationship among coordinate systems

$$\begin{aligned}
 \mathbf{R}_m &= \mathbf{O}_m \vec{O}_c + \mathbf{R}_c \\
 &= [x_c + (\rho_c + s \sin \phi_c)(\cos \sigma \cos \Theta - \sin \sigma \cos \zeta \sin \Theta) \\
 &\quad + s \cos \phi_c \sin \zeta \sin \Theta] \mathbf{i}_m \\
 &\quad + [y_c + (\rho_c + s \sin \phi_c)(\cos \sigma \sin \Theta + \sin \sigma \cos \zeta \cos \Theta) \\
 &\quad - s \cos \phi_c \sin \zeta \cos \Theta] \mathbf{j}_m \\
 &\quad + [z_c + (\rho_c + s \sin \phi_c) \sin \sigma \sin \zeta + s \cos \phi_c \cos \zeta] \mathbf{k}_m
 \end{aligned} \tag{5.8}$$

Further, if we assume that the cutting position of the point on the cutter corresponding to reference point P_b on the workpiece is in coordinate plane $\mathbf{i}_c - \mathbf{O}_c - \mathbf{j}_c$, i.e., $s = 0$, then the position vector of the point on the cutter corresponding to the reference point P_b on the workpiece can be simplified in the form

$$\begin{aligned}
 \mathbf{R}_{mb} &= (x_c + \rho_c \cos \sigma \cos \Theta - \rho_c \sin \sigma \cos \zeta \sin \Theta) \mathbf{i}_m \\
 &\quad + (y_c + \rho_c \cos \sigma \sin \Theta + \rho_c \sin \sigma \cos \zeta \cos \Theta) \mathbf{j}_m \\
 &\quad + (z_c + \rho_c \sin \sigma \sin \zeta) \mathbf{k}_m
 \end{aligned} \tag{5.9}$$

where, for the concave flank: $\rho_c = \rho_c^o$, $\sigma = \sigma^o$, $\Theta = \Theta^o$, $x_c = x_c^o$, $y_c = y_c^o$, $z_c = z_c^o$; for the convex flank: $\rho_c = \rho_c^i$, $\sigma = \sigma^i$, $\Theta = \Theta^i$, $x_c = x_c^i$, $y_c = y_c^i$, $z_c = z_c^i$.

Correspondingly, the unit normal \mathbf{N}_c to the cutter surface is found in the form

$$\left. \begin{aligned} \mathbf{N}_c &= N_{cx}\mathbf{i}_m + N_{cy}\mathbf{j}_m + N_{cz}\mathbf{k}_m \\ N_{cx} &= -\cos\phi_c \cos\sigma \cos\Theta + \cos\phi_c \sin\sigma \cos\zeta \sin\Theta + \sin\phi_c \sin\zeta \sin\Theta \\ N_{cy} &= -\cos\phi_c \cos\sigma \sin\Theta - \cos\phi_c \sin\sigma \cos\zeta \cos\Theta - \sin\phi_c \sin\zeta \cos\Theta \\ N_{cz} &= -\cos\phi_c \sin\sigma \sin\zeta + \sin\phi_c \cos\zeta \end{aligned} \right\} \quad (5.10)$$

Without the tilt device, i.e., $\Theta = \zeta = 0$, expressions (5.8) and (5.9) become

$$\mathbf{R}_m = [x_c + (\rho_c + s \sin\phi_c) \cos\sigma]\mathbf{i}_m + [y_c + (\rho_c + s \sin\phi_c) \sin\sigma]\mathbf{j}_m + (z_c + s \cos\phi_c)\mathbf{k}_m \quad (5.11)$$

$$\mathbf{R}_{mb} = (x_c + \rho_c \cos\sigma)\mathbf{i}_m + (y_c + \rho_c \sin\sigma)\mathbf{j}_m + z_c\mathbf{k}_m \quad (5.12)$$

Correspondingly, the unit normal \mathbf{N}_c to the cutter surface in the case of the no tilt device is found as follows

$$\begin{aligned} \mathbf{N}_c &= (\sigma\mathbf{k}_c) \otimes (-\cos\phi_c\mathbf{i}_c + \sin\phi_c\mathbf{k}_c) \\ &= -\cos\phi_c \cos\sigma\mathbf{i}_m - \cos\phi_c \sin\sigma\mathbf{j}_m + \sin\phi_c\mathbf{k}_m \end{aligned} \quad (5.13)$$

where, for the convex side: $\phi_c = \phi_c^i$, $\sigma = \sigma^i$; for the concave side: $\phi_c = \phi_c^o$, $\sigma = \sigma^o$.

5.2 Cutting Position of the Reference Point P_b on the Workpiece

The initial position of reference point P_b on the workpiece can be assumed to be in coordinate plane $\mathbf{i} - O - \mathbf{k}$, that is

$$\mathbf{R}_{gbo} = \rho_b\mathbf{i} + z_b\mathbf{k} \quad (5.14)$$

where the coordinate system $O - \mathbf{i}, \mathbf{j}, \mathbf{k}$ is the same as that of chapter 4.1.

Then the cutting position \mathbf{R}_{gb} of reference point P_b on the workpiece can be reached after rotating \mathbf{R}_{gbo} about axis \mathbf{k} through an angle ε_g , that is

$$\begin{aligned} \mathbf{R}_{gb} &= (\varepsilon_g\mathbf{k}) \otimes (\rho_b\mathbf{i} + z_b\mathbf{k}) \\ &= \rho_b \cos\varepsilon_g\mathbf{i} + \rho_b \sin\varepsilon_g\mathbf{j} + z_b\mathbf{k} \end{aligned} \quad (5.15)$$

where, ρ_b is the radial distance of the reference point P_b to axis $\omega_1 = \mathbf{k}$; for the convex side: $\varepsilon_g = \varepsilon_g^i$; for the concave side: $\varepsilon_g = \varepsilon_g^o$; z_b is the axial distance of the reference point P_b to the origin O along direction $\mathbf{k} = \omega_1$.

Likewise, the unit normal vector at reference point P_b to the tooth surface at the initial position is found in the form

$$\begin{aligned} \mathbf{N}_{go} &= (\gamma_g \mathbf{j}) \otimes \{(-\psi_g \mathbf{i}) \otimes [(\phi_g \mathbf{k}) \otimes (-\mathbf{j})]\} \\ &= (\sin \phi_g \cos \gamma_g + \cos \phi_g \sin \psi_g \sin \gamma_g) \mathbf{i} - \cos \phi_g \cos \psi_g \mathbf{j} \\ &\quad + (-\sin \phi_g \sin \gamma_g + \cos \phi_g \sin \psi_g \cos \gamma_g) \mathbf{k} \end{aligned} \quad (5.16)$$

Correspondingly, the unit normal at reference point P_b to the tooth surface at the cutting position is found as follows

$$\begin{aligned} \mathbf{N}_g &= (\varepsilon_g \mathbf{k}) \otimes \mathbf{N}_{go} \\ &= [(\sin \phi_g \cos \gamma_g + \cos \phi_g \sin \psi_g \sin \gamma_g) \cos \varepsilon_g + \cos \phi_g \cos \psi_g \sin \varepsilon_g] \mathbf{i} \\ &\quad + [(\sin \phi_g \cos \gamma_g + \cos \phi_g \sin \psi_g \sin \gamma_g) \sin \varepsilon_g - \cos \phi_g \cos \psi_g \cos \varepsilon_g] \mathbf{j} \\ &\quad + (-\sin \phi_g \sin \gamma_g + \cos \phi_g \sin \psi_g \cos \gamma_g) \mathbf{k} \end{aligned} \quad (5.17)$$

where, for the convex flank: $\phi_g = \phi_g^i$; for the concave flank: $\phi_g = \phi_g^o$.

Now, we embed coordinate system $O - \mathbf{i}, \mathbf{j}, \mathbf{k}$ into $O_g - \mathbf{i}_g, \mathbf{j}_g, \mathbf{k}_g$ as shown in fig.5.4 and the relationship between coordinate systems $O - \mathbf{i}, \mathbf{j}, \mathbf{k}$ and $O_g - \mathbf{i}_g, \mathbf{j}_g, \mathbf{k}_g$ is given as follows

$$\left. \begin{aligned} \mathbf{i} &= \mathbf{i}_g \\ \mathbf{j} &= \mathbf{j}_g \\ \mathbf{k} &= \mathbf{k}_g \\ \vec{O_g O} &= L \mathbf{k} \end{aligned} \right\} \quad (5.18)$$

where, $\mathbf{i}_g, \mathbf{j}_g, \mathbf{k}_g$ are given in expression (5.1).

Then, with the aid of expression (5.18), the cutting position vector \mathbf{R}_{gb} can be expressed in coordinate system $O_g - \mathbf{i}_g, \mathbf{j}_g, \mathbf{k}_g$ as follows

$$\mathbf{R}_{gb} = \rho_b \cos \varepsilon_g \mathbf{i}_g + \rho_b \sin \varepsilon_g \mathbf{j}_g + (z_b + L) \mathbf{k}_g \quad (5.19)$$

Likewise, the unit normal at the reference point to the tooth surface is given in the form

$$\begin{aligned} \mathbf{N}_g &= [(\sin \phi_g \cos \gamma_g + \cos \phi_g \sin \psi_g \sin \gamma_g) \cos \varepsilon_g + \cos \phi_g \cos \psi_g \sin \varepsilon_g] \mathbf{i}_g \\ &\quad + [(\sin \phi_g \cos \gamma_g + \cos \phi_g \sin \psi_g \sin \gamma_g) \sin \varepsilon_g - \cos \phi_g \cos \psi_g \cos \varepsilon_g] \mathbf{j}_g \\ &\quad + (-\sin \phi_g \sin \gamma_g + \cos \phi_g \sin \psi_g \cos \gamma_g) \mathbf{k}_g \end{aligned} \quad (5.20)$$

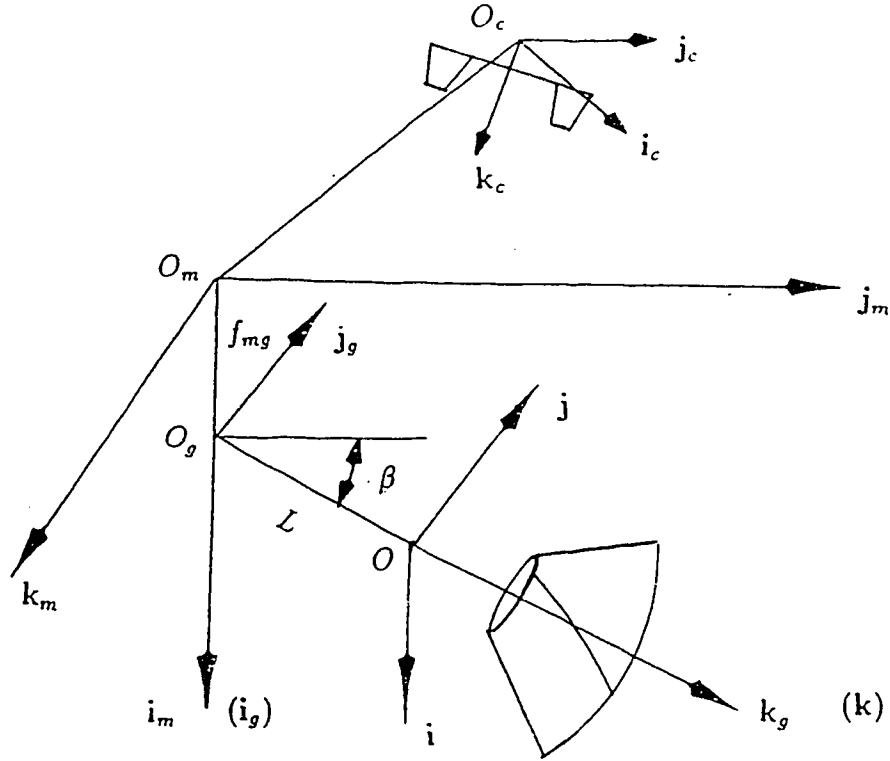


Figure 5.4: Relationship among the coordinate systems

5.3 The Relationship between the Cutter Surface and the Gear Tooth Surface

With the aid of expressions (5.1), (5.9) and (5.19) and taking into consideration $\alpha = 90^\circ - \beta$, expression (2.170) leads to the relationship between \mathbf{R}_{mb} and \mathbf{R}_{gb} as follows

$$\left. \begin{aligned} \rho_b \cos \varepsilon_g &= x_c + \rho_c \cos \sigma \cos \Theta - \rho_c \sin \sigma \cos \zeta \sin \Theta - f_{mg} \\ \rho_b \sin \varepsilon_g &= (y_c + \rho_c \cos \sigma \sin \Theta + \rho_c \sin \sigma \cos \zeta \cos \Theta) \sin \beta \\ &\quad - (z_c + \rho_c \sin \sigma \sin \zeta) \cos \beta \\ z_b + L &= (y_c + \rho_c \cos \sigma \sin \Theta + \rho_c \sin \sigma \cos \zeta \cos \Theta) \cos \beta \\ &\quad + (z_c + \rho_c \sin \sigma \sin \zeta) \sin \beta \end{aligned} \right\} \quad (5.21)$$

Without the tilt device, expression (5.21) can be simplified in the form

$$\left. \begin{aligned} \rho_b \cos \varepsilon_g &= x_c + \rho_c \cos \sigma - f_{mg} \\ \rho_b \sin \varepsilon_g &= (y_c + \rho_c \sin \sigma) \sin \beta - z_c \cos \beta \\ z_b + L &= (y_c + \rho_c \sin \sigma) \cos \beta + z_c \sin \beta \end{aligned} \right\} \quad (5.22)$$

Likewise, substitution of expressions (5.10) and (5.20) into (2.171) together with consideration of $\alpha = 90^\circ - \beta$ yields the relationship between N_c and N_g as follows

$$\left. \begin{aligned} -N_{cx} &= (\sin \phi_g \cos \gamma_g + \cos \phi_g \sin \psi_g \sin \gamma_g) \cos \varepsilon_g \\ &\quad + \cos \phi_g \cos \psi_g \sin \varepsilon_g \\ -N_{cy} \sin \beta + N_{cz} \cos \beta &= (\sin \phi_g \cos \gamma_g + \cos \phi_g \sin \psi_g \sin \gamma_g) \sin \varepsilon_g \\ &\quad - \cos \phi_g \cos \psi_g \cos \varepsilon_g \\ -N_{cy} \cos \beta - N_{cz} \sin \beta &= -\sin \phi_g \sin \gamma_g + \cos \phi_g \sin \psi_g \cos \gamma_g \end{aligned} \right\} \quad (5.23)$$

Without the tilt device, i.e., $\Theta = \zeta = 0$, expression (5.23) may be rewritten in the form

$$\left. \begin{aligned} \cos \phi_c \cos \sigma &= (\sin \phi_g \cos \gamma_g + \cos \phi_g \sin \psi_g \sin \gamma_g) \cos \varepsilon_g \\ &\quad + \cos \phi_g \cos \psi_g \sin \varepsilon_g \\ \cos \phi_c \sin \sigma \sin \beta + \sin \phi_c \cos \beta &= (\sin \phi_g \cos \gamma_g + \cos \phi_g \sin \psi_g \sin \gamma_g) \sin \varepsilon_g \\ &\quad - \cos \phi_g \cos \psi_g \cos \varepsilon_g \\ \cos \phi_c \sin \sigma \cos \beta - \sin \phi_c \sin \beta &= -\sin \phi_g \sin \gamma_g + \cos \phi_g \sin \psi_g \cos \gamma_g \end{aligned} \right\} \quad (5.24)$$

Substitution of expressions (5.9) into (2.129) yields the velocity at the reference point P_b of the cutter relative to the workpiece as follows

$$\begin{aligned} \mathbf{v}_b^{mg} &= [-(1 + M_{mg} \sin \beta)(y_c + \rho_c \cos \sigma \sin \Theta + \rho_c \sin \sigma \cos \zeta \cos \Theta) \\ &\quad + M_{mg}(z_c + \rho_c \sin \sigma \sin \zeta) \cos \beta] \mathbf{i}_m \\ &\quad + [(1 + M_{mg} \sin \beta)(x_c + \rho_c \cos \sigma \cos \Theta - \rho_c \sin \sigma \cos \zeta \sin \Theta) \\ &\quad - M_{mg} f_{mg} \sin \beta] \mathbf{j}_m \\ &\quad + [-M_{mg}(x_c + \rho_c \cos \sigma \cos \Theta - \rho_c \sin \sigma \cos \zeta \sin \Theta) \cos \beta \\ &\quad + M_{mg} f_{mg} \cos \beta] \mathbf{k}_m \end{aligned} \quad (5.25)$$

where, $M_{mg} = -\frac{d\varepsilon_g}{d\varepsilon_m}$ is the ratio of roll.

Without the tilt device, i.e., $\zeta = \Theta = 0$, the relative velocity is in the form

$$\begin{aligned} \mathbf{v}_b^{mg} &= [-(1 + M_{mg} \sin \beta)(y_c + \rho_c \sin \sigma) + M_{mg} z_c \cos \beta] \mathbf{i}_m \\ &\quad + [(1 + M_{mg} \sin \beta)(x_c + \rho_c \cos \sigma) - M_{mg} f_{mg} \sin \beta] \mathbf{j}_m \\ &\quad + [-M_{mg}(x_c + \rho_c \cos \sigma) \cos \beta + M_{mg} f_{mg} \cos \beta] \mathbf{k}_m \end{aligned} \quad (5.26)$$

Condition (2.157) yields the following equation of conjugacy

$$\begin{aligned} &N_{cx}[-(1 + M_{mg} \sin \beta)(y_c + \rho_c \cos \sigma \sin \Theta + \rho_c \sin \sigma \cos \zeta \cos \Theta) \\ &\quad + M_{mg}(z_c + \rho_c \sin \sigma \sin \zeta) \cos \beta] + N_{cy}[(1 + M_{mg} \sin \beta)(x_c \\ &\quad + \rho_c \cos \sigma \cos \Theta - \rho_c \sin \sigma \cos \zeta \sin \Theta) - M_{mg} f_{mg} \sin \beta] \\ &\quad + N_{cz}[-M_{mg}(x_c + \rho_c \cos \sigma \cos \Theta - \rho_c \sin \sigma \cos \zeta \sin \Theta) \cos \beta \\ &\quad + M_{mg} f_{mg} \cos \beta] = 0 \end{aligned} \quad (5.27)$$

Without the tilt device, equation (5.27) becomes

$$\begin{aligned} & -\cos \phi_c \cos \sigma [-(1 + M_{mg} \sin \beta)(y_c + \rho_c \sin \sigma) + M_{mg} z_c \cos \beta] \\ & -\cos \phi_c \sin \sigma [(1 + M_{mg} \sin \beta)(x_c + \rho_c \cos \sigma) - M_{mg} f_{mg} \sin \beta] \\ & + \sin \phi_c [-M_{mg}(x_c + \rho_c \cos \sigma) \cos \beta + M_{mg} f_{mg} \cos \beta] = 0 \end{aligned} \quad (5.28)$$

5.4 Four Auxiliary Conditions

The point where the cutter axis \mathbf{k}_c intersects the coordinate plane $\mathbf{i}_m - O_m - \mathbf{j}_m$ is named P_{cr} , and then, the position vector \mathbf{R}_{cr} of point P_{cr} is expressed in the form

$$\mathbf{R}_{cr} = x_{cr} \mathbf{i}_m + y_{cr} \mathbf{j}_m \quad (5.29)$$

Therefore, the position vector $O\vec{O}_c$ of the origin O_c of the coordinate system $O_c - \mathbf{i}_c, \mathbf{j}_c, \mathbf{k}_c$ can be found in the form

$$O\vec{O}_c = \mathbf{R}_{cr} + p \mathbf{k}_c \quad (5.30)$$

where, p is the distance from the intersection point P_{cr} to origin O_c along axis \mathbf{k}_c .

With the aid of expression (5.5), removing $p \mathbf{k}_c$ to the left side of the expression above results in

$$\begin{aligned} \mathbf{R}_{cr} &= x_{cr} \mathbf{i}_m + y_{cr} \mathbf{j}_m \\ &= (x_c - p \sin \zeta \sin \Theta) \mathbf{i}_m + (y_c + p \sin \zeta \cos \Theta) \mathbf{j}_m + (z_c - p \cos \zeta) \mathbf{k}_m \end{aligned} \quad (5.31)$$

where, for the concave side: $x_c = x_c^o$, $y_c = y_c^o$, $z_c = z_c^o$, $\Theta = \Theta^o$; for the convex side: $x_c = x_c^i$, $y_c = y_c^i$, $z_c = z_c^i$, $\Theta = \Theta^i$.

Due to $z_c - p \cos \zeta = 0$, then,

$$p = \frac{z_c}{\cos \zeta} \quad (5.32)$$

Substitution of expressions (5.31) into (5.30) leads to

$$\begin{aligned} \mathbf{R}_{cr} &= x_{cr} \mathbf{i}_m + y_{cr} \mathbf{j}_m \\ &= (x_c - z_c \tan \zeta \sin \Theta) \mathbf{i}_m + (y_c + z_c \tan \zeta \cos \Theta) \mathbf{j}_m \end{aligned} \quad (5.33)$$

Since the distance from the intersection point P_{cr} to the cradle axis \mathbf{k}_m is a constant in the whole course of the cutting process, the first auxiliary condition can be found as follows

$$\begin{aligned} & (x_c^o - z_c^o \tan \zeta \sin \Theta^o)^2 + (y_c^o + z_c^o \tan \zeta \cos \Theta^o)^2 \\ &= (x_c^i - z_c^i \tan \zeta \sin \Theta^i)^2 + (y_c^i + z_c^i \tan \zeta \cos \Theta^i)^2 \end{aligned} \quad (5.34)$$

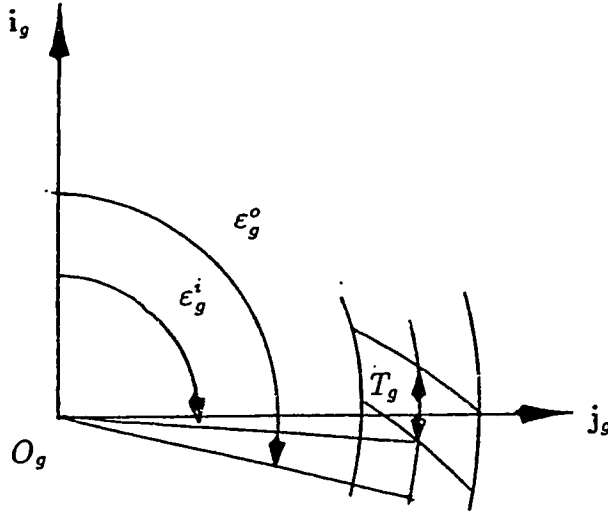


Figure 5.5: The phase angle for gear

and without the tilt device, condition (5.34) can be written in the form

$$(x_c^o)^2 + (y_c^o)^2 = (x_c^i)^2 + (y_c^i)^2 \quad (5.35)$$

Let ε_c be the phase angle made by \mathbf{R}_{cr} with axis \mathbf{i}_m . Then, the second auxiliary condition can be found in the form

$$\varepsilon_c = \arctan \frac{y_c + z_c \tan \zeta \cos \Theta}{x_c - z_c \tan \zeta \sin \Theta} \quad (5.36)$$

Without the tilt device, expression (5.36) results to the form

$$\varepsilon_c = \arctan \frac{y_c}{x_c} \quad (5.37)$$

Since the rotating angle of the gear from the conjugate cutting position of the convex face to the conjugate cutting position of the concave face is $\Delta\varepsilon_g = T_g + \varepsilon_g^o - \varepsilon_g^i$ shown in fig.4.5 and the rotating angle of the cradle corresponding to $\Delta\varepsilon_g$ is $\Delta\varepsilon_c = \varepsilon_c^o - \varepsilon_c^i$ shown in fig. 5.5, the third auxiliary condition can be found as follows

$$\begin{aligned} M_{mg} &= -\frac{d\varepsilon_g}{d\varepsilon_c} = -\frac{\Delta\varepsilon_g}{\Delta\varepsilon_c} \\ &= \frac{T_g + \varepsilon_g^o - \varepsilon_g^i}{\varepsilon_c^i - \varepsilon_c^o} \end{aligned} \quad (5.38)$$

where, M_{mg} is negative, and $T_g = \pm \frac{\pi}{N_g}$, which is the angle corresponding to the tooth space, is positive for a right-hand gear and negative for a left-hand gear, and N_g is the tooth number of the gear.

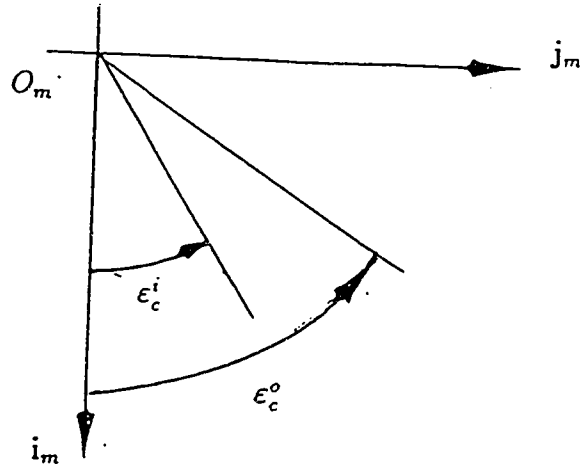


Figure 5.6: The phase angle for cradle

Since the coordinate system $O_c - \mathbf{i}_c, \mathbf{j}_c, \mathbf{k}_c$ is fixed in the cradle, the fourth auxiliary condition can be found as follows

$$\Theta^o = \Theta^i + \epsilon_c^o - \epsilon_c^i \quad (5.39)$$

where, Θ^o and Θ^i are the swivel angles corresponding to the concave and convex sides respectively.

5.5 Simultaneous Equations for Determining the Machine-Setting Parameters and Discussion of the Degrees of Freedom for the Cutting Process

Combination of expressions (5.21), (5.23), (5.27) in the cases of both concave and convex sides, together with the four auxiliary conditions, i.e., (5.34), (5.36), (5.38) and (5.39), leads to the following simultaneous equations for calculating the machine-

setting parameters,

$$\left. \begin{aligned}
 \rho_b \cos \varepsilon_g^o &= x_c^o + \rho_c^o \cos \sigma^o \cos \Theta^o - \rho_c^o \sin \sigma^o \cos \zeta \sin \Theta^o - f_{mg}, \\
 \rho_b \sin \varepsilon_g^o &= (y_c^o + \rho_c^o \cos \sigma^o \sin \Theta^o + \rho_c^o \sin \sigma^o \cos \zeta \cos \Theta^o) \sin \beta \\
 &\quad - (z_c^o + \rho_c^o \sin \sigma^o \sin \zeta) \cos \beta, \\
 z_b + L &= (y_c^o + \rho_c^o \cos \sigma^o \sin \Theta^o + \rho_c^o \sin \sigma^o \cos \zeta \cos \Theta^o) \cos \beta \\
 &\quad + (z_c^o + \rho_c^o \sin \sigma^o \sin \zeta) \sin \beta, \\
 \rho_b \cos \varepsilon_g^i &= x_c^i + \rho_c^i \cos \sigma^i \cos \Theta^i - \rho_c^i \sin \sigma^i \cos \zeta \sin \Theta^i - f_{mg}, \\
 \rho_b \sin \varepsilon_g^i &= (y_c^i + \rho_c^i \cos \sigma^i \sin \Theta^i + \rho_c^i \sin \sigma^i \cos \zeta \cos \Theta^i) \sin \beta \\
 &\quad - (z_c^i + \rho_c^i \sin \sigma^i \sin \zeta) \cos \beta, \\
 z_b + L &= (y_c^i + \rho_c^i \cos \sigma^i \sin \Theta^i + \rho_c^i \sin \sigma^i \cos \zeta \cos \Theta^i) \cos \beta \\
 &\quad + (z_c^i + \rho_c^i \sin \sigma^i \sin \zeta) \sin \beta, \\
 -N_{cx}^o &= (\sin \phi_g^o \cos \gamma_g + \cos \phi_g^o \sin \psi_g \sin \gamma_g) \cos \varepsilon_g^o + \cos \phi_g^o \cos \psi_g \sin \varepsilon_g^o, \\
 -N_{cy}^o \cos \beta - N_{cz}^o \sin \beta &= -\sin \phi_g^o \sin \gamma_g + \cos \phi_g^o \sin \psi_g \cos \gamma_g, \\
 -N_{cx}^i &= (\sin \phi_g^i \cos \gamma_g + \cos \phi_g^i \sin \psi_g \sin \gamma_g) \cos \varepsilon_g^i + \cos \phi_g^i \cos \psi_g \sin \varepsilon_g^i, \\
 -N_{cy}^i \cos \beta - N_{cz}^i \sin \beta &= -\sin \phi_g^i \sin \gamma_g + \cos \phi_g^i \sin \psi_g \cos \gamma_g, \\
 N_{cx}^o [-(1 + M_{mg} \sin \beta)(y_c^o + \rho_c^o \cos \sigma^o \sin \Theta^o + \rho_c^o \sin \sigma^o \cos \zeta \cos \Theta^o) + M_{mg} \\
 (z_c^o + \rho_c^o \sin \sigma^o \sin \zeta) \cos \beta] + N_{cy}^o [(1 + M_{mg} \sin \beta)(x_c^o + \rho_c^o \cos \sigma^o \cos \Theta^o \\
 - \rho_c^o \sin \sigma^o \cos \zeta \sin \Theta^o) - M_{mg} f_{mg} \sin \beta] + N_{cz}^o [-M_{mg} (x_c^o + \rho_c^o \cos \sigma^o \cos \Theta^o \\
 - \rho_c^o \sin \sigma^o \cos \zeta \sin \Theta^o) \cos \beta + M_{mg} f_{mg} \cos \beta] = 0, \\
 N_{cx}^i [-(1 + M_{mg} \sin \beta)(y_c^i + \rho_c^i \cos \sigma^i \sin \Theta^i + \rho_c^i \sin \sigma^i \cos \zeta \cos \Theta^i) + M_{mg} \\
 (z_c^i + \rho_c^i \sin \sigma^i \sin \zeta) \cos \beta] + N_{cy}^i [(1 + M_{mg} \sin \beta)(x_c^i + \rho_c^i \cos \sigma^i \cos \Theta^i \\
 - \rho_c^i \sin \sigma^i \cos \zeta \sin \Theta^i) - M_{mg} f_{mg} \sin \beta] + N_{cz}^i [-M_{mg} (x_c^i + \rho_c^i \cos \sigma^i \cos \Theta^i \\
 - \rho_c^i \sin \sigma^i \cos \zeta \sin \Theta^i) \cos \beta + M_{mg} f_{mg} \cos \beta] = 0, \\
 (x_c^o - z_c^o \tan \zeta \sin \Theta^o)^2 + (y_c^o + z_c^o \tan \zeta \cos \Theta^o)^2 \\
 = (x_c^i - z_c^i \tan \zeta \sin \Theta^i)^2 + (y_c^i + z_c^i \tan \zeta \cos \Theta^i)^2, \\
 M_{mg} = -\frac{d\varepsilon_g}{d\varepsilon_c} = -\frac{\Delta\varepsilon_g}{\Delta\varepsilon_c} = \frac{T_g + \varepsilon_g^o - \varepsilon_g^i}{\varepsilon_c^i - \varepsilon_c^o}, \\
 \Theta^o = \Theta^i + \varepsilon_c^o - \varepsilon_c^i
 \end{aligned} \right\} (5.40)$$

where $N_{cx}^o, N_{cy}^o, N_{cz}^o$ and $N_{cx}^i, N_{cy}^i, N_{cz}^i$ can be calculated by expression (5.10). ε_c^i and ε_c^o can be found as follows

$$\left. \begin{aligned}
 \varepsilon_c^i &= \arctan \frac{y_c^i + z_c^i \tan \zeta \cos \Theta^o}{x_c^i - z_c^i \tan \zeta \sin \Theta^i} \\
 \varepsilon_c^o &= \arctan \frac{y_c^o + z_c^o \tan \zeta \cos \Theta^o}{x_c^o - z_c^o \tan \zeta \sin \Theta^o}
 \end{aligned} \right\} (5.41)$$

Without the tilt device, i.e., $\zeta = \Theta = 0$, equations (5.40) can be expressed in the form

$$\left. \begin{aligned}
\rho_b \cos \varepsilon_g^o &= x_c^o + \rho_c^o \cos \sigma^o - f_{mg}, \\
\rho_b \sin \varepsilon_g^o &= (y_c^o + \rho_c^o \sin \sigma^o) \sin \beta - z_c^o \cos \beta, \\
z_b + L &= (y_c^o + \rho_c^o \sin \sigma^o) \cos \beta + z_c^o \sin \beta, \\
\rho_b \cos \varepsilon_g^i &= x_c^i + \rho_c^i \cos \sigma^i - f_{mg}, \\
\rho_b \sin \varepsilon_g^i &= (y_c^i + \rho_c^i \sin \sigma^i) \sin \beta - z_c^i \cos \beta, \\
z_b + L &= (y_c^i + \rho_c^i \sin \sigma^i) \cos \beta + z_c^i \sin \beta, \\
\cos \phi_c^o \cos \sigma^o &= (\sin \phi_g^o \cos \gamma_g + \cos \phi_g^o \sin \psi_g \sin \gamma_g) \cos \varepsilon_g^o \\
&+ \cos \phi_g^o \cos \psi_g \sin \varepsilon_g^o, \\
\cos \phi_c^o \sin \sigma^o \cos \beta - \sin \phi_c^o \sin \beta &= -\sin \phi_g^o \sin \gamma_g + \cos \phi_g^o \sin \psi_g \cos \gamma_g, \\
\cos \phi_c^i \cos \sigma^i &= (\sin \phi_g^i \cos \gamma_g + \cos \phi_g^i \sin \psi_g \sin \gamma_g) \cos \varepsilon_g^i \\
&+ \cos \phi_g^i \cos \psi_g \sin \varepsilon_g^i, \\
\cos \phi_c^i \sin \sigma^i \cos \beta - \sin \phi_c^i \sin \beta &= -\sin \phi_g^i \sin \gamma_g + \cos \phi_g^i \sin \psi_g \cos \gamma_g, \\
-\cos \phi_c^o \cos \sigma^o [-(1 + M_{mg} \sin \beta)(y_c^o + \rho_c^o \sin \sigma^o) + M_{mg} z_c^o \cos \beta] \\
-\cos \phi_c^o \sin \sigma^o [(1 + M_{mg} \sin \beta)(x_c^o + \rho_c^o \cos \sigma^o) - M_{mg} f_{mg} \sin \beta] \\
+\sin \phi_c^o [-M_{mg}(x_c^o + \rho_c^o \cos \sigma^o) \cos \beta + M_{mg} f_{mg} \cos \beta] &= 0, \\
-\cos \phi_c^i \cos \sigma^i [-(1 + M_{mg} \sin \beta)(y_c^i + \rho_c^i \sin \sigma^i) + M_{mg} z_c^i \cos \beta] \\
-\cos \phi_c^i \sin \sigma^i [(1 + M_{mg} \sin \beta)(x_c^i + \rho_c^i \cos \sigma^i) - M_{mg} f_{mg} \sin \beta] \\
+\sin \phi_c^i [-M_{mg}(x_c^i + \rho_c^i \cos \sigma^i) \cos \beta + M_{mg} f_{mg} \cos \beta] &= 0, \\
(x_c^o)^2 + (y_c^o)^2 &= (x_c^i)^2 + (y_c^i)^2, \\
M_{mg} &= -\frac{d\varepsilon_g}{d\varepsilon_c} = -\frac{\Delta\varepsilon_g}{\Delta\varepsilon_c} = \frac{T_g + \varepsilon_g^o - \varepsilon_g^i}{\varepsilon_c^i - \varepsilon_c^o}
\end{aligned} \right\} \quad (5.42)$$

where

$$\left. \begin{aligned}
\varepsilon_c^i &= \frac{y_c^i}{x_c^i} \\
\varepsilon_c^o &= \frac{y_c^o}{x_c^o}
\end{aligned} \right\} \quad (5.43)$$

The simultaneous equations (5.40) consist of 15 independent equations. The parameters to be calculated are now 21, i.e., x_c^o , y_c^o , z_c^o , x_c^i , y_c^i , z_c^i , Θ^o , Θ_i , σ^o , σ^i , ε_g^o , ε_g^i , ρ_c^o , ρ_c^i , ϕ_c^o , ϕ_c^i , ζ , β , M_{mg} , f_{mg} and L . Therefore, there are six parameters whose values must be prescribed. In order to limit the number of cutters, the radii and the blade angles of the cutter, i.e., ρ_c^o , ρ_c^i and ϕ_c^o , ϕ_c^i can be prescribed. In the current practice of hypoid gearing, the tilt device is usually used to allow for a difference between the gear pressure angle and the cutter blade angle. In this case, the minimum value of the tilt angle ζ can be achieved by letting the phase angles of the cutting edges be right angles, i.e., $\sigma^o = \sigma^i = 90^\circ$. The simultaneous equations (5.40) can then be

further simplified as

$$\left. \begin{aligned}
 \rho_b \cos \varepsilon_g^o &= x_c^o - \rho_c^o \cos \zeta \sin \Theta^o - f_{mg}, \\
 \rho_b \sin \varepsilon_g^o &= (y_c^o + \rho_c^o \cos \zeta \cos \Theta^o) \sin \beta - (z_c^o + \rho_c^o \sin \zeta) \cos \beta, \\
 z_b + L &= (y_c^o + \rho_c^o \cos \zeta \cos \Theta^o) \cos \beta + (z_c^o + \rho_c^o \sin \zeta) \sin \beta, \\
 \rho_b \cos \varepsilon_g^i &= x_c^i - \rho_c^i \cos \zeta \sin \Theta^i - f_{mg}, \\
 \rho_b \sin \varepsilon_g^i &= (y_c^i + \rho_c^i \cos \zeta \cos \Theta^i) \sin \beta - (z_c^i + \rho_c^i \sin \zeta) \cos \beta, \\
 z_b + L &= (y_c^i + \rho_c^i \cos \zeta \cos \Theta^i) \cos \beta + (z_c^i + \rho_c^i \sin \zeta) \sin \beta, \\
 -N_{cx}^o &= (\sin \phi_g^o \cos \gamma_g + \cos \phi_g^o \sin \psi_g \sin \gamma_g) \cos \varepsilon_g^o + \cos \phi_g^o \cos \psi_g \sin \varepsilon_g^o, \\
 -N_{cy}^o \cos \beta - N_{cz}^o \sin \beta &= -\sin \phi_g^o \sin \gamma_g + \cos \phi_g^o \sin \psi_g \cos \gamma_g, \\
 -N_{cx}^i &= (\sin \phi_g^i \cos \gamma_g + \cos \phi_g^i \sin \psi_g \sin \gamma_g) \cos \varepsilon_g^i + \cos \phi_g^i \cos \psi_g \sin \varepsilon_g^i, \\
 -N_{cy}^i \cos \beta - N_{cz}^i \sin \beta &= -\sin \phi_g^i \sin \gamma_g + \cos \phi_g^i \sin \psi_g \cos \gamma_g, \\
 N_{cx}^o [-(1 + M_{mg} \sin \beta)(y_c^o + \rho_c^o \cos \zeta \cos \Theta^o) + M_{mg}(z_c^o + \rho_c^o \sin \zeta) \cos \beta] \\
 + N_{cy}^o [(1 + M_{mg} \sin \beta)(x_c^o - \rho_c^o \cos \zeta \sin \Theta^o) - M_{mg} f_{mg} \sin \beta] \\
 + N_{cz}^o [-M_{mg}(x_c^o - \rho_c^o \cos \zeta \sin \Theta^o) \cos \beta + M_{mg} f_{mg} \cos \beta] &= 0, \\
 N_{cx}^i [-(1 + M_{mg} \sin \beta)(y_c^i + \rho_c^i \cos \zeta \cos \Theta^i) + M_{mg}(z_c^i + \rho_c^i \sin \zeta) \cos \beta] \\
 + N_{cy}^i [(1 + M_{mg} \sin \beta)(x_c^i - \rho_c^i \cos \zeta \sin \Theta^i) - M_{mg} f_{mg} \sin \beta] \\
 + N_{cz}^i [-M_{mg}(x_c^i - \rho_c^i \cos \zeta \sin \Theta^i) \cos \beta + M_{mg} f_{mg} \cos \beta] &= 0, \\
 (x_c^o - z_c^o \tan \zeta \sin \Theta^o)^2 + (y_c^o + z_c^o \tan \zeta \cos \Theta^o)^2 \\
 = (x_c^i - z_c^i \tan \zeta \sin \Theta^i)^2 + (y_c^i + z_c^i \tan \zeta \cos \Theta^i)^2, \\
 M_{mg} = -\frac{d\varepsilon_g}{d\varepsilon_c} = -\frac{\Delta \varepsilon_g}{\Delta \varepsilon_c} = \frac{T_g + \varepsilon_g^o - \varepsilon_g^i}{\varepsilon_c^i - \varepsilon_c^o}, \\
 \Theta^o = \Theta^i + \varepsilon_c^o - \varepsilon_c^i
 \end{aligned} \right\} \quad (5.44)$$

where, $N_{cx}^o, N_{cy}^o, N_{cz}^o$ and $N_{cx}^i, N_{cy}^i, N_{cz}^i$ are calculated by expression (4.10). ε_c^i and ε_c^o can be found as follows

$$\left. \begin{aligned}
 \varepsilon_c^i &= \arctan \frac{y_c^i + z_c^i \tan \zeta \cos \Theta^i}{x_c^i - z_c^i \tan \zeta \sin \Theta^i} \\
 \varepsilon_c^o &= \arctan \frac{y_c^o + z_c^o \tan \zeta \cos \Theta^o}{x_c^o - z_c^o \tan \zeta \sin \Theta^o}
 \end{aligned} \right\} \quad (5.45)$$

Without the tilt device, the problem can be treated as follows. The simultaneous equations (5.42) consist of 14 independent equations, but the parameters to be solved are 18, i.e., $x_c^o, y_c^o, z_c^o, x_c^i, y_c^i, z_c^i, \sigma^o, \sigma^i, \varepsilon_g^o, \varepsilon_g^i, \rho_c^o, \rho_c^i, \phi_c^o, \phi_c^i, \beta, M_{mg}, f_{mg}$ and L . Therefore, there are four parameters to be prescribed. Usually, β can be assumed to be equal to the root angle γ_{gr} of the gear, i.e., $\beta = \gamma_{gr}$, the blade angles ϕ_c^o and ϕ_c^i can be prescribed, and the inner and outer radii of a cutter can be defined by the following equations, which can be derived by inspection from fig.5.7

$$\left. \begin{aligned}
 \rho_c^o &= r_c - [(L + Z_{gr}) \sin \gamma_{gr} - z_c^o] \tan \phi_c^o + \frac{W_p}{2} \\
 \rho_c^i &= r_c - [(L + Z_{gr}) \sin \gamma_{gr} - z_c^i] \tan \phi_c^i - \frac{W_p}{2}
 \end{aligned} \right\} \quad (5.46)$$

where, W_P is the point width of the cutter, r_c is the nominal radius of the cutter, and Z_{gr} is the root apex beyond the crossing point O between the gear and the pinion.

Therefore, the simultaneous equations for machine-setting parameters in the case of the no tilt device take the following form

$$\left. \begin{aligned}
 \rho_b \cos \varepsilon_g^o &= x_c^o + \rho_c^o \cos \sigma^o - f_{mg}, \\
 \rho_b \sin \varepsilon_g^o &= (y_c^o + \rho_c^o \sin \sigma^o) \sin \gamma_{gr} - z_c^o \cos \gamma_{gr}, \\
 z_b + L &= (y_c^o + \rho_c^o \sin \sigma^o) \cos \gamma_{gr} + z_c^o \sin \gamma_{gr}, \\
 \rho_b \cos \varepsilon_g^i &= x_c^i + \rho_c^i \cos \sigma^i - f_{mg}, \\
 \rho_b \sin \varepsilon_g^i &= (y_c^i + \rho_c^i \sin \sigma^i) \sin \gamma_{gr} - z_c^i \cos \gamma_{gr}, \\
 z_b + L &= (y_c^i + \rho_c^i \sin \sigma^i) \cos \gamma_{gr} + z_c^i \sin \gamma_{gr}, \\
 \cos \phi_c^o \cos \sigma^o &= (\sin \phi_g^o \cos \gamma_g + \cos \phi_g^o \sin \psi_g \sin \gamma_g) \cos \varepsilon_g^o \\
 &+ \cos \phi_g^o \cos \psi_g \sin \varepsilon_g^o, \\
 \cos \phi_c^o \sin \sigma^o \cos \gamma_{gr} - \sin \phi_c^o \sin \gamma_{gr} &= -\sin \phi_g^o \sin \gamma_g + \cos \phi_g^o \sin \psi_g \cos \gamma_g, \\
 \cos \phi_c^i \cos \sigma^i &= (\sin \phi_g^i \cos \gamma_g + \cos \phi_g^i \sin \psi_g \sin \gamma_g) \cos \varepsilon_g^i \\
 \cos \phi_g^i \cos \psi_g \sin \varepsilon_g^i, \\
 \cos \phi_c^i \sin \sigma^i \cos \gamma_{gr} - \sin \phi_c^i \sin \gamma_{gr} &= -\sin \phi_g^i \sin \gamma_g + \cos \phi_g^i \sin \psi_g \cos \gamma_g, \\
 -\cos \phi_c^o \cos \sigma^o [-(1 + M_{mg} \sin \gamma_{gr})(y_c^o + \rho_c^o \sin \sigma^o) + M_{mg} z_c^o \cos \gamma_{gr}] \\
 -\cos \phi_c^o \sin \sigma^o [(1 + M_{mg} \sin \gamma_{gr})(x_c^o + \rho_c^o \cos \sigma^o) - M_{mg} f_{mg} \sin \gamma_{gr} \\
 + \sin \phi_c^o [-M_{mg}(x_c^o + \rho_c^o \cos \sigma^o) \cos \gamma_{gr} + M_{mg} f_{mg} \cos \gamma_{gr}]] &= 0, \\
 -\cos \phi_c^i \cos \sigma^i [-(1 + M_{mg} \sin \gamma_{gr})(y_c^i + \rho_c^i \sin \sigma^i) + M_{mg} z_c^i \cos \gamma_{gr}] \\
 -\cos \phi_c^i \sin \sigma^i [(1 + M_{mg} \sin \gamma_{gr})(x_c^i + \rho_c^i \cos \sigma^i) - M_{mg} f_{mg} \sin \gamma_{gr} \\
 + \sin \phi_c^i [-M_{mg}(x_c^i + \rho_c^i \cos \sigma^i) \cos \gamma_{gr} + M_{mg} f_{mg} \cos \gamma_{gr}]] &= 0, \\
 (x_c^o)^2 + (y_c^o)^2 &= (x_c^i)^2 + (y_c^i)^2, \\
 M_{mg} &= -\frac{d\varepsilon_g}{d\varepsilon_c} = -\frac{\Delta\varepsilon_g}{\Delta\varepsilon_c} = \frac{T_g + \varepsilon_g^o - \varepsilon_g^i}{\varepsilon_c^i - \varepsilon_c^o}
 \end{aligned} \right\} \quad (5.47)$$

Let r_c be prescribed and W_p be calculated. By solving the simultaneous equations (5.47), all 14 remaining parameters can be found.

With the Formate method, we obtain $M_{mg} = \frac{0}{0}$, from expressions (5.38) and (5.39). It follows $x_c^o = x_c^i = x_c$, $y_c^o = y_c^i = y_c$, and $T_g + \varepsilon_g^o - \varepsilon_g^i = 0$. Simultaneous equations for the machine-setting parameters in the case of the formate method are then found in the form

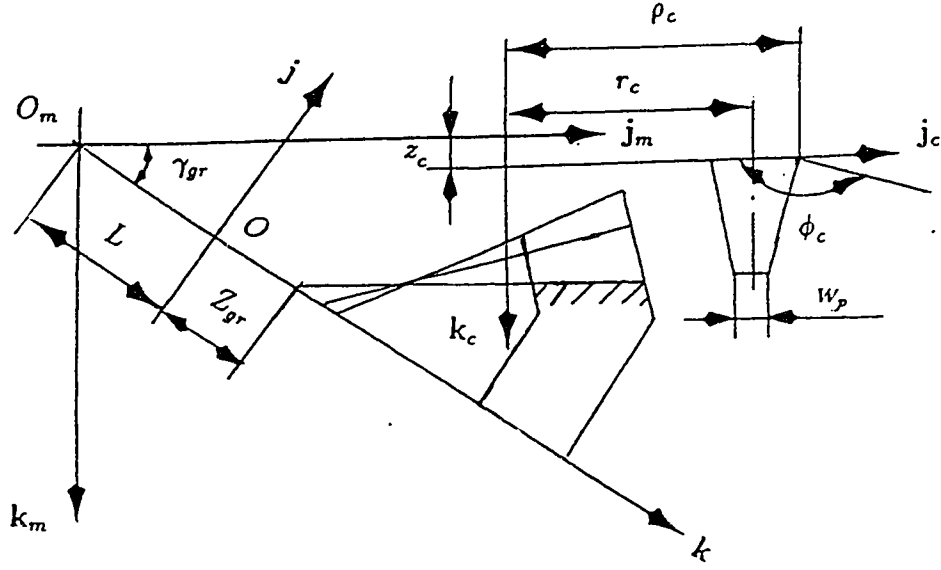


Figure 5.7: Dimension of cutter

$$\left. \begin{aligned}
 \rho_b \cos \varepsilon_g^o &= x_c + \rho_c^o \cos \sigma^o - f_{mg}, \\
 \rho_b \sin \varepsilon_g^o &= (y_c + \rho_c^o \sin \sigma^o) \sin \gamma_{gr} - z_c^o \cos \gamma_{gr}, \\
 z_b + L &= (y_c + \rho_c^o \sin \sigma^o) \cos \gamma_{gr} + z_c^o \sin \gamma_{gr}, \\
 \rho_b \cos \varepsilon_g^i &= x_c + \rho_c^i \cos \sigma^i - f_{mg}, \\
 \rho_b \sin \varepsilon_g^i &= (y_c + \rho_c^i \sin \sigma^i) \sin \gamma_{gr} - z_c^i \cos \gamma_{gr}, \\
 z_b + L &= (y_c + \rho_c^i \sin \sigma^i) \cos \gamma_{gr} + z_c^i \sin \gamma_{gr}, \\
 \cos \phi_c^o \cos \sigma^o &= (\sin \phi_g^o \cos \gamma_g + \cos \phi_g^o \sin \psi_g \sin \gamma_g) \cos \varepsilon_g^o \\
 &\quad + \cos \phi_g^o \cos \psi_g \sin \varepsilon_g^o, \\
 \cos \phi_c^o \sin \sigma^o \cos \gamma_{gr} - \sin \phi_c^o \sin \gamma_{gr} &= -\sin \phi_g^o \sin \gamma_g + \cos \phi_g^o \sin \psi_g \cos \gamma_g, \\
 \cos \phi_c^i \cos \sigma^i &= (\sin \phi_g^i \cos \gamma_g + \cos \phi_g^i \sin \psi_g \sin \gamma_g) \cos \varepsilon_g^i \\
 &\quad + \cos \phi_g^i \cos \psi_g \sin \varepsilon_g^i, \\
 \cos \phi_c^i \sin \sigma^i \cos \gamma_{gr} - \sin \phi_c^i \sin \gamma_{gr} &= -\sin \phi_g^i \sin \gamma_g + \cos \phi_g^i \sin \psi_g \cos \gamma_g, \\
 T_g + \varepsilon_g^o - \varepsilon_g^i &= 0.
 \end{aligned} \right\} \quad (5.48)$$

where, ρ_c^o , ρ_c^i are given by expression (5.46).

There are now 11 equations and 13 parameters, i.e., $x_c, y_c, z_c^o, z_c^i, \varepsilon_g^o, \varepsilon_g^i, \sigma^o, \sigma^i, \phi_c^o, \phi_c^i, W_p, f_{mg}$ and L . Let ϕ_c^o and ϕ_c^i be prescribed. Solving simultaneous equations (5.48) provides all the remaining parameters.

Since the number of calculating parameters is more than that of equations, a optional choice of free parameters is available. In the case of a small amount of production, we can use a currently available cutter rather than invest expensive money to especially design and make a new cutter. But in the case of mass production, we can especially design and make a new cutter according to requirements.

Chapter 6

Calculation of Curvature for the Gear Tooth Surface

Since the gear tooth surface is generated by the cutter surface under a pair of conjugate motions of the gear and cutter, the curvature properties of the gear tooth surface can be obtained by the solution to the first type of problem of conjugate curvatures. Further, the cutter surface is formed by a cutting edge, and therefore, it is necessary to calculate the curvature properties of the cutter surface by the method given in section 2.4.3, before calculating the curvature properties of the gear tooth surface.

6.1 Calculation of Curvatures for Conical and Cylindrical Helicoids with Constant Rate of Lead and Rotating Surface

We assume that the generating curve, i.e., the cutting edge, is fixed in the second reference frame $O' - i', j', k'$ as described in section 2.4.3. If the corresponding conjugate motion is given in the following form

$$\left. \begin{aligned} M = \frac{dM}{d\varepsilon_1} = 0, \quad \frac{d\sigma_2}{d\varepsilon_1} = \frac{d\sigma_2^2}{d\varepsilon_1^2} = 0, \quad \frac{d(l\mathbf{p})}{d\varepsilon_1} = b_r \cos \gamma i + b_r \sin \gamma j, \\ \frac{d^2(l\mathbf{p})}{d\varepsilon_1^2} = 0, \quad \frac{d\sigma_1}{d\varepsilon_1} = b_a, \quad \frac{d^2\sigma_1}{d\varepsilon_1^2} = 0. \end{aligned} \right\} \quad (6.1)$$

then the corresponding conjugate surface formed by the cutting edge under such a type of conjugate motion is a conical helicoid with constant rate of lead. b_r and b_a are two constants which represent the rate of radial and axial leads respectively.

Substituting expressions (2.135) and (2.265) into (2.269) and (2.273) respectively, then expressions (2.267), (2.269) and (2.273) can be simplified in the following forms

$$\left. \begin{aligned} K_{1w} &= -k_c(\mathbf{N}_{1p} \cdot \boldsymbol{\xi}) \\ G_{1w} &= \frac{k_c(\mathbf{v}_p^{12} \cdot \mathbf{W})(\mathbf{N}_{1p} \cdot \boldsymbol{\xi}) + \mathbf{W} \cdot \boldsymbol{\eta}_p}{|\mathbf{W} \times \mathbf{v}_p^{12}|} \\ K_{1q} &= -\frac{\mathbf{W} \cdot (\boldsymbol{\omega}_1 - M\boldsymbol{\omega}_2)}{|\mathbf{W} \times \mathbf{v}_p^{12}|} - \frac{G_{1w}(\mathbf{W} \cdot \mathbf{v}_p^{12})}{|\mathbf{W} \times \mathbf{v}_p^{12}|} - \frac{\mathbf{N}_{1p} \cdot \mathbf{J}_p}{|\mathbf{W} \times \mathbf{v}_p^{12}|^2} \end{aligned} \right\} \quad (6.2)$$

Position vector \mathbf{R}_{1p} of point P on the generating curve can be expressed in the first coordinate system $O - \mathbf{i}, \mathbf{j}, \mathbf{k}$ as follows

$$\mathbf{R}_{1p} = \rho \cos \sigma \mathbf{i} + \rho \sin \sigma \mathbf{j} + z \mathbf{k} \quad (6.3)$$

where, ρ is the radial distance from point P to axis $\omega_1 = \mathbf{k}$; σ is the phase angle made by the radial vector to axis \mathbf{i} and z is the axial distance of point P along axis \mathbf{k} .

The unit radial vector \mathbf{r}_o in the direction from axis $\omega_1 = \mathbf{k}$ to point P is in the form

$$\mathbf{r}_o = \cos \sigma \mathbf{i} + \sin \sigma \mathbf{j} \quad (6.4)$$

and the unit circumferential tangential vector \mathbf{t}_o is found as follows

$$\begin{aligned} \mathbf{t}_o &= \mathbf{k} \times \mathbf{r}_o \\ &= -\sin \sigma \mathbf{i} + \cos \sigma \mathbf{j} \end{aligned} \quad (6.5)$$

Rotating unit vectors \mathbf{r}_o and \mathbf{t}_o about axis \mathbf{k} , each through an angle v , yields new unit vectors \mathbf{W}_o and $\boldsymbol{\xi}_o$ as follows

$$\left. \begin{aligned} \mathbf{W}_o &= (v\mathbf{k}) \otimes \mathbf{r}_o = (v\mathbf{k}) \otimes (\cos \sigma \mathbf{i} + \sin \sigma \mathbf{j}) \\ &= \cos(\sigma + v) \mathbf{i} + \sin(\sigma + v) \mathbf{j} \\ \boldsymbol{\xi}_o &= (v\mathbf{k}) \otimes \mathbf{t}_o = (v\mathbf{k}) \otimes (-\sin \sigma \mathbf{i} + \cos \sigma \mathbf{j}) \\ &= -\sin(\sigma + v) \mathbf{i} + \cos(\sigma + v) \mathbf{j} \end{aligned} \right\} \quad (6.6)$$

The unit tangential vector \mathbf{W} at point P to the generating curve can be obtained by rotating \mathbf{W}_o about axis $\boldsymbol{\xi}_o$ through an angle $\phi_c - 90^\circ$ as follows

$$\begin{aligned} \mathbf{W} &= [(\phi_c - 90^\circ)\boldsymbol{\xi}_o] \otimes \mathbf{W}_o \\ &= \sin \phi_c \cos(\sigma + v) \mathbf{i} + \sin \phi_c \sin(\sigma + v) \mathbf{j} + \cos \phi_c \mathbf{k} \end{aligned} \quad (6.7)$$

The unit principle normal vector $\boldsymbol{\xi}$ at point P to the generating curve results from rotating $\boldsymbol{\xi}_o$ about \mathbf{W} through an angle δ , that is,

$$\begin{aligned} \boldsymbol{\xi} &= (\delta \mathbf{W}) \otimes \boldsymbol{\xi}_o \\ &= [-\cos \delta \sin(\sigma + v) - \sin \delta \cos \phi_c \cos(\sigma + v)] \mathbf{i} \\ &\quad + [\cos \delta \cos(\sigma + v) - \sin \delta \cos \phi_c \sin(\sigma + v)] \mathbf{j} + \sin \delta \sin \phi_c \mathbf{k} \end{aligned} \quad (6.8)$$

With the aid of expression (6.3) and taking into account $M = 0$, application of expression (2.129) yields

$$\left. \begin{aligned} \mathbf{v}_p^{12} &= (-\rho \sin \sigma - b_r \cos \gamma) \mathbf{i} + (\rho \cos \sigma - b_r \sin \gamma) \mathbf{j} + b_a \mathbf{k} \\ |\mathbf{v}_p^{12}| &= \sqrt{\rho^2 + b_r^2 + b_a^2 + 2\rho b_r \sin(\sigma - \gamma)} \end{aligned} \right\} \quad (6.9)$$

and application of expression (2.150) results in

$$\mathbf{J}_p = b_r \sin \gamma \mathbf{i} - b_r \cos \gamma \mathbf{j} \quad (6.10)$$

Substitution of expressions (6.7), (6.9) into (2.265) yields the unit vector \mathbf{N}_{1p} normal to the conjugate surface formed by the generating curve as follows

$$\left. \begin{aligned} \mathbf{N}_{1p} &= \frac{\mathbf{W} \times \mathbf{v}_p^{12}}{|\mathbf{W} \times \mathbf{v}_p^{12}|} \\ &= \frac{\begin{Bmatrix} [b_a \sin \phi_c \sin(\sigma + v) - (\rho \cos \sigma - b_r \sin \gamma) \cos \phi_c] \mathbf{i} \\ + [-b_a \sin \phi_c \cos(\sigma + v) - (\rho \sin \sigma + b_r \cos \gamma) \cos \phi_c] \mathbf{j} \\ + [\rho \sin \phi_c \cos v - b_r \sin \phi_c \sin(\gamma - \sigma - v)] \mathbf{k} \end{Bmatrix}}{Q_p} \\ Q_p &= |\mathbf{W} \times \mathbf{v}_p^{12}| \\ &= \sqrt{\begin{aligned} &b_a^2 \sin^2 \phi_c + \rho^2 (\cos^2 \phi_c + \sin^2 \phi_c \cos^2 v) \\ &+ b_r^2 [\cos^2 \phi_c + \sin^2 \phi_c \sin^2(\gamma - \sigma - v)] \\ &+ 2\rho b_r [\sin(\sigma - \gamma) \cos^2 \phi_c - \sin^2 \phi_c \cos v \sin(\gamma - \sigma - v)] \\ &- 2\rho b_a \sin \phi_c \cos \phi_c \sin v + 2b_a b_r \sin \phi_c \cos \phi_c \cos(\gamma - \sigma - v) \end{aligned}} \end{aligned} \right\} \quad (6.11)$$

Expression (2.133) results in

$$\left. \begin{aligned} \eta_p &= \eta_{p1} \mathbf{i} + \eta_{p2} \mathbf{j} + \eta_{p3} \mathbf{k} \\ \eta_{p1} &= \frac{b_a \sin \phi_c \cos(\sigma + v) + (\rho \sin \sigma + b_r \cos \gamma) \cos \phi_c}{Q_p} \\ \eta_{p2} &= \frac{b_a \sin \phi_c \sin(\sigma + v) - (\rho \cos \sigma - b_r \sin \gamma) \cos \phi_c}{Q_p} \\ \eta_{p3} &= 0 \\ |\eta_p| &= \sqrt{\eta_{p1}^2 + \eta_{p2}^2 + \eta_{p3}^2} \\ &= \frac{\sqrt{b_a^2 \sin^2 \phi_c + [\rho^2 + b_r^2 + 2\rho b_r \sin(\sigma - \gamma)] \cos^2 \phi_c + 2b_a \sin \phi_c \cos \phi_c [b_r \cos(\gamma - \sigma - v) - \rho \sin v]}}{Q_p} \end{aligned} \right\} \quad (6.12)$$

Application of expressions (6.7), (6.9), (6.10), (6.11) and (6.12) results in the following expressions

$$\left. \begin{aligned} \mathbf{N}_{1p} \cdot \mathbf{J}_b &= \frac{b_r[b_a \sin \phi_c \cos(\gamma - \sigma - v) + \rho \cos \phi_c \sin(\sigma - \gamma) + b_r \cos \phi_c]}{Q_p} \\ \mathbf{W} \cdot \mathbf{v}_p^{12} &= \rho \sin \phi_c \sin v - b_r \sin \phi_c \cos(\gamma - \sigma - v) + b_a \cos \phi_c \\ \mathbf{W} \cdot \boldsymbol{\eta}_p &= \frac{\sin \phi_c [b_a \sin \phi_c - \rho \cos \phi_c \sin v + b_r \cos \phi_c \cos(\gamma - \sigma - v)]}{Q_p} \end{aligned} \right\} \quad (6.13)$$

and finally, substitution of expressions (6.7), (6.8), (6.11) and (6.13) into (6.2) leads to the general expressions for calculating the curvatures of conical helicoids with constant rate of lead as follows

$$\left. \begin{aligned} K_{1w} &= \frac{k_c}{Q_p} \left\{ \begin{aligned} &b_a \sin \phi_c \cos \delta - \rho(\sin \delta \cos v + \cos \phi_c \cos \delta \sin v) \\ &+ b_r[\sin \delta \sin(\gamma - \sigma - v) + \cos \phi_c \cos \delta \cos(\gamma - \sigma - v)] \end{aligned} \right\} \\ G_{1w} &= -\frac{K_{1w}[\rho \sin \phi_c \sin v - b_r \sin \phi_c \cos(\gamma - \sigma - v) + b_a \cos \phi_c]}{Q_p} \\ &\quad + \frac{\sin \phi_c [b_a \sin \phi_c - \rho \cos \phi_c \sin v + b_r \cos \phi_c \cos(\gamma - \sigma - v)]}{Q_p^2} \\ K_{1q} &= -\frac{\cos \phi_c}{Q_p} - \frac{G_{1w}[\rho \sin \phi_c \sin v - b_r \sin \phi_c \cos(\gamma - \sigma - v) + b_a \cos \phi_c]}{Q_p} \\ &\quad - \frac{b_r[b_a \sin \phi_c \cos(\gamma - \sigma - v) + \rho \cos \phi_c \sin(\sigma - \gamma) + b_r \cos \phi_c]}{Q_p^3} \end{aligned} \right\} \quad (6.14)$$

If $\gamma = \sigma = v = 0^\circ$ and $\delta = 90^\circ$, the expressions above can be further simplified in the following forms

$$\left. \begin{aligned} \mathbf{N}_{1p} &= \frac{-\rho \cos \phi_c \mathbf{i} - (b_a \sin \phi_c + b_r \cos \phi_c) \mathbf{j} + \rho \sin \phi_c \mathbf{k}}{\sqrt{\rho^2 + (b_a \sin \phi_c + b_r \cos \phi_c)^2}} \\ K_{1w} &= -\frac{k_c \rho}{\sqrt{\rho^2 + (b_a \sin \phi_c + b_r \cos \phi_c)^2}} \\ G_{1w} &= \frac{k_c \rho (b_a \cos \phi_c - b_r \sin \phi_c) + (b_a \sin \phi_c + b_r \cos \phi_c) \sin \phi_c}{\rho^2 + (b_a \sin \phi_c + b_r \cos \phi_c)^2} \\ K_{1q} &= -\frac{\cos \phi_c}{\sqrt{\rho^2 + (b_a \sin \phi_c + b_r \cos \phi_c)^2}} \\ &\quad - \frac{k_c \rho (b_a \cos \phi_c - b_r \sin \phi_c)^2 + (b_a \sin \phi_c + b_r \cos \phi_c)^2 \cos \phi_c}{[\rho^2 + (b_a \sin \phi_c + b_r \cos \phi_c)^2]^{\frac{3}{2}}} \end{aligned} \right\} \quad (6.15)$$

If further we let $k_c = 0$ in expression (6.15), corresponding to a straight cutter blade, then the expression above can be rewritten in the form

$$\left. \begin{aligned} K_{1w} &= 0 \\ G_{1w} &= \frac{(b_a \sin \phi_c + b_r \cos \phi_c) \sin \phi_c}{\rho^2 + (b_a \sin \phi_c + b_r \cos \phi_c)^2} \\ K_{1q} &= -\frac{\cos \phi_c [\rho^2 + 2(b_a \sin \phi_c + b_r \cos \phi_c)^2]}{[\rho^2 + (b_a \sin \phi_c + b_r \cos \phi_c)^2]^{\frac{3}{2}}} \end{aligned} \right\} \quad (6.16)$$

By assuming $b_r = 0$ in the condition of conjugate motion, i.e., in (6.1), the corresponding conjugate surface formed by a cutting edge under the conjugate motions

of this type is a cylindrical helicoid. Substitution of condition (6.1) into expressions (6.11) and (6.14) together with consideration $b_r = 0$ leads to the general formulas to calculate the unit normal and the curvatures of a cylindrical helicoid with a constant rate of lead as follows

$$N_{1p} = \frac{\left\{ \begin{array}{l} [b_a \sin \phi_c \sin(\sigma + \nu) - \rho \cos \sigma \cos \phi_c] \mathbf{i} \\ -[b_a \sin \phi_c \cos(\sigma + \nu) + \rho \sin \sigma \cos \phi_c] \mathbf{j} \\ + \rho \sin \phi_c \cos \nu \mathbf{k} \end{array} \right\}}{\sqrt{b_a^2 \sin^2 \phi_c + \rho^2 (\cos^2 \phi_c + \sin^2 \phi_c \cos^2 \nu) - 2\rho b_a \sin \phi_c \cos \phi_c \sin \nu}} \quad (6.17)$$

and

$$\left. \begin{aligned} K_{1w} &= \frac{k_c [b_a \sin \phi_c \cos \delta - \rho (\sin \delta \cos \nu + \cos \phi_c \cos \delta \sin \nu)]}{\sqrt{b_a^2 \sin^2 \phi_c + \rho^2 (\cos^2 \phi_c + \sin^2 \phi_c \cos^2 \nu) - 2\rho b_a \sin \phi_c \cos \phi_c \sin \nu}} \\ G_{1w} &= \frac{\left\{ \begin{array}{l} \sin \phi_c (b_a \sin \phi_c - \rho \cos \phi_c \sin \nu) \\ -k_c [b_a \sin \phi_c \cos \delta - \rho (\sin \delta \cos \nu + \cos \phi_c \cos \delta \sin \nu)] \\ (\rho \sin \phi_c \sin \nu + b_a \cos \phi_c) \end{array} \right\}}{\sqrt{b_a^2 \sin^2 \phi_c + \rho^2 (\cos^2 \phi_c + \sin^2 \phi_c \cos^2 \nu) - 2\rho b_a \sin \phi_c \cos \phi_c \sin \nu}} \\ K_{1q} &= \frac{\left\{ \begin{array}{l} k_c [b_a \sin \phi_c \cos \delta - \rho (\sin \delta \cos \nu + \cos \phi_c \cos \delta \sin \nu)] \\ (\rho \sin \phi_c \sin \nu + b_a \cos \phi_c)^2 - 2b_a^2 \sin^2 \phi_c \cos \phi_c \\ -\rho^2 (\cos^2 \phi_c + \sin^2 \phi_c \cos^2 \nu - \sin^2 \phi_c \sin^2 \nu) \cos \phi_c \\ -\rho b_a (\sin^2 \phi_c - 3 \cos^2 \phi_c) \sin \phi_c \sin \nu \end{array} \right\}}{[b_a^2 \sin^2 \phi_c + \rho^2 (\cos^2 \phi_c + \sin^2 \phi_c \cos^2 \nu) - 2\rho b_a \sin \phi_c \cos \phi_c \sin \nu]^{\frac{3}{2}}} \end{aligned} \right\} \quad (6.18)$$

If $\sigma = \nu = 0^\circ$, $\delta = 90^\circ$, the expressions above can be simplified in the form

$$\left. \begin{aligned} N_{1p} &= \frac{-\rho \cos \phi_c \mathbf{i} - b_a \sin \phi_c \mathbf{j} + \rho \sin \phi_c \mathbf{k}}{\sqrt{\rho^2 + b_a^2 \sin^2 \phi_c}} \\ K_{1w} &= -\frac{\rho k_c}{\sqrt{\rho^2 + b_a^2 \sin^2 \phi_c}} \\ G_{1w} &= \frac{b_a \sin^2 \phi_c + k_c \rho b_a \cos \phi_c}{\sqrt{\rho^2 + b_a^2 \sin^2 \phi_c}} \\ K_{1q} &= -\frac{\cos \phi_c (\rho^2 + 2b_a^2 \sin^2 \phi_c + k_c \rho b_a \cos \phi_c)}{(\rho^2 + b_a^2 \sin^2 \phi_c)^{\frac{3}{2}}} \end{aligned} \right\} \quad (6.19)$$

Further, assuming $k_c = 0$, besides $\sigma = \nu = 0^\circ$, $\delta = 90^\circ$, then expression (6.19) yields the formulas to calculate curvatures of the surface of the Archimedes worm as follows

$$\left. \begin{aligned} K_{1w} &= 0 \\ G_{1w} &= \frac{b_a \sin^2 \phi_c}{\sqrt{\rho^2 + b_a^2 \sin^2 \phi_c}} \\ K_{1q} &= -\frac{(\rho^2 + 2b_a^2 \sin^2 \phi_c) \cos \phi_c}{(\rho^2 + b_a^2 \sin^2 \phi_c)^{\frac{3}{2}}} \end{aligned} \right\} \quad (6.20)$$

If we choose $b_r = 0$, $b_a \sin \phi_c - \rho \sin v \cos \phi_c = 0$ and $k_c = 0$, the cylindrical helicoid with constant lead of this type is the involute helicoid. The value $\rho \sin v$ represents the radius of the base circle, and ϕ_c is equal to ψ_b , the base helix angle. Substitution of $k_c = 0$, $b_r = 0$ and $b_a = \frac{\rho \sin v \cos \phi_c}{\sin \phi_c}$ into expressions (6.11) and (6.14) leads to the unit normal and the curvatures of the involute helicoid as follows

$$\left. \begin{aligned} N_{1p} &= -\cos \phi_c \cos(\sigma + v)\mathbf{i} - \cos \phi_c \sin(\sigma + v)\mathbf{j} + \sin \phi_c \mathbf{k} \\ K_{1w} &= 0 \\ G_{1w} &= 0 \\ K_{1q} &= -\frac{\cos \phi_c}{\rho \cos v} \end{aligned} \right\} \quad (6.21)$$

Assume $b_r = b_a = 0$ in the condition of conjugate motions, i.e., in (6.1), then the corresponding conjugate surface formed by a cutting edge under this type of conjugate motions is a surface of revolution. Substitution of condition (6.1) into expressions (6.11) and (6.14) together with consideration $b_r = b_a = 0$ leads to the general formulas to calculate the unit normal and curvatures of an axisymmetric surface as follows

$$\left. \begin{aligned} N_{1p} &= \frac{-\cos \sigma \cos \phi_c \mathbf{i} - \sin \sigma \cos \phi_c \mathbf{j} + \sin \phi_c \cos v \mathbf{k}}{\sqrt{\cos^2 \phi_c + \sin^2 \phi_c \cos^2 v}} \\ K_{1w} &= -\frac{k_c (\sin \delta \cos v + \cos \phi_c \cos \delta \sin v)}{\sqrt{\cos^2 \phi_c + \sin^2 \phi_c \cos^2 v}} \\ G_{1w} &= \frac{[k_c \rho (\sin \delta \cos v + \cos \phi_c \cos \delta \sin v) - \cos \phi_c] \sin \phi_c \sin v}{\rho (\cos^2 \phi_c + \sin^2 \phi_c \cos^2 v)} \\ K_{1q} &= -\frac{\left\{ \begin{aligned} &[\cos^2 \phi_c + (\cos^2 v - \sin^2 v) \sin^2 \phi_c] \cos \phi_c \\ &+ k_c \rho (\sin \delta \cos v + \cos \phi_c \cos \delta \sin v) \sin^2 \phi_c \sin^2 v \end{aligned} \right\}}{\rho [\cos^2 \phi_c + \sin^2 \phi_c \cos^2 v]^{\frac{3}{2}}} \end{aligned} \right\} \quad (6.22)$$

Setting $k_c = 0$ in expression (6.22) leads to the formulas to calculate the curvatures of a hyperboloid of revolution as follows

$$\left. \begin{aligned} K_{1w} &= 0 \\ G_{1w} &= -\frac{\sin \phi_c \cos \phi_c \sin v}{\rho (\cos^2 \phi_c + \sin^2 \phi_c \cos^2 v)} \\ K_{1q} &= -\frac{[\cos^2 \phi_c + (\cos^2 v - \sin^2 v) \sin^2 \phi_c] \cos \phi_c}{\rho [\cos^2 \phi_c + \sin^2 \phi_c \cos^2 v]^{\frac{3}{2}}} \end{aligned} \right\} \quad (6.23)$$

If choose $v = 0$ and $k_c = 0$ in expression (6.22), then, expression (6.22) provides the formulas to calculate the unit normal and curvatures of a cone as follows

$$\left. \begin{aligned} N_{1p} &= -\cos \sigma \cos \phi_c \mathbf{i} - \sin \sigma \cos \phi_c \mathbf{j} + \sin \phi_c \mathbf{k} \\ K_{1w} &= 0 \\ G_{1w} &= 0 \\ K_{1q} &= -\frac{\cos \phi_c}{\rho} \end{aligned} \right\} \quad (6.24)$$

Further, assuming $\phi_c = 0^\circ$ or 180° in expression (6.24) gives the unit normal and curvatures of a cylinder as follows

$$\left. \begin{aligned} N_{1p} &= \pm(\cos \sigma \mathbf{i} + \sin \sigma \mathbf{j}) \\ K_{1w} &= 0 \\ G_{1w} &= 0 \\ K_{1q} &= \pm \frac{1}{\rho} \end{aligned} \right\} \quad (6.25)$$

6.2 Selection of the Fundamental Contact point and Determination of the Cutting Position of the Fundamental Contact Point

1. Selection of the fundamental contact point.

A fundamental contact point is an important concept which is a unique feature in this system of design and calculation. In order to realize a pair of tooth surfaces with point contact, it is necessary to select a criterion point on the fundamental surface, i.e., the tooth surface of the gear, first, and then, to carry out curvature modifications to the substituted surface, i.e., the tooth surface of the pinion, at the point corresponding to the criterion point based on a pair of tooth surfaces with line contact, and finally, a pair of tooth surfaces with point contact will be obtained. This criterion point is called the fundamental contact point P_f . The reference point P_b is mainly used to define the shape parameters of the tooth surface. Its position is usually at the mean point of the tooth width and the center of the tooth space on the reference cone. The position of a fundamental contact point P_f can be prescribed and determines the position of contact bearing. Suitable selection of a fundamental contact point P_f is one of the major ways to improve the quality of transmission of gearing and directly affects the strength of bending and contact.

The position of a fundamental contact point P_f can be defined by two parameters with respect to the reference point P_b . Parameter 1 is ξ_f which represents the distance from the reference point P_b to the fundamental contact point P_f in the direction of the generatrix of the reference cone; and parameter 2 is a_f which represents the distance from the reference point P_b to the fundamental contact point P_f in the direction of the tooth height, as shown in fig. 6.1. The radial distance ρ_f from the fundamental contact point P_f to axis $\omega_1 = \mathbf{k}$ and the axial distance z_f to the fundamental contact point P_f from the origin point O along axis \mathbf{k} are found in the form

$$\left. \begin{aligned} \rho_f &= \rho_b + \xi_f \sin \gamma_g + a_f \cos \gamma_g \\ z_f &= z_b + \xi_f \cos \gamma_g - a_f \sin \gamma_g \end{aligned} \right\} \quad (6.26)$$

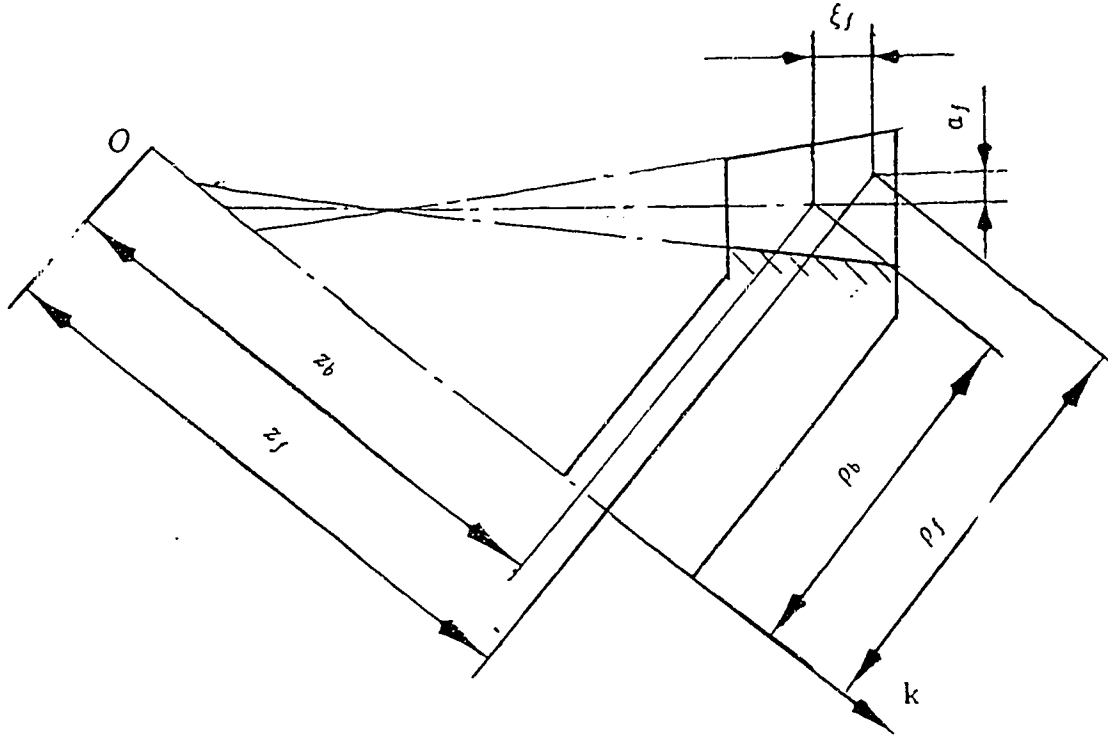


Figure 6.1: The position of the fundamental contact point

where, ρ_b and z_b are defined in chapter 4.1, and γ_g is the gear reference angle which is determined in expression (4.2).

The machine-setting parameters for the gear tooth surface, i.e., M_{mg} , f_{mg} , L , and the blade angle ϕ_c have been given by expressions (5.44) or (5.47). Since the curvature properties at the fundamental contact point P_f of the gear tooth surface are determined by the cutter parameters and the conjugate motion between the cutter and the gear, it is now required to know the cutting position of the fundamental contact point P_f in order to calculate the curvatures at the fundamental contact point P_f . Similar to the derivation of expression (5.9), let $\vec{O_m O_c} = x_c^f \mathbf{i}_m + y_c^f \mathbf{j}_m + z_c^f \mathbf{k}_m$, as shown in fig.5.3, be the position vector of the origin of the coordinate system for the cutter, i.e., $O_c - \mathbf{i}_c, \mathbf{j}_c, \mathbf{k}_c$, corresponding to the fundamental contact point P_f , and let the cutter radius, phase angle and swivel angle corresponding to the cutting position of the fundamental contact point be ρ_c^f , σ^f , and Θ^f respectively. Replacing x_c , y_c , z_c , ρ_c , σ , Θ in expression (5.9) by x_c^f , y_c^f , z_c^f , ρ_c^f , σ^f , Θ^f yields the position vector of the point on the cutter corresponding to the cutting position of the fundamental contact

point in the following form

$$\begin{aligned} \mathbf{R}_{mf} = & (x_c^f + \rho_c^f \cos \sigma^f \cos \Theta^f - \rho_c^f \sin \sigma^f \cos \zeta \sin \Theta^f) \mathbf{i}_m \\ & (y_c^f + \rho_c^f \cos \sigma^f \sin \Theta^f + \rho_c^f \sin \sigma^f \cos \zeta \cos \Theta^f) \mathbf{j}_m \\ & (z_c^f + \rho_c^f \sin \sigma^f \sin \zeta) \mathbf{k}_m \end{aligned} \quad (6.27)$$

As before, the unit normal \mathbf{N}_c^f to the cutter surface is found in the form

$$\left. \begin{aligned} \mathbf{N}_c^f &= N_{cx}^f \mathbf{i}_m + N_{cy}^f \mathbf{j}_m + N_{cz}^f \mathbf{k}_m \\ N_{cx}^f &= -\cos \phi_c \cos \sigma^f \cos \Theta^f + \cos \phi_c \sin \sigma^f \cos \zeta \sin \Theta^f \\ &\quad + \sin \phi_c \sin \zeta \sin \Theta^f \\ N_{cy}^f &= -\cos \phi_c \cos \sigma^f \sin \Theta^f - \cos \phi_c \sin \sigma^f \cos \zeta \cos \Theta^f \\ &\quad - \sin \phi_c \sin \zeta \cos \Theta^f \\ N_{cz}^f &= -\cos \phi_c \sin \sigma^f \sin \zeta + \sin \phi_c \cos \zeta \end{aligned} \right\} \quad (6.28)$$

where, for the convex side: $\phi_c = \phi_c^i$; for the concave side: $\phi_c = \phi_c^o$.

Without the tilt device, i.e., $\Theta^f = \zeta = 0$, expressions (6.29) and (6.30) become

$$\mathbf{R}_{mf} = (x_c^f + \rho_c^f \cos \sigma^f) \mathbf{i}_m + (y_c^f + \rho_c^f \sin \sigma^f) \mathbf{j}_m + z_c^f \mathbf{k}_m \quad (6.29)$$

and

$$\left. \begin{aligned} \mathbf{N}_c^f &= N_{cx}^f \mathbf{i}_m + N_{cy}^f \mathbf{j}_m + N_{cz}^f \mathbf{k}_m \\ N_{cx}^f &= -\cos \phi_c \cos \sigma^f \\ N_{cy}^f &= -\cos \phi_c \sin \sigma^f \\ N_{cz}^f &= \sin \phi_c \end{aligned} \right\} \quad (6.30)$$

The unit normal at the fundamental contact point P_f of the gear tooth surface at the cutting position can be found by application of expression (2.171) together with consideration $\alpha = 90^\circ - \beta$

$$\left. \begin{aligned} \mathbf{N}_g^f &= -\mathbf{N}_c^f = N_{gx}^f \mathbf{i}_g + N_{gy}^f \mathbf{j}_g + N_{gz}^f \mathbf{k}_g \\ N_{gx}^f &= -N_{cx}^f \\ N_{gy}^f &= -N_{cy}^f \sin \beta + N_{cz}^f \cos \beta \\ N_{gz}^f &= -N_{cy}^f \cos \beta - N_{cz}^f \sin \beta \end{aligned} \right\} \quad (6.31)$$

Without the tilt device, i.e., $\Theta^f = \zeta = 0$, expression (6.33) is simplified as follows,

$$\left. \begin{aligned} \mathbf{N}_g^f &= N_{gx}^f \mathbf{i}_g + N_{gy}^f \mathbf{j}_g + N_{gz}^f \mathbf{k}_g \\ N_{gx}^f &= \cos \phi_c \cos \sigma^f \\ N_{gy}^f &= \cos \phi_c \sin \sigma^f \sin \gamma_{gr} + \sin \phi_c \cos \gamma_{gr} \\ N_{gz}^f &= \cos \phi_c \sin \sigma^f \cos \gamma_{gr} - \sin \phi_c \sin \gamma_{gr} \end{aligned} \right\} \quad (6.32)$$

Replacing $x_c, y_c, z_c, \sigma, \Theta, \rho_b, z_b, \varepsilon_g$ in expression (5.21) by $x_c^f, y_c^f, z_c^f, \sigma^f, \Theta^f, \rho_f, z_f, \varepsilon_g^f$ yields the following equations,

$$\left. \begin{aligned} \rho_f \cos \varepsilon_g^f &= x_c^f + \rho_c^f \cos \sigma^f \cos \Theta^f - \rho_c^f \sin \sigma^f \cos \zeta \sin \Theta^f - f_{mg} \\ \rho_f \sin \varepsilon_g^f &= (y_c^f + \rho_c^f \cos \sigma^f \sin \Theta^f + \rho_c^f \sin \sigma^f \cos \zeta \cos \Theta^f) \sin \beta \\ &\quad - (z_c^f + \rho_c^f \sin \sigma^f \sin \zeta) \cos \beta \\ z_f + L &= (y_c^f + \rho_c^f \cos \sigma^f \sin \Theta^f + \rho_c^f \sin \sigma^f \cos \zeta \cos \Theta^f) \cos \beta \\ &\quad + (z_c^f + \rho_c^f \sin \sigma^f \sin \zeta) \sin \beta \end{aligned} \right\} \quad (6.33)$$

Without the tilt device, expression (6.35) with consideration $\beta = \gamma_{gr}$ can be simplified in the form

$$\left. \begin{aligned} \rho_f \cos \varepsilon_g^f &= x_c^f + \rho_c^f \cos \sigma^f - f_{mg} \\ \rho_f \sin \varepsilon_g^f &= (y_c^f + \rho_c^f \sin \sigma^f) \sin \gamma_{gr} - z_c^f \cos \gamma_{gr} \\ z_f + L &= (y_c^f + \rho_c^f \sin \sigma^f) \cos \gamma_{gr} + z_c^f \sin \gamma_{gr} \end{aligned} \right\} \quad (6.34)$$

Likewise, expression (5.25) yields the velocity at the fundamental contact point P_f of the cutter relative to the gear as follows

$$\left. \begin{aligned} \mathbf{v}_f^{mg} &= v_{f1}^{mg} \mathbf{i}_m + v_{f2}^{mg} \mathbf{j}_m + v_{f3}^{mg} \mathbf{k}_m \\ v_{f1}^{mg} &= -(1 + M_{mg} \sin \beta)(y_c^f + \rho_c^f \cos \sigma^f \sin \Theta^f + \rho_c^f \sin \sigma^f \cos \zeta \cos \Theta^f) \\ &\quad + M_{mg}(z_c^f + \rho_c^f \sin \sigma^f \sin \zeta) \cos \beta \\ v_{f2}^{mg} &= (1 + M_{mg} \sin \beta)(x_c^f + \rho_c^f \cos \sigma^f \cos \Theta^f - \rho_c^f \sin \sigma^f \cos \zeta \sin \Theta^f) \\ &\quad - M_{mg} f_{mg} \sin \beta \\ v_{f3}^{mg} &= -M_{mg}(x_c^f + \rho_c^f \cos \sigma^f \cos \Theta^f - \rho_c^f \sin \sigma^f \cos \zeta \sin \Theta^f) \cos \beta \\ &\quad + M_{mg} f_{mg} \cos \beta \\ |\mathbf{v}_f^{mg}| &= \sqrt{(v_{f1}^{mg})^2 + (v_{f2}^{mg})^2 + (v_{f3}^{mg})^2} \end{aligned} \right\} \quad (6.35)$$

where, M_{mg} , f_{mg} and ζ can be determined from expression (5.44).

Without the tilt device, i.e., $\Theta^f = \zeta = 0$, the relative velocity reduces to the form

$$\left. \begin{aligned} \mathbf{v}_f^{mg} &= v_{f1}^{mg} \mathbf{i}_m + v_{f2}^{mg} \mathbf{j}_m + v_{f3}^{mg} \mathbf{k}_m \\ v_{f1}^{mg} &= -(1 + M_{mg} \sin \gamma_{gr})(y_c^f + \rho_c^f \sin \sigma^f) + M_{mg} z_c^f \cos \gamma_{gr} \\ v_{f2}^{mg} &= (1 + M_{mg} \sin \gamma_{gr})(x_c^f + \rho_c^f \cos \sigma^f) - M_{mg} f_{mg} \sin \gamma_{gr} \\ v_{f3}^{mg} &= -M_{mg}(x_c^f + \rho_c^f \cos \sigma^f) \cos \gamma_{gr} + M_{mg} f_{mg} \cos \gamma_{gr} \\ |\mathbf{v}_f^{mg}| &= \sqrt{(v_{f1}^{mg})^2 + (v_{f2}^{mg})^2 + (v_{f3}^{mg})^2} \end{aligned} \right\} \quad (6.36)$$

Correspondingly, expression (5.27) becomes

$$\begin{aligned}
& N_{cx}^f [-(1 + M_{mg} \sin \beta)(y_c^f + \rho_c^f \cos \sigma^f \sin \Theta^f + \rho_c^f \sin \sigma^f \cos \zeta \cos \Theta^f) \\
& + M_{mg}(z_c^f + \rho_c^f \sin \sigma^f \sin \zeta) \cos \beta] + N_{cy}^f [(1 + M_{mg} \sin \beta)(x_c^f \\
& + \rho_c^f \cos \sigma^f \cos \Theta^f - \rho_c^f \sin \sigma^f \cos \zeta \sin \Theta^f) - M_{mg} f_{mg} \sin \beta] \\
& + N_{cz} [-M_{mg}(x_c^f + \rho_c^f \cos \sigma^f \cos \Theta^f - \rho_c^f \sin \sigma^f \cos \zeta \sin \Theta^f) \cos \beta \\
& + M_{mg} f_{mg} \cos \beta] = 0
\end{aligned} \tag{6.37}$$

and without the tilt device, expression (6.37) becomes

$$\begin{aligned}
& -\cos \phi_c \cos \sigma^f [-(1 + M_{mg} \sin \gamma_{gr})(y_c^f + \rho_c^f \sin \sigma^f) + M_{mg} z_c^f \cos \gamma_{gr}] \\
& -\cos \phi_c \sin \sigma^f [(1 + M_{mg} \sin \gamma_{gr})(x_c^f + \rho_c^f \cos \sigma^f) - M_{mg} f_{mg} \sin \gamma_{gr}] \\
& + \sin \phi_c [-M_{mg}(x_c^f + \rho_c^f \cos \sigma^f) \cos \gamma_{gr} + M_{mg} f_{mg} \cos \gamma_{gr}] = 0
\end{aligned} \tag{6.38}$$

2. Three auxiliary relationships

Application of expression (5.34), which represents the distance between the center of the cutter and the center of the cradle, leads to the first auxiliary relationship as follows for the outer and inner sides of the cutter,

$$\left. \begin{aligned}
& (x_c^o - z_c^o \tan \zeta \sin \Theta^o)^2 + (y_c^o + z_c^o \tan \zeta \cos \Theta^o)^2 \\
& = (x_c^f - z_c^f \tan \zeta \sin \Theta^f)^2 + (y_c^f + z_c^f \tan \zeta \cos \Theta^f)^2 \\
& \quad \text{and} \\
& (x_c^i - z_c^i \tan \zeta \sin \Theta^i)^2 + (y_c^i + z_c^i \tan \zeta \cos \Theta^i)^2 \\
& = (x_c^f - z_c^f \tan \zeta \sin \Theta^f)^2 + (y_c^f + z_c^f \tan \zeta \cos \Theta^f)^2
\end{aligned} \right\} \tag{6.39}$$

Without the tilt device, condition (6.39) becomes

$$\left. \begin{aligned}
& (x_c^o)^2 + (y_c^o)^2 = (x_c^f)^2 + (y_c^f)^2 \\
& \quad \text{and} \\
& (x_c^i)^2 + (y_c^i)^2 = (x_c^f)^2 + (y_c^f)^2
\end{aligned} \right\} \tag{6.40}$$

With the aid of expression (5.32) and the definition of the blade angle of the cutter, the second auxiliary relationship can be found

$$\rho_c - \rho_c^f = (p - p_f) \tan \phi_c \tag{6.41}$$

that is

$$\rho_c^f = \rho_c - \left(\frac{z_c}{\cos \zeta} - \frac{z_c^f}{\cos \zeta} \right) \tan \phi_c \tag{6.42}$$

where, ρ_c^f is the radius of the cutter corresponding to the fundamental contact point P_f . ρ_c can be determined from expression (5.44), for the convex side: $\rho_c = \rho_c^i$, $z_c = z_c^i$, $\phi_c = \phi_c^i$; for the concave side: $\rho_c = \rho_c^o$, $z_c = z_c^o$, $\phi_c = \phi_c^o$.

Without the tilt device, i.e., $\zeta = 0$, expression (6.42) becomes

$$\rho_c^f = \rho_c - (z_c - z_c^f) \tan \phi_c \quad (6.43)$$

where, ρ_c is determined by expression (5.46) and z_c is determined by expression (5.47).

With the aid of expression (5.36), application of expression (5.39) yields the third auxiliary relationship as follows

$$\Theta^f = \Theta + \arctan \frac{y_c^f + z_c^f \tan \zeta \cos \Theta^f}{x_c^f - z_c^f \tan \zeta \sin \Theta^f} - \arctan \frac{y_c + z_c \tan \zeta \cos \Theta}{x_c - z_c \tan \zeta \sin \Theta} \quad (6.44)$$

where, for the convex side: $\Theta = \Theta^i$, $x_c = x_c^i$, $y_c = y_c^i$, $z_c = z_c^i$; for the concave side: $\Theta = \Theta^o$, $x_c = x_c^o$, $y_c = y_c^o$, $z_c = z_c^o$.

3. Simultaneous equations for determining the cutting position of the fundamental contact point.

Combining expressions (6.33), (6.37), (6.39), (6.42) and (6.44) gives rise to the following simultaneous equations for calculating the cutting position of the fundamental contact point P_f .

$$\left. \begin{aligned} \rho_f \cos \varepsilon_g^f &= x_c^f + \rho_c^f \cos \sigma^f \cos \Theta^f - \rho_c^f \sin \sigma^f \cos \zeta \sin \Theta^f - f_{mg}, \\ \rho_f \sin \varepsilon_g^f &= (y_c^f + \rho_c^f \cos \sigma^f \sin \Theta^f + \rho_c^f \sin \sigma^f \cos \zeta \cos \Theta^f) \sin \beta \\ &\quad - (z_c^f + \rho_c^f \sin \sigma^f \sin \zeta) \cos \beta, \\ z_f + L &= (y_c^f + \rho_c^f \cos \sigma^f \sin \Theta^f + \rho_c^f \sin \sigma^f \cos \zeta \cos \Theta^f) \cos \beta \\ &\quad + (z_c^f + \rho_c^f \sin \sigma^f \sin \zeta) \sin \beta, \\ N_{cx}^f &[-(1 + M_{mg} \sin \beta)(y_c^f + \rho_c^f \cos \sigma^f \sin \Theta^f + \rho_c^f \sin \sigma^f \cos \zeta \cos \Theta^f) \\ &\quad + M_{mg}(z_c^f + \rho_c^f \sin \sigma^f \sin \zeta) \cos \beta] + N_{cy}^f[(1 + M_{mg} \sin \beta)(x_c^f \\ &\quad + \rho_c^f \cos \sigma^f \cos \Theta^f - \rho_c^f \sin \sigma^f \cos \zeta \sin \Theta^f) - M_{mg} f_{mg} \sin \beta] \\ &\quad + N_{cz}^f[-M_{mg}(x_c^f + \rho_c^f \cos \sigma^f \cos \Theta^f - \rho_c^f \sin \sigma^f \cos \zeta \sin \Theta^f) \cos \beta \\ &\quad + M_{mg} f_{mg} \cos \beta] = 0, \\ (x_c - z_c \tan \zeta \sin \Theta)^2 &+ (y_c + z_c \tan \zeta \cos \Theta)^2 \\ &= (x_c^f - z_c^f \tan \zeta \sin \Theta^f)^2 + (y_c^f + z_c^f \tan \zeta \cos \Theta^f)^2, \\ \rho_c^f &= \rho_c - \left(\frac{z_c}{\cos \zeta} - \frac{z_c^f}{\cos \zeta} \right) \tan \phi_c, \\ \Theta^f &= \Theta + \arctan \frac{y_c^f + z_c^f \tan \zeta \cos \Theta^f}{x_c^f - z_c^f \tan \zeta \sin \Theta^f} - \arctan \frac{y_c + z_c \tan \zeta \cos \Theta}{x_c - z_c \tan \zeta \sin \Theta}. \end{aligned} \right\} \quad (6.45)$$

where, L , M_{mg} , f_{mg} and ζ can be determined by equation (5.44). For the convex side: $x_c = x_c^i$, $y_c = y_c^i$, $z_c = z_c^i$, and $\Theta = \Theta^i$; for the concave side: $x_c = x_c^o$, $y_c = y_c^o$, $z_c = z_c^o$, and $\Theta = \Theta^o$. These quantities are also determined by equation (5.44).

Solving simultaneous equations (6.45) results in $x_c^f, y_c^f, z_c^f, \Theta^f, \varepsilon_g^f, \sigma^f$ and ρ_c^f .

Without the tilt device, the simultaneous equations for determining the cutting position of the fundamental contact point P_f are simplified as following form

$$\left. \begin{aligned} \rho_f \cos \varepsilon_g^f &= x_c^f + \rho_c^f \cos \sigma^f - f_{mg}, \\ \rho_f \sin \varepsilon_g^f &= (y_c^f + \rho_c^f \sin \sigma^f) \sin \gamma_{gr} - z_c^f \cos \gamma_{gr}, \\ z_f + L &= (y_c^f + \rho_c^f \sin \sigma^f) \cos \gamma_{gr} + z_c^f \sin \gamma_{gr}, \\ &- \cos \phi_c \cos \sigma^f [-(1 + M_{mg} \sin \gamma_{gr})(y_c^f + \rho_c^f \sin \sigma^f) + M_{mg} z_c^f \cos \gamma_{gr}] \\ &- \cos \phi_c \sin \sigma^f [(1 + M_{mg} \sin \gamma_{gr})(x_c^f + \rho_c^f \cos \sigma^f) - M_{mg} f_{mg} \sin \gamma_{gr}] \\ &+ \sin \phi_c [-M_{mg}(x_c^f + \rho_c^f \cos \sigma^f) \cos \gamma_{gr} + M_{mg} f_{mg} \cos \gamma_{gr}] = 0, \\ (x_c^f)^2 + (y_c^f)^2 &= (x_c^f)^2 + (y_c^f)^2, \\ \rho_c^f &= \rho_c - (z_c - z_c^f) \tan \phi_c. \end{aligned} \right\} \quad (6.46)$$

Solving equations (6.46) results in $x_c^f, y_c^f, z_c^f, \varepsilon_g^f, \sigma^f$ and ρ_c^f .

With the formate method, expression (6.46) is simplified in the form

$$\left. \begin{aligned} \rho_f \cos \varepsilon_g^f &= x_c + \rho_c^f \cos \sigma^f - f_{mg}, \\ \rho_f \sin \varepsilon_g^f &= (y_c + \rho_c^f \sin \sigma^f) \sin \gamma_{gr} - z_c^f \cos \gamma_{gr}, \\ z_f + L &= (y_c + \rho_c^f \sin \sigma^f) \cos \gamma_{gr} + z_c^f \sin \gamma_{gr}, \\ \rho_c^f &= \rho_c - (z_c - z_c^f) \tan \phi_c. \end{aligned} \right\} \quad (6.47)$$

Solving the simultaneous equations (6.47) results in $z_c^f, \varepsilon_g^f, \sigma^f$, and ρ_c^f .

6.3 Determination of the Curvature Properties of the Gear Tooth Surface

The direction \mathbf{W} of the cutting edge corresponding to the cutting position of the fundamental contact point P_f can be found from expression (6.7) by setting $v = 0$,

$$\mathbf{W} = \sin \phi_c \cos \sigma^f \mathbf{i}_c + \sin \phi_c \sin \sigma^f \mathbf{j}_c + \cos \phi_c \mathbf{k}_c \quad (6.48)$$

With the aid of equation (5.5), expression (6.48) can be written in coordinate system $O_m - \mathbf{i}_m, \mathbf{j}_m, \mathbf{k}_m$ as follows

$$\left. \begin{aligned} \mathbf{W} &= W_1 \mathbf{i}_m + W_2 \mathbf{j}_m + W_3 \mathbf{k}_m \\ W_1 &= \sin \phi_c \cos \sigma^f \cos \Theta^f - \sin \phi_c \sin \sigma^f \cos \zeta \sin \Theta^f + \cos \phi_c \sin \zeta \sin \Theta^f \\ W_2 &= \sin \phi_c \cos \sigma^f \sin \Theta^f + \sin \phi_c \sin \sigma^f \cos \zeta \cos \Theta^f - \cos \phi_c \sin \zeta \cos \Theta^f \\ W_3 &= \sin \phi_c \sin \sigma^f \sin \zeta + \cos \phi_c \cos \zeta \end{aligned} \right\} \quad (6.49)$$

Without the tilt device, expression (6.49) becomes

$$\left. \begin{aligned} \mathbf{W} &= W_1 \mathbf{i}_m + W_2 \mathbf{j}_m + W_3 \mathbf{k}_m \\ W_1 &= \sin \phi_c \cos \sigma^f \\ W_2 &= \sin \phi_c \sin \sigma^f \\ W_3 &= \cos \phi_c \end{aligned} \right\} \quad (6.50)$$

The direction $\frac{\mathbf{v}_f^{mg}}{|\mathbf{v}_f^{mg}|}$ can be obtained by rotating the tangent vector \mathbf{W} to the cutting edge about unit normal \mathbf{N}_c to the cutter surface through an angle θ_{wv} ,

$$\begin{aligned} \frac{\mathbf{v}_f^{mg}}{|\mathbf{v}_f^{mg}|} &= (\theta_{wv} \mathbf{N}_c^f) \otimes \mathbf{W} \\ &= \cos \theta_{wv} \mathbf{W} + \sin \theta_{wv} \mathbf{N}_c^f \times \mathbf{W} \end{aligned} \quad (6.51)$$

The angle θ_{wv} is then given by

$$\left. \begin{aligned} \cos \theta_{wv} &= \frac{\mathbf{v}_f^{mg} \cdot \mathbf{W}}{|\mathbf{v}_f^{mg}|} \\ &= \frac{v_{f1}^{mg} W_1 + v_{f2}^{mg} W_2 + v_{f3}^{mg} W_3}{|\mathbf{v}_f^{mg}|} \\ \sin \theta_{wv} &= \frac{\mathbf{v}_f^{mg} \cdot (\mathbf{N}_c^f \times \mathbf{W})}{|\mathbf{v}_f^{mg}|} \\ &= \frac{\left\{ \begin{aligned} &-v_{f1}^{mg} (\cos \sigma^f \cos \zeta \sin \Theta^f + \sin \sigma^f \cos \Theta^f) \\ &+v_{f2}^{mg} (\cos \sigma^f \cos \zeta \cos \Theta^f - \sin \sigma^f \sin \Theta^f) \\ &+v_{f3}^{mg} \cos \sigma^f \sin \zeta \end{aligned} \right\}}{|\mathbf{v}_f^{mg}|} \end{aligned} \right\} \quad (6.52)$$

where, $|\mathbf{v}_f^{mg}|$, v_{f1}^{mg} , v_{f2}^{mg} and v_{f3}^{mg} are determined by expressions (6.35).

Without the tilt device, the expressions above become

$$\left. \begin{aligned} \cos \theta_{wv} &= \frac{\mathbf{v}_f^{mg} \cdot \mathbf{W}}{|\mathbf{v}_f^{mg}|} \\ &= \frac{v_{f1}^{mg} W_1 + v_{f2}^{mg} W_2 + v_{f3}^{mg} W_3}{|\mathbf{v}_f^{mg}|} \\ \sin \theta_{wv} &= \frac{\mathbf{v}_f^{mg} \cdot (\mathbf{N}_c^f \times \mathbf{W})}{|\mathbf{v}_f^{mg}|} \\ &= \frac{-v_{f1}^{mg} \sin \sigma^f + v_{f2}^{mg} \cos \sigma^f}{|\mathbf{v}_f^{mg}|} \end{aligned} \right\} \quad (6.53)$$

where, $|\mathbf{v}_f^{mg}|$, v_{f1}^{mg} , v_{f2}^{mg} and v_{f3}^{mg} are determined by expressions (6.36).

With the aid of expressions (6.24), (6.52) or (6.53), application of expressions (2.25) and (2.26) leads to the normal and torsional curvatures of the cutter surface along directions of $\frac{\mathbf{v}_f^{mg}}{|\mathbf{v}_f^{mg}|}$ and $\Delta_f = \mathbf{N}_c^f \times \frac{\mathbf{v}_f^{mg}}{|\mathbf{v}_f^{mg}|}$ as follows

$$\left. \begin{aligned} K_{1v} &= K_{1w} \cos^2 \theta_{wv} + K_{1q} \sin^2 \theta_{wv} + 2G_{1w} \sin \theta_{wv} \cos \theta_{wv} \\ &= -\frac{\cos \phi_c}{\rho_c} \sin^2 \theta_{wv} \\ G_{1v} &= -(K_{1w} - K_{1q}) \sin \theta_{wv} \cos \theta_{wv} + G_{1w} (\cos^2 \theta_{wv} - \sin^2 \theta_{wv}) \\ &= -\frac{\cos \phi_c}{\rho_c} \sin \theta_{wv} \cos \theta_{wv} \\ K_{1\Delta} &= K_{1w} \sin^2 \theta_{wv} + K_{1q} \cos^2 \theta_{wv} - 2G_{1w} \sin \theta_{wv} \cos \theta_{wv} \\ &= -\frac{\cos \phi_c}{\rho_c} \cos^2 \theta_{wv} \end{aligned} \right\} \quad (6.54)$$

where, in the case of the tilt device, $\sin \theta_{wv}$ and $\cos \theta_{wv}$ are determined by expressions (6.52); in the case of no tilt device, $\sin \theta_{wv}$ and $\cos \theta_{wv}$ are determined by expressions (6.53).

Employment of expression (2.133) yields the direction η_f perpendicular to the relative angular velocity component in the tangent plane,

$$\left. \begin{aligned} \eta_f &= \eta_{f1} \mathbf{i}_m + \eta_{f2} \mathbf{j}_m + \eta_{f3} \mathbf{k}_m \\ \eta_{f1} &= -N_{cy}^f (1 + M_{mg} \sin \beta) + N_{cz}^f M_{mg} \cos \beta \\ \eta_{f2} &= N_{cx}^f (1 + M_{mg} \sin \beta) \\ \eta_{f3} &= -N_{cx}^f M_{mg} \cos \beta \\ |\eta_f| &= \sqrt{\eta_{f1}^2 + \eta_{f2}^2 + \eta_{f3}^2} \end{aligned} \right\} \quad (6.55)$$

where, N_{c1}^f , N_{c2}^f , and N_{c3}^f are determined by expression (6.28).

Expression (2.135) yields the angle between $\frac{\mathbf{v}_f^{mg}}{|\mathbf{v}_f^{mg}|}$ and η_f as follows,

$$\left. \begin{aligned} \sin \theta_{v\eta} &= \frac{\mathbf{N}_c^f \cdot (\mathbf{v}_f^{mg} \times \eta_f)}{|\mathbf{v}_f^{mg}| |\eta_f|} \\ &= -\frac{\mathbf{v}_f^{mg} \cdot (\omega_1 - M_{mg} \omega_2)}{|\mathbf{v}_f^{mg}| |\eta_f|} \\ &= -\frac{M_{mg} f_{mg} \cos \beta}{|\mathbf{v}_f^{mg}| |\eta_f|} \\ \cos \theta_{v\eta} &= \frac{\mathbf{v}_f^{mg} \cdot \eta_f}{|\mathbf{v}_f^{mg}| |\eta_f|} \\ &= \frac{v_{f1}^{mg} \eta_{f1} + v_{f2}^{mg} \eta_{f2} + v_{f3}^{mg} \eta_{f3}}{|\mathbf{v}_f^{mg}| |\eta_f|} \end{aligned} \right\} \quad (6.56)$$

where, v_{f1}^{mg} , v_{f2}^{mg} , v_{f3}^{mg} and $|\mathbf{v}_f^{mg}|$ are determined by expression (6.35).

Without the tilt device, expressions (6.55) and (6.56) become

$$\left. \begin{aligned} \eta_f &= \eta_{f1}\mathbf{i}_m + \eta_{f2}\mathbf{j}_m + \eta_{f3}\mathbf{k}_m \\ \eta_{f1} &= -N_{cy}^f(1 + M_{mg} \sin \gamma_{gr}) + N_{cz}^f M_{mg} \cos \gamma_{gr} \\ &= \cos \phi_c \sin \sigma^f (1 + M_{mg} \sin \gamma_{gr}) + M_{mg} \sin \phi_c \cos \gamma_{gr} \\ \eta_{f2} &= N_{cx}^f(1 + M_{mg} \sin \gamma_{gr}) \\ &= -\cos \phi_c \cos \sigma^f (1 + M_{mg} \sin \gamma_{gr}) \\ \eta_{f3} &= -N_{cz}^f M_{mg} \cos \gamma_{gr} \\ &= M_{mg} \cos \phi_c \cos \sigma^f \cos \gamma_{gr} \\ |\eta_f| &= \sqrt{\eta_{f1}^2 + \eta_{f2}^2 + \eta_{f3}^2} \end{aligned} \right\} \quad (6.57)$$

where, M_{mg} , and σ^f are determined by expressions (5.47) and (6.46). and

$$\left. \begin{aligned} \sin \theta_{v\eta} &= \frac{\mathbf{N}_c^f \cdot (\mathbf{v}_f^{mg} \times \eta_f)}{|\mathbf{v}_f^{mg}| |\eta_f|} \\ &= -\frac{\mathbf{v}_f^{mg} \cdot (\omega_1 - M_{mg} \omega_2)}{|\mathbf{v}_f^{mg}| |\eta_f|} \\ &= -\frac{M_{mg} f_{mg} \cos \gamma_{gr}}{|\mathbf{v}_f^{mg}| |\eta_f|} \\ \cos \theta_{v\eta} &= \frac{\mathbf{v}_f^{mg} \cdot \eta_f}{|\mathbf{v}_f^{mg}| |\eta_f|} \\ &= \frac{v_{f1}^{mg} \eta_{f1} + v_{f2}^{mg} \eta_{f2} + v_{f3}^{mg} \eta_{f3}}{|\mathbf{v}_f^{mg}| |\eta_f|} \end{aligned} \right\} \quad (6.58)$$

where, v_{f1}^{mg} , v_{f2}^{mg} , v_{f3}^{mg} , $|\mathbf{v}_f^{mg}|$, η_{f1} , η_{f2} and η_{f3} are determined by expressions (6.36) and (6.57) respectively.

Expression (2.151) gives the components of the conjugate relative acceleration,

$$\left. \begin{aligned} \mathbf{J}_f &= J_{f1}\mathbf{i}_m + J_{f2}\mathbf{j}_m + J_{f3}\mathbf{k}_m \\ J_{f1} &= M_{mg} f_{mg} \sin \beta \\ J_{f2} &= M_{mg} (z_c^f + \rho_c^f \sin \sigma^f \sin \zeta) \cos \beta \\ J_{f3} &= -M_{mg} (y_c^f + \rho_c^f \cos \sigma^f \sin \Theta^f + \rho_c^f \sin \sigma^f \cos \zeta \cos \Theta^f) \cos \beta \end{aligned} \right\} \quad (6.59)$$

and

$$\begin{aligned} \mathbf{N}_c^f \cdot \mathbf{J}_f &= N_{cx}^f M_{mg} f_{mg} \sin \beta + N_{cy}^f M_{mg} (z_c^f + \rho_c^f \sin \sigma^f \sin \zeta) \cos \beta \\ &\quad - N_{cz}^f M_{mg} (y_c^f + \rho_c^f \cos \sigma^f \sin \Theta^f + \rho_c^f \sin \sigma^f \cos \zeta \cos \Theta^f) \cos \beta \end{aligned} \quad (6.60)$$

Without the tilt device, expressions (6.59), and (6.60) become

$$\left. \begin{aligned} \mathbf{J}_f &= J_{f1}\mathbf{i}_m + J_{f2}\mathbf{j}_m + J_{f3}\mathbf{k}_m \\ J_{f1} &= M_{mg} f_{mg} \sin \gamma_{gr} \\ J_{f2} &= M_{mg} z_c^f \cos \gamma_{gr} \\ J_{f3} &= -M_{mg} (y_c^f + \rho_c^f \sin \sigma^f) \cos \gamma_{gr} \end{aligned} \right\} \quad (6.61)$$

and

$$\begin{aligned} \mathbf{N}_c^f \cdot \mathbf{J}_f &= -M_{mg} f_{mg} \sin \gamma_{gr} \cos \phi_c \cos \sigma^f - M_{mg} z_c^f \cos \phi_c \sin \sigma^f \cos \gamma_{gr} \\ &\quad - M_{mg} (y_c^f + \rho_c^f \sin \sigma^f) \sin \phi_c \cos \gamma_{gr} \end{aligned} \quad (6.62)$$

Substitution of expressions (6.35), (6.54), (6.55) and (6.56) into (2.209) yields

$$\left. \begin{aligned} D_p &= K_{1v} |\mathbf{v}_f^{mg}| - |\eta_f| \cos \theta_{v\eta} \\ &= -\frac{|\mathbf{v}_f^{mg}| \cos \phi_c \sin^2 \theta_{wv}}{\rho_c^f} - |\eta_f| \cos \theta_{v\eta} \\ E_p &= G_{1v} |\mathbf{v}_f^{mg}| - |\eta_f| \sin \theta_{v\eta} \\ &= -\frac{|\mathbf{v}_f^{mg}| \cos \phi_c \sin \theta_{wv} \cos \theta_{wv}}{\rho_c^f} - |\eta_f| \sin \theta_{v\eta} \end{aligned} \right\} \quad (6.63)$$

where, in the case of the tilt device, $|\mathbf{v}_f^{mg}|$, $|\eta_f|$, $\sin \theta_{wv}$, and $\cos \theta_{wv}$ are determined by expressions (6.35), (6.55) and (6.56) respectively; in the case of no tilt device, $|\mathbf{v}_f^{mg}|$, $|\eta_f|$, $\sin \theta_{wv}$, and $\cos \theta_{wv}$ are determined by expressions (6.36), (6.57) and (6.58) respectively.

With the aid of expression (6.54), application of expressions (2.239) and (2.240) yields the conjugate curvatures properties of the gear tooth surface in the directions of $\frac{\mathbf{v}_f^{mg}}{|\mathbf{v}_f^{mg}|}$ and $\Delta_f = \mathbf{N}_c^f \times \frac{\mathbf{v}_f^{mg}}{|\mathbf{v}_f^{mg}|}$ as follows

$$\left. \begin{aligned} K'_{gv} &= \frac{D_p^2}{D_p |\mathbf{v}_f^{mg}| + \mathbf{N}_c^f \cdot \mathbf{J}_f} - K_{1v} \\ &= \frac{D_p^2}{D_p |\mathbf{v}_f^{mg}| + \mathbf{N}_c^f \cdot \mathbf{J}_f} + \frac{\cos \phi_c \sin^2 \theta_{wv}}{\rho_c^f} \\ G'_{gv} &= \frac{D_p E_p}{D_p |\mathbf{v}_f^{mg}| + \mathbf{N}_c^f \cdot \mathbf{J}_f} - G_{1v} \\ &= \frac{D_p E_p}{D_p |\mathbf{v}_f^{mg}| + \mathbf{N}_c^f \cdot \mathbf{J}_f} + \frac{\cos \phi_c \sin \theta_{wv} \cos \theta_{wv}}{\rho_c^f} \\ K'_{g\Delta} &= \frac{E_p^2}{D_p |\mathbf{v}_f^{mg}| + \mathbf{N}_c^f \cdot \mathbf{J}_f} - K_{1\Delta} \\ &= \frac{E_p^2}{D_p |\mathbf{v}_f^{mg}| + \mathbf{N}_c^f \cdot \mathbf{J}_f} + \frac{\cos \phi_c \cos^2 \theta_{wv}}{\rho_c^f} \end{aligned} \right\} \quad (6.64)$$

where, D_p , and E_p are determined by the expression (6.63), in the case of the tilt device: $|\mathbf{v}_f^{mg}|$ and $\mathbf{N}_c^f \cdot \mathbf{J}_f$ are determined by expressions (6.35) and (6.60) respectively; in the case of no tilt device: $|\mathbf{v}_f^{mg}|$ and $\mathbf{N}_c^f \cdot \mathbf{J}_f$ are determined by expressions (6.36) and (6.62) respectively.

With the aid of expression (2.28), the normal and torsional curvatures of the gear tooth surface in directions of $\frac{\mathbf{v}_f^{mg}}{|\mathbf{v}_f^{mg}|}$ and $\Delta_f = \mathbf{N}_c^f \times \frac{\mathbf{v}_f^{mg}}{|\mathbf{v}_f^{mg}|}$ are found in the form

$$\left. \begin{aligned} K_{gv} &= K'_{gv} \\ G_{gv} &= -G'_{gv} \\ K_{g\Delta} &= K'_{g\Delta} \end{aligned} \right\} \quad (6.65)$$

If we construct a cone with the root angle γ_{gr} of the gear through the fundamental contact point P_f at the cutting position, the unit normal \mathbf{N}_{gr} to this cone at the fundamental contact point P_f is found in the form

$$\begin{aligned}\mathbf{N}_{gr} &= (\varepsilon_g^f \mathbf{k}) \otimes (\cos \gamma_{gr} \mathbf{i} - \sin \gamma_{gr} \mathbf{k}) \\ &= \cos \gamma_{gr} (\cos \varepsilon_g^f \mathbf{i} + \sin \varepsilon_g^f \mathbf{j}) - \sin \gamma_{gr} \mathbf{k}\end{aligned}\quad (6.66)$$

With the aid of expressions (6.31) or (6.32) and (6.66), the unit vector \mathbf{t}_{gr} tangential to the intersection of the gear tooth surface with the cone constructed above is found in the form

$$\left. \begin{aligned}t_{gr} &= \pm \frac{\mathbf{N}_g^f \times \mathbf{N}_{gr}}{|\mathbf{N}_g^f \times \mathbf{N}_{gr}|} = t_{gr1} \mathbf{i} + t_{gr2} \mathbf{j} + t_{gr3} \mathbf{k} \\ t_{gr1} &= -\frac{N_{gy}^f \sin \gamma_{gr} + N_{gz}^f \cos \gamma_{gr} \sin \varepsilon_g^f}{Q_{gr}} \\ t_{gr2} &= \frac{N_{gz}^f \cos \gamma_{gr} \cos \varepsilon_g^f + N_{gx}^f \sin \gamma_{gr}}{Q_{gr}} \\ t_{gr3} &= \frac{N_{gz}^f \cos \gamma_{gr} \sin \varepsilon_g^f - N_{gy}^f \cos \gamma_{gr} \cos \varepsilon_g^f}{Q_{gr}} \\ Q_{gr} &= \pm \sqrt{\begin{aligned} & (N_{gy}^f \sin \gamma_{gr} + N_{gz}^f \cos \gamma_{gr} \sin \varepsilon_g^f)^2 \\ & + (N_{gz}^f \cos \gamma_{gr} \cos \varepsilon_g^f + N_{gx}^f \sin \gamma_{gr})^2 \\ & + (N_{gx}^f \cos \gamma_{gr} \sin \varepsilon_g^f - N_{gy}^f \cos \gamma_{gr} \cos \varepsilon_g^f)^2 \end{aligned}}\end{aligned}\right\} \quad (6.67)$$

where, for the convex side: " \pm " is positive; for the concave side: " \pm " is negative.

Expression (6.35) or (6.36) can be written in the coordinate system $O - \mathbf{i}, \mathbf{j}, \mathbf{k}$ as follows

$$\begin{aligned}\mathbf{v}_f^{mg} &= v_{f1}^{mg} \mathbf{i}_m + v_{f2}^{mg} \mathbf{j}_m + v_{f3}^{mg} \mathbf{k}_m \\ &= v_{f1}^{mg} \mathbf{i} + (v_{f2}^{mg} \sin \beta - v_{f3}^{mg} \cos \beta) \mathbf{j} + (v_{f2}^{mg} \cos \beta + v_{f3}^{mg} \sin \beta) \mathbf{k}\end{aligned}\quad (6.68)$$

and

$$\begin{aligned}\mathbf{v}_f^{mg} &= v_{f1}^{mg} \mathbf{i}_m + v_{f2}^{mg} \mathbf{j}_m + v_{f3}^{mg} \mathbf{k}_m \\ &= v_{f1}^{mg} \mathbf{i} + (v_{f2}^{mg} \sin \gamma_{gr} - v_{f3}^{mg} \cos \gamma_{gr}) \mathbf{j} + (v_{f2}^{mg} \cos \gamma_{gr} + v_{f3}^{mg} \sin \gamma_{gr}) \mathbf{k}\end{aligned}\quad (6.69)$$

On the other hand, \mathbf{t}_{gr} can be obtained by the following method, i.e.,

$$\begin{aligned}\mathbf{t}_{gr} &= (\theta_{vt} \mathbf{N}_g^f) \otimes \frac{\mathbf{v}_f^{mg}}{|\mathbf{v}_f^{mg}|} \\ &= \cos \theta_{vt} \frac{\mathbf{v}_f^{mg}}{|\mathbf{v}_f^{mg}|} + \sin \theta_{vt} \mathbf{N}_g^f \times \frac{\mathbf{v}_f^{mg}}{|\mathbf{v}_f^{mg}|}\end{aligned}\quad (6.70)$$

Angle θ_{vt} is given by

$$\begin{aligned}
\sin \theta_{vt} &= \frac{\mathbf{t}_{gr} \cdot (\mathbf{N}_g^f \times \mathbf{v}_f^{mg})}{|\mathbf{v}_f^{mg}|} \\
&= \left\{ \begin{aligned} &v_{f1}^{mg} (t_{gr2} N_{gz}^f - t_{gr3} N_{gy}^f) \\ &+ (v_{f2}^{mg} \sin \beta - v_{f3}^{mg} \cos \beta) (t_{gr3} N_{gx}^f - t_{gr1} N_{gz}^f) \\ &+ (v_{f2}^{mg} \cos \beta + v_{f3}^{mg} \sin \beta) (t_{gr1} N_{gy}^f - t_{gr2} N_{gx}^f) \end{aligned} \right\} \\
\cos \theta_{vt} &= \frac{t_{gr1} v_{f1}^{mg} + t_{gr2} (v_{f2}^{mg} \sin \beta - v_{f3}^{mg} \cos \beta) + t_{gr3} (v_{f2}^{mg} \cos \beta + v_{f3}^{mg} \sin \beta)}{|\mathbf{v}_f^{mg}|}
\end{aligned} \quad (6.71)$$

In the case of no tilt device, the angle β is replaced by γ_{gr}

$$\begin{aligned}
\sin \theta_{vt} &= \frac{\mathbf{t}_{gr} \cdot (\mathbf{N}_g^f \times \mathbf{v}_f^{mg})}{|\mathbf{v}_f^{mg}|} \\
&= \left\{ \begin{aligned} &v_{f1}^{mg} (t_{gr2} N_{gz}^f - t_{gr3} N_{gy}^f) \\ &+ (v_{f2}^{mg} \sin \gamma_{gr} - v_{f3}^{mg} \cos \gamma_{gr}) (t_{gr3} N_{gx}^f - t_{gr1} N_{gz}^f) \\ &+ (v_{f2}^{mg} \cos \gamma_{gr} + v_{f3}^{mg} \sin \gamma_{gr}) (t_{gr1} N_{gy}^f - t_{gr2} N_{gx}^f) \end{aligned} \right\} \\
\cos \theta_{vt} &= \frac{t_{gr1} v_{f1}^{mg} + t_{gr2} (v_{f2}^{mg} \sin \gamma_{gr} - v_{f3}^{mg} \cos \gamma_{gr}) + t_{gr3} (v_{f2}^{mg} \cos \gamma_{gr} + v_{f3}^{mg} \sin \gamma_{gr})}{|\mathbf{v}_f^{mg}|}
\end{aligned} \quad (6.72)$$

Application of expressions (2.25) and (2.26) yields the normal and torsional curvatures of the gear tooth surface in directions \mathbf{t}_{gr} and $\mathbf{s}_{gr} = \mathbf{N}_g^f \times \mathbf{t}_{gr}$ in the following form

$$\begin{aligned}
K_{gt} &= K_{gv} \cos^2 \theta_{vt} + K_{g\Delta} \sin^2 \theta_{vt} + 2G_{gv} \sin \theta_{vt} \cos \theta_{vt} \\
G_{gt} &= -(K_{gv} - K_{g\Delta}) \sin \theta_{vt} \cos \theta_{vt} + G_{gv} (\cos^2 \theta_{vt} - \sin^2 \theta_{vt}) \\
K_{gs} &= K_{gv} \sin^2 \theta_{vt} + K_{g\Delta} \cos^2 \theta_{vt} - 2G_{gv} \sin \theta_{vt} \cos \theta_{vt}
\end{aligned} \quad (6.73)$$

where, K_{gv} , G_{gv} , $K_{g\Delta}$, $\sin \theta_{vt}$ and $\cos \theta_{vt}$ are determined by expressions (6.65), (6.71) or (6.72) respectively.

With the Formate method, the normal and torsional curvatures of the gear tooth surface in directions \mathbf{W} and $\mathbf{q} = \mathbf{N}_g^f \times \mathbf{W}$ are found in the following form

$$\begin{aligned}
K_{gw} &= 0 \\
G_{gw} &= 0 \\
K_{gq} &= \frac{\cos \phi_c}{\rho_c}
\end{aligned} \quad (6.74)$$

Since expression (6.48) can be written in coordinate system $O - \mathbf{i}, \mathbf{j}, \mathbf{k}$, that is,

$$\begin{aligned}
\mathbf{W} &= \sin \phi_c \cos \sigma^f \mathbf{i} + (\sin \phi_c \sin \sigma^f \sin \gamma_{gr} - \cos \phi_c \cos \gamma_{gr}) \mathbf{j} \\
&\quad + (\sin \phi_c \sin \sigma^f \cos \gamma_{gr} + \cos \phi_c \sin \gamma_{gr}) \mathbf{k}
\end{aligned} \quad (6.75)$$

and \mathbf{t}_{gr} can be obtained by the following way

$$\begin{aligned}\mathbf{t}_{gr} &= (\theta_{wt}\mathbf{N}_g^f) \otimes \mathbf{W} \\ &= \cos \theta_{wt}\mathbf{W} + \sin \theta_{wt}\mathbf{N}_g^f \times \mathbf{W}\end{aligned}\quad (6.76)$$

then, we can find angle θ_{wt} as follows

$$\left. \begin{aligned}\sin \theta_{wt} &= \mathbf{t}_{gr} \cdot (\mathbf{N}_g^f \times \mathbf{W}) \\ &= (t_{gr2}N_{gz}^f - t_{gr3}N_{gy}^f) \sin \phi_c \cos \sigma^f \\ &\quad + (t_{gr3}N_{gx}^f - t_{gr1}N_{gz}^f)(\sin \phi_c \sin \sigma^f \sin \gamma_{gr} - \cos \phi_c \cos \gamma_{gr}) \\ &\quad + (t_{gr1}N_{gy}^f - t_{gr2}N_{gx}^f)(\sin \phi_c \sin \sigma^f \cos \gamma_{gr} + \cos \phi_c \sin \gamma_{gr}) \\ \cos \theta_{wt} &= t_{gr1} \sin \phi_c \cos \sigma^f + t_{gr2}(\sin \phi_c \sin \sigma^f \sin \gamma_{gr} - \cos \phi_c \cos \gamma_{gr}) \\ &\quad + t_{gr3}(\sin \phi_c \sin \sigma^f \cos \gamma_{gr} + \cos \phi_c \sin \gamma_{gr})\end{aligned}\right\} \quad (6.77)$$

Application of expressions (2.25) and (2.26) yields the normal and torsional curvatures of the gear tooth surface in directions of \mathbf{t}_{gr} and $\mathbf{s}_{gr} = \mathbf{N}_g^f \times \mathbf{t}_{gr}$ in the following form

$$\left. \begin{aligned}K_{gt} &= K_{gw} \cos^2 \theta_{wt} + K_{gq} \sin^2 \theta_{wt} + 2G_{gw} \sin \theta_{wt} \cos \theta_{wt} \\ &= \frac{\cos \phi_c \sin^2 \theta_{wt}}{\rho_c} \\ G_{gt} &= -(K_{gw} - K_{gq}) \sin \theta_{wt} \cos \theta_{wt} + G_{gw}(\cos^2 \theta_{wt} - \sin^2 \theta_{wt}) \\ &= \frac{\cos \phi_c \sin \theta_{wt} \cos \theta_{wt}}{\rho_c} \\ K_{gs} &= K_{gw} \sin^2 \theta_{wt} + K_{gq} \cos^2 \theta_{wt} - 2G_{gw} \sin \theta_{wt} \cos \theta_{wt} \\ &= \frac{\cos \phi_c \cos^2 \theta_{wt}}{\rho_c}\end{aligned}\right\} \quad (6.78)$$

Chapter 7

Calculation of Curvatures for the Pinion Tooth Surface with Line Contact

Since precise conjugate motions between a pair of hypoid gears are prescribed by the users of hypoid gearing, and the tooth surface of the gear member is already determined in previous sections, the curvature values of the pinion tooth surface can be determined by application of the solution to the first type of problem of conjugate surfaces and curvatures.

7.1 Determination of the Conjugate Contact Position at the Fundamental Contact Point P_f of the Gear Relative to the Pinion

The fundamental contact point P_f of the gear will reach the conjugate contact position with the pinion after rotating about the axis \mathbf{k} of the gear through an angle $\delta\epsilon_g$ from the cutting position, that is, the conjugate contact position \mathbf{R}_{gp}^f at the fundamental contact point of the gear with the pinion is derived in the following way

$$\left. \begin{aligned} \mathbf{R}_{gp}^f &= (\delta\epsilon_g \mathbf{k}) \otimes [(\epsilon_g^f \mathbf{k}) \otimes (\rho_f \mathbf{i} + z_f \mathbf{k})] = [(\epsilon_g^f + \delta\epsilon_g) \mathbf{k}] \otimes (\rho_f \mathbf{i} + z_f \mathbf{k}) \\ &= x_{gp}^f \mathbf{i} + y_{gp}^f \mathbf{j} + z_{gp}^f \mathbf{k} \\ x_{gp}^f &= \rho_f \cos(\epsilon_g^f + \delta\epsilon_g) \\ y_{gp}^f &= \rho_f \sin(\epsilon_g^f + \delta\epsilon_g) \\ z_{gp}^f &= z_f \end{aligned} \right\} \quad (7.1)$$

where, ρ_f and z_f are determined by expression (6.26); in the case of the tilt device: ε_g^f is determined by expression (6.45); in the case of the no tilt device: ε_g^f is calculated by expression (6.46) and in the case of the Formate method: ε_g^f is calculated by expression (6.47).

Consequently, the unit normal N_{gp}^f at the fundamental contact point P_f to the gear tooth surface at the conjugate contact position of the gear with the pinion is found by making the same rotation

$$\left. \begin{aligned} N_{gp}^f &= (\delta\varepsilon_g \mathbf{k}) \otimes N_g^f \\ &= N_{gpx}^f \mathbf{i} + N_{gpy}^f \mathbf{j} + N_{gpz}^f \mathbf{k} \\ N_{gpx}^f &= N_{gx}^f \cos \delta\varepsilon_g - N_{gy}^f \sin \delta\varepsilon_g \\ N_{gpy}^f &= N_{gy}^f \sin \delta\varepsilon_g + N_{gx}^f \cos \delta\varepsilon_g \\ N_{gpz}^f &= N_{gz}^f \end{aligned} \right\} \quad (7.2)$$

where, in the case of the tilt device: N_{gx}^f , N_{gy}^f and N_{gz}^f are determined by expression (6.31) and in the cases of the no tilt device and the Formate method: N_{gx}^f , N_{gy}^f and N_{gz}^f are determined by expression (6.32).

Application of expression (2.167) together with the shaft angle set at $\alpha = -90^\circ$ leads to angle $\delta\varepsilon_g$ in the following form

$$\delta\varepsilon_g = \arccos\left(\frac{W_{gp}}{\sqrt{U_{gp}^2 + V_{gp}^2}}\right) - \arctan\left(\frac{V_{gp}}{U_{gp}}\right) \quad (7.3)$$

where

$$\left. \begin{aligned} U_{gp} &= N_{gz}^f M_{gp} \rho_f \cos \varepsilon_g^f - N_{gx}^f M_{gp} z_f \\ V_{gp} &= N_{gz}^f M_{gp} \rho_f \sin \varepsilon_g^f - N_{gy}^f M_{gp} z_f \\ W_{gp} &= N_{gx}^f \rho_f \sin \varepsilon_g^f - N_{gy}^f \rho_f \cos \varepsilon_g^f + N_{gz}^f M_{gp} f_{gp} \end{aligned} \right\} \quad (7.4)$$

and M_{gp} is determined by expression (4.1).

With the aid of expression (2.123), the conjugate contact position at the fundamental contact point P_f of the gear with the pinion can be expressed in the coordinate system $O' - \mathbf{i}', \mathbf{j}', \mathbf{k}'$ of the pinion, that is,

$$\left. \begin{aligned} \mathbf{R}_p^f &= x_p^f \mathbf{i}' + y_p^f \mathbf{j}' + z_p^f \mathbf{k}' \\ x_p^f &= x_{gp}^f - f_{gp} \\ y_p^f &= z_{gp}^f \\ z_p^f &= -y_{gp}^f \end{aligned} \right\} \quad (7.5)$$

7.2 Calculation of Curvatures

Since a pair of tooth surfaces with point contact is obtained by applying curvature modification to the substituted surface, i.e., the pinion tooth surface, of a pair of tooth surfaces with line contact, thus, a pair of tooth surfaces with line contact is the basis for a pair of tooth surfaces with point contact. It is necessary to obtain a clear understanding of the curvature properties for a pair of tooth surfaces with line contact before obtaining a pair of tooth surfaces with point contact.

The phase angle ε_p^f of vector \mathbf{r}_p^f with respect to coordinate plane $\mathbf{i}' - \mathbf{O}' - \mathbf{x}'$ is found from its coordinates

$$\left. \begin{aligned} \sin \varepsilon_p^f &= \frac{y_p^f}{\sqrt{(x_p^f)^2 + (y_p^f)^2}} \\ \cos \varepsilon_p^f &= \frac{x_p^f}{\sqrt{(x_p^f)^2 + (y_p^f)^2}} \end{aligned} \right\} \quad (7.6)$$

With the aid of expression (2.171), the unit normal \mathbf{N}_p^f at point P_{fp} , corresponding to the fundamental contact point, of the pinion tooth surface is found in the following form

$$\left. \begin{aligned} \mathbf{N}_p^f &= -\mathbf{N}_{gp}^f = N_{px}^f \mathbf{i}' + N_{py}^f \mathbf{j}' + N_{pz}^f \mathbf{k}' \\ N_{px}^f &= -N_{gpx}^f \\ N_{py}^f &= -N_{gpy}^f \\ N_{pz}^f &= N_{gpz}^f \end{aligned} \right\} \quad (7.7)$$

The unit normal \mathbf{N}_{po}^f at point P_{fp} , corresponding to the fundamental contact point, of the pinion tooth surface at the position where point P_{fp} returns to the coordinate plane $\mathbf{i}' - \mathbf{O}' - \mathbf{k}'$ is found in the following form

$$\begin{aligned} \mathbf{N}_{po}^f &= (-\varepsilon_p^f \mathbf{k}') \otimes \mathbf{N}_p^f \\ &= (N_{px}^f \cos \varepsilon_p^f + N_{py}^f \sin \varepsilon_p^f) \mathbf{i}' + (-N_{px}^f \sin \varepsilon_p^f + N_{py}^f \cos \varepsilon_p^f) \mathbf{j}' + N_{pz}^f \mathbf{k}' \\ &= (-N_{gpx}^f \cos \varepsilon_p^f - N_{gpy}^f \sin \varepsilon_p^f) \mathbf{i}' + (N_{gpx}^f \sin \varepsilon_p^f - N_{gpy}^f \cos \varepsilon_p^f) \mathbf{j}' + N_{gpz}^f \mathbf{k}' \end{aligned} \quad (7.8)$$

On the other hand, \mathbf{N}_{po}^f can be obtained as a series of rotations

$$\begin{aligned} \mathbf{N}_{po}^f &= (\gamma_{pr} \mathbf{j}') \otimes \{(-\psi_{pr} \mathbf{i}') \otimes [(\phi_{pr} \mathbf{k}') \otimes (-\mathbf{j}')] \} \\ &= (\sin \phi_{pr} \cos \gamma_{pr} + \cos \phi_{pr} \sin \psi_{pr} \sin \gamma_{pr}) \mathbf{i}' - \cos \phi_{pr} \cos \psi_{pr} \mathbf{j}' \\ &\quad + (-\sin \phi_{pr} \sin \gamma_{pr} + \cos \phi_{pr} \sin \psi_{pr} \cos \gamma_{pr}) \mathbf{k}' \end{aligned} \quad (7.9)$$

where, ϕ_{pr} and ψ_{pr} are the pressure angle and the spiral angle of the pinion at point P_{fp} with respect to the root cone of the pinion. γ_{pr} is the root angle of the pinion and is determined by expression (4.56).

Combination of expressions (7.8) and (7.9) yields the values of ψ_{pr} and ϕ_{pr} as follows

$$\left. \begin{aligned} \tan \psi_{pr} &= \frac{N_{gpy}^f \cos \gamma_{pr} - (N_{gpz}^f \cos \varepsilon_p^f + N_{gpz}^f \sin \varepsilon_p^f) \sin \gamma_{pr}}{N_{gpz}^f \cos \varepsilon_p^f - N_{gpz}^f \sin \varepsilon_p^f} \\ \sin \phi_{pr} &= -\frac{(N_{gpx}^f \cos \varepsilon_p^f + N_{gpz}^f \sin \varepsilon_p^f) \cos \gamma_{pr} - N_{gpy}^f \sin \gamma_{pr}}{N_{gpz}^f \cos \varepsilon_p^f - N_{gpz}^f \sin \varepsilon_p^f} \\ \cos \phi_{pr} &= \frac{N_{gpz}^f \cos \varepsilon_p^f - N_{gpz}^f \sin \varepsilon_p^f}{\cos \psi_{pr}} \end{aligned} \right\} \quad (7.10)$$

where, $0^\circ \leq \psi_{pr} \leq 180^\circ$ and $0^\circ \leq \phi_{pr} \leq 180^\circ$.

The use of expression (2.129) gives rise to velocity \mathbf{v}_f^{gp} at the fundamental contact point P_f of the gear relative to the pinion as follows

$$\left. \begin{aligned} \mathbf{v}_f^{gp} &= v_{f1}^{gp} \mathbf{i} + v_{f2}^{gp} \mathbf{j} + v_{f3}^{gp} \mathbf{k} \\ v_{f1}^{gp} &= -\rho_f \sin(\varepsilon_g^f + \delta \varepsilon_g) - M_{gp} z_f \\ v_{f2}^{gp} &= \rho_f \cos(\varepsilon_g^f + \delta \varepsilon_g) \\ v_{f3}^{gp} &= M_{gp} \rho_f \cos(\varepsilon_g^f + \delta \varepsilon_g) - M_{gp} f_{gp} \end{aligned} \right\} \quad (7.11)$$

Application of expression (2.150) yields the conjugate relative acceleration at the fundamental contact point P_f

$$\left. \begin{aligned} \mathbf{J}_p &= J_{p1} \mathbf{i} + J_{p2} \mathbf{j} + J_{p3} \mathbf{k} \\ J_{p1} &= 0 \\ J_{p2} &= -M_{gp} z_f \\ J_{p3} &= M_{gp} \rho_f \sin(\varepsilon_g^f + \delta \varepsilon_g) \end{aligned} \right\} \quad (7.12)$$

and

$$\mathbf{J}_p \cdot \mathbf{N}_{gp}^f = -M_{gp} z_f N_{gpy}^f + M_{gp} \rho_f N_{gpz}^f \sin(\varepsilon_g^f + \delta \varepsilon_g) \quad (7.13)$$

Expression (2.133) gives

$$\left. \begin{aligned} \eta_p &= (\mathbf{k} + M_{gp} \mathbf{k}') \times \mathbf{N}_{gp}^f \\ &= \eta_{p1} \mathbf{i} + \eta_{p2} \mathbf{j} + \eta_{p3} \mathbf{k} \\ \eta_{p1} &= -N_{gpy}^f - N_{gpz}^f M_{gp} \\ \eta_{p2} &= N_{gpx}^f \\ \eta_{p3} &= N_{gpx}^f M_{gp} \\ |\eta_p| &= \sqrt{\eta_{p1}^2 + \eta_{p2}^2 + \eta_{p3}^2} \end{aligned} \right\} \quad (7.14)$$

The direction of \mathbf{t}_{gr} at the conjugate contact position of the fundamental contact point P_f is found in the following way

$$\left. \begin{aligned} \mathbf{t}_{gr}^f &= (\delta \varepsilon_g^f \mathbf{k}) \otimes \mathbf{t}_{gr} = t_{gr1}^f \mathbf{i} + t_{gr2}^f \mathbf{j} + t_{gr3}^f \mathbf{k} \\ t_{gr1}^f &= t_{gr1} \cos \delta \varepsilon_g^f - t_{gr2} \sin \delta \varepsilon_g^f \\ t_{gr2}^f &= t_{gr1} \sin \delta \varepsilon_g^f + t_{gr2} \cos \delta \varepsilon_g^f \\ t_{gr3}^f &= t_{gr3} \end{aligned} \right\} \quad (7.15)$$

where, t_{gr1} , t_{gr2} and t_{gr3} are determined by expression (6.67).

Since $\frac{\eta_p}{|\eta_p|}$, i.e., expression (7.14), can be expressed as a rotation from the sliding velocity direction,

$$\begin{aligned} \frac{\eta_p}{|\eta_p|} &= (\theta_{v\eta}^f \mathbf{N}_{gp}^f) \otimes \frac{\mathbf{v}_f^{gp}}{|\mathbf{v}_f^{gp}|} \\ &= \cos \theta_{v\eta}^f \frac{\mathbf{v}_f^{gp}}{|\mathbf{v}_f^{gp}|} + \sin \theta_{v\eta}^f \mathbf{N}_{gp}^f \times \frac{\mathbf{v}_f^{gp}}{|\mathbf{v}_f^{gp}|} \end{aligned} \quad (7.16)$$

angle $\theta_{v\eta}^f$ is therefore given by

$$\left. \begin{aligned} \sin \theta_{v\eta}^f &= \frac{\eta_p \cdot (\mathbf{N}_{gp}^f \times \mathbf{v}_f^{gp})}{|\eta_p| |\mathbf{v}_f^{gp}|} \\ &= \frac{M_{gp} v_{f2}^{gp} - v_{f3}^{gp}}{|\eta_p| |\mathbf{v}_f^{gp}|} \\ \cos \theta_{v\eta}^f &= \frac{\eta_p \cdot \mathbf{v}_f^{gp}}{|\eta_p| |\mathbf{v}_f^{gp}|} \\ &= \frac{\eta_{p1} v_{f1}^{gp} + \eta_{p2} v_{f2}^{gp} + \eta_{p3} v_{f3}^{gp}}{|\eta_p| |\mathbf{v}_f^{gp}|} \end{aligned} \right\} \quad (7.17)$$

where, v_{f1}^{gp} , v_{f2}^{gp} and v_{f3}^{gp} are determined by expression (7.11).

On the other hand, since \mathbf{v}_f^{gp} , i.e., expression (7.11), can also be expressed as a rotation from vector \mathbf{t}_{gr}^f

$$\begin{aligned} \frac{\mathbf{v}_f^{gp}}{|\mathbf{v}_f^{gp}|} &= (\theta_{tv}^f \mathbf{N}_{gp}^f) \otimes \mathbf{t}_{gr}^f \\ &= \cos \theta_{tv}^f \mathbf{t}_{gr}^f + \sin \theta_{tv}^f \mathbf{N}_{gp}^f \times \mathbf{t}_{gr}^f \end{aligned} \quad (7.18)$$

Angle θ_{tv}^f is therefore given by

$$\left. \begin{aligned}
\sin \theta_{tv}^f &= \frac{\mathbf{v}_f^{gp} \cdot (\mathbf{N}_{gp}^f \times \mathbf{t}_{gr}^f)}{|\mathbf{v}_f^{gp}|} \\
&= \frac{\left\{ \begin{aligned} &v_{f1}^{gp}(N_{gpy}^f t_{gr3}^f - N_{gpz}^f t_{gr2}^f) + v_{f2}^{gp}(N_{gpx}^f t_{gr1}^f - N_{gpy}^f t_{gr3}^f) \\ &+ v_{f3}^{gp}(N_{gpz}^f t_{gr2}^f - N_{gpx}^f t_{gr1}^f) \end{aligned} \right\}}{|\mathbf{v}_f^{gp}|} \\
\cos \theta_{tv}^f &= \frac{\mathbf{v}_f^{gp} \cdot \mathbf{t}_{gr}^f}{|\mathbf{v}_f^{gp}|} \\
&= \frac{v_{f1}^{gp} t_{gr1}^f + v_{f2}^{gp} t_{gr2}^f + v_{f3}^{gp} t_{gr3}^f}{|\mathbf{v}_f^{gp}|}
\end{aligned} \right\} \quad (7.19)$$

Consequently, application of expression (2.39) yields the normal and torsional curvatures of the gear tooth surface in directions \mathbf{v}_f^{gp} and $\Delta_f^{gp} = \mathbf{N}_{gp}^f \times \frac{\mathbf{v}_f^{gp}}{|\mathbf{v}_f^{gp}|}$ as follows

$$\left. \begin{aligned}
K_{gpv} &= K_{gt} \cos^2 \theta_{tv}^f + K_{gs} \sin^2 \theta_{tv}^f + 2G_{gt} \sin \theta_{tv}^f \cos \theta_{tv}^f \\
G_{gpv} &= -(K_{gt} - K_{gs}) \sin \theta_{tv}^f \cos \theta_{tv}^f + G_{gt} (\cos^2 \theta_{tv}^f - \sin^2 \theta_{tv}^f) \\
K_{gp\Delta} &= K_{gt} \sin^2 \theta_{tv}^f + K_{gs} \cos^2 \theta_{tv}^f - 2G_{gt} \sin \theta_{tv}^f \cos \theta_{tv}^f
\end{aligned} \right\} \quad (7.20)$$

where, K_{gt} , G_{gt} and K_{gs} are determined by expression (6.73) or (6.78).

Expression (2.209) leads to

$$\left. \begin{aligned}
D_p &= K_{gpv} |\mathbf{v}_f^{gp}| - |\eta_p| \cos \theta_{v\eta}^f \\
E_p &= G_{gpv} |\mathbf{v}_f^{gp}| - |\eta_p| \sin \theta_{v\eta}^f
\end{aligned} \right\} \quad (7.21)$$

where, $|\eta_p|$ is determined by expression (7.14) and $\sin \theta_{v\eta}^f$ and $\cos \theta_{v\eta}^f$ are determined by expression (7.17).

With the aid of expression (2.218), the angle θ_{ve}^f shown in fig.7.1 of $\frac{\mathbf{v}_f^{gp}}{|\mathbf{v}_f^{gp}|}$ rotating about \mathbf{N}_{gp}^f to the direction \mathbf{e} of the instantaneous line of contact is found in the following form

$$\left. \begin{aligned}
\sin \theta_{ve}^f &= -\frac{D_p}{\sqrt{D_p^2 + E_p^2}} \\
\cos \theta_{ve}^f &= \frac{E_p}{\sqrt{D_p^2 + E_p^2}}
\end{aligned} \right\} \quad (7.22)$$

where, D_p and E_p are determined by expression (7.21).

With the aid of expressions (7.20) and (7.22), application of expression (2.39) yields the normal and torsional curvatures of the gear tooth surface in directions \mathbf{e} and $\mathbf{g} = \mathbf{N}_{gp}^f \times \mathbf{e}$ as follows

$$\left. \begin{aligned}
K_{gpe} &= K_{gpv} \cos^2 \theta_{ve}^f + K_{gp\Delta} \sin^2 \theta_{ve}^f + 2G_{gpv} \sin \theta_{ve}^f \cos \theta_{ve}^f \\
G_{gpe} &= -(K_{gpv} - K_{gp\Delta}) \sin \theta_{ve}^f \cos \theta_{ve}^f + G_{gpv} (\cos^2 \theta_{ve}^f - \sin^2 \theta_{ve}^f) \\
K_{gpg} &= K_{gpv} \sin^2 \theta_{ve}^f + K_{gp\Delta} \cos^2 \theta_{ve}^f - 2G_{gpv} \sin \theta_{ve}^f \cos \theta_{ve}^f
\end{aligned} \right\} \quad (7.23)$$

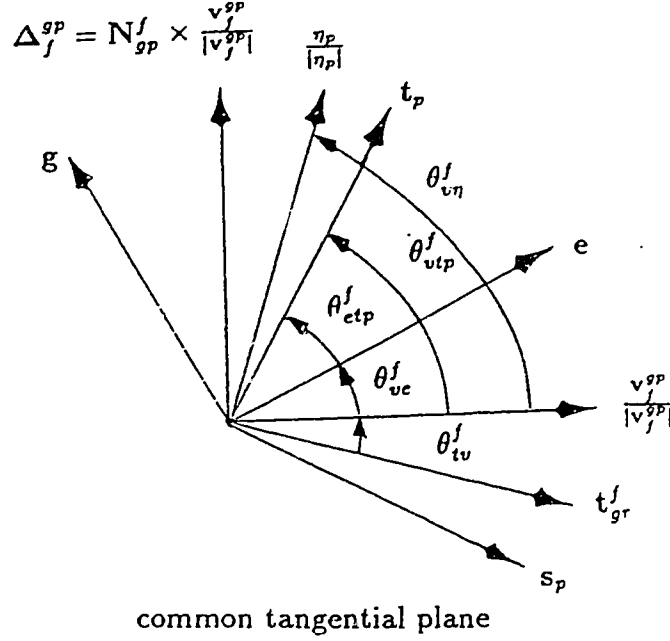


Figure 7.1: Several tangential vectors

Expression (2.233) gives rise to the relative normal curvature \overline{K}_g in the direction perpendicular to the instantaneous line of contact in the following form

$$\overline{K}_g = \frac{D_p^2 + E_p^2}{D_p |v_f^{gp}| + J_p \cdot N_{gp}^f} \quad (7.24)$$

where, D_p and E_p are determined by expression (7.21), $|v_f^{gp}|$ is determined by expression (7.11) and $J_p \cdot N_{gp}^f$ is calculated by expression (7.13).

Application of expressions (2.238) and (2.241) yields the conjugate normal and torsional curvatures of the pinion tooth surface in directions e and $g = N_{gp}^f \times e$ in the following form

$$\left. \begin{aligned} K'_{pe} &= -K_{gpc} \\ G'_{pe} &= -G_{gpe} \\ K'_{pg} &= \overline{K}_g - K_{gpg} = \frac{D_p^2 + E_p^2}{D_p |v_f^{gp}| + J_p \cdot N_{gp}^f} - K_{gpg} \end{aligned} \right\} \quad (7.25)$$

If we construct a cone with the root angle of the pinion through the point on the pinion corresponding to the fundamental contact point, the unit vector t_p tangential

to the intersection of the pinion tooth surface with the cone constructed above is found as follows

$$\left. \begin{aligned} \mathbf{t}_p &= (\varepsilon_p^f \mathbf{k}') \otimes (\gamma_{pr} \mathbf{j}') \otimes [(-\psi_{pr} \mathbf{i}') \otimes \mathbf{k}'] \\ &= t_{p1} \mathbf{i} + t_{p2} \mathbf{j} + t_{p3} \mathbf{k} \\ t_{p1} &= \cos \psi_{pr} \sin \gamma_{pr} \cos \varepsilon_p^f - \sin \psi_{pr} \sin \varepsilon_p^f \\ t_{p2} &= -\cos \psi_{pr} \cos \gamma_{pr} \\ t_{p3} &= \cos \psi_{pr} \sin \gamma_{pr} \sin \varepsilon_p^f + \sin \psi_{pr} \cos \varepsilon_p^f \end{aligned} \right\} \quad (7.26)$$

The unit vector $\mathbf{s}_p = -\mathbf{N}_{gp}^f \times \mathbf{t}_p$ can then be found

$$\left. \begin{aligned} \mathbf{s}_p &= s_{p1} \mathbf{i} + s_{p2} \mathbf{j} + s_{p3} \mathbf{k} \\ s_{p1} &= t_{p2} N_{gpy}^f - t_{p3} N_{gpz}^f \\ s_{p2} &= t_{p3} N_{gpx}^f - t_{p1} N_{gpz}^f \\ s_{p3} &= t_{p1} N_{gpy}^f - t_{p2} N_{gpx}^f \end{aligned} \right\} \quad (7.27)$$

where, N_{gpx}^f , N_{gpy}^f and N_{gpz}^f are determined by expression (7.2).

Angle θ_{utp}^f of \mathbf{v}_f^{gp} rotating about \mathbf{N}_{gp}^f to \mathbf{t}_p is found in the following way

$$\left. \begin{aligned} \mathbf{t}_p &= (\theta_{utp}^f \mathbf{N}_{gp}^f) \otimes \frac{\mathbf{v}_f^{gp}}{|\mathbf{v}_f^{gp}|} \\ &= \cos \theta_{utp}^f \frac{\mathbf{v}_f^{gp}}{|\mathbf{v}_f^{gp}|} + \sin \theta_{utp}^f \mathbf{N}_{gp}^f \times \frac{\mathbf{v}_f^{gp}}{|\mathbf{v}_f^{gp}|} \\ \sin \theta_{utp}^f &= \frac{\mathbf{t}_p \cdot (\mathbf{N}_{gp}^f \times \mathbf{v}_f^{gp})}{|\mathbf{v}_f^{gp}|} \\ &= \frac{\left\{ t_{p1} (N_{gpy}^f v_{f3}^{gp} - N_{gpz}^f v_{f2}^{gp}) + t_{p2} (N_{gpz}^f v_{f1}^{gp} - N_{gpx}^f v_{f3}^{gp}) \right.}{|\mathbf{v}_f^{gp}|} \\ &\quad \left. + t_{p3} (N_{gpx}^f v_{f2}^{gp} - N_{gpy}^f v_{f1}^{gp}) \right\}}{|\mathbf{v}_f^{gp}|} \\ \cos \theta_{utp}^f &= \frac{\mathbf{t}_p \cdot \mathbf{v}_f^{gp}}{|\mathbf{v}_f^{gp}|} \\ &= \frac{t_{p1} v_{f1}^{gp} + t_{p2} v_{f2}^{gp} + t_{p3} v_{f3}^{gp}}{|\mathbf{v}_f^{gp}|} \end{aligned} \right\} \quad (7.28)$$

It can be seen in fig.7.1 that

$$\theta_{utp}^f = \theta_{ve}^f + \theta_{etp}^f \quad (7.29)$$

so that

$$\theta_{etp}^f = \theta_{utp}^f - \theta_{ve}^f \quad (7.30)$$

Consequently,

$$\left. \begin{aligned} \sin \theta_{etp}^f &= \sin \theta_{utp}^f \cos \theta_{ve}^f - \cos \theta_{utp}^f \sin \theta_{ve}^f \\ \cos \theta_{etp}^f &= \cos \theta_{utp}^f \cos \theta_{ve}^f + \sin \theta_{utp}^f \sin \theta_{ve}^f \end{aligned} \right\} \quad (7.31)$$

Finally, the conjugate normal and torsional curvatures of the pinion tooth surface in directions \mathbf{t}_p and $\mathbf{s}_p = \mathbf{N}_p^f \times \mathbf{t}_p$ are found in the following way

$$\left. \begin{aligned} K'_{pt} &= K'_{pe} \cos^2 \theta_{etp}^f + K'_{pg} \sin^2 \theta_{etp}^f + 2G'_{pe} \sin \theta_{etp}^f \cos \theta_{etp}^f \\ G'_{pt} &= -(K'_{pe} - K'_{pg}) \sin \theta_{etp}^f \cos \theta_{etp}^f + G'_{pe} (\cos^2 \theta_{etp}^f - \sin^2 \theta_{etp}^f) \\ K'_{ps} &= K'_{pe} \sin^2 \theta_{etp}^f + K'_{pg} \cos^2 \theta_{etp}^f - 2G'_{pe} \sin \theta_{etp}^f \cos \theta_{etp}^f \end{aligned} \right\} \quad (7.32)$$

where, K'_{pe} , G'_{pe} and K'_{pg} are determined by expression (7.25).

Chapter 8

Calculation of the Quantity for the Curvature Modification to the Pinion Tooth Surface to Obtain Point Contact

The pair of tooth surfaces of hypoid gearing obtained in the previous sections have line contact. A pair of line contact tooth surfaces are very difficult to manufacture and are very sensitive to any errors. In order to alleviate the above two deficiencies, we can make a small curvature modification to the pinion tooth surface, and then a pair of point contact tooth surfaces will be obtained.

The selection of the fundamental contact point and the determination of the modified curvature values at the fundamental contact point on the pinion tooth surface constitute the two indispensable conditions to realize a pair of controlled point-contacting tooth surfaces. The amount of curvature modification determines the magnitude and the shape of the contact bearing between a pair of tooth surfaces, and directly affects the strength of contact and bending, the ability to absorb errors and deformations, the motion precision, the noise, vibration and the lubrication properties. Therefore, the amount of curvature modification should be determined taking these factors into account.

8.1 Angle between the Virtual instantaneous Line of Contact and the Contact Locus.

In the case of a pair of point-contacting conjugate surfaces A and \bar{A} , selecting arbitrarily one surface, say A , as the fundamental surface, due to the conjugate motions being given, it is definitely possible to derive the virtual conjugate surface \bar{A}^* which is in line-contact with the fundamental surface A . At any given instant, the three surfaces A , \bar{A} and \bar{A}^* will touch each other at the common conjugate contact point. However, it is obvious that, at the common conjugate contact point, the relative curvatures of A with \bar{A}^* along the virtual instantaneous line of contact e_v are zero, i.e., $\bar{K}_{e_v}^* = K_{1e_v} + K_{2e_v}^* = 0$, and $\bar{G}_{e_v}^* = G_{1e_v} + G_{2e_v}^* = 0$, or

$$\left. \begin{aligned} K_{2e_v}^{I*} &= -K_{1e_v} \\ G_{2e_v}^{I*} &= -G_{1e_v} \end{aligned} \right\} \quad (8.1)$$

while the relative curvatures, \bar{K}_{e_v} and \bar{G}_{e_v} of surfaces A with \bar{A} along e_v are not zero. Due to the identity of the conjugate motions between A and \bar{A} , and A and \bar{A}^* , the two surfaces \bar{A} and \bar{A}^* will certainly touch each other not only at the common conjugate contact point, but also along a curve, which is just the very contact locus on \bar{A} for a pair of point-contacting conjugate surfaces A and \bar{A} . Hence, the conjugate curvatures of the surfaces \bar{A} and \bar{A}^* at the common conjugate contact point along the contact curve direction τ' (unit vector) will be identical, i.e.,

$$\left. \begin{aligned} K_{2\tau'}' &= K_{2\tau'}^{I*} \\ G_{2\tau'}' &= G_{2\tau'}^{I*} \end{aligned} \right\} \quad (8.2)$$

Using the compatible equation of surface curvatures, i.e., expression (2.42), we obtain

$$\tan \theta_{e_v \tau'} = \frac{K_{2\tau'}^{I*} - K_{2e_v}^{I*}}{G_{2\tau'}^{I*} + G_{2e_v}^{I*}} \quad (8.3)$$

and

$$\tan \theta_{e_v \tau'} = \frac{K_{2\tau'}' - K_{2e_v}'}{G_{2\tau'}' + G_{2e_v}'} \quad (8.4)$$

Substitution of expressions (8.1) and (8.2) into (8.3) gives

$$\tan \theta_{e_v \tau'} = \frac{K_{2\tau'}' + K_{1e_v}}{G_{2\tau'}' - G_{1e_v}} \quad (8.5)$$

With the aid of expressions (8.4) and (8.5), the angle $\theta_{e_v\tau'}$ between the virtual instantaneous line of contact e_v on surface A and the contact locus τ' on surface \bar{A} is expressed as follows

$$\begin{aligned}\tan \theta_{e_v\tau'} &= \frac{(K_{1e_v} + K'_{2\tau'}) - (K'_{2\tau'} - K'_{2e_v})}{(G'_{2\tau'} - G_{1e_v}) - (G'_{2\tau'} + G'_{2e_v})} \\ &= -\frac{K_{1e_v} + K'_{2e_v}}{G_{1e_v} + G'_{2e_v}} = -\frac{K_{e_v}}{G_{e_v}}\end{aligned}\quad (8.6)$$

It is worth notice that since there is actually a point contact between a pair of surfaces A and \bar{A} , the instantaneous line of contact does not exactly exist between A and \bar{A} , that is why e_v is called the virtual instantaneous line of contact. On the other hand, if, on the contrary, selecting \bar{A} as the fundamental surface among the same pair of surfaces A and \bar{A} , it is also possible to derive a virtual instantaneous line of contact e'_v between A and \bar{A} , but e'_v is usually not equal to e_v , i.e., $e'_v \neq e_v$. If $e'_v = e_v$, A and \bar{A} become in line contact with each other.

8.2 The Modification $\Delta K'_{2e}$ of the Conjugate Normal Curvature to the Pinion Tooth Surface in the Direction of the Instantaneous Line of Contact.

The modified value $\Delta K'_{2e}$ of the conjugate normal curvature to the pinion tooth surface in the direction e of the instantaneous line of contact depends on the expected semi-width F_{Ge} of the contact bearing, and the impact of $\Delta K'_{2e}$ is upon the length of the major axis of the elliptic contact bearing. The value $2F_{Ge}$ is defined to be the product of the actual tooth width along the direction e and the proportional coefficient F_c . In actual calculation, the following two cases should be considered, and the smaller value of the two cases should be used:

1. If the instantaneous line of contact e intersects the toe and the heel of the gear tooth surface as shown in fig. 8.1 (a), $2F_{Ge}$ is found in the following form

$$\begin{aligned}2F_{Ge} &\approx \frac{F_c F_G}{|\cos \psi_g \cos(\theta_{te}^f - \delta_g)|} \\ &\approx \frac{F_c F_G}{|\cos \delta_g \cos \theta_{tv}^f \cos \theta_{ve}^f \cos \psi_g|}\end{aligned}\quad (8.7)$$

where, F_c is prescribed, F_G is given in chapter 4.1, and ψ_g , δ_g , θ_{tv}^f and θ_{ve}^f are determined by expressions (4.8), (4.43), (7.19) and (7.22) respectively.

2. If the instantaneous line of contact e intersects the top and bottom of the gear

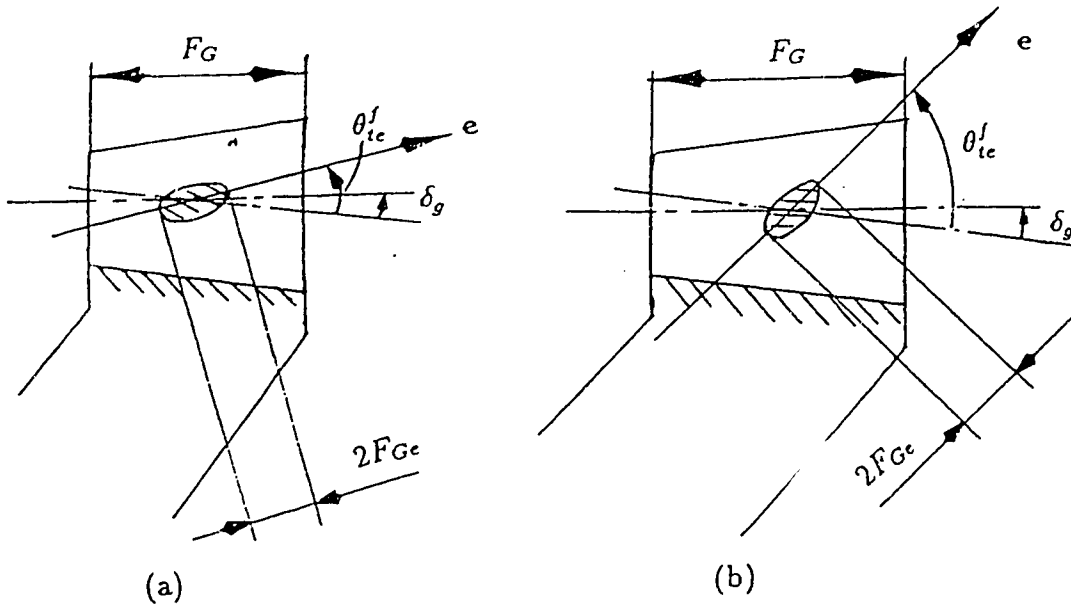


Figure 8.1: Determination of $2F_{Ge}$

tooth surface as shown in fig. 8.2 (b), $2F_{Ge}$ is found in the following form

$$\begin{aligned} 2F_{Ge} &\approx \frac{F_c h \cos \delta_g}{|\cos \Phi_g \sin \theta_{te}^j|} \\ &\approx \frac{F_c h \cos \delta_g}{|\cos \Phi_g (\sin \theta_{te}^j \cos \theta_{ve}^j + \cos \theta_{te}^j \sin \theta_{ve}^j)|} \end{aligned} \quad (8.8)$$

where, Φ_g is determined by expression (4.17), and h is determined by expression (4.18).

Since the actual exhibition of the value $2F_{Ge}$ is the length of the major axis of the elliptic contact bearing in the inspection of the tooth contact quality, and at both ends of the major axis of the elliptic contact, the value of separation between the pinion and the gear tooth surfaces reaches the specified value δ , i.e., the value of the diameter of a particle of the color compound, $\Delta K'_{2e}$ can be determined in terms of F_{Ge} and δ . It is known from chapter 2.4.3 that among a pair of line-contacting tooth surfaces, the fundamental surface, i.e., the gear tooth surface, can be reduced to a plane, and the substituted surface, i.e., the pinion tooth surface, can be reduced to a cylinder whose axis is parallel to the direction e of the instantaneous line of contact, as shown in fig. 8.2 (a). After the curvature modification to the pinion tooth surface, the original reduced pinion tooth surface, i.e., the cylinder, becomes an ellipsoid which is used as a substituting reduced pinion tooth surface, as shown in fig. 8.2 (b). The original direction e of the instantaneous line of contact becomes now the direction e_v of the virtual instantaneous line of contact after curvature modification.

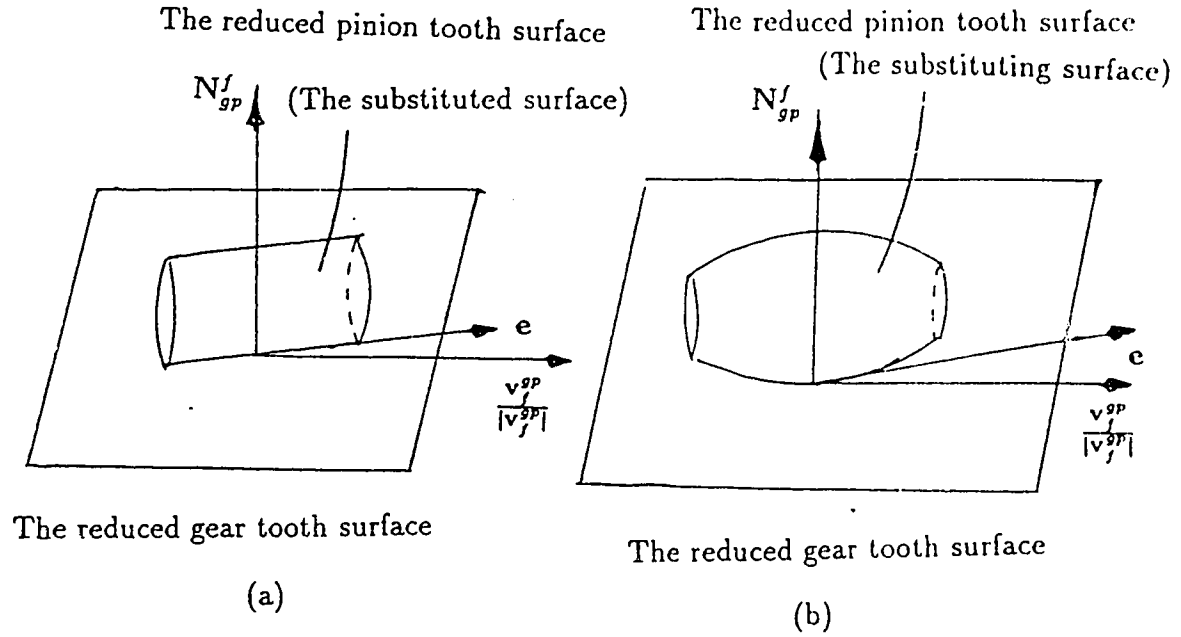


Figure 8.2:Curvature Modification

The direction e' of the major axis of the ellipsoid, i.e., the substituting surface, might be different from that of the virtual instantaneous line of contact, i.e., $e' \neq e_v \approx e$, but since the modified value of the curvature is very small, it can be assumed that $e' \approx e_v \approx e$.

Let K_{2e}'' be the reduced pinion conjugate normal curvature in the direction e of the instantaneous line of contact before the modification, i.e., in the state of line contact, thus,

$$K_{2e}'' = 0 \quad (8.9)$$

and let $K_{2e}'^p$ be the reduced pinion conjugate normal curvature in the direction $e' \approx e_v \approx e$ after the modification, i.e., in the state of point contact

$$K_{2e}'^p = \frac{1}{R_e} \quad (8.10)$$

where, R_e is the radius of curvature in direction e .

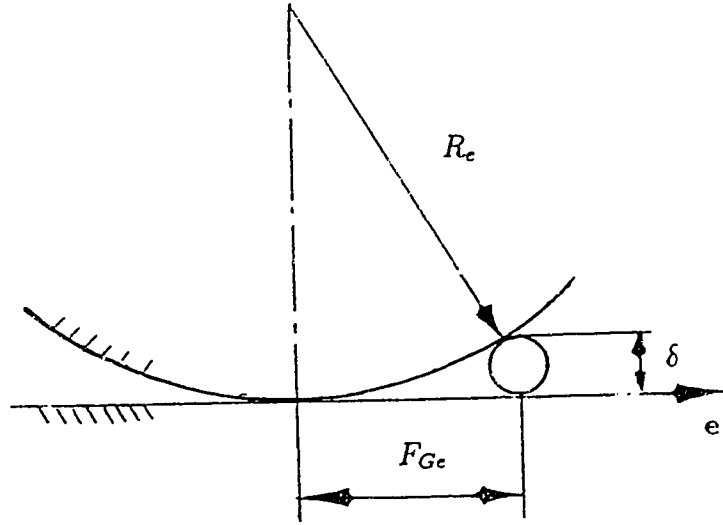


Figure 8.3: Normal intersection in direction e of instantaneous line of contact

Then, examination of fig.8.3 yields

$$\frac{2\delta}{F_{Ge}} \approx \frac{1}{R_e} \quad (8.11)$$

Hence, the reduced pinion conjugate normal curvature K_{2e}^{ip} after the modification can be expressed as follows

$$K_{2e}^{ip} = \frac{1}{R_e} \approx \frac{2\delta}{F_{Ge}^2} \quad (8.12)$$

With the aid of expressions (8.9), (8.10) and (8.11), the incremental conjugate normal curvature defined in chapter 2.2.13 is found in the following form

$$\begin{aligned} \Delta K_{2e}' &= K_{2e}^{ip} - K_{2e}^{il} \\ &= \frac{2\delta}{F_{Ge}^2} \end{aligned} \quad (8.13)$$

Finally, conjugate normal curvature K_{pe}^{ip} of the pinion tooth surface in direction e after the curvature modification is found in the following form

$$K_{pe}^{ip} = K_{pe}' + \Delta K_{2e}' \quad (8.14)$$

where, K_{pe}' is determined by expression (7.25).

8.3 The Modification $\Delta G'_{2e}$ of the Conjugate Torsional Curvature in the Direction of the Instantaneous Line of Contact

The fundamental surface A_g , i.e., the gear tooth surface, is in line contact with the substituted surface A_p , i.e., the pinion tooth surface before the curvature modification. The conjugate motion and the direction of the instantaneous line of contact between A_g and A_p are designated as Σ and e . By replacing the substituted surface A_p with the substituting surface \bar{A}_p , the pinion tooth surface after the curvature modification, the fundamental surface A_g is in point contact with the substituting surface \bar{A}_p , and thus, the conjugate motion between A_g and \bar{A}_p is designated as $\bar{\Sigma}$. The virtual instantaneous line e_v of contact can be derived under the base of A_g and $\bar{\Sigma}$. If the substituted surface A_p and the substituting surface \bar{A}_p are in line contact, then the conjugate motions Σ and $\bar{\Sigma}$ are identical, and consequently, the virtual instantaneous line e_v of contact between A_g and \bar{A}_p is identical to the instantaneous line e of contact between A_g and A_p . If A_p and \bar{A}_p are in point contact, then the conjugate motions Σ and $\bar{\Sigma}$ are not identical, and consequently, the virtual instantaneous line e_v of contact between A_g and \bar{A}_p is not identical to the instantaneous line e of contact between A_g and A_p .

Application of expression (8.6) yields

$$\tan \theta_{e\tau'}^f \approx -\frac{K_{gp} + K_{pe}^{ip}}{G_{gpe} + G_{pe}^{ip}} \quad (8.15)$$

where, K_{gpe} and G_{gpe} are calculated by expression (7.23).

K_{pe}^{ip} and G_{pe}^{ip} in expression (8.15) are the conjugate normal and torsional curvatures of the pinion tooth surface after the curvature modification, and are found in the following form

$$\left. \begin{aligned} K_{pe}^{ip} &= K_{pe}' + \Delta K_{2e}' \\ G_{pe}^{ip} &= G_{pe}' + \Delta G_{2e}' \end{aligned} \right\} \quad (8.16)$$

where, K_{pe}' and G_{pe}' are determined by expression (7.25).

With the aid of expressions (7.25) and (8.16), expression (8.15) can be rewritten in the following form

$$\tan \theta_{e\tau'}^f \approx -\frac{\Delta K_{2e}'}{\Delta G_{2e}'} \quad (8.17)$$

Consequently, the modified value $\Delta G'_{2e}$ of the conjugate torsional curvature in direction \mathbf{e} is found as follows

$$\Delta G'_{2e} \approx -\frac{\Delta K'_{2e}}{\tan \theta_{e\tau'}^f} \quad (8.18)$$

and

$$\begin{aligned} \theta_{e\tau'}^f &= \theta_{ev}^f + \theta_{v\tau}^f + \theta_{\tau\tau'}^f \\ &= -\theta_{ve}^f + \theta_{v\tau}^f + \theta_{\tau\tau'}^f \end{aligned} \quad (8.19)$$

where θ_{ve}^f can be determined in expression (7.22) and $\theta_{\tau\tau'}^f$ can be found by expression (2.244), and $\theta_{v\tau}^f$ can be prescribed, usually assuming $\theta_{v\tau}^f = 90^\circ$.

Finally, the conjugate torsional curvature G'_{2e} of the pinion tooth surface in direction \mathbf{e} is found in the following form

$$G'_{pe} = G'_{pe} + \Delta G'_{2e} \quad (8.20)$$

8.4 The Modification $\Delta K'_{2g}$ of the Conjugate Normal Curvature in Direction \mathbf{g} Perpendicular to Direction \mathbf{e} .

With the curvature modification to the pinion tooth surface, the previous pair of tooth surfaces with line contact becomes a pair of tooth surfaces with point contact. The curve on the tooth surface formed by the set of contact points is called the contact locus. Obviously, if we consider only the contact transmission between one pair of tooth surfaces, the contact locus on the tooth surface will extend from the bottom to the top of the tooth surface which is called the theoretical contact locus as shown in fig. 8.4 (a), no matter how the curvature modifications have been done. But, in fact, since the two adjacent tooth surfaces will also contribute to the contact transmission, the actual contact locus occupies only one portion of the theoretical contact locus as shown in fig. 8.4 (b).

Let the ordinate designate the rotating angle ε_p of the pinion and the abscissa designate the rotating angle ε_g of the gear. Then, without the curvature modification to the pinion tooth surface, due to the transmission ratio $M_{gp} = \frac{d\varepsilon_p}{d\varepsilon_g} = \text{constant}$, i.e., expression (4.1), the motion diagram of $\varepsilon_p^l = \varepsilon_p^l(\varepsilon_g)$ should be the straight line as shown in fig. 8.5 (a). With the curvature modification to the pinion tooth surface, the motion diagram of $\varepsilon_p^p = \varepsilon_p^p(\varepsilon_g)$ might be the convex curve as shown in fig. 8.5 (a). If, alternatively, let the ordinate designate the error $\Delta\varepsilon_p$ of the rotating angle of

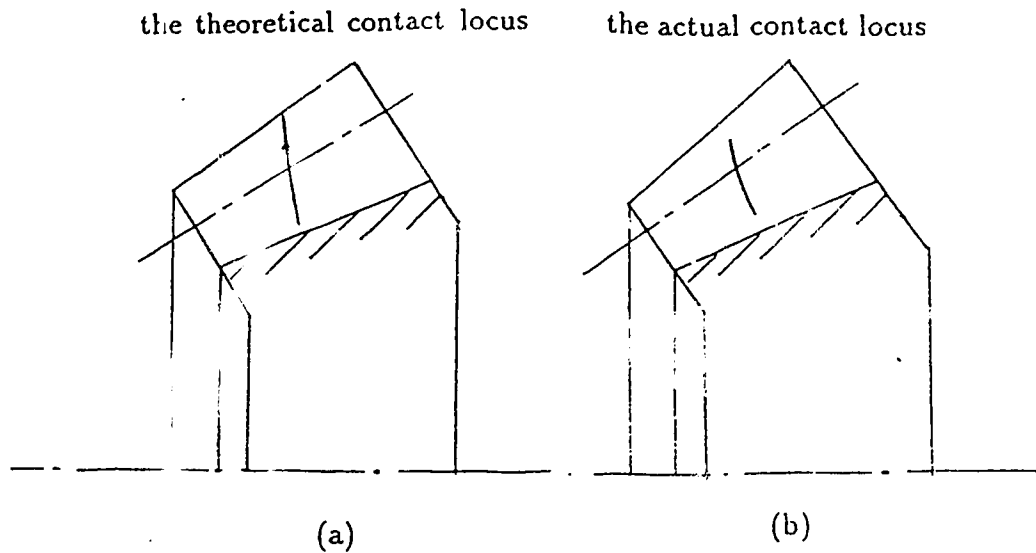


Figure 8.4: Contact locus

the pinion, i.e., $\Delta\epsilon_p = \epsilon_p^p - \epsilon_p^l$ and the abscissa designate the rotating angle ϵ_g of the gear, the motion diagram, i.e., fig. 8.5 (a), can be re-depicted as shown in fig. 8.5 (b).

If the contact transmission occurs only between one pair of tooth surfaces, the contact locus should correspond to the curve CC' of the motion diagram. Due to the succeeding contact of the adjacent tooth pair, tooth 2 is about to be in advance of tooth 1 at point B' of the motion diagram, and accordingly, the contact will be transferred from tooth 1 to tooth 2 and therefore, tooth 1 works only in the range of rotating angle corresponding to the curve BB' of the motion diagram.

If the motion diagram is the concave curve as shown in fig. 8.6, in such a case, since tooth 2 is in advance of tooth 1 at point A of the motion diagram, the contact suddenly jumps from tooth 1 to the tip edge of tooth 2 of the pinion, and in turn, tooth 1 is about to be in advance of tooth 2 at point B' of the motion diagram, and thus the contact transmission will be transferred more than once from tooth 2 to tooth 1. Finally, at point C' of the motion diagram, the contact point reaches the tip edge of tooth 1 of the gear, and therefore, the contact suddenly jumps from tooth 1 to tooth 2 again. So, the intermittent contact locus corresponding to this case is as shown in fig. 8.6 (c). The same situation will occur repeatedly, and cause vibration, noise and instability. Therefore, such a situation is not permissible. From the analyses above, the motion diagram should be convex curve as shown in figs. 8.5 (a) and (b) or 8.7 (a) and (b).

Since in the course of manufacture, assembly and transmission of gearing, errors and

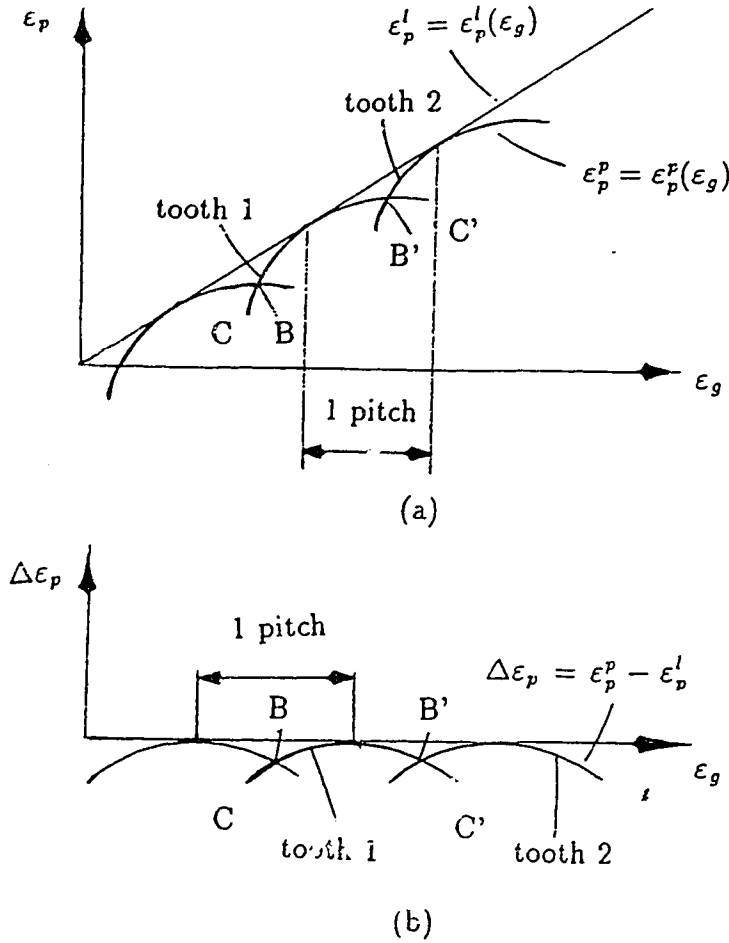


Figure 8.5: Motion diagram

deformation are inevitable, thus, it is impossible to achieve exactly the required transmission ratio. But, because there exists an intrinsically interchangeable relationship between geometry and motion, the error of transmission can be, to some extent, compensated through the curvature modification.

Let the allowed error in the transmission ratio be ΔM_{gp} within the range of a single pitch. Then, the modified value of the angular acceleration $\Lambda(\frac{dM_{gp}}{d\epsilon_g})$ is found in the following form

$$\Delta(\frac{dM_{gp}}{d\epsilon_g}) = \pm \frac{N_g \Delta M_{gp}}{2\pi} \quad (8.21)$$

where, N_g is the number of teeth in the gear.

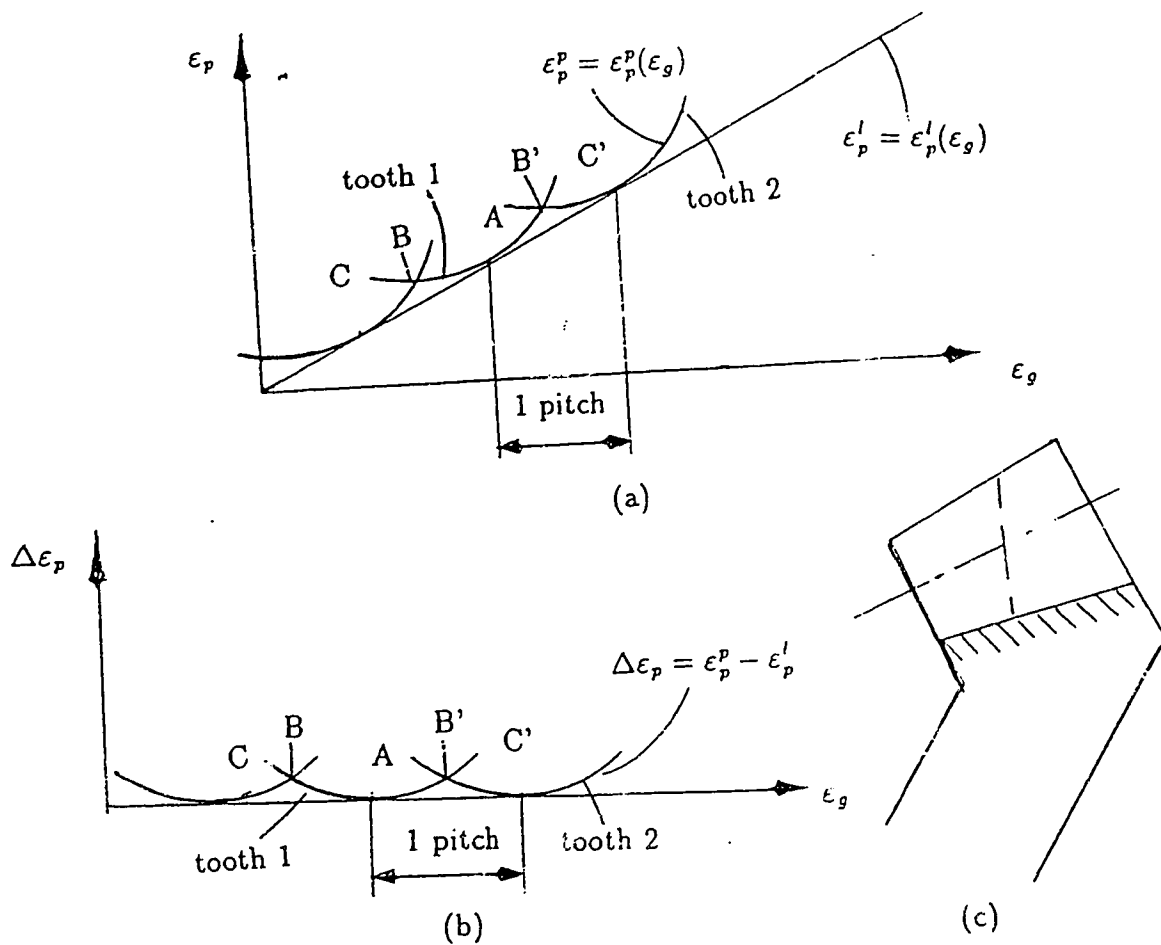


Figure 8.6: Motion diagram and contact locus

The motion diagram is shown in fig. 8.7 (a), and its first-order derivative is the instantaneous transmission ratio $M_{gp} = \frac{d\epsilon_p}{d\epsilon_g}$, shown in fig. 8.7 (c). Since the motion diagram for the theoretical line-contacting tooth surfaces is a straight line, thus, the instantaneous transmission ratio is constant, i.e., $(M_{gp})_l = (\frac{d\epsilon_p}{d\epsilon_g})_l = \text{const.}$, as shown in fig. 8.7 (c), and the instantaneous angular acceleration is zero, i.e., $(\frac{dM_{gp}}{d\epsilon_g})_l = 0$ as shown in fig. 8.7 (d). If the motion diagram for the point-contacting tooth surfaces is assumed to be approximately a second order curve, then, the curve for the instantaneous transmission ratio $(M_{gp})_p = (\frac{d\epsilon_p}{d\epsilon_g})_p$ is a straight line as shown in fig. 8.7 (c), and the instantaneous angular acceleration is a constant as shown in fig. 8.7 (d). Consequently, the modified value of the angular acceleration is found as

follows

$$\Delta\left(\frac{dM_{gp}}{d\varepsilon_g}\right) = \left(\frac{dM_{gp}}{d\varepsilon_g}\right)_p - \left(\frac{dM_{gp}}{d\varepsilon_g}\right)_l \begin{cases} < 0, & \text{forward transmission;} \\ > 0, & \text{reverse transmission.} \end{cases} \quad (8.22)$$

Since the transmission ratio at the fundamental contact point P_f remains unchanged before and after the curvature modification, and only the derivative to the transmission ratio at the fundamental contact point P_f is changed after the curvature modification, i.e., $\Delta\left(\frac{dM_{gp}}{d\varepsilon_g}\right) \neq 0$, with the aid of the definition of \mathbf{J}_p , i.e., expression (2.150), and expressions (2.123), (7.5) and (7.7), the corresponding modified value of $\Delta(\mathbf{J}_p \cdot \mathbf{N}_{gp}^f)$ is found in the following form

$$\begin{aligned} \Delta(\mathbf{J}_p \cdot \mathbf{N}_{gp}^f) &= \left\{ \left(\frac{dM_{gp}}{d\varepsilon_g} \right)_p \omega_2 \times (\mathbf{R}_{gp}^f - l\mathbf{p}) + M_{gp} \omega_2 \times (\omega_1 \times \mathbf{R}_{gp}^f) \right. \\ &\quad \left. - \omega_1 \times [M_{gp} \omega_2 \times (\mathbf{R}_{gp}^f - l\mathbf{p})] \right\} \cdot \mathbf{N}_{gp}^f - \left\{ M_{gp} \omega_2 \times (\omega_1 \times \mathbf{R}_{gp}^f) \right. \\ &\quad \left. - \omega_1 \times [M_{gp} \omega_2 \times (\mathbf{R}_{gp}^f - l\mathbf{p})] \right\} \cdot \mathbf{N}_{gp}^f \\ &= -\Delta\left(\frac{dM_{gp}}{d\varepsilon_g}\right)(\mathbf{k}' \times \mathbf{R}_p^f) \cdot \mathbf{N}_{gp}^f \\ &= \Delta\left(\frac{dM_{gp}}{d\varepsilon_g}\right)[z_{gp}^f N_{gpx}^f - N_{gpz}^f(x_{gp}^f - f_{gp})] \end{aligned} \quad (8.23)$$

where $\Delta\left(\frac{dM_{gp}}{d\varepsilon_g}\right)$ is determined by expression (8.21), N_{gpx}^f , N_{gpz}^f are determined by expression (7.2) and x_{gp}^f , f_{gp} are determined by expression (7.1).

The increment $\Delta(\mathbf{J}_p \cdot \mathbf{N}_{gp}^f)$ can be achieved through the modification of the conjugate normal curvature to the pinion tooth surface along direction \mathbf{g} perpendicular to direction \mathbf{e} of the instantaneous line of contact. Taking the increment of expression (2.241) yields

$$\begin{aligned} \Delta K'_{2g} &= \frac{d\bar{K}_g}{d(\mathbf{J}_p \cdot \mathbf{N}_{gp}^f)} \Delta(\mathbf{J}_p \cdot \mathbf{N}_{gp}^f) - \frac{dK_{gpg}}{d(\mathbf{J}_p \cdot \mathbf{N}_{gp}^f)} \Delta(\mathbf{J}_p \cdot \mathbf{N}_{gp}^f) \\ &= -\frac{\bar{K}_g^2}{D_p^2 + E_p^2} \Delta(\mathbf{J}_p \cdot \mathbf{N}_{gp}^f) - \frac{dK_{gpg}}{d(\mathbf{J}_p \cdot \mathbf{N}_{gp}^f)} \Delta(\mathbf{J}_p \cdot \mathbf{N}_{gp}^f) \end{aligned} \quad (8.24)$$

where, D_p and E_p are determined by expression (7.21), and \bar{K}_g can be determined by expression (7.24).

Since no curvature modification is applied to the gear tooth surface, the value $\frac{dK_{gpg}}{d(\mathbf{J}_p \cdot \mathbf{N}_{gp}^f)}$ is equal to zero. Finally, the modified value $\Delta K'_{2g}$ of the conjugate normal curvature to the pinion tooth surface is found in the following form

$$\Delta K'_{2g} = -\frac{\bar{K}_g^2}{D_p^2 + E_p^2} \Delta(\mathbf{J}_p \cdot \mathbf{N}_{gp}^f) \quad (8.25)$$

Consequently, the value K'_{pg} of the conjugate normal curvature for the pinion tooth surface is found as follows

$$K'_{pg} = \Delta K'_{2g} + K'_{pg} \quad (8.26)$$

where, K'_{pg} is determined by expression (7.25).

With the aid of expression (7.31), application of expression (2.39) yields the conjugate normal and torsional curvatures of the pinion tooth surface in directions of \mathbf{t}_p and \mathbf{s}_p as follows

$$\left. \begin{aligned} K'_{pt} &= K'_{pe} \cos^2 \theta_{etp}^f + K'_{pg} \sin^2 \theta_{etp}^f + 2G'_{pe} \sin \theta_{etp}^f \cos \theta_{etp}^f \\ G'_{pt} &= -(K'_{pe} - K'_{pg}) \sin \theta_{etp}^f \cos \theta_{etp}^f + G'_{pe} (\cos^2 \theta_{etp}^f - \sin^2 \theta_{etp}^f) \\ K'_{ps} &= K'_{pe} \sin^2 \theta_{etp}^f + K'_{pg} \cos^2 \theta_{etp}^f - 2G'_{pe} \sin \theta_{etp}^f \cos \theta_{etp}^f \end{aligned} \right\} \quad (8.27)$$

where, K'_{pe} , G'_{pe} and K'_{pg} are determined by expressions (8.14), (8.20) and (8.26) respectively, and θ_{etp}^f is determined by expression (7.31).

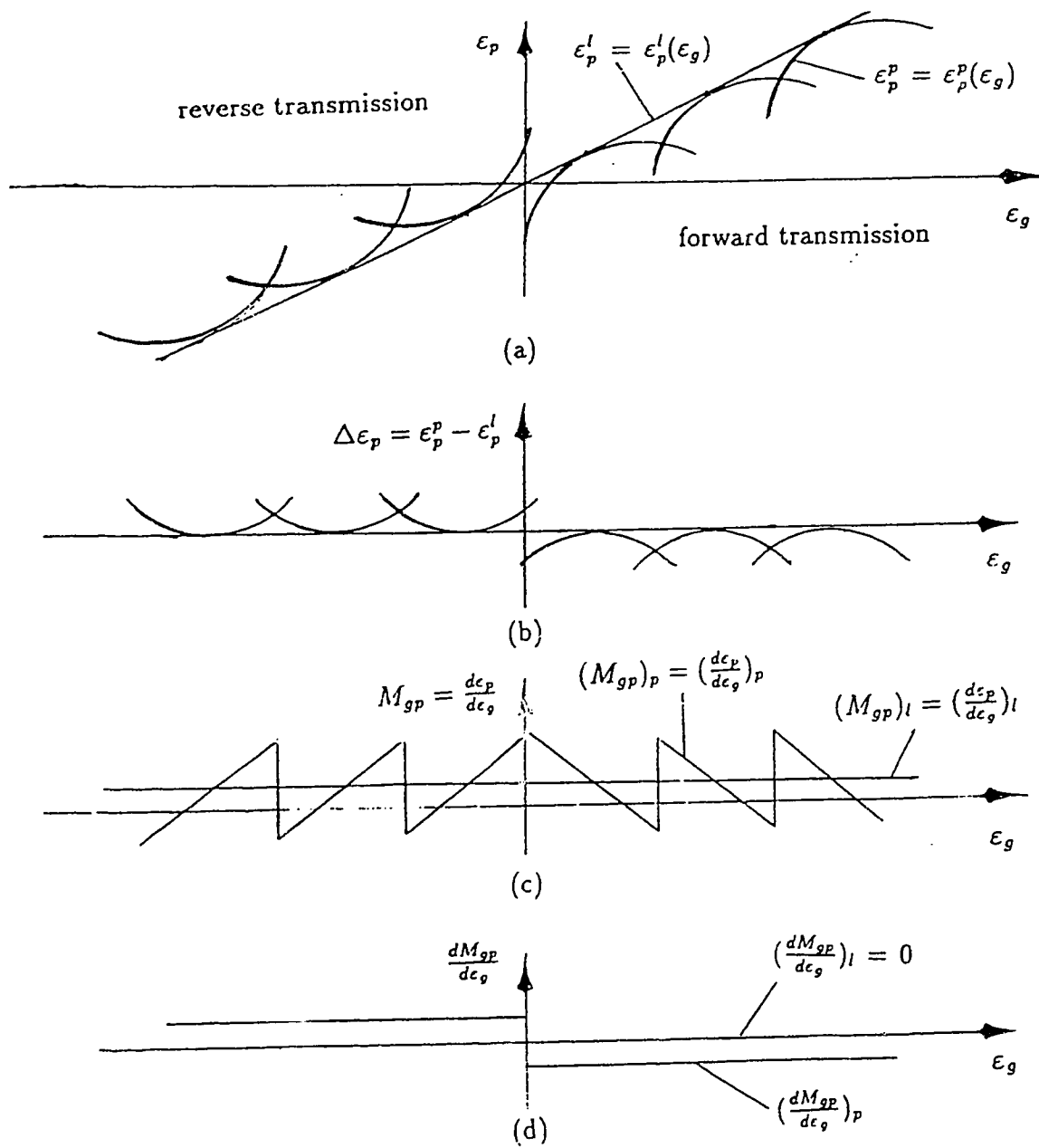


Figure 8.7:Diagrams for motion analyses

Chapter 9

Determination of Machine-Setting Parameters for the Generation of the Pinion Tooth Surface

The manufacture of the pinion tooth surface is a very critical and practical step to achieve a pair of point-contacting tooth surfaces with good mismatch. The pinion tooth surface finally obtained should have the specified curvature properties besides the prescribed unit normal at the fundamental contact point. Therefore, the procedure for choosing the cutting parameters for the pinion tooth surface is more complicated than that for the gear tooth surface. In the current practice of manufacturing hypoid gears, the pinion tooth surface is generated by the single side method, i.e., the two faces on each side of a tooth space are cut independently.

9.1 The Cutting Position Vector of the Point on the Cutter Corresponding to the Fundamental Contact Point

Similar to chapter 2.3.2, we use dual coordinate systems $O_m - \mathbf{i}_m, \mathbf{j}_m, \mathbf{k}_m$ and $O_p - \mathbf{i}_p, \mathbf{j}_p, \mathbf{k}_p$ as shown in fig.9.1. We choose coordinate system $O_m - \mathbf{i}_m, \mathbf{j}_m, \mathbf{k}_m$ to correspond to the machine frame, \mathbf{k}_m being coincident with the axis of the cradle, \mathbf{i}_m being vertically down; and we choose coordinate system $O_p - \mathbf{i}_p, \mathbf{j}_p, \mathbf{k}_p$ to correspond to the workpiece, \mathbf{k}_p being coincident with the rotating axis of workpiece. The relationship between $O_m - \mathbf{i}_m, \mathbf{j}_m, \mathbf{k}_m$ and $O_p - \mathbf{i}_p, \mathbf{j}_p, \mathbf{k}_p$ is found as follows,

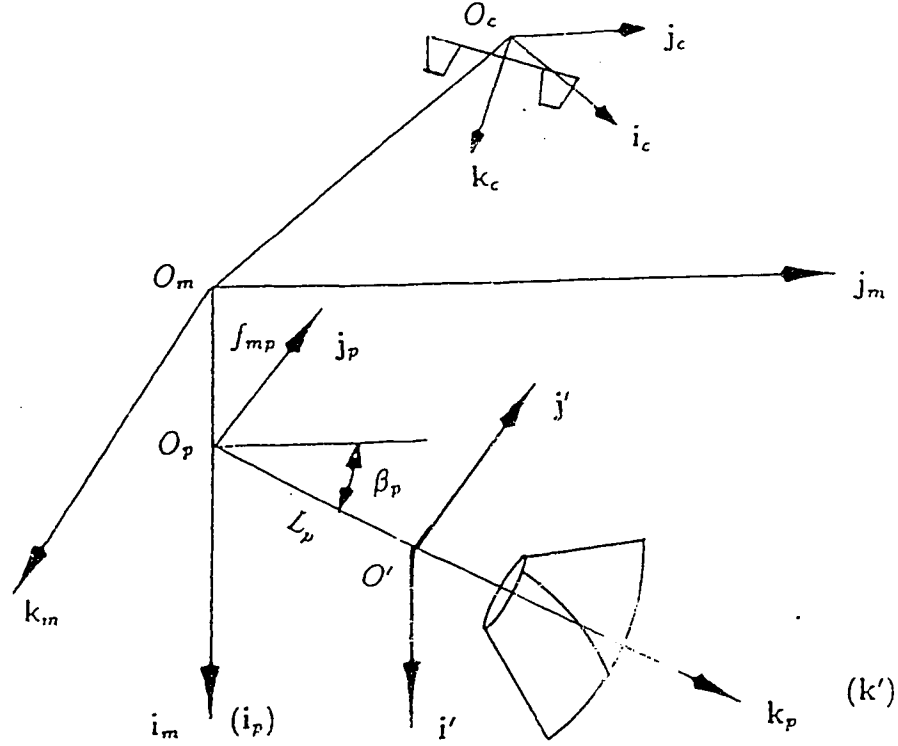


Figure 9.1: Relationship among coordinate systems

$$\left. \begin{aligned} \vec{O_m O_p} &= f_{mp} \mathbf{i}_m \\ \mathbf{i}_p &= \mathbf{i}_m \\ \mathbf{j}_p &= (\beta_p \mathbf{i}_m) \otimes (-\mathbf{k}_m) = -\cos \beta_p \mathbf{k}_m + \sin \beta_p \mathbf{j}_m \\ \mathbf{k}_p &= (\beta_p \mathbf{i}_m) \otimes \mathbf{j}_m = \sin \beta_p \mathbf{k}_m + \cos \beta_p \mathbf{j}_m \end{aligned} \right\} \quad (9.1)$$

In the same manner as chapter 5.1, we establish coordinate system $O_c - \mathbf{i}_c, \mathbf{j}_c, \mathbf{k}_c$ corresponding to the cutter, and then with the method used to derive expression (5.5), we show that the coordinate system $O_c - \mathbf{i}_c, \mathbf{j}_c, \mathbf{k}_c$ is related to the coordinate system $O_m - \mathbf{i}_m, \mathbf{j}_m, \mathbf{k}_m$ as follows

$$\left. \begin{aligned} \mathbf{i}_c &= (\Theta_p \mathbf{k}_m) \otimes \mathbf{i}_m = \cos \Theta_p \mathbf{i}_m + \sin \Theta_p \mathbf{j}_m \\ \mathbf{k}_c &= (\zeta_p \mathbf{i}_c) \otimes \mathbf{k}_m = \sin \zeta_p \sin \Theta_p \mathbf{i}_m - \sin \zeta_p \cos \Theta_p \mathbf{j}_m + \cos \zeta_p \mathbf{k}_m \\ \mathbf{j}_c &= \mathbf{k}_c \times \mathbf{i}_c = -\cos \zeta_p \sin \Theta_p \mathbf{i}_m + \cos \zeta_p \cos \Theta_p \mathbf{j}_m + \sin \zeta_p \mathbf{k}_m \end{aligned} \right\} \quad (9.2)$$

where, Θ_p is the swivel angle, and ζ_p is the tilt angle.

Without the tilt device, i.e., $\Theta_p = \zeta_p = 0$, the relationship above is simplified as follows

$$\left. \begin{aligned} \mathbf{i}_c &= \mathbf{i}_m \\ \mathbf{j}_c &= \mathbf{j}_m \\ \mathbf{k}_c &= \mathbf{k}_m \end{aligned} \right\} \quad (9.3)$$

and

$$\vec{O_m O_c} = x_{cp} \mathbf{i}_m + y_{cp} \mathbf{j}_m + z_{cp} \mathbf{k}_m \quad (9.4)$$

Let ρ_{cp} designate the radius of the cutter corresponding to the fundamental contact point P_f , ϕ_{cp} designate the blade angle of the cutter for the pinion and σ_p designate the phase angle of the cutting edge in the coordinate system $O_c - \mathbf{i}_c, \mathbf{j}_c, \mathbf{k}_c$. Then following the derivation of expression (5.9), and knowing that the conjugate cutting position lies in coordinate plane $\mathbf{i}_c - O_c - \mathbf{j}_c$, the position vector of the point on the cutter corresponding to the fundamental contact point on the pinion is found as follows

$$\left. \begin{aligned} \mathbf{R}_{mp} &= x_{mp} \mathbf{i}_m + y_{mp} \mathbf{j}_m + z_{mp} \mathbf{k}_m \\ x_{mp} &= x_{cp} + \rho_{cp} \cos \sigma_p \cos \Theta_p - \rho_{cp} \sin \sigma_p \cos \zeta_p \sin \Theta_p \\ y_{mp} &= y_{cp} + \rho_{cp} \cos \sigma_p \sin \Theta_p + \rho_{cp} \sin \sigma_p \cos \zeta_p \cos \Theta_p \\ z_{mp} &= z_{cp} + \rho_{cp} \sin \sigma_p \sin \zeta_p \end{aligned} \right\} \quad (9.5)$$

Correspondingly, the unit normal \mathbf{N}_{cp} to the cutter surface is found in the form

$$\left. \begin{aligned} \mathbf{N}_{cp} &= N_{cpx} \mathbf{i}_m + N_{cpy} \mathbf{j}_m + N_{cpz} \mathbf{k}_m \\ N_{cpx} &= -\cos \phi_{cp} \cos \sigma_p \cos \Theta_p + \cos \phi_{cp} \sin \sigma_p \cos \zeta_p \sin \Theta_p \\ &\quad + \sin \phi_{cp} \sin \zeta_p \sin \Theta_p \\ N_{cpy} &= -\cos \phi_{cp} \cos \sigma_p \sin \Theta_p - \cos \phi_{cp} \sin \sigma_p \cos \zeta_p \cos \Theta_p \\ &\quad - \sin \phi_{cp} \sin \zeta_p \cos \Theta_p \\ N_{cpz} &= -\cos \phi_{cp} \sin \sigma_p \sin \zeta_p + \sin \phi_{cp} \cos \zeta_p \end{aligned} \right\} \quad (9.6)$$

and the unit vector tangential to the cutting edge at the point corresponding to the fundamental contact point is given by

$$\left. \begin{aligned} \mathbf{W}_{cp} &= W_{cp1}\mathbf{i}_m + W_{cp2}\mathbf{j}_m + W_{cp3}\mathbf{k}_m \\ W_{cp1} &= \sin \phi_{cp} \cos \sigma_p \cos \Theta_p - \sin \phi_{cp} \sin \sigma_p \cos \zeta_p \sin \Theta_p \\ &\quad + \cos \phi_{cp} \sin \zeta_p \sin \Theta_p \\ W_{cp2} &= \sin \phi_{cp} \cos \sigma_p \sin \Theta_p + \sin \phi_{cp} \sin \sigma_p \cos \zeta_p \cos \Theta_p \\ &\quad - \cos \phi_{cp} \sin \zeta_p \cos \Theta_p \\ W_{cp3} &= \sin \phi_{cp} \sin \sigma_p \sin \zeta_p + \cos \phi_{cp} \cos \zeta_p \end{aligned} \right\} \quad (9.7)$$

Without the tilt device, i.e., $\Theta_p = \zeta_p = 0$, expressions (9.5) become

$$\left. \begin{aligned} \mathbf{R}_{m;p} &= x_{mp}\mathbf{i}_m + y_{mp}\mathbf{j}_m + z_{mp}\mathbf{k}_m \\ x_{mp} &= x_{cp} + \rho_{cp} \cos \sigma_p \\ y_{mp} &= y_{cp} + \rho_{cp} \sin \sigma_p \\ z_{mp} &= z_{cp} \end{aligned} \right\} \quad (9.8)$$

Correspondingly, the unit normal \mathbf{N}_{cp} to the cutter surface in the case of no tilt device is found as follows

$$\left. \begin{aligned} \mathbf{N}_{cp} &= (\sigma_p \mathbf{k}_c) \otimes (-\cos \phi_{cp} \mathbf{i}_c + \sin \phi_{cp} \mathbf{k}_c) \\ &= N_{cpz}\mathbf{i}_m + N_{cpy}\mathbf{j}_m + N_{cpz}\mathbf{k}_m \\ N_{cpz} &= -\cos \phi_{cp} \cos \sigma_p \\ N_{cpy} &= -\cos \phi_{cp} \sin \sigma_p \\ N_{cpz} &= \sin \phi_{cp} \end{aligned} \right\} \quad (9.9)$$

and the unit vector tangential to the cutting edge is found in the following form

$$\left. \begin{aligned} \mathbf{W}_{cp} &= W_{cp1}\mathbf{i}_m + W_{cp2}\mathbf{j}_m + W_{cp3}\mathbf{k}_m \\ W_{cp1} &= \sin \phi_{cp} \cos \sigma_p \\ W_{cp2} &= \sin \phi_{cp} \sin \sigma_p \\ W_{cp3} &= \cos \phi_{cp} \end{aligned} \right\} \quad (9.10)$$

9.2 The Cutting Position Vector of the Fundamental Contact Point on the Pinion

The cutting position vector \mathbf{R}_p of the fundamental contact point P_f on the pinion can be reached by rotating vector \mathbf{R}_p^f , i.e., expression (7.5), representing the conjugate

contact position at the fundamental contact point of the pinion with the gear, about axis \mathbf{k}' through an angle $\delta\varepsilon_p^f$, that is,

$$\left. \begin{aligned} \mathbf{R}_p &= (\delta\varepsilon_p^f \mathbf{k}') \otimes \mathbf{R}_p^f = (\delta\varepsilon_p^f \mathbf{k}') \otimes (x_p^f \mathbf{i}' + y_p^f \mathbf{j}' + z_p^f \mathbf{k}') \\ &= x_p^f \mathbf{i}' + y_p^f \mathbf{j}' + z_p^f \mathbf{k}' \\ x_p &= x_p^f \cos \delta\varepsilon_p^f - y_p^f \sin \delta\varepsilon_p^f \\ y_p &= x_p^f \sin \delta\varepsilon_p^f + y_p^f \cos \delta\varepsilon_p^f \\ z_p &= z_p^f \end{aligned} \right\} \quad (9.11)$$

where, x_p^f , y_p^f and z_p^f are determined by expression (7.5).

With the aid of expression (2.153), \mathbf{R}_p is related to \mathbf{R}_{mp} , i.e., expression (9.5), as follows

$$\left. \begin{aligned} \mathbf{R}_{mp} &= \mathbf{R}_p + f_{mp} \mathbf{i}_m + L_p \mathbf{k}' \\ x_{cp} + \rho_{cp} \cos \sigma_p \cos \zeta_p + \rho_{cp} \sin \sigma_p \cos \zeta_p \sin \Theta_p &= x_p^f \cos \delta\varepsilon_p^f - y_p^f \sin \delta\varepsilon_p^f \\ &\quad + f_{mp}, \\ y_{cp} + \rho_{cp} \cos \sigma_p \sin \zeta_p + \rho_{cp} \sin \sigma_p \cos \zeta_p \cos \Theta_p &= (z_p^f + L_p) \cos \beta_p \\ &\quad - (x_p^f \sin \delta\varepsilon_p^f + y_p^f \cos \delta\varepsilon_p^f) \sin \beta_p, \\ z_{cp} + \rho_{cp} \sin \sigma_p \sin \zeta_p &= (z_p^f + L_p) \sin \beta_p \\ &\quad - (x_p^f \sin \delta\varepsilon_p^f + y_p^f \cos \delta\varepsilon_p^f) \cos \beta_p, \end{aligned} \right\} \quad (9.12)$$

Consequently, with the aid of expression (7.7), the unit vector at the fundamental contact point P_f normal to the pinion tooth surface corresponding to the cutting position is found in the following form

$$\left. \begin{aligned} \mathbf{N}_p &= (\delta\varepsilon_p^f \mathbf{k}') \otimes \mathbf{N}_p^f = (\delta\varepsilon_p^f \mathbf{k}') \otimes (N_{px}^f \mathbf{i}' + N_{py}^f \mathbf{j}' + N_{pz}^f \mathbf{k}') \\ &= N_{px}^f \mathbf{i}' + N_{py}^f \mathbf{j}' + N_{pz}^f \mathbf{k}' \\ N_{px} &= N_{px}^f \cos \delta\varepsilon_p^f - N_{py}^f \sin \delta\varepsilon_p^f \\ N_{py} &= N_{px}^f \sin \delta\varepsilon_p^f + N_{py}^f \cos \delta\varepsilon_p^f \\ N_{pz} &= N_{pz}^f \end{aligned} \right\} \quad (9.13)$$

With the aid of expression (2.171), \mathbf{N}_p is related to \mathbf{N}_{cp} , i.e., expression (9.6), in the following form

$$\left. \begin{aligned} N_{px}^f \cos \delta\varepsilon_p^f - N_{py}^f \sin \delta\varepsilon_p^f &= -N_{cpz} \\ N_{px}^f \sin \delta\varepsilon_p^f + N_{py}^f \cos \delta\varepsilon_p^f &= -N_{cpy} \sin \beta_p + N_{cpz} \cos \beta_p \\ N_{pz}^f &= -N_{cpy} \cos \beta_p - N_{cpz} \sin \beta_p \end{aligned} \right\} \quad (9.14)$$

Without the tilt device, expressions (9.12) and (9.14) are simplified to the following forms

$$\left. \begin{aligned} x_{cp} + \rho_{cp} \cos \sigma_p &= x_p^f \cos \delta \varepsilon_p^f - y_p^f \sin \delta \varepsilon_p^f + f_{mp}, \\ y_{cp} + \rho_{cp} \sin \sigma_p &= (z_p^f + L_p) \cos \gamma_{pr} + (x_p^f \sin \delta \varepsilon_p^f + y_p^f \cos \delta \varepsilon_p^f) \sin \gamma_{pr}, \\ z_{cp} &= (z_p^f + L_p) \sin \gamma_{pr} - (x_p^f \sin \delta \varepsilon_p^f + y_p^f \cos \delta \varepsilon_p^f) \cos \gamma_{pr} \end{aligned} \right\} \quad (9.15)$$

and

$$\left. \begin{aligned} N_{px}^f \cos \delta \varepsilon_p^f - N_{py}^f \sin \delta \varepsilon_p^f &= \cos \phi_{cp} \cos \sigma_p, \\ N_{px}^f \sin \delta \varepsilon_p^f + N_{py}^f \cos \delta \varepsilon_p^f &= \cos \phi_{cp} \sin \sigma_p \sin \gamma_{pr} + \sin \phi_{cp} \cos \gamma_{pr}, \\ N_{pz}^f &= \cos \phi_{cp} \sin \sigma_p \cos \gamma_{pr} - \sin \phi_{cp} \sin \gamma_{pr} \end{aligned} \right\} \quad (9.16)$$

9.3 Calculation of Curvatures for the Pinion Tooth Surface

The required curvature properties for the pinion tooth surface have been determined in Chapter 8, but on the other hand, the pinion tooth surface is generated by the cutter surface under the conjugate motions of the cutter and the pinion. Therefore, machine-setting parameters for the pinion tooth surface should satisfy the curvature requirements obtained in Chapter 8.

With aid of expression (2.129), the velocity at the fundamental contact point of the cutter relative to the pinion corresponding to the cutting position is found in the following form

$$\left. \begin{aligned} \mathbf{v}_p^{mp} &= v_{p1}^{mp} \mathbf{i}_m + v_{p2}^{mp} \mathbf{j}_m + v_{p3}^{mp} \mathbf{k}_m \\ v_{p1}^{mp} &= -(1 + M_{mp} \sin \beta_p) y_{mp} + z_{mp} M_{mp} \cos \beta_p, \\ v_{p2}^{mp} &= (1 + M_{mp} \sin \beta_p) x_{mp} - M_{mp} f_{mp} \sin \beta_p, \\ v_{p3}^{mp} &= -M_{mp} x_{mp} \cos \beta_p + M_{mp} f_{mp} \cos \beta_p \end{aligned} \right\} \quad (9.17)$$

where, M_{mp} is the ratio of roll for the pinion, and x_{mp} , y_{mp} , z_{mp} are determined by expression (9.5).

Expression (2.133) results in

$$\left. \begin{aligned} \eta_p^p &= \eta_{p1}^p \mathbf{i}_m + \eta_{p2}^p \mathbf{j}_m + \eta_{p3}^p \mathbf{k}_m, \\ \eta_{p1}^p &= -N_{cpx} (1 + M_{mp} \sin \beta_p) + N_{cpz} M_{mp} \cos \beta_p, \\ \eta_{p2}^p &= N_{cpx} (1 + M_{mp} \sin \beta_p), \\ \eta_{p3}^p &= -N_{cpx} M_{mp} \cos \beta_p, \\ |\eta_p^p| &= \sqrt{(\eta_{p1}^p)^2 + (\eta_{p2}^p)^2 + (\eta_{p3}^p)^2} \end{aligned} \right\} \quad (9.18)$$

where, N_{cpx} , N_{cpx} and N_{cpz} are determined by expression (9.6).

The requirement of conjugacy, i.e., expression (2.157), yields

$$\begin{aligned} & [-(1 + M_{mp} \sin \beta_p) y_{mp} + z_{mp} M_{mp} \cos \beta_p] N_{cpz} + [(1 + M_{mp} \sin \beta_p) x_{mp} \\ & - M_{mp} f_{mp} \sin \beta_p] N_{cpy} + (-M_{mp} x_{mp} \cos \beta_p + M_{mp} f_{mp} \cos \beta_p) N_{cpz} = 0 \end{aligned} \quad (9.19)$$

Without the tilt device, expressions (9.17), (9.18) and (9.19) are simplified to the following forms

$$\left. \begin{aligned} \mathbf{v}_p^{mp} &= v_{p1}^{mp} \mathbf{i}_m + v_{p2}^{mp} \mathbf{j}_m + v_{p3}^{mp} \mathbf{k}_m \\ v_{p1}^{mp} &= -(1 + M_{mp} \sin \gamma_{pr}) y_{mp} + z_{mp} M_{mp} \cos \gamma_{pr}, \\ v_{p2}^{mp} &= (1 + M_{mp} \sin \gamma_{pr}) x_{mp} - M_{mp} f_{mp} \sin \gamma_{pr}, \\ v_{p3}^{mp} &= -M_{mp} x_{mp} \cos \gamma_{pr} + M_{mp} f_{mp} \cos \gamma_{pr} \end{aligned} \right\} \quad (9.20)$$

where, x_{mp} , y_{mp} and z_{mp} are determined from expression (9.8).
and

$$\left. \begin{aligned} \eta_p^p &= \eta_{p1}^p \mathbf{i}_m + \eta_{p2}^p \mathbf{j}_m + \eta_{p3}^p \mathbf{k}_m, \\ \eta_{p1}^p &= (1 + M_{mp} \sin \gamma_{pr}) \cos \phi_{cp} \sin \sigma_p + M_{mp} \cos \gamma_{pr} \sin \phi_{cp}, \\ \eta_{p2}^p &= -(1 + M_{mp} \sin \gamma_{pr}) \cos \phi_{cp} \cos \sigma_p, \\ \eta_{p3}^p &= M_{mp} \cos \phi_{cp} \cos \sigma_p \cos \gamma_{pr}, \\ |\eta_p^p| &= \sqrt{(\eta_{p1}^p)^2 + (\eta_{p2}^p)^2 + (\eta_{p3}^p)^2} \end{aligned} \right\} \quad (9.21)$$

and

$$\begin{aligned} & [-(1 + M_{mp} \sin \gamma_{pr}) y_{mp} + z_{mp} M_{mp} \cos \gamma_{pr}] \cos \phi_{cp} \cos \sigma_p \\ & + [(1 + M_{mp} \sin \gamma_{pr}) x_{mp} - M_{mp} f_{mp} \sin \gamma_{pr}] \cos \phi_{cp} \sin \sigma_p \\ & - (-M_{mp} x_{mp} \cos \gamma_{pr} + M_{mp} f_{mp} \cos \gamma_{pr}) \sin \phi_{cp} = 0 \end{aligned} \quad (9.22)$$

Since the unit vector $\frac{\eta_p^p}{|\eta_p^p|}$ can be obtained by rotating $\frac{\mathbf{v}_p^{mp}}{|\mathbf{v}_p^{mp}|}$ about \mathbf{N}_{cp} as an axis through an angle $\theta_{v\eta}^{mp}$, that is,

$$\begin{aligned} \frac{\eta_p^p}{|\eta_p^p|} &= (\theta_{v\eta}^{mp} \mathbf{N}_{cp}) \otimes \frac{\mathbf{v}_p^{mp}}{|\mathbf{v}_p^{mp}|} \\ &= \cos \theta_{v\eta}^{mp} \frac{\mathbf{v}_p^{mp}}{|\mathbf{v}_p^{mp}|} + \sin \theta_{v\eta}^{mp} \mathbf{N}_{cp} \times \frac{\mathbf{v}_p^{mp}}{|\mathbf{v}_p^{mp}|} \end{aligned} \quad (9.23)$$

then,

$$\left. \begin{aligned} \cos \theta_{v\eta}^{mp} &= \frac{\mathbf{v}_p^{mp} \cdot \eta_p^p}{|\mathbf{v}_p^{mp}| |\eta_p^p|} \\ &= \frac{v_{p1}^{mp} \eta_{p1}^p + v_{p2}^{mp} \eta_{p2}^p + v_{p3}^{mp} \eta_{p3}^p}{|\mathbf{v}_p^{mp}| |\eta_p^p|} \\ \sin \theta_{v\eta}^{mp} &= \frac{\mathbf{N}_{cp} \cdot (\mathbf{v}_p^{mp} \times \eta_p^p)}{|\mathbf{v}_p^{mp}| |\eta_p^p|} \\ &= -\frac{M_{mp} f_{mp} \cos \beta_p}{|\mathbf{v}_p^{mp}| |\eta_p^p|} \end{aligned} \right\} \quad (9.24)$$

where, in the case of the tilt device, v_{p1}^{mp} , v_{p2}^{mp} and v_{p3}^{mp} are determined by expression (9.17), and η_{p1}^p , η_{p2}^p and η_{p3}^p are determined by expression (9.18); in the case of no tilt device, v_{p1}^{mp} , v_{p2}^{mp} and v_{p3}^{mp} are determined by expression (9.20), and η_{p1}^p , η_{p2}^p and η_{p3}^p are determined by expression (9.21), with $\beta_p = \gamma_{pr}$.

Since vector $\frac{\mathbf{v}_p^{mp}}{|\mathbf{v}_p^{mp}|}$ can be expressed in the following form

$$\begin{aligned} \frac{\mathbf{v}_p^{mp}}{|\mathbf{v}_p^{mp}|} &= (\eta_{wv}^{mp} \mathbf{N}_{cp}) \otimes \mathbf{W}_{cp} \\ &= \cos \theta_{wv}^{mp} \mathbf{W}_{cp} + \sin \theta_{wv}^{mp} \mathbf{N}_{cp} \times \mathbf{W}_{cp} \end{aligned} \quad (9.25)$$

then

$$\left. \begin{aligned} \cos \theta_{wv}^{mp} &= \frac{\mathbf{v}_p^{mp} \cdot \mathbf{W}_{cp}}{|\mathbf{v}_p^{mp}|} \\ &= \frac{v_{p1}^{mp} W_{cp1} + v_{p2}^{mp} W_{cp2} + v_{p3}^{mp} W_{cp3}}{|\mathbf{v}_p^{mp}|}, \\ \sin \theta_{wv}^{mp} &= \frac{\mathbf{v}_p^{mp} \cdot (\mathbf{N}_{cp} \times \mathbf{W}_{cp})}{|\mathbf{v}_p^{mp}|} \\ &= \frac{\begin{cases} v_{p1}^{mp} (N_{cpy} W_{cp3} - N_{cpz} W_{cp2}) \\ + v_{p2}^{mp} (N_{cpz} W_{cp1} - N_{cp x} W_{cp3}) \\ + v_{p3}^{mp} (N_{cp x} W_{cp2} - N_{cpy} W_{cp1}) \end{cases}}{|\mathbf{v}_p^{mp}|} \end{aligned} \right\} \quad (9.26)$$

where, $N_{cp x}$, N_{cpy} and N_{cpz} are determined by expression (9.6), W_{cp1} , W_{cp2} and W_{cp3} are determined by expression (9.7), and v_{p1}^{mp} , v_{p2}^{mp} and v_{p3}^{mp} are calculated by expression (9.17).

Without the tilt device, the expression above simplifies to the following form

$$\left. \begin{aligned} \cos \theta_{wv}^{mp} &= \frac{v_{p3}^{mp}}{|\mathbf{v}_p^{mp}| \cos \phi_{cp}}, \\ \sin \theta_{wv}^{mp} &= \frac{v_{p2}^{mp} \cos \sigma_p - v_{p1}^{mp} \sin \sigma_p}{|\mathbf{v}_p^{mp}|} \end{aligned} \right\} \quad (9.27)$$

where, v_{p1}^{mp} , v_{p2}^{mp} and v_{p3}^{mp} are determined by expression (9.20).

With the aid of expressions (2.39) and (6.24), the curvature properties of the cutter surface in directions of $\frac{\mathbf{v}_p^{mp}}{|\mathbf{v}_p^{mp}|}$ and $\Delta_{mp} = \mathbf{N}_{cp} \times \frac{\mathbf{v}_p^{mp}}{|\mathbf{v}_p^{mp}|}$ are found as follows

$$\left. \begin{aligned} K_{cpv} &= K_{cpw} \cos^2 \theta_{wv}^{mp} + K_{cpq} \sin^2 \theta_{wv}^{mp} + 2G_{cpw} \sin \theta_{wv}^{mp} \cos \theta_{wv}^{mp} \\ &= -\frac{\rho_{cp}}{\cos \phi_{cp} \sin^2 \theta_{wv}^{mp}}, \\ G_{cpv} &= -(K_{cpw} - K_{cpq}) \sin \theta_{wv}^{mp} \cos \theta_{wv}^{mp} + G_{cpw} (\cos^2 \theta_{wv}^{mp} - \sin^2 \theta_{wv}^{mp}) \\ &= -\frac{\rho_{cp}}{\cos \phi_{cp} \sin \theta_{wv}^{mp} \cos \theta_{wv}^{mp}}, \\ K_{cp\Delta} &= K_{cpw} \sin^2 \theta_{wv}^{mp} + K_{cpq} \cos^2 \theta_{wv}^{mp} - 2G_{cpw} \sin \theta_{wv}^{mp} \cos \theta_{wv}^{mp} \\ &= -\frac{\rho_{cp}}{\cos \phi_{cp} \cos^2 \theta_{wv}^{mp}} \end{aligned} \right\} \quad (9.28)$$

where, in the case of the tilt device: $\sin \theta_{uv}^{mp}$ and $\cos \theta_{uv}^{mp}$ are determined by expression (9.26); in the case of no tilt device: $\sin \theta_{uv}^{mp}$ and $\cos \theta_{uv}^{mp}$ are determined by expression (9.27).

Expression (2.151) results in

$$\left. \begin{aligned} \mathbf{J}_p &= J_{p1}\mathbf{i}_m + J_{p2}\mathbf{j}_m + J_{p3}\mathbf{k}_m, \\ J_{p1} &= M_{mp}f_{mp} \sin \beta_p, \\ J_{p2} &= M_{mp}z_{mp} \cos \beta_p, \\ J_{p3} &= -M_{mp}y_{mp} \cos \beta_p \end{aligned} \right\} \quad (9.29)$$

where, y_{mp} and z_{mp} are determined by expression (9.5).

Then, the combination of expressions (9.6) and (9.29) yields

$$\mathbf{J}_p \cdot \mathbf{N}_{cp} = N_{cpz}M_{mp}f_{mp} \sin \beta_p + N_{cpy}M_{mp}z_{mp} \cos \beta_p - N_{cpz}M_{mp}y_{mp} \cos \beta_p \quad (9.30)$$

Without the tilt device, expressions (9.29) and (9.30) become

$$\left. \begin{aligned} \mathbf{J}_p &= J_{p1}\mathbf{i}_m + J_{p2}\mathbf{j}_m + J_{p3}\mathbf{k}_m, \\ J_{p1} &= M_{mp}f_{mp} \sin \gamma_{pr}, \\ J_{p2} &= M_{mp}z_{mp} \cos \gamma_{pr}, \\ J_{p3} &= -M_{mp}y_{mp} \cos \gamma_p \end{aligned} \right\} \quad (9.31)$$

where, y_{mp} and z_{mp} are determined by expression (9.8).

and

$$\begin{aligned} \mathbf{J}_p \cdot \mathbf{N}_{cp} = & -M_{mp}f_{mp} \sin \gamma_{pr} \cos \phi_{cp} \cos \sigma_p - M_{mp}z_{mp} \cos \gamma_{pr} \cos \phi_{cp} \sin \sigma_p \\ & - M_{mp}y_{mp} \cos \gamma_{pr} \sin \phi_{cp} \end{aligned} \quad (9.32)$$

Expression (2.209) results in

$$\left. \begin{aligned} D_p &= K_{cpv}|\mathbf{v}_p^{mp}| - |\eta_p^p| \cos \theta_{v\eta}^{mp}, \\ E_p &= G_{cpv}|\mathbf{v}_p^{mp}| - |\eta_p^p| \sin \theta_{v\eta}^{mp} \end{aligned} \right\} \quad (9.33)$$

where, K_{cpv} and G_{cpv} are determined by expression (9.28), and $\sin \theta_{v\eta}^{mp}$, $\cos \theta_{v\eta}^{mp}$ are determined by expression (9.24); in the case of the tilt device: $|\mathbf{v}_p^{mp}|$ and $|\eta_p^p|$ are determined by expressions (9.17) and (9.18); in the case of no tilt device: $|\mathbf{v}_p^{mp}|$ and $|\eta_p^p|$ are determined by expressions (9.20) and (9.21).

Application of expressions (2.239) and (2.240) yields the conjugate normal and torsional curvatures of the pinion tooth surface in directions of $\frac{\mathbf{v}_p^{mp}}{|\mathbf{v}_p^{mp}|}$ and

$\Delta_{mp} = \mathbf{N}_{cp} \times \frac{\mathbf{v}_p^{mp}}{|\mathbf{v}_p^{mp}|}$ in the following forms

$$\left. \begin{aligned} K'_{pv} &= \frac{D_p^2}{D_p |\mathbf{v}_p^{mp}| + \mathbf{J}_p \cdot \mathbf{N}_{cp}} - K_{cpv}, \\ G'_{pv} &= \frac{D_p E_p}{D_p |\mathbf{v}_p^{mp}| + \mathbf{J}_p \cdot \mathbf{N}_{cp}} - G_{cpv}, \\ K'_{p\Delta} &= \frac{E_p^2}{D_p |\mathbf{v}_p^{mp}| + \mathbf{J}_p \cdot \mathbf{N}_{cp}} - K_{cp\Delta}, \end{aligned} \right\} \quad (9.34)$$

where, K_{cpv} , G_{cpv} and $K_{cp\Delta}$ are determined by expression (9.28); in the case of the tilt device, $|\mathbf{v}_p^{mp}|$, and $\mathbf{J}_p \cdot \mathbf{N}_{cp}$ are determined by expressions (9.17) and (9.30) respectively; in the case of no tilt device, $|\mathbf{v}_p^{mp}|$, and $\mathbf{J}_p \cdot \mathbf{N}_{cp}$ are determined by expressions (9.20) and (9.32) respectively.

In the cutting position, vector \mathbf{t}_p defined by expression (7.26) becomes

$$\left. \begin{aligned} \mathbf{t}_{pc} &= (\delta \varepsilon_p^f \mathbf{k}') \otimes \mathbf{t}_p \\ &= t_{pc1} \mathbf{i}_m + t_{pc2} \mathbf{j}_m + t_{pc3} \mathbf{k}_m, \\ t_{pc1} &= t_{p1} \cos \delta \varepsilon_p^f - t_{p3} \sin \delta \varepsilon_p^f, \\ t_{pc2} &= (t_{p1} \sin \delta \varepsilon_p^f + t_{p3} \cos \delta \varepsilon_p^f) \sin \beta_p - t_{p2} \cos \beta_p, \\ t_{pc3} &= -(t_{p1} \sin \delta \varepsilon_p^f + t_{p3} \cos \delta \varepsilon_p^f) \cos \beta_p - t_{p2} \sin \beta_p \end{aligned} \right\} \quad (9.35)$$

Consequently, vector \mathbf{s}_p defined by expression (7.27) is given by

$$\left. \begin{aligned} \mathbf{s}_{pc} &= (\delta \varepsilon_p^f \mathbf{k}') \otimes \mathbf{s}_p \\ &= s_{pc1} \mathbf{i}_m + s_{pc2} \mathbf{j}_m + s_{pc3} \mathbf{k}_m, \\ s_{pc1} &= s_{p1} \cos \delta \varepsilon_p^f - s_{p3} \sin \delta \varepsilon_p^f, \\ s_{pc2} &= (s_{p1} \sin \delta \varepsilon_p^f + s_{p3} \cos \delta \varepsilon_p^f) \sin \beta_p - s_{p2} \cos \beta_p, \\ s_{pc3} &= -(s_{p1} \sin \delta \varepsilon_p^f + s_{p3} \cos \delta \varepsilon_p^f) \cos \beta_p - s_{p2} \sin \beta_p \end{aligned} \right\} \quad (9.36)$$

Without the tilt device, expressions (9.35) and (9.36) become

$$\left. \begin{aligned} \mathbf{t}_{pc} &= (\delta \varepsilon_p^f \mathbf{k}') \otimes \mathbf{t}_p \\ &= t_{pc1} \mathbf{i}_m + t_{pc2} \mathbf{j}_m + t_{pc3} \mathbf{k}_m, \\ t_{pc1} &= \cos \psi_{pr} \sin \gamma_{pr} \cos(\varepsilon_p^f + \delta \varepsilon_p^f) - \sin \psi_{pr} \sin(\varepsilon_p^f + \delta \varepsilon_p^f), \\ t_{pc2} &= \sin \gamma_{pr} \sin \psi_{pr} \cos(\varepsilon_p^f + \delta \varepsilon_p^f) + [\sin^2 \gamma_{pr} \sin(\varepsilon_p^f + \delta \varepsilon_p^f) \\ &\quad + \cos^2 \gamma_{pr}] \cos \psi_{pr}, \\ t_{pc3} &= [1 - \sin(\varepsilon_p^f + \delta \varepsilon_p^f)] \cos \psi_{pr} \sin \gamma_{pr} \cos \gamma_{pr} \\ &\quad - \cos \gamma_{pr} \sin \psi_{pr} \cos(\varepsilon_p^f + \delta \varepsilon_p^f) \end{aligned} \right\} \quad (9.37)$$

and

$$\left. \begin{aligned} \mathbf{s}_{pc} &= (\delta \varepsilon_p^f \mathbf{k}') \otimes \mathbf{s}_p \\ &= s_{pc1} \mathbf{i}_m + s_{pc2} \mathbf{j}_m + s_{pc3} \mathbf{k}_m, \\ s_{pc1} &= s_{p1} \cos \delta \varepsilon_p^f - s_{p3} \sin \delta \varepsilon_p^f, \\ s_{pc2} &= (s_{p1} \sin \delta \varepsilon_p^f + s_{p3} \cos \delta \varepsilon_p^f) \sin \gamma_{pr} - s_{p2} \cos \gamma_{pr}, \\ s_{pc3} &= -(s_{p1} \sin \delta \varepsilon_p^f + s_{p3} \cos \delta \varepsilon_p^f) \cos \gamma_{pr} - s_{p2} \sin \gamma_{pr} \end{aligned} \right\} \quad (9.38)$$

Since vector \mathbf{t}_{pc} can be derived by rotating $\frac{\mathbf{v}^{mp}}{|\mathbf{v}^{mp}|}$ about \mathbf{N}_{cp} as an axis through an angle θ_{vt}^{mp} , that is,

$$\begin{aligned} \mathbf{t}_{pc} &= (\theta_{vt}^{mp} \mathbf{N}_{cp}) \times \frac{\mathbf{v}^{mp}}{|\mathbf{v}^{mp}|} \\ &= \cos \theta_{vt}^{mp} \frac{\mathbf{v}^{mp}}{|\mathbf{v}^{mp}|} + \sin \theta_{vt}^{mp} \mathbf{N}_{cp} \times \frac{\mathbf{v}^{mp}}{|\mathbf{v}^{mp}|} \end{aligned} \quad (9.39)$$

therefore, the angle θ_{vt}^{mp} is given by

$$\left. \begin{aligned} \cos \theta_{vt}^{mp} &= \frac{\mathbf{t}_{pc} \cdot \mathbf{v}_p^{mp}}{|\mathbf{v}^{mp}|} \\ &= \frac{t_{pc1} v_{p1}^{mp} + t_{pc2} v_{p2}^{mp} + t_{pc3} v_{p3}^{mp}}{|\mathbf{v}^{mp}|}, \\ \sin \theta_{vt}^{mp} &= \frac{|\mathbf{t}_{pc} \cdot (\mathbf{N}_{cp} \times \mathbf{v}_p^{mp})|}{|\mathbf{v}^{mp}|} \\ &= \frac{t_{pc1} (N_{cpy} v_{p3}^{mp} - N_{cpz} v_{p2}^{mp}) + t_{pc2} (N_{cpz} v_{p1}^{mp} - N_{cpz} v_{p3}^{mp}) + t_{pc3} (N_{cpz} v_{p2}^{mp} - N_{cpy} v_{p1}^{mp})}{|\mathbf{v}^{mp}|} \end{aligned} \right\} \quad (9.40)$$

where, in the case of the tilt device, N_{cpz} , N_{cpy} and N_{cpz} are determined by expression (9.6), v_{p1}^{mp} , v_{p2}^{mp} and v_{p3}^{mp} are found in expression (9.17), and t_{pc1} , t_{pc2} and t_{pc3} are calculated by expression (9.35); in the case of no tilt device, N_{cpz} , N_{cpy} and N_{cpz} are determined by expression (9.9), v_{p1}^{mp} , v_{p2}^{mp} and v_{p3}^{mp} are found in expression (9.20), and t_{pc1} , t_{pc2} and t_{pc3} are calculated by expression (9.37).

With the aid of expressions (9.34) and (9.40), application of expression (2.39) yields the conjugate normal and torsional curvatures of the pinion tooth surface in directions of \mathbf{t}_{pc} and \mathbf{s}_{pc} in the following form

$$\left. \begin{aligned} K'_{ptp} &= K'_{pv} \cos^2 \theta_{vt}^{mp} + K'_{p\Delta} \sin^2 \theta_{vt}^{mp} + 2G'_{pv} \sin \theta_{vt}^{mp} \cos \theta_{vt}^{mp}, \\ G'_{ptp} &= -(K'_{pv} - K'_{p\Delta}) \sin \theta_{vt}^{mp} \cos \theta_{vt}^{mp} + G'_{pv} (\cos^2 \theta_{vt}^{mp} - \sin^2 \theta_{vt}^{mp}), \\ K'_{psp} &= K'_{pv} \sin^2 \theta_{vt}^{mp} + K'_{p\Delta} \cos^2 \theta_{vt}^{mp} - 2G'_{pv} \sin \theta_{vt}^{mp} \cos \theta_{vt}^{mp} \end{aligned} \right\} \quad (9.41)$$

9.4 Simultaneous Equations for Machine-Setting Parameters of the Pinion Tooth Surface

The values of the conjugate normal and torsional curvatures of the pinion tooth surface in directions of \mathbf{t}_{pc} and \mathbf{s}_{pc} have been given by expression (8.27). Setting

$K'_{ptp} = K'_{ptp}$, $G'_{ptp} = G'_{ptp}$ and $K'_{psp} = K'_{psp}$ and combining equations (9.12), (9.14) and (9.19), we obtain the simultaneous equations for determining the machine-setting parameters of the pinion tooth surface in the following form

$$\left. \begin{aligned} x_{cp} + \rho_{cp} \cos \sigma_p \cos \Theta_p - \rho_{cp} \sin \sigma_p \cos \zeta_p \sin \Theta_p &= x_p^f \cos \delta \varepsilon_p^f - y_p^f \sin \delta \varepsilon_p^f + f_{mp}, \\ y_{cp} + \rho_{cp} \cos \sigma_p \sin \Theta_p + \rho_{cp} \sin \sigma_p \cos \zeta_p \cos \Theta_p &= (z_p^f + L_p) \cos \beta_p \\ &\quad + (x_p^f \sin \delta \varepsilon_p^f + y_p^f \cos \delta \varepsilon_p^f) \sin \beta_p, \\ z_{cp} + \rho_{cp} \sin \sigma_p \sin \zeta_p &= (z_p^f + L_p) \sin \beta_p \\ &\quad - (x_p^f \sin \delta \varepsilon_p^f + y_p^f \cos \delta \varepsilon_p^f) \cos \beta_p, \\ N_{px}^f \cos \delta \varepsilon_p^f - N_{py}^f \sin \delta \varepsilon_p^f &= -N_{cpz}, \\ N_{px}^f \sin \delta \varepsilon_p^f + N_{py}^f \cos \delta \varepsilon_p^f &= -N_{cpy} \sin \beta_p + N_{cpz} \cos \beta_p, \\ [- (1 + M_{mp} \sin \beta_p) y_{mp} + z_{mp} M_{mp} \cos \beta_p] N_{cpz} &+ [(1 + M_{mp} \sin \beta_p) x_{mp} \\ - M_{mp} f_{mp} \sin \beta_p] N_{cpy} &+ (-M_{mp} x_{mp} \cos \beta_p + M_{mp} f_{mp} \cos \beta_p) N_{cpz} = 0, \\ K'_{ptp} &= K'_{pv} \cos^2 \theta_{vt}^{mp} + K'_{p\Delta} \sin^2 \theta_{vt}^{mp} + 2G'_{pv} \sin \theta_{vt}^{mp} \cos \theta_{vt}^{mp}, \\ G'_{ptp} &= -(K'_{pv} - K'_{p\Delta}) \sin \theta_{vt}^{mp} \cos \theta_{vt}^{mp} + G'_{pv} (\cos^2 \theta_{vt}^{mp} - \sin^2 \theta_{vt}^{mp}), \\ K'_{psp} &= K'_{pv} \sin^2 \theta_{vt}^{mp} + K'_{p\Delta} \cos^2 \theta_{vt}^{mp} - 2G'_{pv} \sin \theta_{vt}^{mp} \cos \theta_{vt}^{mp} \end{aligned} \right\} \quad (9.42)$$

Simultaneous equations (9.42) consist of nine equations, and there are twelve parameters to be determined, i.e., x_{cp} , y_{cp} , z_{cp} , σ_p , ζ_p , Θ_p , ϕ_{cp} , ρ_{cp} , f_{mp} , L_p , $\delta \varepsilon_p^f$, and M_{mp} . Therefore, the values of three parameters among them be prescribed.

Without the tilt device, simultaneous equations for determining the machine-setting parameters of the pinion tooth surface are found in the following form

$$\left. \begin{aligned} x_{cp} + \rho_{cp} \cos \sigma_p &= x_p^f \cos \delta \varepsilon_p^f - y_p^f \sin \delta \varepsilon_p^f + f_{mp}, \\ y_{cp} + \rho_{cp} \sin \sigma_p &= (z_p^f + L_p) \cos \gamma_{pr} + (x_p^f \sin \delta \varepsilon_p^f + y_p^f \cos \delta \varepsilon_p^f) \sin \gamma_{pr}, \\ z_{cp} &= (z_p^f + L_p) \sin \gamma_{pr} - (x_p^f \sin \delta \varepsilon_p^f + y_p^f \cos \delta \varepsilon_p^f) \cos \gamma_{pr}, \\ N_{px}^f \cos \delta \varepsilon_p^f - N_{py}^f \sin \delta \varepsilon_p^f &= \cos \phi_{cp} \cos \sigma_p, \\ N_{px}^f \sin \delta \varepsilon_p^f + N_{py}^f \cos \delta \varepsilon_p^f &= \cos \phi_{cp} \sin \sigma_p \sin \gamma_{pr} + \sin \phi_{cp} \cos \gamma_{pr}, \\ [- (1 + M_{mp} \sin \gamma_{pr}) y_{mp} + z_{mp} M_{mp} \cos \gamma_{pr}] \cos \phi_{cp} \cos \sigma_p \\ &+ [(1 + M_{mp} \sin \gamma_{pr}) x_{mp} - M_{mp} f_{mp} \sin \gamma_{pr}] \cos \phi_{cp} \sin \sigma_p \\ &- (-M_{mp} x_{mp} \cos \gamma_{pr} + M_{mp} f_{mp} \cos \gamma_{pr}) \sin \phi_{cp} = 0, \\ K'_{ptp} &= K'_{pv} \cos^2 \theta_{vt}^{mp} + K'_{p\Delta} \sin^2 \theta_{vt}^{mp} + 2G'_{pv} \sin \theta_{vt}^{mp} \cos \theta_{vt}^{mp}, \\ G'_{ptp} &= -(K'_{pv} - K'_{p\Delta}) \sin \theta_{vt}^{mp} \cos \theta_{vt}^{mp} + G'_{pv} (\cos^2 \theta_{vt}^{mp} - \sin^2 \theta_{vt}^{mp}), \\ K'_{psp} &= K'_{pv} \sin^2 \theta_{vt}^{mp} + K'_{p\Delta} \cos^2 \theta_{vt}^{mp} - 2G'_{pv} \sin \theta_{vt}^{mp} \cos \theta_{vt}^{mp} \end{aligned} \right\} \quad (9.43)$$

Simultaneous equations (9.43) consist of nine equations, and there are ten parameters to be determined, i.e., x_{cp} , y_{cp} , z_{cp} , σ_p , ϕ_{cp} , ρ_{cp} , f_{mp} , L_p , $\delta \varepsilon_p^f$, and M_{mp} .

Hence, the value of ϕ_{cp} must be prescribed, and the remaining nine parameters are calculated.

Chapter 10

Summary of the Procedure for Design and Calculation

Given a pair of line-contacting surfaces, we select one surface as the fundamental surface, and use the other surface as the substituted surface. Then, from the requirements, we select a fundamental contact point and replace the substituted surface at the fundamental contact point by the substituting surface which shares the same unit normal with the substituted surface but whose curvature properties have been slightly modified. Consequently, a pair of new surfaces, i.e., the fundamental surface and the substituting surface, are obtained. Such a pair of surfaces is obviously a point-contacting pair.

Since the contact strength for a pair of point-contacting surfaces is low, much gearing in current use is designed with line-contacting surfaces. But a pair of line-contacting surfaces have the following two major defects: 1. high sensitivity to all kinds of inevitable errors; 2. difficulty to manufacture. Substitution of a pair of point-contacting surfaces for a pair of line-contacting surfaces can overcome the two shortcomings above, and meanwhile, preserve almost the same contact strength and the precision of transmission. This is based on the following two reasons:

1. These kinds of inevitable errors mentioned above are very small in value, so, very little modification to the curvatures is required in order to compensate for these errors. Thus, it is possible to eliminate the sensitivity to errors and to retain almost the original contact strength.

2. There are a few constraints to the substituting surface as follows: (1). The substituting surface must pass through the fundamental contact point; (2). The substituting surface must have the required unit normal at the fundamental contact point;

(3). The substituting surface should have the required curvature properties at the fundamental contact point. On the contrary, the constraints to a pair of line-contacting surfaces are much more stringent than those of a pair of point-contacting surfaces, for every point on a pair of line-contacting surfaces has to satisfy the requirement of conjugation. Therefore, a pair of point-contacting surfaces can be manufactured much more easily than a pair of line-contacting surfaces.

As stated before, the basic principle for this system of design and calculation can be summarized as the following points:

1. Design of the Gear Blank.

Use the gear tooth surface as the fundamental surface, select the reference point for calculation on the fundamental surface, and calculate the basic shape parameters and the gear blank parameters for the gear and the pinion respectively in order to determine the basic shapes and the scope of the tooth solid.

2. Determination of the Machine-Setting Parameters and the Cutter Parameters for the Gear.

According to the requirement for the unit normal to the gear tooth surface at the calculation reference point, determine the machine-setting parameters and the cutter parameters.

3. Analysis of the Tooth Surface Structure.

Select the fundamental contact point, and then calculate the curvature properties of the gear tooth surface at the fundamental contact point, and finally with the aid of the solution to the first type of the conjugate curvature problem, determine the curvature properties at the fundamental contact point of the pinion tooth surface for the state of line contact.

4. Calculation of the Curvature Modification.

Use the pinion tooth surface with the line contact as the substituted tooth surface, according to the requirement for the strength, the direction of the contact locus, the ability to absorb errors caused by elastic deformation and assembly, and the precision of transmission, carry out the curvature modification at the fundamental contact point to the pinion tooth surface in order to derive a pair of tooth surfaces with point contact.

5. Calculation of the Machine-Setting Parameters and the Cutter Parameters for the Pinion.

According to the requirements for the unit normal and the required curvature properties at the fundamental contact point of the pinion tooth surface, determine the machine-setting parameters and the cutter parameters for the pinion tooth surface.

Finally, from the above analysis, it can be concluded that this method can precisely control the position of the contact point, and make good use of all the parameters of adjustment provided by the Gleason No.16 Bevel-Gear Generator and approximately control the contact pattern. Other methods such as the Gleason Works and F. Litvin's methods need many cycles of trial and error through the TCA before they reach the required position of the contact point and the required contact pattern. In the present method, the machine settings can be calculated directly, to give contact at exactly the chosen fundamental point, and the specified curvature conditions.

Chapter 11

Immediate Future Challenge

So far, we have used the theory of conjugate surfaces to derive a pair of hypoid gears with point contact whose geometric properties and transmission properties at the fundamental contact point are controlled under comparatively ideal working conditions. In order to grasp comprehensively, deeply and precisely the performance of the hypoid gearing obtained in the whole course of transmission under realistic conditions, it is necessary to take into account not only the normal displacement caused by the profile error and the elastic deformation at the corresponding conjugate contact point but also the effect of the tangential location change of the conjugate contact point due to profile error and elastic deformation under dynamic loads. Obviously, the use of just the theory of conjugate surfaces is not sufficient to deal with this problem, and we have to perform analysis of dynamic loads on gear teeth with the aid of the theory of dynamics, which, as is well-known, deals with the laws of interrelationship between forces and kinematical motions, and the theory of elasticity, which, as is well-known, deals with the laws of interrelationship between forces and geometric configuration, and the aid of the theory of conjugate surfaces which deals with the laws of interrelationship between kinematical motion and geometric configuration. A general analytical theory to this problem has been given in reference [19]. Since three theories, i.e., theory of conjugate surfaces, theory of elasticity, and theory of dynamics, are involved, this analytical theory is called Conjugato-Elasto-Dynamics, or simply CED. This is, in the author's prediction, the direction of the future development.

Bibliography

- [1] Ernest Wildhaber, "Basic Relationship of Hypoid Gears," *American Machinist*, Vol. 90, No.4, February 14, 1946.
- [2] Ernest Wildhaber, "Basic Relationship of Hypoid Gears-II," *American Machinist*, Vol. 90, No.5, February 28, 1946.
- [3] Ernest Wildhaber, "Basic Relationship of Hypoid Gears-III," *American Machinist*, Vol. 90, No.6, March 14, 1946.
- [4] Chih-Hsin Chen, *Fundamentals of the Theory of Conjugate Surfaces*, Science Press, Beijing, 1985(in Chinese).
- [5] Chih-Hsin Chen, *Theory of Conjugate Surfaces*, Science Press, Peking, Vol.1, 1974, Vol. 2, 1977(in Chinese).
- [6] Chih-Hsin Chen, (Chen Ji-Shien), "On Theory of Conjugate Surfaces," *Proceedings of the Word Symposium on Gears and Gear Transmissions*, IFToM-MJuDEKO, Dubrovnik, Vol. A, 1978, pp. 119-132.
- [7] Chih-Hsin Chen, "Contact Pattern and Transmission Quality Analysis of Point Contact Conjugation With One Degree-of-Freedom," *ASME Journal of Mechanism, Transmission, and Automation in Design*, 1983, Vol. 105, pp, 392-399.
- [8] Chih-Hsin Chen, "Tooth Form of PK Conjugation — A New Design Concept for Gear Tooth Form," *Proceedings of the International Symposium on Gearing and Power Transmissions*, JSME, IFToMM, ASME. JSPE, Tokyo, Vol. I, 1981, pp. 11-15.
- [9] M.L. Baxter, "Basic Geometry and Tooth Contact of Hypoid Gears," *Industrial Mathematics*, Vol. 11, Part 2, 1961, pp. 19-42.
- [10] B. Shtipelman, *Design and Manufacture of Hypoid gears*, A wiley- interscience publication, John Wiley and Sons, 1978.

- [11] J.R. Colbourne "The Curvature of Helicoids," *Mech. Mach. Theory* Vol. 24, No. 3, pp. 213-221, 1989.
- [12] Gosselin C., Cloutier L., Sankar S. "On the Control of the Profile Kinematical Transmission Error in Spiral Bevel Gears Cut by the Gleason Method," 5th ASME Power Transmission and Gearing Conference, Chicago, April 1989.
- [13] Gosselin C., Cloutier L., Sankar S. "Effects of the Machine Settings on the Transmission Error of Spiral Bevel Gears Cut by the Gleason Method," 5th ASME Power Transmission and Gearing Conference, Chicago, April, 1989.
- [14] Gleason Works, "Understanding Tooth Contact Analysis," Gleason, Rochester (1981).
- [15] Gosselin C., Cloutier L., Nguyen D. "A General Formulation for the Calculation of the Load Sharing and Transmission Error under Load of Spiral Bevel and Hypoid Gears," *Mech. Mach Theory*, Vol. 30. No. 3. 1995.
- [16] Litvin. F., *Theory of Gearing*, NASA Reference Publication 1212, 1989.
- [17] Litvin. F., *Gear Geometry and Applied Theory*, Prentice Hall, 1994.
- [18] Stadtfeld, H.J. "Handbook of Bevel and Hypoid Gears," Rochester Institute of Technology, March, 1993.
- [19] AGMA, "Design Manual for Bevel Gears", ANSI/AGMA 2005-B88, 1989.
- [20] J.R. Colbourne "The Contact Stress in Novikov Gears," *Mech. Mach. Theory* Vol. 24, No. 3, pp. 223-229, 1989.
- [21] J.R. Colbourne, *The Geometry of Involute Gears*. Springer, New York, 1987.
- [22] J.R. Colbourne, "The Curvature of Surface Formed by a Cutting Edge," *Mech. Mach. Theory* Vol. 29, No. 5, pp. 767-775, 1994.
- [23] J.R. Colbourne "Compensating for Spindle Tilt in the Cutting of Spiral Bevel Gears". Pwc 1989 International Power Transmission and Gearing Conference, ASME, Chicago, PP 727-743.
- [24] C.J. Gosselin, L.Cloutier "The Generating Space for Parabolic Motion Error Spiral Bevel Gears Cut By the Gleason Method," *ASME Journal of Mechanical Design*, 1993, Vol. 115 483-489.

- [25] Chih-Hsin Chen, Yuri Wang, and J.R. Colbourne, " A General Formula for Determining the Normal to the Path of Contact in Parallel-Axis Gearing," DE-Vol. 43-2, International Power Transmission and Gearing Conference, ASME 1992.
- [26] Chih-Hsin Chen, "Applications of Algebra of Rotations in Robot Kinematics," Mech. Mach. Theory Vol. 22, No. 1, pp. 77-83, 1987.
- [27] Chih-Hsin Chen, "Analysis of Dynamic Loads on Gear Teeth by Conjugato-Elasto- Dynamics(CED)," ASME Journal of Mechanisms, Transmissions, and Automation in Design, 1988, Vol. 110, pp. 100-104.
- [28] The Gleason Works, "Calculating Instructions Formate Hypoid Gears," HFM-116, Gears Engineering Standard, Gleason Works, Rochester, N.Y., 1962.
- [29] The Gleason Works, "Calculating Instructions Generated Hypoid Gears," HGM-26, Gears Engineering Standard, Gleason Works, Rochester, N.Y., 1959.
- [30] The Gleason Works, "Method for Designing Hypoid Gear Blanks," Gleason Works, Rochester, N.Y., 1971.

Appendix A

Numerical Example

The original parameters for the design of a gear blank are quoted from AGMA standard. The figure in bracket refers to the number of equation in the thesis. The units of length is millimeters

A.1 Design of Gear Blank

Input parameters:

Item	Expression	Value
The Number of Gear Teeth	N_g	45
The Number of Pinion Teeth	N_p	11
The Hypoid Offset	f_{gp}	38.1
The Radial Distance of the Reference Point	ρ_b	117.29628
The Phase Angle of the Reference Point	μ_b	-72.829584°
The Axial Distance of the Reference Point	z_b	36.934075
The Face Width of the Gear	F_G	40.64
The Nominal Radius of Cutter	r_c	150

Intermediate Parameters and Output Parameters:

Item	Expression	Value
Transmission Ratio	$M_{gp} = \frac{N_g}{N_p}$ that is, expression (4.1)	4.090909091
Intermediate Parameter	$\rho_b \cos \mu_b - f_{gp}$	-3.472406499
Intermediate Parameter	$Q_b = \sqrt{(\rho_b \cos \mu_b - f_{gp})^2 + z_b^2 \cos^2 \mu_b}$ that is, expression (4.3)	11.44305792
Gear Pitch Angle	$\gamma_g = \arccos \frac{ \rho_b \cos \mu_b - f_{gp} }{Q_b}$ that is, expression (4.2)	72.335014°
The Radial Distance of Point P'_b	$\rho'_b = \sqrt{(\rho_b \cos \mu_b - f_{gp})^2 + z_b^2}$ that is, expression (4.4)	37.09694735
The Phase Angle of Point P'_b	$\tan \mu'_b = \frac{z_b}{\rho_b \cos \mu_b - f_{gp}}$ that is, expression (4.4)	-10.63644911
The Axial Distance of Point P'_b	$z'_b = -\rho_b \sin \mu_b$ that is, expression (4.4)	112.0684927
Pinion Pitch Angle	$\gamma_p = \arccos \frac{ \cos \mu_b \sqrt{(\rho_b \cos \mu_b - f_{gp})^2 + z_b^2} }{Q_b}$ that is, expression (4.5)	16.853544°
Relative Velocity at the Reference Point	$\mathbf{v}_b^{12} = v_{b1}^{12} \mathbf{i} + v_{b2}^{12} \mathbf{j} + v_{b3}^{12} \mathbf{k}$ $v_{b1}^{12} = -\rho_b \sin \mu_b - M_{gp} z_b$ $v_{b2}^{12} = \rho_b \cos \mu_b$ $v_{b3}^{12} = M_{gp} (\rho_b \cos \mu_b - f_{gp})$ $ \mathbf{v}_b^{12} = \sqrt{(v_{b1}^{12})^2 + (v_{b2}^{12})^2 + (v_{b3}^{12})^2}$ that is, expression (4.6)	-39.02545048 34.6275935 -14.20529931 54.07260439
The Generatrix of the Gear Reference Cone	$\mathbf{S}_b = S_{b1} \mathbf{i} + S_{b2} \mathbf{j} + S_{b3} \mathbf{k}$ $S_{b1} = \frac{z_b \cos^2 \mu_b}{Q_b}$ $S_{b2} = \frac{z_b \cos \mu_b \sin \mu_b}{Q_b}$ $S_{b3} = -\frac{\rho_b \cos \mu_b - f_{gp}}{Q_b}$ that is, expression (4.7)	0.281294521 -0.910379551 0.303450924
Gear Spiral Angle	$\psi_g = \arccos \frac{ v_{b1}^{12} S_{b1} + v_{b2}^{12} S_{b2} + v_{b3}^{12} S_{b3} }{ \mathbf{v}_b^{12} }$ that is, expression (4.7)	30.033337°

The Generatrix of the Pinion Reference Cone	$\mathbf{S}'_b = S'_{b1}\mathbf{i} + S'_{b2}\mathbf{j} + S'_{b3}\mathbf{k}$ $S'_{b1} = \frac{(\rho_b \cos \mu_b - f_{gp})^2 \sin \mu_b}{Q_b \sqrt{(\rho_b \cos \mu_b - f_{gp})^2 + z_b^2}}$ $S'_{b2} = \frac{z_b (\rho_b \cos \mu_b - f_{gp}) \sin \mu_b}{Q_b \sqrt{(\rho_b \cos \mu_b - f_{gp})^2 + z_b^2}}$ $S'_{b3} = \frac{\cos \mu_b \sqrt{(\rho_b \cos \mu_b - f_{gp})^2 + z_b^2}}{Q_b}$	-0.027138144 0.288653487 0.957048945
Relative Velocity at the reference point	<p>that is, expression (4.9)</p> $\mathbf{v}_b^{12} = v_{b1'}^{12}\mathbf{i}' + v_{b2'}^{12}\mathbf{j}' + v_{b3'}^{12}\mathbf{k}'$ $v_{b1'}^{12} = v_{b1}^{12}$ $v_{b2'}^{12} = v_{b3}^{12}$ $v_{b3'}^{12} = -v_{b2}^{12}$	-39.02545048 -14.20529931 -34.6275935
Pinion Spiral Angle	<p>that is, expression (4.10)</p> $\psi_p = \arccos \frac{ S'_{b1}v_{b1'}^{12} + S'_{b2}v_{b2'}^{12} + S'_{b3}v_{b3'}^{12} }{ \mathbf{v}_b^{12} }$	132°
Conjugate Acceleration of Reference Point P_b	<p>that is, expression (4.11)</p> $\mathbf{J}_b = J_{b1}\mathbf{i} + J_{b2}\mathbf{j} + J_{b3}\mathbf{k}$ $J_{b1} = 0$ $J_{b2} = -M_{gp}z_b$ $J_{b3} = M_{gp}\rho_b \sin \mu_b$	0 -151.0939432 -458.4620156
Unit Normal to the Gear Blank Pitch Surface	<p>that is, expression (4.12)</p> $\mathbf{N}_{1b} = A_b\mathbf{i} + B_b\mathbf{j} + C_b\mathbf{k}$ $A_b = -\frac{(\rho_b \cos \mu_b - f_{gp}) \cos \mu_b}{Q_b}$ $B_b = -\frac{(\rho_b \cos \mu_b - f_{gp}) \sin \mu_b}{Q_b}$ $C_b = -\frac{z_b \cos \mu_b}{Q_b}$	0.089583192 -0.289926395 -0.952847068
Intermediate Parameters	<p>that is, expression (4.13)</p> $\mathbf{t} = t_1\mathbf{i} + t_2\mathbf{j} + t_3\mathbf{k}$ $t_1 = S_{b1} \cos \psi_g - (B_b S_{b3} - C_b S_{b2}) \sin \psi_g$ $t_2 = S_{b2} \cos \psi_g - (C_b S_{b1} - A_b S_{b3}) \sin \psi_g$ $t_3 = S_{b3} \cos \psi_g - (A_b S_{b2} - B_b S_{b1}) \sin \psi_g$	0.721723152 -0.640390709 0.26270788
Limit Pressure Angle	<p>that is, expression (3.48)</p> $\tan \phi_o = \frac{\left\{ \begin{array}{l} \rho_b(t_1 B_b - t_2 A_b) \sin \mu_b \\ -z_b(t_3 A_b - t_1 C_b) \end{array} \right\}}{\rho_b C_b \sin \mu_b - z_b B_b}$ <p>that is, expression (4.14)</p>	-4.5004158°

Average Pressure Angle of Gear	$\Phi_g = \phi_{gm}$ that is, expression (4.17)	20°
Gear Pressure Angle on Convex Side	$\phi_{gi} = \phi_{gm} + \phi_o$ that is, expression (4.15)	15.499584°
Gear Pressure Angle on Concave Side	$\phi_{go} = 180^\circ - \phi_{gm} + \phi_o$ that is, expression (4.16)	155.49958°
Depth Factor	k_1 that is, table 6-1 in AGMA standard	2.0
Mean Addendum Factor	c_1 that is, table 6-2 in AGMA standard	0.2384
Clearance Factor	k_2 that is, section 6.5 in AGMA standard	0.125
Mean Working Depth	$h = \frac{2k_1\rho_b \cos \psi_g}{N_g}$ that is, expression (4.18)	9.0264373
Mean Addendum for Gear	$a_g = c_1 h$ that is, expression (4.19)	2.1519026
Mean Addendum for Pinion	$a_p = h - a_g$ that is, expression (4.20)	6.8745347
Mean Dedendum for Gear	$b_g = h(1 + k_2 - c_1)$ that is, expression (4.21)	8.0028393
Mean Dedendum for Pinion	$b_p = b_g + a_g - a_p$ that is, expression (4.22)	3.28020721
Clearance	$c = k_2 h$ that is, expression (4.23)	1.1283047
Mean Pitch Cone Distance	$A_{mG} = \frac{\rho_b}{\sin \gamma_g}$ that is, expression (4.38)	123.1008416
Sum of Dedendum Angles	$\Sigma\delta_D = \frac{\pi \sin \gamma_g}{N_g \tan \Phi_g \cos \psi_g } (1 - \frac{A_{mG} \sin \psi_g}{r_c})$ that is, expression (4.39)	7.1274237°
Dedendum Angle of Gear	$\delta_g = \Sigma\delta_D - \Sigma\delta_D(\frac{a_g}{h})$ that is, expression (4.43)	5.4282459°
Addendum Angle of Gear	$\alpha_g = \Sigma\delta_D - \delta_g$ that is, expression (4.44)	1.6991778°
Face Angle of Gear	$\gamma_{gf} = \gamma_g + \alpha_g$ that is, expression (4.45)	74.0341918°
Root Angle of Gear	$\gamma_{gr} = \gamma_g - \delta_g$ that is, expression (4.46)	66.9067681°
Pitch Apex Beyond Crossing Point	$Z_{go} = z_b - \frac{\rho_b}{\tan \gamma_g}$ that is, expression (4.47)	-0.4209788

Face Apex Beyond Crossing Point	$Z_{gf} = z_b - \left(\frac{\rho_b + a_g \cos \gamma_g}{\tan \gamma_{gf}} + a_g \sin \gamma_g \right)$ that is, expression (4.48)	1.138391799
Root Apex Beyond Crossing Point	$Z_{gr} = z_b - \left(\frac{\rho_b - b_g \cos \gamma_g}{\tan \gamma_{gr}} - b_g \sin \gamma_g \right)$ that is, expression (4.49)	-4.41967989
Intermediate Para- meters	$\rho_D = \rho_b - (b_g - c) \cos \gamma_g$ $z_D = z_b + (b_g - c) \sin \gamma_g$ that is, expression (4.50)	115.2101968 43.48445536
Intermediate Para- meters	$\cos \mu_D = \frac{f_{gp} \tan \gamma_{gr}}{z_D + \rho_D \tan \gamma_{gr}}$ that is, expression (4.51)	0.284855941
	$Q_D = \sqrt{(\rho_D \cos \mu_D - f_{gp})^2 + z_D^2 \cos^2 \mu_D}$ that is, expression (4.53)	13.46585344
Face Angle of Pinion	$\gamma_{pf} = \arccos \left \frac{\cos \mu_D \sqrt{(\rho_D \cos \mu_D - f_{gp})^2 + z_D^2}}{Q_D} \right $ that is, expression (4.52)	22.08480729
Intermediate Para- meters	$\rho_t = \rho_b + (a_g + c) \cos \gamma_g$ $z_t = z_b - (a_g + c) \sin \gamma_g$ that is, expression (4.54)	118.2916616 33.80853899
Intermediate Para- meters	$\cos \mu_t = \frac{f_{gp} \tan \gamma_{gf}}{z_t + \rho_t \tan \gamma_{gf}}$ that is, expression (4.55)	0.297739353
	$Q_t = \sqrt{(\rho_t \cos \mu_t - f_{gp})^2 + z_t^2 \cos^2 \mu_t}$ that is, expression (4.57)	10.47000225
Root Angle of Pinion	$\gamma_{pr} = \arccos \left \frac{\cos \mu_t \sqrt{(\rho_t \cos \mu_t - f_{gp})^2 + z_t^2}}{Q_t} \right $ that is, expression (4.56)	15.22372558
Intermediate Para- meters	$\rho'_D = \sqrt{(\rho_D \cos \mu_D - f_{gp})^2 + z_D^2}$ that is, expression (4.59)	43.8040225
Face Apex Beyond Crossing Point	$Z_{pf} = -\rho_D \sin \mu_D - \frac{\rho'_D}{\tan \gamma_{pf}}$ that is, expression (4.58)	2.478663941
Intermediate Para- meters	$\rho'_t = \sqrt{(\rho_t \cos \mu_t - f_{gp})^2 + z_t^2}$ that is, expression (4.61)	33.93097746
Root Apex Beyond Crossing Point	$Z_{pr} = -\rho_t \sin \mu_t - \frac{\rho'_t}{\tan \gamma_{pr}}$ that is, expression (4.60)	-11.7558611

A.2 Machine-Setting Parameters for Gear

The input parameters were obtained in the design of the gear blank together with the following parameters:

Item	Expression	Value
Outer Blade Angle	ϕ_c^o	160°
Inner Blade Angle	ϕ_c^i	14°

Output Parameters:

Item	Expression	Value
Vertical Position of Gear	f_{mg}	0.87699787
Horizontal Position of Gear	that is, by solving equations (5.44) L	-14.094601
The Point Width of Cutter	W_p	1.7458611
The Ratio of Roll	that is, by solving equations (5.44) M_{mg}	-1.0121695
The Phase Angles for Gear Cutting Position	ε_g^o	95.2441723°
	ε_g^i	78.46167698°
The Phase Angles for Cutting Edge	that is, by solving equations (5.44) σ^o	36.40313597°
	σ^i	17.4713471°
The Coordinates of Cutter Center at the Cutting Position	that is, by solving equations (5.44) x_c^o	-133.55318
	y_c^o	25.186956
	z_c^o	-24.805069
	x_c^i	-116.23481
	y_c^i	70.429421
	z_c^i	-24.067896
Unit Normal to the Cutter Surfaces	$N_c = N_{cx}i_m + N_{cy}j_m + N_{cz}k_m$ $N_{cx}^o = -\cos \phi_c^o \cos \sigma^o$ $N_{cy}^o = -\cos \phi_c^o \sin \sigma^o$ $N_{cz}^o = \sin \phi_c^o$ $N_{cx}^i = -\cos \phi_c^i \cos \sigma^i$ $N_{cy}^i = -\cos \phi_c^i \sin \sigma^i$ $N_{cz}^i = \sin \phi_c^i$ that is, expression (5.13)	0.756322233 0.557672745 0.342020143 -0.925533277 -0.291310741 0.241921895

Intermediate Parameters:

Item	Expression	Value
Unit Normal to the Gear	$\mathbf{N}_g = N_{gx}\mathbf{i} + N_{gy}\mathbf{j} + N_{gz}\mathbf{k}$	
Tooth Surfaces	$N_{gx}^o = (\sin \phi_{go} \cos \gamma_g + \cos \phi_{go} \sin \psi_g \sin \gamma_g) \cos \varepsilon_g^o + \cos \phi_{go} \cos \psi_g \sin \varepsilon_g^o$	-0.756322219
	$N_{gy}^o = (\sin \phi_{go} \cos \gamma_g + \cos \phi_{go} \sin \psi_g \sin \gamma_g) \sin \varepsilon_g^o - \cos \phi_{go} \cos \psi_g \cos \varepsilon_g^o$	-0.378835142
	$N_{gz}^o = \cos \phi_{go} \sin \psi_g \cos \gamma_g - \sin \phi_{go} \sin \gamma_g$	-0.533348509
	$N_{gx}^i = (\sin \phi_{gi} \cos \gamma_g + \cos \phi_{gi} \sin \psi_g \sin \gamma_g) \cos \varepsilon_g^i + \cos \phi_{gi} \cos \psi_g \sin \varepsilon_g^i$	0.925533288
	$N_{gy}^i = (\sin \phi_{gi} \cos \gamma_g + \cos \phi_{gi} \sin \psi_g \sin \gamma_g) \sin \varepsilon_g^i - \cos \phi_{gi} \cos \psi_g \cos \varepsilon_g^i$	0.362855997
	$N_{gz}^i = \cos \phi_{gi} \sin \psi_g \cos \gamma_g - \sin \phi_{gi} \sin \gamma_g$	-0.108275803
Cutter Radius	that is, expression (5.20)	
	$-N_{cy}^o \sin \gamma_{gr} + N_{cz}^o \cos \gamma_{gr}$	-0.378835187
	$-N_{cy}^o \cos \gamma_{gr} - N_{cz}^o \sin \gamma_{gr}$	-0.533348449
	$-N_{cy}^i \sin \gamma_{gr} + N_{cz}^i \cos \gamma_{gr}$	0.362856032
	$-N_{cy}^i \cos \gamma_{gr} - N_{cz}^i \sin \gamma_{gr}$	-0.108275802
	that is, condition (5.24) is satisfied	
	$\rho_c^o = r_c - [(L + Z_{gr}) \sin \gamma_{gr} - z_c^o] \tan \phi_c^o + \frac{W_p}{2}$	153.7025726
	$\rho_c^i = r_c - [(L + Z_{gr}) \sin \gamma_{gr} - z_c^i] \tan \phi_c^i - \frac{W_p}{2}$	147.3724974
Cutting Position	that is, expression (5.46)	
	$\mathbf{R}_{mb} = (x_c + \rho_c \cos \sigma)\mathbf{i}_m + (y_c + \rho_c \sin \sigma)\mathbf{j}_m + z_c\mathbf{k}_m$	
	$x_c^o + \rho_c^o \cos \sigma^o$	-9.843925059
	$y_c^o + \rho_c^o \sin \sigma^o$	116.4037366
	z_c^o	-24.805069
	$x_c^i + \rho_c^i \cos \sigma^i$	24.33898303
	$y_c^i + \rho_c^i \sin \sigma^i$	114.674892
	z_c^i	-24.067896
	that is expression (5.12)	
	$\mathbf{R}_{gb} = \rho_b \cos \varepsilon_g \mathbf{i} + \rho_b \sin \varepsilon_g \mathbf{j} + (z_b + L)\mathbf{k}$ $\rho_b \cos \varepsilon_g^o$	-10.72091897

Velocities of Cutter relative to Gear	$\rho_b \sin \varepsilon_g^o$	116.8053047
	$z_b + L$	22.839474
	$\rho_b \cos \varepsilon_g^i$	23.46199194
	$\rho_b \sin \varepsilon_g^i$	114.9258554
	that is, expression (5.19)	
	$x_c^o + \rho_c^o \cos \sigma^o - f_{mg}$	-10.72092293
	$(y_c^o + \rho_c^o \sin \sigma^o) \sin \gamma_{gr} - z_c^o \cos \gamma_{gr}$	116.8053073
	$(y_c^o + \rho_c^o \sin \sigma^o) \cos \gamma_{gr} + z_c^o \sin \gamma_{gr}$	22.83947313
	$x_c^i + \rho_c^i \cos \sigma^i - f_{mg}$	23.46198516
	$(y_c^i + \rho_c^i \sin \sigma^i) \sin \gamma_{gr} - z_c^i \cos \gamma_{gr}$	114.9258585
Center Distance From Cradle to Cutter The Phase Angle of the Cutter Center	$(y_c^i + \rho_c^i \sin \sigma^i) \cos \gamma_{gr} + z_c^i \sin \gamma_{gr}$	22.83947281
	that is, equation (5.22) is satisfied	
	$\mathbf{v}_b^{mg} = v_x^{mg} \mathbf{i}_m + v_y^{mg} \mathbf{j}_m + v_z^{mg} \mathbf{k}_m$	
	$v_{xo}^{mg} = M_{mg} z_c^o \cos \gamma_{gr}$	1.823032917
	$-(1 + M_{mg} \sin \gamma_{gr})(y_c^o + \rho_c^o \sin \sigma^o)$	
	$v_{yo}^{mg} = (1 + M_{mg} \sin \gamma_{gr})(x_c^o + \rho_c^o \cos \sigma^o)$	0.137920685
	$-M_{mg} f_{mg} \sin \gamma_{gr}$	
	$v_{zo}^{mg} = -M_{mg}(x_c^o + \rho_c^o \cos \sigma^o) \cos \gamma_{gr}$	-4.256224452
	$+M_{mg} f_{mg} \cos \gamma_{gr}$	
	$v_{xi}^{mg} = M_{mg} z_c^i \cos \gamma_{gr}$	1.649556794
Ratio of Roll	$-(1 + M_{mg} \sin \gamma_{gr})(y_c^i + \rho_c^i \sin \sigma^i)$	
	$v_{yi}^{mg} = (1 + M_{mg} \sin \gamma_{gr})(x_c^i + \rho_c^i \cos \sigma^i)$	2.49441626
	$-M_{mg} f_{mg} \sin \gamma_{gr}$	
	$v_{zi}^{mg} = -M_{mg}(x_c^i + \rho_c^i \cos \sigma^i) \cos \gamma_{gr}$	9.314447609
	$+M_{mg} f_{mg} \cos \gamma_{gr}$	
	that is, expression (5.26)	
	$N_{cx}^o v_{xo}^{mg} + N_{cy}^o v_{yo}^{mg} + N_{cz}^o v_{zo}^{mg}$	0.000000437
	$N_{cx}^i v_{xi}^{mg} + N_{cy}^i v_{yi}^{mg} + N_{cz}^i v_{zi}^{mg}$	-0.000001137
	that is, condition (5.28) is satisfied	
	$\sqrt{(x_c^o)^2 + (y_c^o)^2}$	135.9074488
Ratio of Roll	$\sqrt{(x_c^i)^2 + (y_c^i)^2}$	135.9074479
	that is, condition (5.35) is satisfied	
	$\varepsilon_c^o = \arctan \frac{y_c^o}{x_c^o}$	169.3199583
	$\varepsilon_c^i = \arctan \frac{y_c^i}{x_c^i}$	148.7873364
	that is, expression (5.37)	
	$T_g = \frac{180}{N_g}$	4°
	$M_{mg} = \frac{T_g + \varepsilon_g^o - \varepsilon_g^i}{\varepsilon_c^i \varepsilon_c^o}$	-1.012169579
	that is, condition (5.38) is satisfied	

A.3 Calculation of Curvatures for the Gear Tooth Surface

Input parameters were obtained in the previous sections.

Output Parameters and Intermediate Parameters:

(All calculations from A.3 to A.6 correspond to the concave face of the gear and the convex face of pinion).

Item	Expression	Value
The Position of the Fundamental Contact Point	ξ_f	0
	a_f	0
	$\rho_f = \rho_b$	117.29628
	$z_f = z_b$	36.934075
	$\varepsilon_g^f = \varepsilon_g^o$	95.2441723°
	$x_c^f = x_c^o$	-133.55318
	$y_c^f = y_c^o$	25.186956
	$z_c^f = z_c^o$	-24.805069
	$\rho_c^f = \rho_c^o$	153.7025726
	$\sigma^f = \sigma^o$	36.40313597°
The Tangential Direction to the Cutting Edge	$\mathbf{W} = W_1 \mathbf{i}_m + W_2 \mathbf{j}_m + W_3 \mathbf{k}_m$	
	$W_1 = \sin \phi_c^o \cos \sigma^f$	0.275278782
	$W_2 = \sin \phi_c^o \sin \sigma^f$	0.202976279
	$W_3 = \cos \phi_c^o$	-0.93969262
Relative Velocity of Fundamental Contact Point	that is, expression (6.50)	
	$\mathbf{v}_f^{mg} = v_{f1}^{mg} \mathbf{i}_m + v_{f2}^{mg} \mathbf{j}_m + v_{f3}^{mg} \mathbf{k}_m$	
	$v_{f1}^{mg} = v_{x0}^{mg}$	1.823032917
	$v_{f2}^{mg} = v_{y0}^{mg}$	0.137920685
	$v_{f3}^{mg} = v_{z0}^{mg}$	-4.256224452
	$ \mathbf{v}_f^{mg} = \sqrt{(v_{f1}^{mg})^2 + (v_{f2}^{mg})^2 + (v_{f3}^{mg})^2}$	4.632269176
Intermediate Parameters	that is, expression (6.36)	
	$\cos \theta_{wv} = \frac{v_{f1}^{mg} W_1 + v_{f2}^{mg} W_2 + v_{f3}^{mg} W_3}{ \mathbf{v}_f^{mg} }$	0.977788518
	$\sin \theta_{wv} = \frac{-v_{f1}^{mg} \sin \sigma^f + v_{f2}^{mg} \cos \sigma^f}{ \mathbf{v}_f^{mg} }$	-0.209593919
	that is, expression (6.53)	
Curvatures of the Cutter Surface in Direction $\frac{\mathbf{v}_f^{mg}}{ \mathbf{v}_f^{mg} }$ and Δ_f	$K_{1v} = -\frac{\cos \phi_c^o}{\rho_c^f} \sin^2 \theta_{wv}$	0.268572×10^{-3}
	$G_{1v} = -\frac{\cos \phi_c^o}{\rho_c^f} \sin \theta_{wv} \cos \theta_{wv}$	$-0.1252934 \times 10^{-2}$
	$K_{1\Delta} = -\frac{\cos \phi_c^o}{\rho_c^f} \cos^2 \theta_{wv}$	0.5845134×10^{-2}
	that is, expression (6.54)	

Intermediate Parameters	$\eta_f = \eta_{f1}\mathbf{i}_m + \eta_{f2}\mathbf{j}_m + \eta_{f3}\mathbf{k}_m$	
	$\eta_{f1} = -N_{cy}^f(1 + M_{mg} \sin \gamma_{gr})$	-0.174227322
	$+ N_{cz}^f M_{mg} \cos \gamma_{gr}$	
	$\eta_{f2} = N_{cx}^f(1 + M_{mg} \sin \gamma_{gr})$	0.052139215
	$\eta_{f3} = -N_{cx}^f M_{mg} \cos \gamma_{gr}$	0.300261199
	$ \eta_f = \sqrt{\eta_{f1}^2 + \eta_{f2}^2 + \eta_{f3}^2}$	0.351041941
	that is, expression (6.57)	
	$\sin \theta_{v\eta} = -\frac{M_{mg} f_{mg} \cos \gamma_{gr}}{ \mathbf{v}_f^{mg} \eta_f }$	0.214110562
	$\cos \theta_{v\eta} = \frac{v_{f1}^{mg} \eta_{f1} + v_{f2}^{mg} \eta_{f2} + v_{f3}^{mg} \eta_{f3}}{ \mathbf{v}_f^{mg} \eta_f }$	-0.976809447
	that is, expression (6.58)	
	$\mathbf{J}_f = J_{f1}\mathbf{i}_m + J_{f2}\mathbf{j}_m + J_{f3}\mathbf{k}_m$	
	$J_{f1} = M_{mg} f_{mg} \sin \gamma_{gr}$	-0.81653953
	$J_{f2} = M_{mg} z_c^f \cos \gamma_{gr}$	9.8476544
	$J_{f3} = -M_{mg} (y_c^f + \rho_c^f \sin \sigma^f) \cos \gamma_{gr}$	46.21248
Conjugate Curvatures of Gear Tooth Surface in Directions $\frac{\mathbf{v}_f^{mg}}{ \mathbf{v}_f^{mg} }$ and Δ_f Curvatures of Gear Tooth Surface	that is, expression (6.61)	
	$\mathbf{N}_c^f \cdot \mathbf{J}_f = N_{cx}^f J_{f1} + N_{cy}^f J_{f2} + N_{cz}^f J_{f3}$	20.67980014
	that is, expression (6.62)	
	$D_p = K_{1v} \mathbf{v}_f^{mg} - \eta_f \cos \theta_{v\eta}$	0.34414519
	$E_p = G_{1v} \mathbf{v}_f^{mg} - \eta_f \sin \theta_{v\eta}$	-0.080965733
	that is, expression (6.63)	
	$K'_{gv} = \frac{D_p^2}{D_p \mathbf{v}_f^{mg} + \mathbf{N}_c^f \cdot \mathbf{J}_f} - K_{1v}$	0.50486606 $\times 10^{-2}$
	$G'_{gv} = \frac{D_p E_p}{D_p \mathbf{v}_f^{mg} + \mathbf{N}_c^f \cdot \mathbf{J}_f} - G_{1v}$	0.1968525 $\times 10^{-5}$
	$K'_{g\Delta} = \frac{E_p^2}{D_p \mathbf{v}_f^{mg} + \mathbf{N}_c^f \cdot \mathbf{J}_f} - K_{1\Delta}$	-0.55508254 $\times 10^{-2}$
	that is, expression (6.64)	
	$K_{gv} = K'_{gv}$	
	$G_{gv} = -G'_{gv}$	
	$K_{g\Delta} = K'_{g\Delta}$	
	that is, expression (6.65)	

Intermediate	$Q_{gr} = - \sqrt{ \begin{aligned} &(N_{gy}^f \sin \gamma_{gr} + N_{gz}^f \cos \gamma_{gr} \sin \varepsilon_g^f)^2 \\ &+ (N_{gz}^f \cos \gamma_{gr} \cos \varepsilon_g^f + N_{gx}^f \sin \gamma_{gr})^2 \\ &+ (N_{gx}^f \cos \gamma_{gr} \sin \varepsilon_g^f \\ &- N_{gy}^f \cos \gamma_{gr} \cos \varepsilon_g^f)^2 \end{aligned} }$	-0.929128813
Parameters	$\mathbf{t}_{gr} = t_{gr1}\mathbf{i} + t_{gr2}\mathbf{j} + t_{gr3}\mathbf{k}$ $t_{gr1} = - \frac{N_{gy}^f \sin \gamma_{gr} + N_{gz}^f \cos \gamma_{gr} \sin \varepsilon_g^f}{Q_{gr}}$ $t_{gr2} = \frac{N_{gz}^f \cos \gamma_{gr} \cos \varepsilon_g^f + N_{gx}^f \sin \gamma_{gr}}{Q_{gr}}$ $t_{gr3} = \frac{N_{gx}^f \cos \gamma_{gr} \sin \varepsilon_g^f - N_{gy}^f \cos \gamma_{gr} \cos \varepsilon_g^f}{Q_{gr}}$ <p>that is expression (6.67)</p> $\sin \theta_{vt} = \frac{ \left\{ \begin{aligned} &v_{f1}^{mg}(t_{gr2}N_{gz}^f - \\ &t_{gr3}N_{gy}^f) + (t_{gr3}N_{gx}^f \\ &- t_{gr1}N_{gz}^f)(v_{f2}^{mg} \sin \gamma_{gr} \\ &- v_{f3}^{mg} \cos \gamma_{gr}) + \\ &(t_{gr1}N_{gy}^f - t_{gr2}N_{gx}^f) \\ &(v_{f2}^{mg} \cos \gamma_{gr} + \\ &v_{f3}^{mg} \sin \gamma_{gr}) \end{aligned} \right\} }{ v_f^{mg} }$ $\cos \theta_{vt} = \frac{ \left\{ \begin{aligned} &t_{gr1}v_{f1}^{mg} + t_{gr2} \\ &(v_{f2}^{mg} \sin \gamma_{gr} - \\ &v_{f3}^{mg} \cos \gamma_{gr}) + \\ &t_{gr3}(v_{f2}^{mg} \cos \gamma_{gr} \\ &+ v_{f3}^{mg} \sin \gamma_{gr}) \end{aligned} \right\} }{ v_f^{mg} }$ <p>that is, expression (6.72)</p>	-0.599267912 0.72820477 0.33255944 -0.97303546 -0.23065557
Curvatures	$K_{gt} = K_{gv} \cos^2 \theta_{vt} + K_{g\Delta} \sin^2 \theta_{vt} + 2G_{gv} \sin \theta_{vt} \cos \theta_{vt}$	-0.49877952 ×10 ⁻²
of Gear in	$G_{gt} = -(K_{gv} - K_{g\Delta}) \sin \theta_{vt} \cos \theta_{vt} + G_{gv}(\cos^2 \theta_{vt} - \sin^2 \theta_{vt})$	-0.23771477 ×10 ⁻²
Directions	$K_{gs} = K_{gv} \sin^2 \theta_{vt} + K_{g\Delta} \cos^2 \theta_{vt} - 2G_{gv} \sin \theta_{vt} \cos \theta_{vt}$ <p>that is, expression (6.73)</p>	0.44856304 ×10 ⁻²
\mathbf{t}_{gr} and $\mathbf{N}_g^f \times \mathbf{t}_{gr}$		

A.4 Calculation of Curvatures for the Pinion Tooth Surface with Line Contact

Input parameters are all obtained in the previous sections.

Output Parameters and Intermediate Parameters:

Item	Expression	Value
The Increment of Rotating Angle	$U_{gp} = N_{gz}^f M_{gp} \rho_f \cos \varepsilon_g^f - N_{gx}^f M_{gp} z_f$	137.6674679
	$V_{gp} = N_{gz}^f M_{gp} \rho_f \sin \varepsilon_g^f - N_{gy}^f M_{gp} z_f$	-197.6154936
	$W_{gp} = N_{gx}^f \rho_f \sin \varepsilon_g^f + N_{gz}^f M_{gp} f_{gp} - N_{gy}^f \rho_f \cos \varepsilon_g^f$	-175.5335461
	that is, expression (7.4) $\delta \varepsilon_g = \arccos\left(\frac{W_{gp}}{\sqrt{U_{gp}^2 + V_{gp}^2}}\right) - \arctan\left(\frac{V_{gp}}{U_{gp}}\right)$	191.9262439°
Contact Position of Fundamental Contact Point	that is, expression (7.3) $\mathbf{R}_{gp}^f = [(\varepsilon_g^f + \delta \varepsilon_g) \mathbf{k}] \otimes (\rho_f \mathbf{i} + z_f \mathbf{k})$	
	$x_{gp}^f = \rho_f \cos(\varepsilon_g^f + \delta \varepsilon_g)$	34.627594
	$y_{gp}^f = \rho_f \sin(\varepsilon_g^f + \delta \varepsilon_g)$	-112.0684926
	$z_{gp}^f = z_f$	36.934075
Corresponding Unit Normal	that is, expression (7.1) $\mathbf{N}_{gp}^f = (\delta \varepsilon_g \mathbf{k}) \otimes \mathbf{N}_g^f$	
	$N_{gpx}^f = N_{gx}^f \cos \delta \varepsilon_g - N_{gy}^f \sin \delta \varepsilon_g$	0.661709394
	$N_{gpy}^f = N_{gx}^f \sin \delta \varepsilon_g + N_{gy}^f \cos \delta \varepsilon_g$	0.526953544
	$N_{gpz}^f = N_{gz}^f$	-0.533348509
Contact Position in Pinion Coordinate System	that is, expression (7.2) $\mathbf{R}_p^f = x_p^f \mathbf{i}' + y_p^f \mathbf{j}' + z_p^f \mathbf{k}'$	
	$x_p^f = x_{gp}^f - f_{gp}$	-3.47240596
	$y_p^f = z_{gp}^f$	36.934075
	$z_p^f = -y_{gp}^f$	112.0684926
Phase Angle of Contact Point	that is, expression (7.5) $\sin \varepsilon_p^f = \frac{y_p^f}{\sqrt{(x_p^f)^2 + (y_p^f)^2}}$	0.995609549
	$\cos \varepsilon_p^f = \frac{x_p^f}{\sqrt{(x_p^f)^2 + (y_p^f)^2}}$	-0.093603549
Unit Normal to the Pinion Tooth Surface	that is, expression (7.6) $\mathbf{N}_p^f = -\mathbf{N}_{gp}^f = N_{px}^f \mathbf{i}' + N_{py}^f \mathbf{j}' + N_{pz}^f \mathbf{k}'$	
	$N_{px}^f = -N_{gpx}^f$	-0.661709394
	$N_{py}^f = -N_{gpy}^f$	0.533348509
	$N_{pz}^f = N_{gpz}^f$	0.526953544
	that is, expression (7.7)	

Intermediate Parameters	$\psi_{pr} = \arctan \frac{\left\{ \begin{array}{l} N_{gpy}^f \cos \gamma_{pr} - \\ (N_{gpx}^f \cos \varepsilon_p^f + N_{gpz}^f \sin \varepsilon_p^f) \sin \gamma_{pr} \end{array} \right\}}{N_{gpx}^f \cos \varepsilon_p^f - N_{gpz}^f \sin \varepsilon_p^f}$ $\sin \phi_{pr} = -\frac{(N_{gpx}^f \cos \varepsilon_p^f + N_{gpz}^f \sin \varepsilon_p^f) \cos \gamma_{pr} - N_{gpy}^f \sin \gamma_{pr}}{\cos \psi_{pr}}$ $\cos \phi_{pr} = \frac{N_{gpx}^f \cos \varepsilon_p^f - N_{gpz}^f \sin \varepsilon_p^f}{\cos \psi_{pr}}$	132.5135127° 0.43376541 0.901025825
Velocity of Gear with Respect to Pinion	<p>that is, expression (7.10)</p> $\mathbf{v}_f^{gp} = v_{f1}^{gp} \mathbf{i} + v_{f2}^{gp} \mathbf{j} + v_{f3}^{gp} \mathbf{k}$ $v_{f1}^{gp} = -\rho_f \sin(\varepsilon_g^f + \delta \varepsilon_g) - M_{gp} z_f$ $v_{f2}^{gp} = \rho_f \cos(\varepsilon_g^f + \delta \varepsilon_g)$ $v_{f3}^{gp} = M_{gp} \rho_f \cos(\varepsilon_g^f + \delta \varepsilon_g) - M_{gp} f_{gp}$ $ \mathbf{v}_f^{gp} = \sqrt{(v_{f1}^{gp})^2 + (v_{f2}^{gp})^2 + (v_{f3}^{gp})^2}$	-39.02545048 34.62759404 -14.20529711 54.07260416
Conjugate Acceleration	<p>that is, expression (7.11)</p> $\mathbf{J}_p = J_{p1} \mathbf{i} + J_{p2} \mathbf{j} + J_{p3} \mathbf{k}$ $J_{p1} = 0$ $J_{p2} = -M_{gp} z_f$ $J_{p3} = M_{gp} \rho_f \sin(\varepsilon_g^f + \delta \varepsilon_g)$	0 -151.0939432 -458.4620152
Intermediate Parameters	<p>that is, expression (7.12)</p> $\mathbf{J}_p \cdot \mathbf{N}_{gp}^f = N_{gpy}^f J_{p2} + N_{gpz}^f J_{p3}$ <p>that is, expression (7.13)</p> $\eta_p = \eta_{p1} \mathbf{i} + \eta_{p2} \mathbf{j} + \eta_{p3} \mathbf{k}$ $\eta_{p1} = -N_{gpy}^f - N_{gpz}^f M_{gp}$ $\eta_{p2} = N_{gpx}^f$ $\eta_{p3} = N_{gpz}^f M_{gp}$ $ \eta_p = \sqrt{\eta_{p1}^2 + \eta_{p2}^2 + \eta_{p3}^2}$ <p>that is, expression (7.14)</p> $\mathbf{t}_{gr}^f = t_{gr1}^f \mathbf{i} + t_{gr2}^f \mathbf{j} + t_{gr3}^f \mathbf{k}$ $t_{gr1}^f = t_{gr1} \cos \delta \varepsilon_g^f - t_{gr2} \sin \delta \varepsilon_g^f$ $t_{gr2}^f = t_{gr1} \sin \delta \varepsilon_g^f + t_{gr2} \cos \delta \varepsilon_g^f$ $t_{gr3}^f = t_{gr3}$ <p>that is, expression (7.15)</p> $\sin \theta_{v\eta}^f = \frac{M_{gp} v_{f2}^{gp} - v_{f3}^{gp}}{ \eta_p \mathbf{v}_f^{gp} }$ $\cos \theta_{v\eta}^f = \frac{\eta_{p1} v_{f1}^{gp} + \eta_{p2} v_{f2}^{gp} + \eta_{p3} v_{f3}^{gp}}{ \eta_p \mathbf{v}_f^{gp} }$ <p>that is, expression (7.17)</p>	164.9005434 1.65492672 0.661709394 2.706992975 3.241057349 0.736817609 -0.588645927 0.33255944 0.889366573 -0.457194828

Intermediate Parameters	$\sin \theta_{tv}^f = \frac{\begin{Bmatrix} v_{f1}^{gp}(N_{gpy}^f t_{gr3}^f - N_{gpz}^f t_{gr2}^f) \\ + v_{f2}^{gp}(N_{gpz}^f t_{gr1}^f - N_{gpx}^f t_{gr3}^f) \\ + v_{f3}^{gp}(N_{gpx}^f t_{gr2}^f - N_{gpy}^f t_{gr1}^f) \end{Bmatrix}}{ v_f^{gp} }$	-0.088144664
	$\cos \theta_{tv}^f = \frac{v_{f1}^{gp} t_{gr1}^f + v_{f2}^{gp} t_{gr2}^f + v_{f3}^{gp} t_{gr3}^f}{ v_f^{gp} }$	-0.996107692
	that is, expression (7.19)	
	$K_{gpv} = K_{gt} \cos^2 \theta_{tv}^f + K_{gs} \sin^2 \theta_{tv}^f + 2G_{gt} \sin \theta_{tv}^f \cos \theta_{tv}^f$	-0.53316263 $\times 10^{-3}$
	$G_{gpv} = -(K_{gt} - K_{gs}) \sin \theta_{tv}^f \cos \theta_{tv}^f + G_{gt}(\cos^2 \theta_{tv}^f - \sin^2 \theta_{tv}^f)$	-0.15084276 $\times 10^{-2}$
	$K_{gp\Delta} = K_{gt} \sin^2 \theta_{tv}^f + K_{gs} \cos^2 \theta_{tv}^f - 2G_{gt} \sin \theta_{tv}^f \cos \theta_{tv}^f$	0.48294615 $\times 10^{-2}$
	that is, expression (7.20)	
	$D_p = K_{gpv} v_f^{gp} - \eta_p \cos \theta_{v\eta}^f$	1.1934993
	$E_p = G_{gpv} v_f^{gp} - \eta_p \sin \theta_{v\eta}^f$	-2.9640528
	$\sin \theta_{ve}^f = -\frac{D_p}{\sqrt{D_p^2 + E_p^2}}$	-0.373515168
Curvatures of Gear in Dire- ctions e and g	$\cos \theta_{ve}^f = \frac{E_p}{\sqrt{D_p^2 + E_p^2}}$	-0.927624072
	θ_{ve}^f	201.9325709
	that is, expression (7.22)	
	$K_{gpe} = K_{gpv} \cos^2 \theta_{ve}^f + K_{gp\Delta} \sin^2 \theta_{ve}^f + 2G_{gpv} \sin \theta_{ve}^f \cos \theta_{ve}^f$	-0.49593016 $\times 10^{-2}$
	$G_{gpe} = -(K_{gpv} - K_{gp\Delta}) \sin \theta_{ve}^f \cos \theta_{ve}^f + G_{gpv}(\cos^2 \theta_{ve}^f - \sin^2 \theta_{ve}^f)$	0.24330951 $\times 10^{-2}$
	$K_{gpg} = K_{gpv} \sin^2 \theta_{ve}^f + K_{gp\Delta} \cos^2 \theta_{ve}^f - 2G_{gpv} \sin \theta_{ve}^f \cos \theta_{ve}^f$	0.44571368 $\times 10^{-2}$
	that is, expression (7.23)	
	$\bar{K}_g = \frac{D_p^2 + E_p^2}{D_p v_f^{gp} + J_p \cdot N_{gp}^f}$	0.044500619
	that is, expression (7.24)	
	$K'_{pe} = -K_{gpe}$	0.49593016 $\times 10^{-2}$
Conjugate Cur- vatures of Pinion in Directions e and g	$G'_{pe} = -G_{gpe}$	-0.24330951 $\times 10^{-2}$
	$K'_{pg} = \bar{K}_g - K_{gpg}$ that is, expression (7.25)	0.040043483

Intermediate Parameters	$\mathbf{t}_p = t_{p1}\mathbf{i} + t_{p2}\mathbf{j} + t_{p3}\mathbf{k}$	
	$t_{p1} = \cos \psi_{pr} \sin \gamma_{pr} \cos \varepsilon_p^f - \sin \psi_{pr} \sin \varepsilon_p^f$	-0.717271937
	$t_{p2} = -\cos \psi_{pr} \cos \gamma_{pr}$	0.652050049
	$t_{p3} = \cos \psi_{pr} \sin \gamma_{pr} \sin \varepsilon_p^f + \sin \psi_{pr} \cos \varepsilon_p^f$	-0.24566583
	$\mathbf{s}_p = s_{p1}\mathbf{i} + s_{p2}\mathbf{j} + s_{p3}\mathbf{k}$	
	$s_{p1} = t_{p2}N_{gpx}^f - t_{p3}N_{gpy}^f$	-0.218315441
	$s_{p2} = t_{p3}N_{gpx}^f - t_{p1}N_{gpz}^f$	-0.545115305
	$s_{p3} = t_{p1}N_{gpy}^f - t_{p2}N_{gpz}^f$	-0.809436632
	$\sin \theta_{vt_p}^f = \frac{\begin{Bmatrix} t_{p1}(N_{gpy}^f v_{f3}^{gp} - N_{gpz}^f v_{f2}^{gp}) \\ + t_{p2}(N_{gpx}^f v_{f1}^{gp} - N_{gpz}^f v_{f3}^{gp}) \\ + t_{p3}(N_{gpx}^f v_{f2}^{gp} - N_{gpy}^f v_{f1}^{gp}) \end{Bmatrix}}{ v_f^{gp} }$	0.021121875
	$\cos \theta_{vt_p}^f = \frac{t_{p1}v_{f1}^{gp} + t_{p2}v_{f2}^{gp} + t_{p3}v_{f3}^{gp}}{ v_f^{gp} }$	0.99977691
Conjugate Curvatures of Pinion	$\theta_{vt_p}^f$	1.210278966°
	that is, expression (7.28)	
	$\theta_{et_p}^f = \theta_{vt_p}^f - \theta_{ve}^f$	-200.7222919°
	that is, expression (7.31)	
	$K'_{pt} = K'_{pe} \cos^2 \theta_{et_p}^f + K'_{pg} \sin^2 \theta_{et_p}^f$	1.0962361
	$+ 2G'_{pe} \sin \theta_{et_p}^f \cos \theta_{et_p}^f$	$\times 10^{-2}$
	$G'_{pt} = -(K'_{pe} - K'_{pg}) \sin \theta_{et_p}^f \cos \theta_{et_p}^f$	-1.3434867
	$+ G'_{pe} (\cos^2 \theta_{et_p}^f - \sin^2 \theta_{et_p}^f)$	$\times 10^{-2}$
	$K'_{ps} = K'_{pe} \sin^2 \theta_{et_p}^f + K'_{pg} \cos^2 \theta_{et_p}^f$	3.4040423
	$- 2G'_{pe} \sin \theta_{et_p}^f \cos \theta_{et_p}^f$	$\times 10^{-2}$
	that is, expression (7.32)	

A.5 Calculation of the Quantity for the Curvature Modification to the Pinion Tooth Surface

Input parameters are all obtained in the previous sections.

Output parameters and intermediate parameters:

Item	Expression	Value
Proportional coefficient	F_c	0.4
Actual contact width	$2F_{Ge1} \approx \frac{F_c F_G}{ \cos \delta_g \cos \theta_{tv}^f \cos \theta_{ve}^f \cos \psi_g }$ that is, expression (8.7) $2F_{Ge1} \approx \frac{F_c h \cos \delta_g}{ \cos \Phi_g (\sin \theta_{tv}^f \cos \theta_{ve}^f + \cos \theta_{tv}^f \sin \theta_{ve}^f) }$ that is, expression (8.8)	20.41280746 8.428470146
Allowable error of transmission ratio	F_{Ge} ΔM_{gp} $\Delta(\frac{dM_{gp}}{d\varepsilon_g}) = -\frac{N_g \Delta M_{gp}}{2\pi}$ that is, expression (8.21)	4.214235073 0.00259 -0.018549508
Diameter of color compound	δ	0.00635
Modified value of Curvature in Directions e and g	$\Delta K'_{2e} = \frac{2\delta}{F_{Ge}^2}$ that is, expression (8.13) $g_f = \frac{\sqrt{D_p^2 + E_p^2}}{N_{gp}^f \cdot J_p}$ $\tan \theta_{er'}^f = \frac{1 - g_f \mathbf{v}_{gp}^{fp} \sin \theta_{ve}^f}{\tan \theta_{ve}^f + g_f \mathbf{v}_{gp}^{fp} \cos \theta_{ve}^f}$ that is, expression (8.19) $\Delta G'_{2e} = -\frac{\Delta K'_{2e}}{\tan \theta_{er'}^f}$ that is, expression (8.18) $\Delta(\mathbf{J}_p \cdot \mathbf{N}_{gp}^f) = \Delta(\frac{dM_{gp}}{d\varepsilon_g}) [z_{gp}^f N_{gpx}^f - N_{gpz}^f (x_{gp}^f - f_{gp})]$ $\Delta K'_{2g} = -\frac{\bar{K}_g^2}{D_p^2 + E_p^2} \Delta(\mathbf{J}_p \cdot \mathbf{N}_{gp}^f)$ that is, expression (8.25)	0.000715099 0.019377236 -2.444046149 0.000292588 -0.418989272 0.000081266
Curvatures of Pinion in Directions e and g	$K_{pe}^{ip} = K_{pe}' + \Delta K'_{2e}$ $G_{pe}^{ip} = G_{pe}' + \Delta G'_{2e}$ that is, expression (8.16) $K_{pg}^{ip} = K_{pg}' + \Delta K'_{2g}$ that is, expression (8.26)	0.56744 $\times 10^{-2}$ -0.2140507 $\times 10^{-2}$ 0.040124749

Curvatures of	$K_{pt}^{ip} = K_{pe}^{ip} \cos^2 \theta_{etp}^f + K_{pg}^{ip} \sin^2 \theta_{etp}^f + 2G_{pe}^{ip} \sin \theta_{etp}^f \cos \theta_{etp}^f$	1.140444×10^{-2}
Pinion in Direc-	$G_{pt}^{ip} = -(K_{pe}^{ip} - K_{pg}^{ip}) \sin \theta_{etp}^f \cos \theta_{etp}^f + G_{pe}^{ip} (\cos^2 \theta_{etp}^f - \sin^2 \theta_{etp}^f)$	$-1.3005779 \times 10^{-2}$
tions t_p and s_p	$K_{ps}^{ip} = K_{pe}^{ip} \sin^2 \theta_{etp}^f + K_{pg}^{ip} \cos^2 \theta_{etp}^f - 2G_{pe}^{ip} \sin \theta_{etp}^f \cos \theta_{etp}^f$ that is, expression (8.27)	3.4394709×10^{-2}

A.6 Determination of Machine-Setting Parameters for the Pinion Tooth Surface

Input parameters are all obtained in the previous sections and together with:

Item	Expression	Value
Blade Angle for Pinion	ϕ_{cp}^i	24°

Output parameters:

Item	Expression	Value
Vertical Position of Pinion	f_{mp} that is, by solving equation (9.43)	32.195057
Horizontal Position of Pinion	L_p that is, by solving equation (9.43)	0.91700418
The Ratio of Roll	M_{mp}	-4.2258279
The Increment of Phase Angle for Pinion Cutting Position	$\delta \varepsilon_p^f$ that is, by solving equation (9.43)	-2.790746357°
The Phase Angle for Cutting Edge	σ_p that is, equation (9.43)	134.0309399°
The Coordinate of Cutter Center at the Cutting Position	x_{cp} y_{cp} z_{cp} that is, by solving equation (9.43)	130.91316 14.909281 -6.0901225
Cutter Radius at Cutting Position	ρ_{cp} that is, by solving equation (9.43)	144.43365

Intermediate Parameters:

The Position of Cutting Point on Cutter	$\mathbf{R}_{mp} = x_{mp}\mathbf{i}_m + y_{mp}\mathbf{j}_m + z_{mp}\mathbf{k}_m$	30.52502605
	$x_{mp} = x_{cp} + \rho_{cp} \cos \sigma_p$	118.7519592
	$y_{mp} = y_{cp} + \rho_{cp} \sin \sigma_p$	-6.0901225
The Position of Cutting Point on Pinion	$z_{mp} = z_{cp}$	
	that is, expression (9.8)	
	$\mathbf{R}_p = x_p\mathbf{i}' + y_p\mathbf{j}' + z_p\mathbf{k}'$	-1.67002467
Unit Normal to Cutter	$x_p = x_p^f \cos \delta \varepsilon_p^f - y_p^f \sin \delta \varepsilon_p^f$	37.05933778
	$y_p = x_p^f \sin \delta \varepsilon_p^f + y_p^f \cos \delta \varepsilon_p^f$	112.0684926
	$z_p = z_p^f$	
Unit Normal to Pinion	that is, expression (9.11)	
	$x_p + f_{mp}$	30.52503233
	$y_p \sin \gamma_{pr} + (L_p + z_p) \cos \gamma_{pr}$	118.7519574
Unit Tangent to Cutting Edge	$(L_p + z_p) \sin \gamma_{pr} - y_p \cos \gamma_{pr}$	-6.090124212
	that is, equation (9.15) is satisfied	
	$\mathbf{N}_{cp} = N_{cpz}\mathbf{i}_m + N_{cpy}\mathbf{j}_m + N_{cpz}\mathbf{k}_m$	
Velocity of Cutter Relative to Pinion	$N_{cpz} = -\cos \phi_{cp}^i \cos \sigma_p$	0.634956769
	$N_{cpy} = -\cos \phi_{cp}^i \sin \sigma_p$	-0.656806825
	$N_{cpz} = \sin \phi_{cp}^i$	0.406736643
Unit Tangent to Cutting Edge	that is, expression (9.9)	
	$\mathbf{N}_p = N_{px}\mathbf{i}' + N_{py}\mathbf{j}' + N_{pz}\mathbf{k}'$	
	$N_{px} = N_{px}^f \cos \delta \varepsilon_p^f - N_{py}^f \sin \delta \varepsilon_p^f$	-0.634956701
Velocity of Cutter Relative to Pinion	$N_{py} = N_{px}^f \sin \delta \varepsilon_p^f + N_{py}^f \cos \delta \varepsilon_p^f$	0.564933573
	$N_{pz} = N_{pz}^f$	0.526953544
	$-N_{cpy} \sin \gamma_{pr} + N_{cpz} \cos \gamma_{pr}$	0.564933465
Unit Tangent to Cutting Edge	$-N_{cpy} \cos \gamma_{pr} - N_{cpz} \sin \gamma_{pr}$	0.526953586
	that is, equation (9.16) is satisfied	
	$\mathbf{W}_{cp} = W_{cp1}\mathbf{i}_m + W_{cp2}\mathbf{j}_m + W_{cp3}\mathbf{k}_m$	
Velocity of Cutter Relative to Pinion	$W_{cp1} = \sin \phi_{cp}^i \cos \sigma_p$	-0.282700968
	$W_{cp2} = \sin \phi_{cp}^i \sin \sigma_p$	0.292429239
	$W_{cp3} = \cos \phi_{cp}^i$	0.913545458
Unit Tangent to Cutting Edge	that is, expression (9.10)	
	$\mathbf{v}_p^{mp} = v_{p1}^{mp}\mathbf{i}_m + v_{p2}^{mp}\mathbf{j}_m$	
	$v_{p1}^{mp} = -(1 + M_{mp} \sin \gamma_{pr})y_{mp}$	37.85441933
Velocity of Cutter Relative to Pinion	$+ z_{mp} M_{mp} \cos \gamma_{pr}$	

Intermediate Parameters	$v_{p2}^{mp} = (1 + M_{mp} \sin \gamma_{pr})x_{mp} - M_{mp}f_{mp} \sin \gamma_{pr}$	32.378184
	$v_{p3}^{mp} = -M_{mp}x_{mp} \cos \gamma_{pr} + M_{mp}f_{mp} \cos \gamma_{pr}$	-6.8095895
	$ \mathbf{v}_p^{mp} = \sqrt{(v_{p1}^{mp})^2 + (v_{p2}^{mp})^2 + (v_{p3}^{mp})^2}$	50.27598205
	that is, expression (9.20)	
	$v_{p1}^{mp} N_{cpz} + v_{p2}^{mp} N_{cpy} + v_{p3}^{mp} N_{cpz}$	-0.000002013
	that is, equation (9.20) is satisfied	
	$\eta_p^p = \eta_{p1}^p \mathbf{i}_m + \eta_{p2}^p \mathbf{j}_m + \eta_{p3}^p \mathbf{k}_m$	
	$\eta_{p1}^p = -N_{cpy}(1 + M_{mp} \sin \gamma_{pr}) + N_{cpz} M_{mp} \cos \gamma_{pr}$	-1.7305048
	$\eta_{p2}^p = N_{cpz}(1 + M_{mp} \sin \gamma_{pr})$	-0.06962614
	$\eta_{p3}^p = -N_{cpz} M_{mp} \cos \gamma_{pr}$	2.5890581
	$ \eta_p^p = \sqrt{(\eta_{p1}^p)^2 + (\eta_{p2}^p)^2 + (\eta_{p3}^p)^2}$	3.114918379
	that is, expression (9.18)	
	$\cos \theta_{v\eta}^{mp} = \frac{v_{p1}^{mp} \eta_{p1}^p + v_{p2}^{mp} \eta_{p2}^p + v_{p3}^{mp} \eta_{p3}^p}{ \mathbf{v}_p^{mp} \eta_p^p }$	-0.545268214
	$\sin \theta_{v\eta}^{mp} = -\frac{M_{mp} f_{mp} \cos \gamma_{pr}}{ \mathbf{v}_p^{mp} \eta_p^p }$	0.838261667
Curvatures of Cutter Surface	that is, expression (9.24)	
	$\cos \theta_{wv}^{mp} = \frac{v_{p3}^{mp}}{ \mathbf{v}_p^{mp} \cos \phi_{cp}^i}$	-0.14826212
	$\sin \theta_{wv}^{mp} = \frac{v_{p2}^{mp} \cos \sigma_p - v_{p1}^{mp} \sin \sigma_p}{ \mathbf{v}_p^{mp} }$	-0.988948102
	that is, expression (9.27)	
	$K_{cpv} = -\frac{\cos \phi_{cp}^i \sin^2 \theta_{wv}^{mp}}{\rho_{cp}}$	-0.6185984 $\times 10^{-2}$
Conjugate Accele- ration	$G_{cpv} = -\frac{\cos \phi_{cp}^i \sin \theta_{wv}^{mp} \cos \theta_{wv}^{mp}}{\rho_{cp}}$	-0.92739653 $\times 10^{-3}$
	$K_{cp\Delta} = -\frac{\cos \phi_{cp}^i \cos^2 \theta_{wv}^{mp}}{\rho_{cp}}$	-0.13903436 $\times 10^{-3}$
	that is, expression (9.28)	
	$\mathbf{J}_p = J_{p1} \mathbf{i}_m + J_{p2} \mathbf{j}_m + J_{p3} \mathbf{k}_m$	
	$J_{p1} = M_{mp} f_{mp} \sin \gamma_{pr}$	-35.725404
	$J_{p2} = M_{mp} z_{mp} \cos \gamma_{pr}$	24.832685
	$J_{p3} = -M_{mp} y_{mp} \cos \gamma_{pr}$	484.21521
	that is, expression (9.31)	
	$\mathbf{J}_p \cdot \mathbf{N}_{cp} = J_{p1} N_{cpz} + J_{p2} N_{cpy} + J_{p3} N_{cpz}$	157.9537049

Intermediate Parameters	$D_p = K_{cpv} \mathbf{v}_p^{mp} - \eta_p^p \cos \theta_{v\eta}^{mp}$ $E_p = G_{cpv} \mathbf{v}_p^{mp} - \eta_p^p \sin \theta_{v\eta}^{mp}$ that is, expression (9.33)	1.3874596 -2.6577423
Conjugate	$K'_{pv} = \frac{D_p^2}{D_p \mathbf{v}_p^{mp} + \mathbf{J}_p \cdot \mathbf{N}_{cp}} - K_{cpv}$	1.4639927 $\times 10^{-2}$
Curvatures of	$G'_{pv} = \frac{D_p E_p}{D_p \mathbf{v}_p^{mp} + \mathbf{J}_p \cdot \mathbf{N}_{cp}} - G_{cpv}$	-1.526652 $\times 10^{-2}$
Pinion	$K'_{p\Delta} = \frac{E_p^2}{D_p \mathbf{v}_p^{mp} + \mathbf{J}_p \cdot \mathbf{N}_{cp}} - K_{cp\Delta}$ that is, expression (9.34)	3.1159221 $\times 10^{-2}$
Intermediate Parameters	$\mathbf{t}_{pc} = t_{pc1} \mathbf{i}_m + t_{pc2} \mathbf{j}_m + t_{pc3} \mathbf{k}_m$ $t_{pc1} = t_{p1} \cos \delta \varepsilon_p^f - t_{p3} \sin \delta \varepsilon_p^f$ $t_{pc2} = (t_{p1} \sin \delta \varepsilon_p^f + t_{p3} \cos \delta \varepsilon_p^f) \sin \gamma_{pr}$ $\quad - t_{p2} \cos \gamma_{pr}$ $t_{pc3} = -(t_{p1} \sin \delta \varepsilon_p^f + t_{p3} \cos \delta \varepsilon_p^f) \cos \gamma_{pr}$ $\quad - t_{p2} \sin \gamma_{pr}$ that is, expression (9.35)	-0.728382352 -0.684430433 0.031845397
	$\cos \theta_{vt}^{mp} = \frac{t_{pc1} v_{p1}^{mp} + t_{pc2} v_{p2}^{mp} + t_{pc3} v_{p3}^{mp}}{ \mathbf{v}_p^{mp} }$	-0.993515343
	$\sin \theta_{vt}^{mp} = \frac{\begin{Bmatrix} t_{pc1} (N_{cpy} v_{p3}^{mp} - N_{cpz} v_{p2}^{mp}) \\ + t_{pc2} (N_{cpz} v_{p1}^{mp} - N_{cp x} v_{p3}^{mp}) \\ + t_{pc3} (N_{cp x} v_{p2}^{mp} - N_{cpy} v_{p1}^{mp}) \end{Bmatrix}}{ \mathbf{v}_p^{mp} }$ that is, expression (9.40)	-0.113698111
Conjugate	$K'_{pt_p} = K'_{pv} \cos^2 \theta_{vt}^{mp} + K'_{p\Delta} \sin^2 \theta_{vt}^{mp}$ $\quad + 2G'_{pv} \sin \theta_{vt}^{mp} \cos \theta_{vt}^{mp}$	1.140444 $\times 10^{-2}$
Curvatures of	$G'_{pt_p} = -(K'_{pv} - K'_{p\Delta}) \sin \theta_{vt}^{mp} \cos \theta_{vt}^{mp}$ $\quad + G'_{pv} (\cos^2 \theta_{vt}^{mp} - \sin^2 \theta_{vt}^{mp})$	-1.3005778 $\times 10^{-2}$
Pinion	$K'_{ps_p} = K'_{pv} \sin^2 \theta_{vt}^{mp} + K'_{p\Delta} \cos^2 \theta_{vt}^{mp}$ $\quad - 2G'_{pv} \sin \theta_{vt}^{mp} \cos \theta_{vt}^{mp}$ that is, requirement (9.41) is satisfied	3.4394709 $\times 10^{-2}$

A.7 Calculation of Curvatures for the Gear Tooth Surface

Input parameters were obtained in the previous sections.

Output Parameters and Intermediate Parameters:

(All calculations from A.7 to A.10 correspond to the convex face of the gear and the concave face of the pinion).

Item	Expression	Value
The Position of the Fundamental Contact Point	ξ_f	0
	a_f	0
	$\rho_f = \rho_b$	117.29628
	$z_f = z_b$	36.934075
	$\varepsilon_g^f = \varepsilon_g^i$	78.46167698°
	$x_c^f = x_c^i$	-116.23481
	$y_c^f = y_c^i$	70.429421
	$z_c^f = z_c^i$	-24.067896
	$\rho_c^f = \rho_c^i$	147.3724974
	$\sigma^f = \sigma^i$	17.4713471°
The Tangential Direction to the Cutting Edge	$\mathbf{W} = W_1 \mathbf{i}_m + W_2 \mathbf{j}_m + W_3 \mathbf{k}_m$	
	$W_1 = \sin \phi_c^i \cos \sigma^f$	0.230761364
	$W_2 = \sin \phi_c^i \sin \sigma^f$	0.072631925
	$W_3 = \cos \phi_c^i$	0.970295726
Relative Velocity of Fundamental Contact Point	that is, expression (6.50)	
	$\mathbf{v}_f^{mg} = v_{f1}^{mg} \mathbf{i}_m + v_{f2}^{mg} \mathbf{j}_m + v_{f3}^{mg} \mathbf{k}_m$	
	$v_{f1}^{mg} = v_{xi}^{mg}$	1.649556794
	$v_{f2}^{mg} = v_{yi}^{mg}$	2.49441626
	$v_{f3}^{mg} = v_{zi}^{mg}$	9.314447609
	$ \mathbf{v}_f^{mg} = \sqrt{(v_{f1}^{mg})^2 + (v_{f2}^{mg})^2 + (v_{f3}^{mg})^2}$	9.782744214
	that is, expression (6.36)	
Intermediate Parameters	$\cos \theta_{wv} = \frac{v_{f1}^{mg} W_1 + v_{f2}^{mg} W_2 + v_{f3}^{mg} W_3}{ \mathbf{v}_f^{mg} }$	0.981278538
	$\sin \theta_{wv} = \frac{-v_{f1}^{mg} \sin \sigma^f + v_{f2}^{mg} \cos \sigma^f}{ \mathbf{v}_f^{mg} }$	0.19259401
	that is, expression (6.53)	
Curvatures of the Cutter Surface in Direction $\frac{\mathbf{v}_f^{mg}}{ \mathbf{v}_f^{mg} }$ and Δ_f	$K_{1v} = -\frac{\cos \phi_c^i}{\rho_c^f} \sin^2 \theta_{wv}$	$-0.2442155 \times 10^{-3}$
	$G_{1v} = -\frac{\cos \phi_c^i}{\rho_c^f} \sin \theta_{wv} \cos \theta_{wv}$	$-0.1244293 \times 10^{-2}$
	$K_{1\Delta} = -\frac{\cos \phi_c^o}{\rho_c^f} \cos^2 \theta_{wv}$	$-0.63397519 \times 10^{-2}$
	that is, expression (6.54)	

Intermediate Parameters	$\eta_f = \eta_{f1}\mathbf{i}_m + \eta_{f2}\mathbf{j}_m + \eta_{f3}\mathbf{k}_m$	
	$\eta_{f1} = -N_{cy}^f(1 + M_{mg} \sin \gamma_{gr})$	-0.075961069
	$+ N_{cx}^f M_{mg} \cos \gamma_{gr}$	
	$\eta_{f2} = N_{cx}^f(1 + M_{mg} \sin \gamma_{gr})$	-0.063804267
	$\eta_{f3} = -N_{cx}^f M_{mg} \cos \gamma_{gr}$	-0.36743827
	$ \eta_f = \sqrt{\eta_{f1}^2 + \eta_{f2}^2 + \eta_{f3}^2}$	0.380594207
	that is, expression (6.57)	
	$\sin \theta_{v\eta} = -\frac{M_{mg} f_{mg} \cos \gamma_{gr}}{ \mathbf{v}_f^{mg} \eta_f }$	0.093512144
	$\cos \theta_{v\eta} = \frac{v_{f1}^{mg} \eta_{f1} + v_{f2}^{mg} \eta_{f2} + v_{f3}^{mg} \eta_{f3}}{ \mathbf{v}_f^{mg} \eta_f }$	-99561814
	that is, expression (6.58)	
	$\mathbf{J}_f = J_{f1}\mathbf{i}_m + J_{f2}\mathbf{j}_m + J_{f3}\mathbf{k}_m$	
	$J_{f1} = M_{mg} f_{mg} \sin \gamma_{gr}$	-0.816539538
	$J_{f2} = M_{mg} z_c^f \cos \gamma_{gr}$	9.5549954
	$J_{f3} = -M_{mg} (y_c^f + \rho_c^f \sin \sigma^f) \cos \gamma_{gr}$	45.526126
Conjugate Curvatures of Gear Tooth Surface in Directions $\frac{\mathbf{v}_f^{mg}}{ \mathbf{v}_f^{mg} }$ and Δ_f Curvatures of Gear Tooth Surface	that is, expression (6.61)	
	$\mathbf{N}_c^f \cdot \mathbf{J}_f = N_{cx}^f J_{f1} + N_{cy}^f J_{f2} + N_{cz}^f J_{f3}$	8.986028398
	that is, expression (6.62)	
	$D_p = K_{1v} \mathbf{v}_f^{mg} - \eta_f \cos \theta_{v\eta}$	0.376537403
	$E_p = G_{1v} \mathbf{v}_f^{mg} - \eta_f \sin \theta_{v\eta}$	-0.047762781
	that is, expression (6.63)	
	$K'_{gv} = \frac{D_p^2}{D_p \mathbf{v}_f^{mg} + \mathbf{N}_c^f \cdot \mathbf{J}_f} - K_{1v}$	1.1434817 $\times 10^{-2}$
	$G'_{gv} = \frac{D_p E_p}{D_p \mathbf{v}_f^{mg} + \mathbf{N}_c^f \cdot \mathbf{J}_f} - G_{1v}$	-0.175205 $\times 10^{-3}$
	$K'_{g\Delta} = \frac{E_p^2}{D_p \mathbf{v}_f^{mg} + \mathbf{N}_c^f \cdot \mathbf{J}_f} - K_{1\Delta}$	0.65198116 $\times 10^{-2}$
	that is, expression (6.64)	
	$K_{gv} = K'_{gv}$	
	$G_{gv} = -G'_{gv}$	
	$K_{g\Delta} = K'_{g\Delta}$	
	that is, expression (6.65)	

Intermediate Parameters	$Q_{gr} = \sqrt{(N_{gy}^f \sin \gamma_{gr} + N_{gz}^f \cos \gamma_{gr} \sin \varepsilon_g^f)^2 + (N_{gz}^f \cos \gamma_{gr} \cos \varepsilon_g^f + N_{gx}^f \sin \gamma_{gr})^2 + (N_{gx}^f \cos \gamma_{gr} \sin \varepsilon_g^f - N_{gy}^f \cos \gamma_{gr} \cos \varepsilon_g^f)^2}$	0.950194249
	$\mathbf{t}_{gr} = t_{gr1}\mathbf{i} + t_{gr2}\mathbf{j} + t_{gr3}\mathbf{k}$	
	$t_{gr1} = -\frac{N_{gy}^f \sin \gamma_{gr} + N_{gz}^f \cos \gamma_{gr} \sin \varepsilon_g^f}{Q_{gr}}$	-0.307483399
	$t_{gr2} = \frac{N_{gz}^f \cos \gamma_{gr} \cos \varepsilon_g^f + N_{gx}^f \sin \gamma_{gr}}{Q_{gr}}$	0.887053929
Curvatures of Gear in Directions \mathbf{t}_{gr} and $\mathbf{N}_g^f \times \mathbf{t}_{gr}$	$t_{gr3} = \frac{N_{gx}^f \cos \gamma_{gr} \sin \varepsilon_g^f - N_{gy}^f \cos \gamma_{gr} \cos \varepsilon_g^f}{Q_{gr}}$	0.34436796
	that is, expression (6.67)	
	$\sin \theta_{vt} = \frac{\left\{ \begin{array}{l} v_{f1}^{mg}(t_{gr2}N_{gz}^f - t_{gr3}N_{gy}^f) + (t_{gr3}N_{gx}^f - t_{gr1}N_{gz}^f)(v_{f2}^{mg} \sin \gamma_{gr} - v_{f3}^{mg} \cos \gamma_{gr}) + (t_{gr1}N_{gy}^f - t_{gr2}N_{gx}^f)(v_{f2}^{mg} \cos \gamma_{gr} + v_{f3}^{mg} \sin \gamma_{gr}) \end{array} \right\}}{ v_f^{mg} }$	-0.986956488
	$\cos \theta_{vt} = \frac{\left\{ \begin{array}{l} t_{gr1}v_{f1}^{mg} + t_{gr2}(v_{f2}^{mg} \sin \gamma_{gr} - v_{f3}^{mg} \cos \gamma_{gr}) + t_{gr3}(v_{f2}^{mg} \cos \gamma_{gr} + v_{f3}^{mg} \sin \gamma_{gr}) \end{array} \right\}}{ v_f^{mg} }$	0.16098728
	that is, expression (6.72)	
	$K_{gt} = K_{gv} \cos^2 \theta_{vt} + K_{g\Delta} \sin^2 \theta_{vt} + 2G_{gv} \sin \theta_{vt} \cos \theta_{vt}$	0.65915175 $\times 10^{-2}$
	$G_{gt} = -(K_{gv} - K_{g\Delta}) \sin \theta_{vt} \cos \theta_{vt} + G_{gv}(\cos^2 \theta_{vt} - \sin^2 \theta_{vt})$	0.61481 $\times 10^{-3}$
	$K_{gs} = K_{gv} \sin^2 \theta_{vt} K_{g\Delta} \cos^2 \theta_{vt} - 2G_{gv} \sin \theta_{vt} \cos \theta_{vt}$	0.011363111
	that is, expression (6.73)	

A.8 Calculation of Curvatures for the Pinion Tooth Surface with Line Contact

Input parameters are all obtained in the previous sections.

Output Parameters and Intermediate Parameters:

Item	Expression	Value
The Increment of Rotating Angle	$U_{gp} = N_{gz}^f M_{gp} \rho_f \cos \varepsilon_g^f - N_{gx}^f M_{gp} z_f$	-150.2348805
	$V_{gp} = N_{gz}^f M_{gp} \rho_f \sin \varepsilon_g^f - N_{gy}^f M_{gp} z_f$	-105.731345
	$W_{gp} = N_{gx}^f \rho_f \sin \varepsilon_g^f + N_{gz}^f M_{gp} f_{gp} - N_{gy}^f \rho_f \cos \varepsilon_g^f$	80.97811994
	that is, expression (7.4) $\delta \varepsilon_g = \arccos\left(\frac{W_{gp}}{\sqrt{U_{gp}^2 + V_{gp}^2}}\right) - \arctan\left(\frac{V_{gp}}{U_{gp}}\right)$	-151.2912602°
Contact Position of Fundamental Contact Point	$\mathbf{R}_{gp}^f = [(\varepsilon_g^f + \delta \varepsilon_g) \mathbf{k}] \otimes (\rho_f \mathbf{i} + z_f \mathbf{k})$	
	$x_{gp}^f = \rho_f \cos(\varepsilon_g^f + \delta \varepsilon_g)$	34.62759519
	$y_{gp}^f = \rho_f \sin(\varepsilon_g^f + \delta \varepsilon_g)$	-112.0685
	$z_{gp}^f = z_f$	36.934075
Corresponding Unit Normal	that is, expression (7.1) $\mathbf{N}_{gp}^f = (\delta \varepsilon_g \mathbf{k}) \otimes \mathbf{N}_g^f$	
	$N_{gpx}^f = N_{gx}^f \cos \delta \varepsilon_g - N_{gy}^f \sin \delta \varepsilon_g$	-0.637459643
	$N_{gpy}^f = N_{gx}^f \sin \delta \varepsilon_g + N_{gy}^f \cos \delta \varepsilon_g$	-0.762837824
	$N_{gpz}^f = N_{gz}^f$	-0.108275803
Contact Position in Pinion Coordinate System	that is, expression (7.2) $\mathbf{R}_p^f = x_p^f \mathbf{i}' + y_p^f \mathbf{j}' + z_p^f \mathbf{k}'$	
	$x_p^f = x_{gp}^f - f_{gp}$	-3.47240481
	$y_p^f = z_{gp}^f$	36.934075
	$z_p^f = -y_{gp}^f$	112.0685
Phase Angle of Contact Point	that is, expression (7.5) $\sin \varepsilon_p^f = \frac{y_p^f}{\sqrt{(x_p^f)^2 + (y_p^f)^2}}$	0.995609553
	$\cos \varepsilon_p^f = \frac{x_p^f}{\sqrt{(x_p^f)^2 + (y_p^f)^2}}$	-0.093603519
Unit Normal to the Pinion Tooth Surface	that is, expression (7.6) $\mathbf{N}_p^f = -\mathbf{N}_{gp}^f = N_{px}^f \mathbf{i}' + N_{py}^f \mathbf{j}' + N_{pz}^f \mathbf{k}'$	
	$N_{px}^f = -N_{gpx}^f$	0.637459643
	$N_{py}^f = -N_{gpy}^f$	0.108275803
	$N_{pz}^f = N_{gpz}^f$	-0.762837824
	that is, expression (7.7)	

Intermediate Parameters	$\psi_{pr} = \arctan \frac{\left\{ \begin{array}{l} N_{gpy}^f \cos \gamma_{pr} - \\ (N_{gpx}^f \cos \varepsilon_p^f + N_{gpz}^f \sin \varepsilon_p^f) \sin \gamma_{pr} \end{array} \right\}}{N_{gpx}^f \cos \varepsilon_p^f - N_{gpz}^f \sin \varepsilon_p^f}$	131.7107678°
	$\sin \phi_{pr} = -\frac{(N_{gpx}^f \cos \varepsilon_p^f + N_{gpz}^f \sin \varepsilon_p^f) \cos \gamma_{pr} - N_{gpy}^f \sin \gamma_{pr}}{\cos \psi_{pr}}$	0.24675552
Velocity of Gear with Respect to Pinion	$\cos \phi_{pr} = \frac{N_{gpx}^f \cos \varepsilon_p^f - N_{gpz}^f \sin \varepsilon_p^f}{\cos \psi_{pr}}$	-0.969077754
	that is, expression (7.10)	
	$\mathbf{v}_f^{gp} = v_{f1}^{gp} \mathbf{i} + v_{f2}^{gp} \mathbf{j} + v_{f3}^{gp} \mathbf{k}$	
	$v_{f1}^{gp} = -\rho_f \sin(\varepsilon_g^f + \delta \varepsilon_g) - M_{gp} z_f$	-39.02545098
	$v_{f2}^{gp} = \rho_f \cos(\varepsilon_g^f + \delta \varepsilon_g)$	34.62759519
Conjugate Acceleration	$v_{f3}^{gp} = M_{gp} \rho_f \cos(\varepsilon_g^f + \delta \varepsilon_g) - M_{gp} f_{gp}$	-14.20529239
	$ \mathbf{v}_f^{gp} = \sqrt{(v_{f1}^{gp})^2 + (v_{f2}^{gp})^2 + (v_{f3}^{gp})^2}$	54.07260397
	that is, expression (7.11)	
	$\mathbf{J}_p = J_{p1} \mathbf{i} + J_{p2} \mathbf{j} + J_{p3} \mathbf{k}$	
	$J_{p1} = 0$	0
Intermediate Parameters	$J_{p2} = -M_{gp} z_f$	-151.0939432
	$J_{p3} = M_{gp} \rho_f \sin(\varepsilon_g^f + \delta \varepsilon_g)$	-458.4620137
	that is, expression (7.12)	
	$\mathbf{J}_p \cdot \mathbf{N}_{gp}^f = N_{gpy}^f J_{p2} + N_{gpz}^f J_{p3}$	164.9005175
	that is, expression (7.13)	
	$\eta_p = \eta_{p1} \mathbf{i} + \eta_{p2} \mathbf{j} + \eta_{p3} \mathbf{k}$	
	$\eta_{p1} = -N_{gpy}^f - N_{gpz}^f M_{gp}$	1.205784291
	$\eta_{p2} = N_{gpx}^f$	-0.637459642
	$\eta_{p3} = N_{gpx}^f M_{gp}$	-2.607789445
	$ \eta_p = \sqrt{\eta_{p1}^2 + \eta_{p2}^2 + \eta_{p3}^2}$	2.942929891
	that is, expression (7.14)	
	$\mathbf{t}_{gr}^f = t_{gr1}^f \mathbf{i} + t_{gr2}^f \mathbf{j} + t_{gr3}^f \mathbf{k}$	
	$t_{gr1}^f = t_{gr1} \cos \delta \varepsilon_g^f - t_{gr2} \sin \delta \varepsilon_g^f$	0.695788179
	$t_{gr2}^f = t_{gr1} \sin \delta \varepsilon_g^f + t_{gr2} \cos \delta \varepsilon_g^f$	-0.630309071
	$t_{gr3}^f = t_{gr3}$	0.34436796
	that is, expression (7.15)	
	$\sin \theta_{v\eta}^f = \frac{M_{gp} v_{f2}^{gp} - v_{f3}^{gp}}{ \eta_p \mathbf{v}_f^{gp} }$	0.979462025
	$\cos \theta_{v\eta}^f = \frac{\eta_{p1} v_{f1}^{gp} + \eta_{p2} v_{f2}^{gp} + \eta_{p3} v_{f3}^{gp}}{ \eta_p \mathbf{v}_f^{gp} }$	-0.2016286
	that is, expression (7.17)	

Intermediate Parameters	$\sin \theta_{tv}^f = \frac{\begin{Bmatrix} v_{f1}^{gp}(N_{gpy}^f t_{gr3}^f - N_{gpz}^f t_{gr2}^f) \\ + v_{f2}^{gp}(N_{gpz}^f t_{gr1}^f - N_{gpx}^f t_{gr3}^f) \\ + v_{f3}^{gp}(N_{gpx}^f t_{gr2}^f - N_{gpy}^f t_{gr1}^f) \end{Bmatrix}}{ \mathbf{v}_f^{gp} }$	0.086190401
	$\cos \theta_{tv}^f = \frac{v_{f1}^{gp} t_{gr1}^f + v_{f2}^{gp} t_{gr2}^f + v_{f3}^{gp} t_{gr3}^f}{ \mathbf{v}_f^{gp} }$	-0.996278678
	that is, expression (7.19)	
	$K_{gpv} = K_{gt} \cos^2 \theta_{tv}^f + K_{gs} \sin^2 \theta_{tv}^f + 2G_{gt} \sin \theta_{tv}^f \cos \theta_{tv}^f$	0.65213778 $\times 10^{-2}$
	$G_{gpv} = -(K_{gt} - K_{gs}) \sin \theta_{tv}^f \cos \theta_{tv}^f + G_{gt}(\cos^2 \theta_{tv}^f - \sin^2 \theta_{tv}^f)$	0.196019 $\times 10^{-3}$
	$K_{gp\Delta} = K_{gt} \sin^2 \theta_{tv}^f + K_{gs} \cos^2 \theta_{tv}^f - 2G_{gt} \sin \theta_{tv}^f \cos \theta_{tv}^f$	0.01143325
	that is, expression (7.20)	
	$D_p = K_{gpv} \mathbf{v}_f^{gp} - \eta_p \cos \theta_{v\eta}^f$	0.94600667
	$E_p = G_{gpv} \mathbf{v}_f^{gp} - \eta_p \sin \theta_{v\eta}^f$	-2.8718933
	$\sin \theta_{ve}^f = -\frac{D_p}{\sqrt{D_p^2 + E_p^2}}$	-0.312864991
Curvatures of Gear in Dire- ctions e and g	$\cos \theta_{ve}^f = \frac{E_p}{\sqrt{D_p^2 + E_p^2}}$	-0.949797608
	θ_{ve}^f	198.2319733
	that is, expression (7.22)	
	$K_{gpe} = K_{gpv} \cos^2 \theta_{ve}^f + K_{gp\Delta} \sin^2 \theta_{ve}^f + 2G_{gpv} \sin \theta_{ve}^f \cos \theta_{ve}^f$	0.71186241 $\times 10^{-2}$
	$G_{gpe} = -(K_{gpv} - K_{gp\Delta}) \sin \theta_{ve}^f \cos \theta_{ve}^f + G_{gpv}(\cos^2 \theta_{ve}^f - \sin^2 \theta_{ve}^f)$	0.1617249 $\times 10^{-2}$
Relative Curva- ture	$K_{gpg} = K_{gpv} \sin^2 \theta_{ve}^f + K_{gp\Delta} \cos^2 \theta_{ve}^f - 2G_{gpv} \sin \theta_{ve}^f \cos \theta_{ve}^f$	0.010836004
	that is, expression (7.23)	
	$\bar{K}_g = \frac{D_p^2 + E_p^2}{D_p \mathbf{v}_f^{gp} + \mathbf{J}_p \cdot \mathbf{N}_{gp}^f}$	0.04231682
	that is, expression (7.24)	
	$K'_{pe} = -K_{gpe}$	-0.71186241 $\times 10^{-2}$
Conjugate Cur- vatures of Pinion in Directions e and g	$G'_{pe} = -G_{gpe}$	-0.1617249 $\times 10^{-2}$
	$K'_{pg} = \bar{K}_g - K_{gpg}$	0.031480816
	that is, expression (7.25)	

Intermediate Parameters	$\mathbf{t}_p = t_{p1}\mathbf{i} + t_{p2}\mathbf{j} + t_{p3}\mathbf{k}$ $t_{p1} = \cos \psi_{pr} \sin \gamma_{pr} \cos \varepsilon_p^f - \sin \psi_{pr} \sin \varepsilon_p^f$ $t_{p2} = -\cos \psi_{pr} \cos \gamma_{pr}$ $t_{p3} = \cos \psi_{pr} \sin \gamma_{pr} \sin \varepsilon_p^f + \sin \psi_{pr} \cos \varepsilon_p^f$ $\mathbf{s}_p = s_{p1}\mathbf{i} + s_{p2}\mathbf{j} + s_{p3}\mathbf{k}$ $s_{p1} = t_{p2}N_{gpx}^f - t_{p3}N_{gpy}^f$ $s_{p2} = t_{p3}N_{gpz}^f - t_{p1}N_{gpx}^f$ $s_{p3} = t_{p1}N_{gpy}^f - t_{p2}N_{gpz}^f$ $\sin \theta_{vt_p}^f = \frac{\begin{Bmatrix} t_{p1}(N_{gpy}^f v_{f3}^{gp} - N_{gpz}^f v_{f2}^{gp}) \\ + t_{p2}(N_{gpz}^f v_{f1}^{gp} - N_{gpx}^f v_{f3}^{gp}) \\ + t_{p3}(N_{gpx}^f v_{f2}^{gp} - N_{gpy}^f v_{f1}^{gp}) \end{Bmatrix}}{ v_f^{gp} }$ $\cos \theta_{vt_p}^f = \frac{t_{p1}v_{f1}^{gp} + t_{p2}v_{f2}^{gp} + t_{p3}v_{f3}^{gp}}{ v_f^{gp} }$ $\theta_{vt_p}^f$ <p>that is, expression (7.28)</p> $\theta_{et_p}^f = \theta_{vt_p}^f - \theta_{ve}^f$ <p>that is, expression (7.31)</p>	-0.726881324 0.642021369 -0.24382802 -0.255516615 0.076726864 0.963755281 -0.019638552 0.99980714 -1.125278472° -199.3572518°
Conjugate	$K'_{pt} = K'_{pe} \cos^2 \theta_{et_p}^f + K'_{pg} \sin^2 \theta_{et_p}^f + 2G'_{pe} \sin \theta_{et_p}^f \cos \theta_{et_p}^f$	-0.18664823 $\times 10^{-2}$
Curvatures of	$G'_{pt} = -(K'_{pe} - K'_{pg}) \sin \theta_{et_p}^f \cos \theta_{et_p}^f + G'_{pe} (\cos^2 \theta_{et_p}^f - \sin^2 \theta_{et_p}^f)$	-0.13332715 $\times 10^{-1}$
Pinion	$K'_{ps} = K'_{pe} \sin^2 \theta_{et_p}^f + K'_{pg} \cos^2 \theta_{et_p}^f - 2G'_{pe} \sin \theta_{et_p}^f \cos \theta_{et_p}^f$ <p>that is, expression (7.32)</p>	0.026228674

A.9 Calculation of the Quantity for the Curvature Modification to the Pinion Tooth Surface

Input parameters are all obtained in the previous sections.

Output parameters and intermediate parameters:

Item	Expression	Value
Proportional coefficient	F_c	0.4
Actual contact width	$2F_{Ge1} \approx \frac{F_c F_G}{ \cos \delta_g \cos \theta_{iv}^f \cos \theta_{ve}^f \cos \psi_g }$ that is, expression (8.7) $2F_{Ge2} \approx \frac{F_c h \cos \delta_g}{ \cos \phi_g (\sin \theta_{iv}^f \cos \theta_{ve}^f + \cos \theta_{iv}^f \sin \theta_{ve}^f) }$ that is, expression (8.8)	19.93283795 16.64248085
Allowable error of transmission ratio	$\frac{F_{Ge}}{\Delta M_{gp}}$ $\Delta(\frac{dM_{gp}}{d\varepsilon_g}) = -\frac{N_g \Delta M_{gp}}{2\pi}$ that is, expression (8.21)	8.321240424 0.00259 0.018549508
Diameter of color compound	δ	0.00635
Modified value of Curvature in Directions e and g	$\Delta K'_{2e} = \frac{2\delta}{F_{Ge}^2}$ that is, expression (8.13) $g_f = \frac{\sqrt{D_p^2 + E_p^2}}{N_{gp}^f \cdot J_p}$ $\tan \theta_{e\tau'}^f = \frac{1 - g_f \mathbf{v}_{fp}^{gp} \sin \theta_{ve}^f}{\tan \theta_{ve}^f + g_f \mathbf{v}_{fp}^{gp} \cos \theta_{ve}^f}$ that is, expression (8.19) $\Delta G'_{2e} = -\frac{\Delta K'_{2e}}{\tan \theta_{e\tau'}^f}$ that is, expression (8.18) $\Delta(\mathbf{J}_p \cdot \mathbf{N}_{gp}^f) = \Delta(\frac{dM_{gp}}{d\varepsilon_g}) [z_{gp}^f N_{gpx}^f - N_{gpz}^f (x_{gp}^f - f_{gp})]$ $\Delta K'_{2g} = -\frac{\bar{K}_g^2}{D_p^2 + E_p^2} \Delta(\mathbf{J}_p \cdot \mathbf{N}_{gp}^f)$ that is, expression (8.25)	0.000183412 0.018336448 -2.139732477 0.000085717 -0.443703483 0.000086905
Curvatures of Pinion in Directions e and g	$K'_{pe} = K'_{pe} + \Delta K'_{2e}$ $G'_{pe} = G'_{pe} + \Delta G'_{2e}$ that is, expression (8.16) $K'_{pg} = K'_{pg} + \Delta K'_{2g}$ that is, expression (8.26)	-0.6935212 $\times 10^{-2}$ -0.1531532 $\times 10^{-2}$ 0.031567721

Curvatures of	$K'_{pt} = K'_{pe} \cos^2 \theta_{etp}^f + K'_{pg} \sin^2 \theta_{etp}^f + 2G'_{pe} \sin \theta_{etp}^f \cos \theta_{etp}^f$	$-0.1747284 \times 10^{-2}$
Pinion in Direc-	$G'_{pt} = -(K'_{pe} - K'_{pg}) \sin \theta_{etp}^f \cos \theta_{etp}^f + G'_{pe} (\cos^2 \theta_{etp}^f - \sin^2 \theta_{etp}^f)$	$-0.13235653 \times 10^{-1}$
tions t_p and s_p	$K'_{ps} = K'_{pe} \sin^2 \theta_{etp}^f + K'_{pg} \cos^2 \theta_{etp}^f - 2G'_{pe} \sin \theta_{etp}^f \cos \theta_{etp}^f$ that is, expression (8.27)	$0.26379792 \times 10^{-1}$

A.10 Determination of Machine-Setting Parameters for the Pinion Tooth Surface

Input parameters are all obtained in the previous sections and together with:

Item	Expression	Value
Blade Angle for Pinion	ϕ_{cp}^o	168.5°

Output parameters:

Item	Expression	Value
Vertical Position of Pinion	f_{mp} that is, by solving equation (9.43)	37.810831
Horizontal Position of Pinion	L_p that is, by solving equation (9.43)	-22.452872
The Ratio of Roll	M_{mp}	-3.8506395
The Increment of Phase Angle for Pinion Cutting Position	$\delta \varepsilon_p^f$ that is, by solving equation (9.43)	-9.726736057°
The Phase Angle for Cutting Edge	σ_p that is, equation (9.43)	131.2873315°
The Coordinate of Cutter Center at the Cutting Position	x_{cp} y_{cp} z_{cp} that is, by solving equation (9.43)	121.80237 3.7442306 -12.159691
Cutter Radius at Cutting Position	ρ_{cp} that is, by solving equation (9.43)	123.02163

Intermediate Parameters:

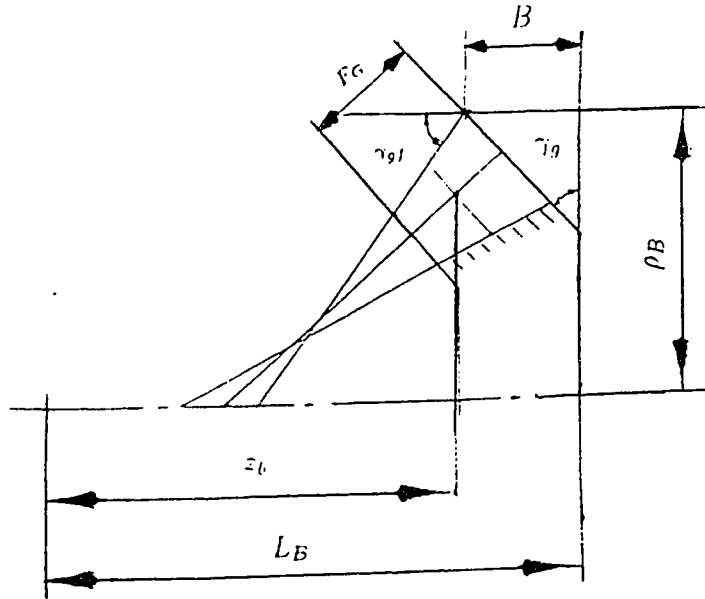
The Position of Cutting Point on Cutter	$\mathbf{R}_{mp} = x_{mp}\mathbf{i}_m + y_{mp}\mathbf{j}_m + z_{mp}\mathbf{k}_m$ $x_{mp} = x_{cp} + \rho_{cp} \cos \sigma_p$ $y_{mp} = y_{cp} + \rho_{cp} \sin \sigma_p$ $z_{mp} = z_{cp}$ that is, expression (9.8)	40.62832609 96.18391928 -12.159691
The Position of Cutting Point on Pinion	$\mathbf{R}_p = x_p\mathbf{i}' + y_p\mathbf{j}' + z_p\mathbf{k}'$ $x_p = x_p^f \cos \delta \varepsilon_p^f - y_p^f \sin \delta \varepsilon_p^f$ $y_p = x_p^f \sin \delta \varepsilon_p^f + y_p^f \cos \delta \varepsilon_p^f$ $z_p = z_p^f$ that is, expression (9.11)	2.817498853 36.98979848 112.0684926
Unit Normal to Cutter	$x_p + f_{mp}$ $y_p \sin \gamma_{pr} + (L_p + z_p) \cos \gamma_{pr}$ $(L_p + z_p) \sin \gamma_{pr} - y_p \cos \gamma_{pr}$ that is, equation (9.15) is satisfied $\mathbf{N}_{cp} = N_{cpz}\mathbf{i}_m + N_{cpy}\mathbf{j}_m + N_{cpz}\mathbf{k}_m$ $N_{cpz} = -\cos \phi_{cp}^i \cos \sigma_p$ $N_{cpy} = -\cos \phi_{cp}^i \sin \sigma_p$ $N_{cpz} = \sin \phi_{cp}^i$ that is, expression (9.9)	40.62832985 96.18392751 -12.15978655
Unit Normal to Pinion	$\mathbf{N}_p = N_{px}\mathbf{i}' + N_{py}\mathbf{j}' + N_{pz}\mathbf{k}'$ $N_{px} = N_{px}^f \cos \delta \varepsilon_p^f - N_{py}^f \sin \delta \varepsilon_p^f$ $N_{py} = N_{px}^f \sin \delta \varepsilon_p^f + N_{py}^f \cos \delta \varepsilon_p^f$ $N_{pz} = N_{pz}^f$ $-N_{cpy} \sin \gamma_{pr} + N_{cpz} \cos \gamma_{pr}$ $-N_{cpy} \cos \gamma_{pr} - N_{cpz} \sin \gamma_{pr}$ that is, equation (9.16) is satisfied	0.646589118 -0.000978945 -0.762837824 -0.000979056 -0.762837803
Unit Tangent to Cutting Edge	$\mathbf{W}_{cp} = W_{cp1}\mathbf{i}_m + W_{cp2}\mathbf{j}_m + W_{cp3}\mathbf{k}_m$ $W_{cp1} = \sin \phi_{cp}^i \cos \sigma_p$ $W_{cp2} = \sin \phi_{cp}^i \sin \sigma_p$ $W_{cp3} = \cos \phi_{cp}^i$ that is, expression (9.10)	-0.131550049 0.149807068 -0.979924705
Velocity of Cutter Relative to Pinion	$\mathbf{v}_p^{mp} = v_{p1}^{mp}\mathbf{i}_m + v_{p2}^{mp}\mathbf{j}_m$ $v_{p1}^{mp} = -(1 + M_{mp} \sin \gamma_{pr})y_{mp}$ $+ z_{mp}M_{mp} \cos \gamma_{pr}$	46.25045504

Intermediate Parameters	$v_{p2}^{mp} = (1 + M_{mp} \sin \gamma_{pr}) x_{mp}$	37.779459
	$v_{p3}^{mp} = -M_{mp} f_{mp} \sin \gamma_{pr}$	10.468446
	$v_{p3}^{mp} = -M_{mp} x_{mp} \cos \gamma_{pr}$	
	$+ M_{mp} f_{mp} \cos \gamma_{pr}$	
	$ v_p^{mp} = \sqrt{(v_{p1}^{mp})^2 + (v_{p2}^{mp})^2 + (v_{p3}^{mp})^2}$	60.62986454
	that is, expression (9.20)	
	$v_{p1}^{mp} N_{cpx} + v_{p2}^{mp} N_{cpy} + v_{p3}^{mp} N_{cpz}$	0.000000351
	that is, equation (9.20) is satisfied	
	$\eta_p^p = \eta_{p1}^p \mathbf{i}_m + \eta_{p2}^p \mathbf{j}_m + \eta_{p3}^p \mathbf{k}_m$	
	$\eta_{p1}^p = -N_{cpy}(1 + M_{mp} \sin \gamma_{pr})$	-0.73255526
	$+ N_{cpz} M_{mp} \cos \gamma_{pr}$	
	$\eta_{p2}^p = N_{cpx}(1 + M_{mp} \sin \gamma_{pr})$	0.007199543
	$\eta_{p3}^p = -N_{cpx} M_{mp} \cos \gamma_{pr}$	-2.4024099
	$ \eta_p^p = \sqrt{(\eta_{p1}^p)^2 + (\eta_{p2}^p)^2 + (\eta_{p3}^p)^2}$	2.511625444
Curvatures of Cutter Surface	that is, expression (9.18)	
	$\cos \theta_{v\eta}^{mp} = \frac{v_{p1}^{mp} \eta_{p1}^p + v_{p2}^{mp} \eta_{p2}^p + v_{p3}^{mp} \eta_{p3}^p}{ v_p^{mp} \eta_p^p }$	-0.385859643
	$\sin \theta_{v\eta}^{mp} = -\frac{M_{mp} f_{mp} \cos \gamma_{pr}}{ v_p^{mp} \eta_p^p }$	0.922557509
	that is, expression (9.24)	
	$\cos \theta_{wv}^{mp} = \frac{v_{p3}^{mp}}{ v_p^{mp} \cos \phi_{cp}^i}$	-0.176198786
	$\sin \theta_{wv}^{mp} = \frac{v_{p2}^{mp} \cos \sigma_p - v_{p1}^{mp} \sin \sigma_p}{ v_p^{mp} }$	-0.984354605
	that is, expression (9.27)	
	$K_{cpv} = -\frac{\cos \phi_{cp}^i \sin^2 \theta_{wv}^{mp}}{\rho_{cp}}$	0.77181707 $\times 10^{-2}$
	$G_{cpv} = -\frac{\cos \phi_{cp}^i \sin \theta_{wv}^{mp} \cos \theta_{wv}^{mp}}{\rho_{cp}}$	0.1381547 $\times 10^{-2}$
	$K_{cp\Delta} = -\frac{\cos \phi_{cp}^i \cos^2 \theta_{wv}^{mp}}{\rho_{cp}}$	0.24729594 $\times 10^{-3}$
	that is, expression (9.28)	
	$\mathbf{J}_p = J_{p1} \mathbf{i}_m + J_{p2} \mathbf{j}_m + J_{p3} \mathbf{k}_m$	
	$J_{p1} = M_{mp} f_{mp} \sin \gamma_{pr}$	-38.23184133
	$J_{p2} = M_{mp} z_{mp} \cos \gamma_{pr}$	45.179481
	$J_{p3} = -M_{mp} y_{mp} \cos \gamma_{pr}$	357.37255
Conjugate Accele- ration	that is, expression (9.31)	
	$\mathbf{J}_p \cdot \mathbf{N}_{cp} = J_{p1} N_{cpx} + J_{p2} N_{cpy} + J_{p3} N_{cpz}$	129.2357142

Intermediate Parameters	$D_p = K_{cpv} \mathbf{v}_p^{mp} - \eta_p^p \cos \theta_{v\eta}^{mp}$ $E_p = G_{cpv} \mathbf{v}_p^{mp} - \eta_p^p \sin \theta_{v\eta}^{mp}$ that is, expression (9.33)	1.437086499 -2.2333558
Conjugate	$K'_{pv} = \frac{D_p^2}{D_p \mathbf{v}_p^{mp} + \mathbf{J}_p \cdot \mathbf{N}_{cp}} - K_{cpv}$	0.18268453 $\times 10^{-2}$
Curvatures of	$G'_{pv} = \frac{D_p E_p}{D_p \mathbf{v}_p^{mp} + \mathbf{J}_p \cdot \mathbf{N}_{cp}} - G_{cpv}$	-1.6215321 $\times 10^{-2}$
Pinion	$K'_{p\Delta} = \frac{E_p^2}{D_p \mathbf{v}_p^{mp} + \mathbf{J}_p \cdot \mathbf{N}_{cp}} - K_{cp\Delta}$ that is, expression (9.34)	2.2805663 $\times 10^{-2}$
Intermediate Parameters	$\mathbf{t}_{pc} = t_{pc1} \mathbf{i}_m + t_{pc2} \mathbf{j}_m + t_{pc3} \mathbf{k}_m$ $t_{pc1} = t_{p1} \cos \delta \varepsilon_p^f - t_{p3} \sin \delta \varepsilon_p^f$ $t_{pc2} = (t_{p1} \sin \delta \varepsilon_p^f + t_{p3} \cos \delta \varepsilon_p^f) \sin \gamma_{pr}$ $\quad - t_{p2} \cos \gamma_{pr}$ $t_{cp3} = -(t_{p1} \sin \delta \varepsilon_p^f + t_{p3} \cos \delta \varepsilon_p^f) \cos \gamma_{pr}$ $\quad - t_{p2} \sin \gamma_{pr}$ that is, expression (9.35)	-0.757626794 -0.65035005 -0.055194692
	$\cos \theta_{vt}^{mp} = \frac{t_{pc1} v_{p1}^{mp} + t_{pc2} v_{p2}^{mp} + t_{pc3} v_{p3}^{mp}}{ \mathbf{v}_p^{mp} }$	-0.99271638
	$\sin \theta_{vt}^{mp} = \frac{\begin{Bmatrix} t_{pc1}(N_{cpy} v_{p3}^{mp} - N_{cpz} v_{p2}^{mp}) \\ + t_{pc2}(N_{cpz} v_{p1}^{mp} - N_{cpv} v_{p3}^{mp}) \\ + t_{pc3}(N_{cpv} v_{p2}^{mp} - N_{cpy} v_{p1}^{mp}) \end{Bmatrix}}{ \mathbf{v}_p^{mp} }$ that is, expression (9.40)	-0.120474847
Conjugate	$K'_{pt_p} = K'_{pv} \cos^2 \theta_{vt}^{mp} + K'_{p\Delta} \sin^2 \theta_{vt}^{mp}$ $\quad + 2G'_{pv} \sin \theta_{vt}^{mp} \cos \theta_{vt}^{mp}$	-0.1747283 $\times 10^{-2}$
Curvatures of	$G'_{pt_p} = -(K'_{pv} - K'_{p\Delta}) \sin \theta_{vt}^{mp} \cos \theta_{vt}^{mp}$ $\quad + G'_{pv} (\cos^2 \theta_{vt}^{mp} - \sin^2 \theta_{vt}^{mp})$	-1.3235606 $\times 10^{-2}$
Pinion	$K'_{ps_p} = K'_{pv} \sin^2 \theta_{vt}^{mp} + K'_{p\Delta} \cos^2 \theta_{vt}^{mp}$ $\quad - 2G'_{pv} \sin \theta_{vt}^{mp} \cos \theta_{vt}^{mp}$ that is, requirement (9.41) is satisfied	2.6379791 $\times 10^{-2}$

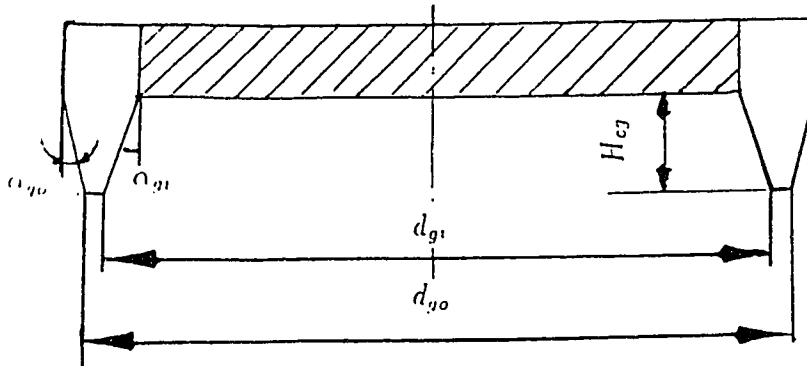
Parameters for Gear Blank

$$\left. \begin{aligned} B &> [a_g + b_g + \frac{F_G}{2} (\tan \alpha_g + \tan \delta_g)] \sin \gamma_g \\ \rho_B &= \rho_b + \frac{F_G}{2} \sin \gamma_g + (a_g + \frac{F_G}{2} \tan \alpha_g) \cos \gamma_g \end{aligned} \right\} \quad (A.1)$$



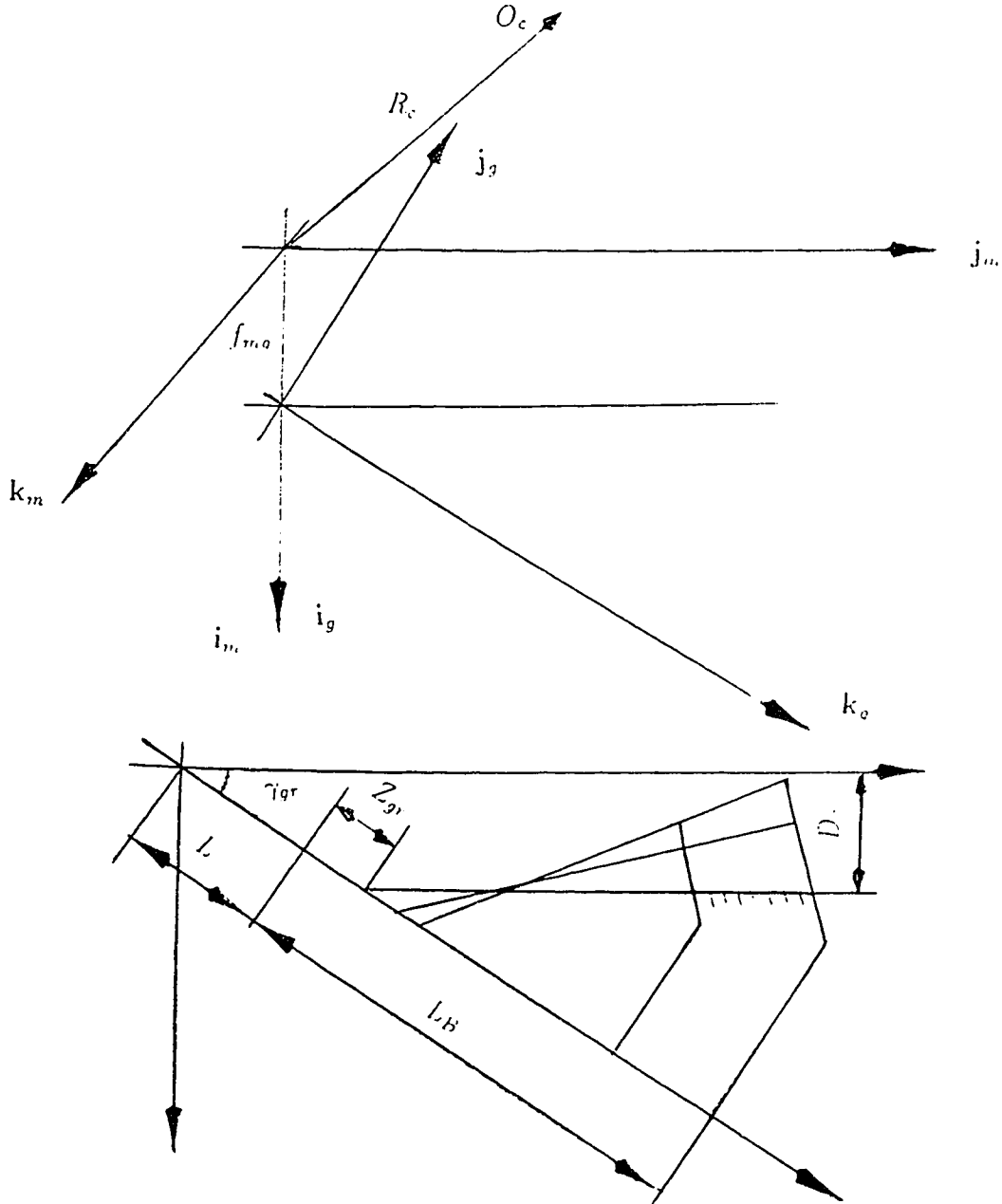
Parameters for Cutter of Gear

$$\left. \begin{aligned} d_{gi} &= 2r_c - W_p \\ d_{go} &= 2r_c + W_p \\ \alpha_{gi} &= \phi_c^i \\ \alpha_{go} &= 180^\circ - \phi_c^o \\ H_{cg} &> [a_g + b_g + \frac{F_G}{2} (\tan \alpha_g + \tan \delta_g)] \cos \delta_g \end{aligned} \right\} \quad (A.2)$$



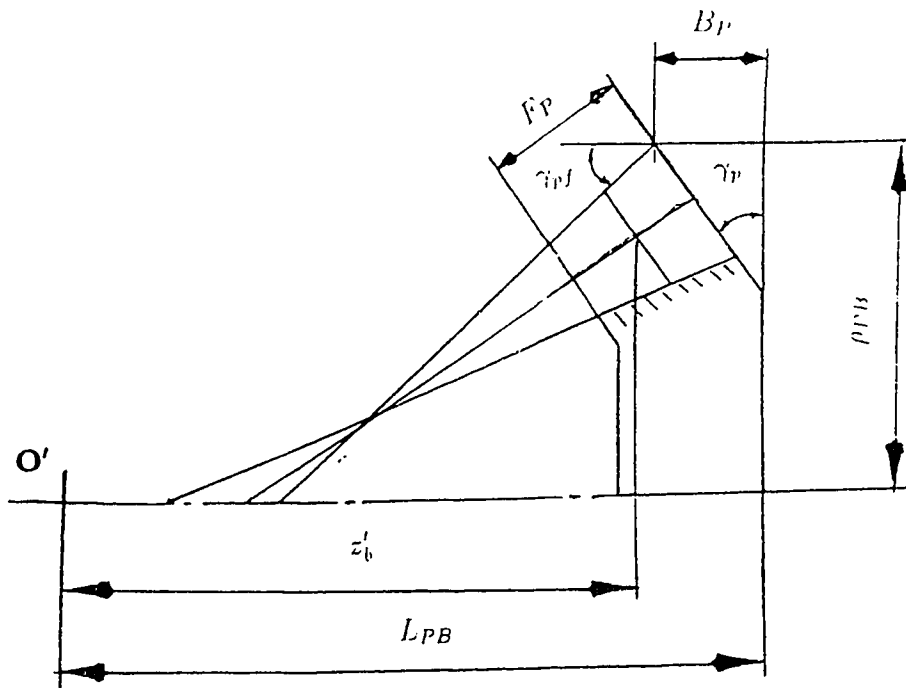
Parameters for Machine-Setting of Gear

$$\left. \begin{aligned} L_B &= z_b - a_g \sin \gamma_g + \frac{F_G \cos \gamma_{gl}}{2 \cos \alpha_g} + B \\ R_c &= \sqrt{(x_c^o)^2 + (y_c^o)^2} = \sqrt{(x_c^i)^2 + (y_c^i)^2} \\ D_c &= (L + Z_{gr}) \sin \gamma_{gr} \end{aligned} \right\} \quad (A.3)$$



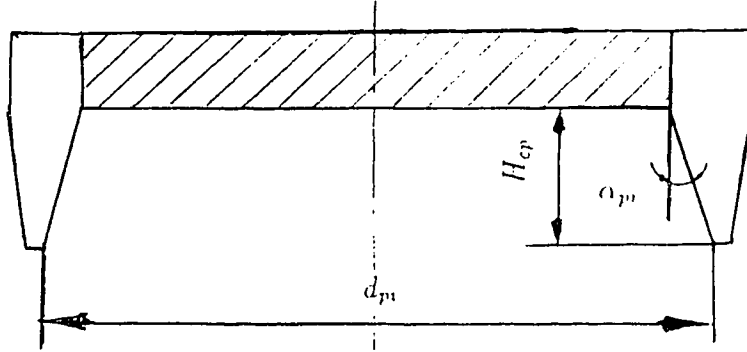
Parameters for Pinion Blank

$$\left. \begin{aligned} F_P &> F_G \\ B_P &> \{a_p + b_p + \frac{F_P}{2}[\tan(\gamma_{pf} - \gamma_p) + \tan(\gamma_p - \gamma_{pr})]\} \sin \gamma_p \\ \rho_{PB} &= \rho'_b + a_p \cos \gamma_p + \frac{F_P \sin \gamma_{pf}}{2 \cos(\gamma_{pf} - \gamma_p)} \\ L_{PB} &= z'_b - a_p \sin \gamma_p + \frac{F_P \cos \gamma_{pf}}{2 \cos(\gamma_{pf} - \gamma_p)} + B_P \end{aligned} \right\} \quad (\text{A.4})$$



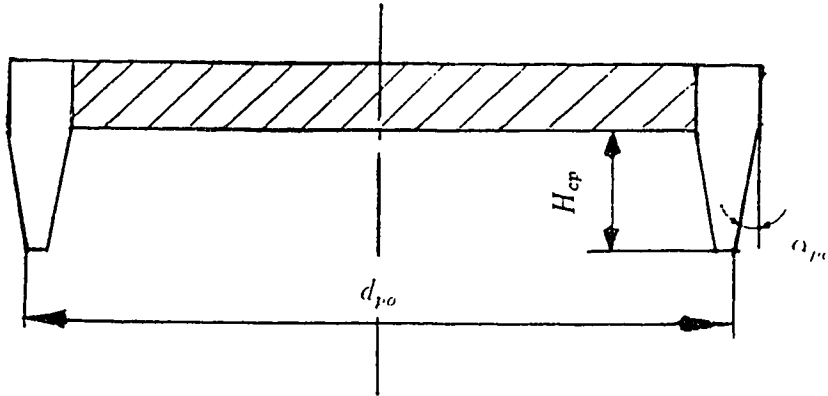
Parameters for Cutter of Pinion (Convex)

$$\left. \begin{aligned} H_{cp} &> \left\{ a_p + b_p + \frac{F_p}{2} [\tan(\gamma_{pf} - \gamma_p) + \tan(\gamma_p - \gamma_{pr})] \right\} \cos(\gamma_p - \gamma_{pr}) \\ d_{pi} &= 2\rho_{cp}^i + 2[(L_p + Z_{pr}) \sin \gamma_{pr} - z_{cp}^i] \tan \phi_{cp}^i \\ \alpha_{pi} &= \phi_{cp}^i \end{aligned} \right\} \quad (A.5)$$



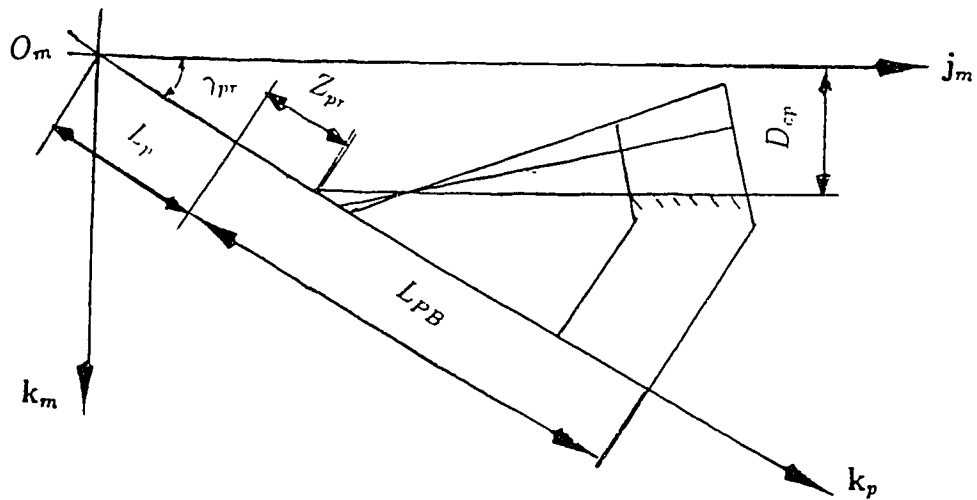
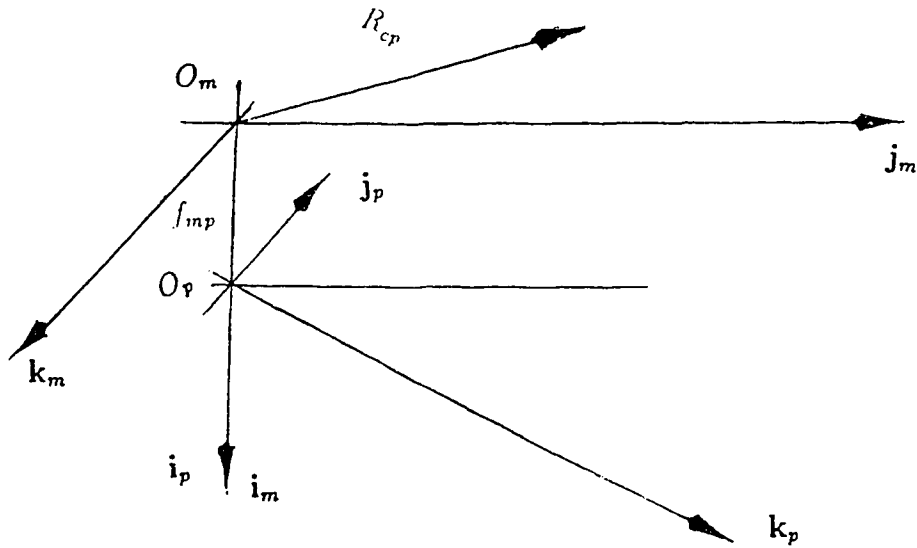
Parameters for Cutter of Pinion (Concave)

$$\left. \begin{aligned} d_{po} &= 2\rho_{cp}^o + 2[(L_p + Z_{pr}) \sin \gamma_{pr} - z_{cp}^o] \tan \phi_{cp}^o \\ \alpha_{po} &= 180^\circ - \phi_{cp}^o \end{aligned} \right\} \quad (A.6)$$



Parameters for Machine-Setting of Pinion

$$\left. \begin{aligned} D_{cp} &= (L_p + Z_{pr}) \sin \gamma_{pr} \\ R_{cp} &= \sqrt{x_{cp}^2 + y_{cp}^2} \end{aligned} \right\} \quad (A.7)$$



Data of Gear Blank

$$B = 30 > 12.09$$

$$\rho_B = 137.494$$

Data for Cutter of Gear

$$d_{gi} = 298.254$$

$$d_{go} = 301.749$$

$$\alpha_{gi} = 14^\circ$$

$$\alpha_{go} = 20^\circ$$

$$H_{cg} = 20 > 12.632$$

Data for Machine-Setting of Gear

$$L_B = 70.475$$

$$R_c = 135.907$$

$$D_c = -17.031$$

Data for Pinion Blank

$$F_P = 43 > 40.64$$

$$B_P = 10 > 3.692$$

$$\rho_{PB} = 51.794$$

$$L_{PB} = 140.681$$

Data for Cutter of Pinion (Convex)

$$H_{cp} = 20 > 12.588$$

$$d_{pi} = 291.756$$

$$\alpha_{pi} = 24^\circ$$

Data for Cutter of Pinion (concave)

$$d_{po} = 244.75$$

$$\alpha_{po} = 11.5^\circ$$

Data for Machine-Setting of Pinion

$$D_{cp}^i = -2.846$$

$$D_{cp}^o = -8.983$$

$$f_{mp}^i = 32.195$$

$$f_{mp}^o = 37.81$$

$$R_{cp}^i = 131.759$$

$$R_{cp}^o = 121.86$$